The Role of CC-Chemokine Receptor-Like 2 in the B cell Response

Sarah Cook

A thesis submitted to
The University of Birmingham
for the degree of
DOCTOR OF PHILOSOPHY

September 2014

School of Immunity and Infection
College of Medical and Dental Sciences
The University of Birmingham
Edgbaston
B15 2TT
United Kingdom

Abstract

CCRL2 is a member of the atypical chemattractant family. It has been proposed to bind the chemokines CCL19 and CCL5, as well as the adipokine chemerin. Unlike typical chemokine receptors, atypical chemoattractant receptors do not undergo conventional G protein signalling upon binding, but instead degrade, transcytose or present their ligands on the cell surface. This study aims to characterise the role of CCRL2 in B cells upon their activation and differentiation into either extrafollicular plasmablasts or germinal centre B cells.

CCRL2 mRNA is upregulated upon plasmablast differentiation. In order to assess the role of CCRL2 in the plasmablast response, wild type and CCRL2 deficient mice were immunised with the thymus independent type 2 antigen NP-Ficoll. Upon immunisation, CCRL2 deficient mice produce more NP-specific antibody and larger numbers of NP-specific plasmablasts. Adoptive transfer of NP-specific $CCRL2^{+/+}$ or $CCRL2^{-/-}$ cells into wild type hosts show that the increase in antibody levels is due to B cell intrinsic effects. CCRL2 deficient plasmablasts tend to proliferate more and undergo less apoptosis than CCRL2 expressing plasmablasts. Analysis of mRNA produced by $CCRL2^{+/+}$ and $CCRL2^{-/-}$ plasmablasts show no the major differences in a panel of mRNAs analysed, with the exception of TACI mRNA, which is reduced.

The role of CCRL2 in the germinal centre was also assessed. To this end, wild type and CCRL2 deficient mice were immunised with thymus dependent antigen NP-CGG to induce germinal centre formation. Germinal centres formed normally, including polarisation into light and dark zones in CCRL2 deficient mice. However, FDCs within the germinal

centre appeared to extend further into the follicular mantle in CCRL2 deficient mice. This may be the cause of an increased proportion of germinal centres over the whole spleen in CCRL2 deficient mice. Analysis of mRNAs in GC B cells from CCRL2$^{-/-}$ mice show a reduction in Bcl6 and *Aicda* mRNA compared to CCRL2$^{+/+}$ GC B cells. Nevertheless, these differences did not result in significant changes in affinity maturation.

Together, this shows a novel role for CCRL2 in the regulation of the extrafollicular plasmablast response to NP-Ficoll. However, minor differences in CCRL2 deficient germinal centres do not affect high affinity plasma cell output, suggesting a minimal role of CCRL2 in GC function.

Acknowledgements

Firstly, I would like to thank my supervisor Dr. Kai Toellner for giving me the chance to work on this project. Thank you for all your help, support and encouragement during my time as a PhD student. I would also like to thank Prof. Antal Rot for his help during my time here. Thank you to the Wellcome Trust, for providing me with the funding to complete this study.

A big thank you also needs to go to: Jenny, super Postdoc extraordinaire, who has taught me everything I know and I am truly grateful; Yang and Laura (Walsall), for allowing me constantly pester you for help and advice, allowing me to blabber on at you and teaching me so much; Maria, your patience with me at the beginning was second-to-none, thank you for always giving me your time and expertise, even after you moved away; Laura (Spanish) thanks for all your help since you started, I couldn't have done some days without you; and to the remainder (and ex) members of the lab; Tom, Charlie, Ciaran and Ben, thanks for all your help, advice and (most importantly!) your friendship.

For all of Prof. Adam Cunninghams lab, thank you so much with your help in the Salmonella aspects of this thesis as well as everything else you have done over the three years to ensure "Calamity Cook" submitted! Adriana, Coral, Jessie and Spyda, you have helped make this a brilliant place to work and somewhere I want to go every morning! Poonam and Beth, you are both amazing! I already miss our lunches together. For everyone on the fourth floor, thank you for providing endless reagents, antibodies and MACS magnets, and giving some great advice to me at the fourth floor meetings. A special mention must also go to Roger Bird for your hours on the MoFlo. I'd also like to show my appreciation to everyone at BMSU, in particular Ian, Jim and Jenny. Thanks also to Chris Hansell at The University of Glasgow, for providing the fluorescent CCL19. A huge thank you to Jenny, Jessie, Laura, Spyda, Tom and Yang for proof-reading.

Finally, some special mentions. Ditte, Maaike, Simone and Suzi - thanks for everything you superstars! Mum, Dad, Laura and Ciaran "Cooky" Cook, thank you for your never ending love, support, laughs and Fish 'n' Chips!

Abbreviations

7-AAD	7-Aminoactinomycin D
β2-M	β2-Microglobulin
ACKR	Atypical Chemokine Receptor
AID	Activation Induced Cytidine Deaminase
APRIL	A Proliferation Induced Ligand
BAFF	B Cell Activating Factor of the TNF Family
Bcl6	B Cell Lymphoma 6
BCMA	B Cell Maturation Antigen
BCR	B Cell Receptor
BLIMP-1	B Lymphocyte-Induced Maturation Protein-1
BMSU	Biomedical Services Unit
BrdU	5-bromo-2'-deoxyuridine
BSA	Bovine Serum Albumin
CB2	Cannabinoid Receptor 2
$CCL19^{AF647}$	Alexa Fluor 647 conjugated CCL19
CCRL1	CC Chemokine Receptor Like-1
CCRL2	CC Chemokine Receptor Like-2
$CCRL2^{+/-}$	CCRL2 heterozygous
$CCRL2^{-/-}$	CCRL2 knock out
CGG	Chicken Gamma Globulin
Cq	Quantification Cycle
CRAM	Chemokine Receptor on Activated Macrophage
CSR	Class Switch Recombination
DC	Dendritic Cell
dC	deoxycytidine
dU	deoxyuridine
DZ	Dark Zone
EBI2	Epstein-Barr Virus-Induced GPCR 2
EDTA	Ethylenediaminetetraacetic acid
EdU	5-ethylnyl-2'-deoxyuridine

ELISA	Enzyme Linked Immunosorbent Assay
ELISPOT	Enzyme Linked Immunosorbent Spot
FACS	Fluorescent Activated Cell Sorting
FCS	Fetal Calf Serum
FDC	Follicular Dendritic Cell
GC	Germinal Centre
GPCR	G Protein Coupled Receptor
HIGM2	Hyper-IgM syndrome type 2
IFN	Interferon
Ig	Immunoglobulin
IL	Interleukin
iNKT	invariant NK T cells
i.p.	Intraperitoneal
IRF4	Interferon Regulatory Factor 4
i.v.	Intravenous
KLF2	Krüppel-like factor 2
KO	Knock Out
LN	Lymph Node
LPM	Large Peritoneal Macrophage
LPS	Lipopolysaccharide
LZ	Light Zone
MACS	Magnetic-Activated Cell Sorting
MFI	Mean Fluorescence Intensity
MGI	Mouse Genome Informatics
MHC	Major Histocompatibility Complex
miRNA	microRNAs
MZ	Marginal Zone
MZM	Marginal Zone Macrophages
NP	4-hydroxy-3-nitrophenyl
NP-CGG	4-hydroxy-3-nitrophenyl - Chicken Gamma Globulin
OD	Optical Density
OMP	Outer Membrane Protein

OVA	Ovalbumin
PALS	Periarteriolar Lymphoid Sheath
PB	Plasmablast
PBS	Phosphate Buffered Saline
PBS-1%BSA	Phosphate Buffered Saline containing 1% Bovine Serum Albumin
PCA	Passive Cutaneous Anaphylaxis
PE	Phosphatidylethanolamine
PS	Phosphatidylserine
QM	Quasi-Monoclonal
QM^{KO}	CCRL2 deficient QM B cells or mice
QM^{WT}	Wild type QM B cells or mice
RGS13	Regulator of G protein Signalling 13
RT	Room Temperature
RT-qPCR	Reverse Transcription-quantitative real-time PCR
S1P	Sphingosine-1-Phosphate
S1PR1	Sphingosine-1-Phosphate Receptor 1
S1PR2	Sphingosine-1-Phosphate Receptor 2
SHM	Somatic Hypermutation
SPM	Small Peritoneal Macrophage
STm	Salmonella Typhimurium
TACI	Transmembrane Activator and Calcium-modulator and cyclophilin ligand Interactor
TD	Thymus Dependent
Tfh	T follicular helper
TI	Thymus Independent
TLR	Toll Like Receptor
TNP-LPS	Trinitrophenyl-lipopolysaccharide
TZ	T Zone
WT	Wild Type

Contents

List of Figures

Chapter 1. Introduction

For a multicellular organism to function, cells must be directed to specific niches, where they will be able to fulfil their role through cellular interactions. In order to direct cells to the correct location, species have evolved a system of ligand-receptor interactions, which attract or repel cells from distinct anatomical sites. The major family involved in this process are chemokines, which guide cells to specific organs or microanatomical compartments within those organs.

1.1 Chemokines and their receptors

Chemokines ("chemotactic cytokines") are a superfamily of 8-10kDa glycoproteins which are involved in numerous physiological functions including angiogenesis, organogenesis and haematopoiesis. The role of chemokines is to guide the migration of cells. Cellular locomotion requires polarisation of the cell; the forming of lamellipodia at the leading edge, where the receptors of chemokines gather to induce signals that either attract, or repel, the cell from the area (Lauffenburger and Horwitz, 1996, Nieto et al., 1997).

Chemokines are defined through a set of 4 conserved cysteine residues linked by disulphide bonds (Baggiolini et al., 1997). The two major subfamilies of chemokines are named CC or CXC, depending on whether the two first cysteines are adjacent or separated by another amino acid (Baggiolini et al., 1997). Other chemokines that do not belong to either of these major families include CX3CL1, XCL1 and XCL2 (Rot and von Andrian, 2004). Chemokines can be classified into two broad groups; homeostatic or inflammatory, which are all similar in structure, and signal via G protein coupled receptors (GPCRs).

Chemokines bind to GPCRs on the cell surface to produce their effect on the target cell. GPCRs are seven transmembrane receptors, in which binding of ligand to the extracellular portion of the GPCR causes signalling via the G protein (figure 1.1). There are more than 1000 GPCRs, making this the largest known receptor family. Human GPCRs are split into five subfamilies, with chemokine receptors belonging to the Rhodopsin family (Fredriksson et al., 2003).

1.2 Atypical chemokine receptors

Atypical chemokine receptors (ACKRs) are serpentine receptors, however, unlike a typical chemokine receptors a DRYLAIV motif in the second intracellular loop is either missing or modified, and therefore ACKRs are unable to couple to a G-protein (Ulvmar et al., 2011) (figure 1.1). The ACKR family has 4 confirmed members: DARC (Duffy Antigen Receptor for Chemokines), D6, CXCR7 and CCRL1 (CC-Chemokine Receptor Like 1) (Ulvmar et al., 2011). Within the last year, a more conserved naming strategy for ACKRs was implemented, with each containing the prefix "ACKR" (table 1.1) (Bachelerie et al., 2014). Two other receptors, CCRL2 and PITPNM3, are reserved as part of this group of receptors (as ACKR5 and 6, respectively), but further analysis of their properties is required to confirm their chemokine-binding ability (Bachelerie et al., 2014).

GPCRs can transduce signals in the absence of G proteins (reviewed in (Sun et al., 2007)), disputing initial ideas that ACKRs are "silent". Indeed, a recent review on ACKRs has debated how and why ACKRs undergo unconventional signalling (Nibbs and Graham, 2013). One known response upon ligand binding to ACKRs is the internalisation of the

ligand, hence an alternative name for ACKRs; “interceptors” (internalising receptors) (Ulvmar et al., 2011).

Traditional Name	New Nomenclature
DARC	ACKR1
D6	ACKR2
CXCR7	ACKR3
CCRL1	ACKR4
CCRL2	ACKR5 (Reserved)
PITPNM3	ACKR6 (Reserved)

Table 1.1. New nomenclature for atypical chemokine receptors. *ACKR5 and ACKR6 are reserved for CCRL2 and PITPNM3, respectively, pending confirmation of their status of ACKRs.*

Binding of chemokine by ACKRs has been shown to have different consequences under certain conditions (reviewed in (Ulvmar et al., 2011) and (Nibbs and Graham, 2013)). For example, *in vitro* studies have shown ACKR1 is able to transport chemokine from the baso-lateral to the apical side of the cell (Pruenster et al., 2009) and ACKR4 has been shown to internalise chemokine ligand for lysosomal degradation (Comerford et al., 2006).

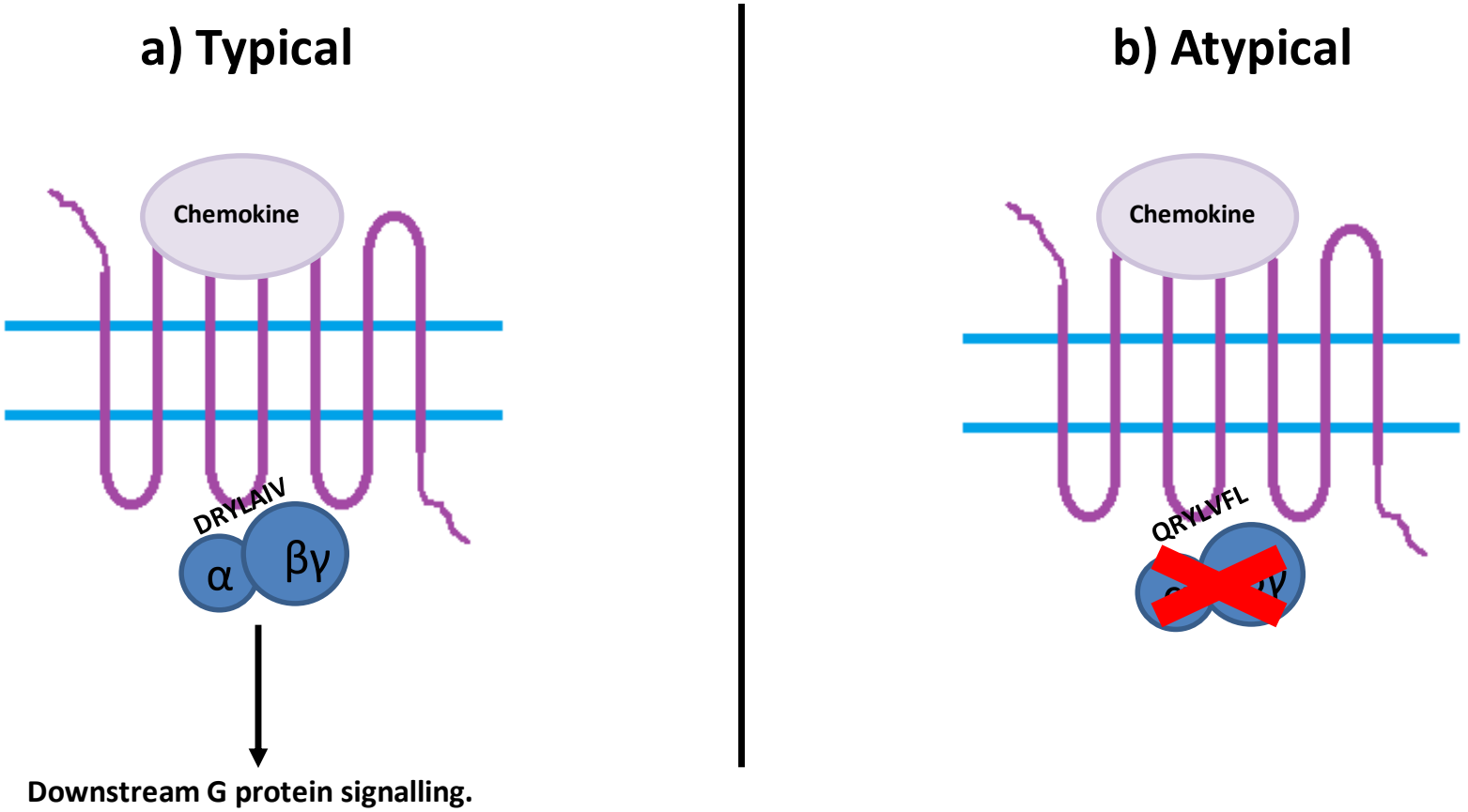

Figure 1.1. Atypical chemokine receptors are unable to couple to G proteins. Both atypical and typical chemokine receptors are seven-transmembrane receptors; a) typical chemokine receptors contain a canonical DRYLAIV motif in the second intracellular loop which enables G protein binding. Upon binding of chemokine ligand, the G protein dissociates and normal G-protein signalling occurs; b) in atypical chemokine receptors the DRYLAIV motif is either missing or modified, meaning G proteins are unable to bind. Upon chemokine ligand binding, non-G protein signalling takes place. Example here is CCRL2, with a QRYLVFL motif.

The consequence of this internalisation and movement of chemokine ligand has been conveyed in three recent *in vivo* studies; two reports have shown the formation of a CXCL12 gradient in zebrafish by the ACKR3 (Venkiteswaran et al., 2013, Dona et al., 2013) and another the formation of a CCL21 gradient in the mouse by ACKR4 (Ulvmar et al., 2014).

In both of the former studies the authors follow the migration of epithelial-like cells across the primordium of the zebrafish, from the front (ear) to the rear (tail); a process which requires CXCL12, CXCR4 and ACKR3. ACKR3 is expressed at the tail-end, but CXCR4 and CXCL12 are uniformally expressed along the length of the zebrafish. Nevertheless, CXCL12 signalling is under a gradient, with reduced signalling at the tail-end of the zebrafish. This chemokine gradient is generated through ACKR3 because 1) in the absence of ACKR3 there is a 30-40% reduction in the gradient of CXCL12, 2) in ACKR3$^{-/-}$ zebrafish CXCL12 signalling at the tail-end is equivalent to that at the front and 3) overexpression of ACKR3 causes a reduction in CXCL12 signalling across the embryo (Venkiteswaran et al., 2013, Dona et al., 2013).

In the latter study, a gradient of CCL21 formed by ACKR4 was demonstrated in the mouse. ACKR4 was shown to be expressed in the subcapsular sinus of the lymph node (LN). In ACKR4$^{-/-}$ LNs CCL21 is found within the subcapsular sinus, which is not the case in wild type (WT) LNs. This shows that a physiological gradient of CCL21 between the subcapsular sinus and parenchyma is reliant on the expression of ACKR4. This gradient, and ACKR4 expression, is required for the migration of dendritic cells (DCs), with DCs accumulating in the subcapsular sinus of ACKR4$^{-/-}$ LNs (Ulvmar et al., 2014).

Together, these publications show the ability of ACKRs to shape chemokine gradients, and these gradients are required for the migration of cells in both the zebrafish and the mouse.

1.3 CCRL2

CCRL2 (C-C chemokine receptor like 2) is potentially the newest member of the ACKR family. CCRL2 is also known by alternative names, such as L-CCR (Lipopolysaccharide-inducible CC chemokine receptor related gene), HCR (human chemokine receptor) and CRAM (chemokine receptor on activated macrophages) (Shimada et al., 1998, Fan et al., 1998, Galligan et al., 2004). Compared to other members of the chemokine receptor family, CCRL2 has the highest degree of homology with CCR1, an inflammatory chemokine receptor (Otero et al., 2010), however, CCRL2 is also highly homologous to the chemokine receptor CCR5 (NCBI BLAST search, (Altschul et al., 1990)). Human CCRL2 has two transcript variants, named CCRL2A and CCRL2B. However the mouse only contains one transcript, more similar to the human CCRL2B (Del Prete et al., 2013).

Like other ACKRs, CCRL2 has a modified DRYLAIV motif, which reads QRYLVFL (Del Prete et al., 2013). There has, however, recently been some debate whether CCRL2 is specifically an atypical chemokine receptor; although the name ACKR5 is reserved for CCRL2, this is pending confirmatory reports of chemokine binding and lack of typical signalling (Bachelerie et al., 2014).

1.3.1 Ligands of CCRL2

1.3.1.1 Binding of chemokines to CCRL2

Currently there is wide debate as to whether CCRL2 belongs to the ACKR family of receptors. Indeed, two recent reviews on ACKRs did not include CCRL2 (Graham et al., 2012, Nibbs and Graham, 2013). CCRL2 has been proposed to bind the chemokines CCL2 and CCL5 (Biber et al., 2003) as CCRL2 expressing HEK293 showed small intracellular calcium flux signalling in response to four chemokines (CCL -2, -5, -7 and -8). Upon incubation with CCL5, a cell line transfected with human CCRL2 has also been shown to undergo actin reorganisation (Hartmann et al., 2008). However, two independent studies contradict these findings; the first did not detect functional response in CCRL2 expressing cells to CCL2 (Galligan et al., 2004), and the second found no detectable binding of the four stated chemokines on HEK293 cells transfected with CCRL2 (Zabel et al., 2008).

Another chemokine, CCL19, has been suggested to bind human CCRL2 (Leick et al., 2010). In addition, results from the same laboratory showed that CCRL2 expression on a B cell chronic lymphocytic leukaemia cell line causes a reduction in CCL19- but not CCL21-induced chemotaxis via CCR7 (Catusse et al., 2010), however no studies have yet confirmed these findings, nor shown the binding of CCL19 to mouse CCRL2.

1.3.1.2 Chemerin is a functional ligand of CCRL2

Two signalling receptors bind the adipokine chemerin (previously known as RARRES2); ChemR23 (CMKLR1) (Meder et al., 2003, Wittamer et al., 2003) and GPR1 (Barnea et al., 2008). However, in 2008, CCRL2 was also proposed to bind chemerin (Zabel et al., 2008). CCRL2 is a non-signalling receptor of chemerin, and is able to present chemerin on the

cell surface (Zabel et al., 2008) and also regulate chemerin plasma levels (Monnier et al., 2012).

Chemerin is important in glucose homeostasis, with chemerin deficient mice being glucose intolerant (Takahashi et al., 2011). Chemerin promotes DC transmigration, making it a chemotactic factor (Gonzalvo-Feo et al., 2014), however it is not a chemokine, as it does not have the defining C-C motif. This binding of a non-chemokine ligand has caused CCRL2 to be defined as a "fringe" member of the ACKR family (Del Prete et al., 2013).

1.3.2 Expression of CCRL2

Expression of CCRL2 has been widely studied since it was first described in 1998 by Shimada and colleagues (Shimada et al., 1998). CCRL2 has been described in detail as a gene upregulated during inflammation in multiple cell types.

Originally, CCRL2 was shown to be upregulated upon lipopolysaccharide (LPS) stimulation of the macrophage cell line RAW264, as well as in mouse macrophages stimulated with LPS (Shimada et al., 1998). Macrophages and epithelial cells were also shown to express CCRL2 at an mRNA level in ovalbumin (OVA)-induced airway inflammation (Oostendorp et al., 2004). Macrophages are not the only LPS-stimulated cell type to upregulate CCRL2; with neutrophils (Galligan et al., 2004) and endothelial cells (Monnier et al., 2012) also upregulating the receptor upon LPS stimulation. Endothelial cells also upregulate CCRL2 in response to retinoic acid stimulation (Gonzalvo-Feo et al., 2014).

CCRL2 is not only upregulated in cells during mouse models of inflammation or *in vitro* stimulation; CCRL2 expression has also been observed on neutrophils and some

macrophages of the synovial fluid from rheumatoid arthritis patients (Galligan et al., 2004), probably due to the presence of inflammatory mediators within the synovial fluid.

CCRL2 expression has also been analysed within astrocytes and microglia of the brain, as the latter are bone marrow derived cells which have macrophage-like properties (Zuurman et al., 2003). Expression of CCRL2 at an mRNA level was enhanced in both cell types upon LPS stimulation both *in vitro* and *in vivo* (Zuurman et al., 2003), which was confirmed in astrocytes using whole genome expression profiling techniques (Hamby et al., 2012). In a differing study, CCRL2 mRNA expression was also detected in astrocytes, microglia and infiltrating macrophages in both the brains of experimental autoimmune encephalomyelitis mice (Brouwer et al., 2004) and mouse brains incubated with ischemic solution (a solution that causes a restriction of blood supply and oxygen) (Douglas et al., 2013). Further to this, elevated CCRL2 expression has been detected in human glioblastoma patient samples, which is thought to enhance migration and invasion of the tumour cells (Yin et al., 2012).

Recently, Zhao *et al.* conducted a global analysis of changes in gene expression in a murine microglial cell line during rabies virus infection. CCRL2 was described as one of the top 20 most upregulated genes, along with the chemokines CXCL5 and CXCL10 (Zhao et al., 2013).

Although highly upregulated during inflammation models, CCRL2 is also expressed in cells in steady state conditions. Peritoneal mast cells of the mouse have been shown to express CCRL2 at both the mRNA and protein level (Zabel et al., 2008). A recent study has also assessed the expression of CCRL2 in human and rat testes (Li et al., 2014). CCRL2

mRNA was found at relatively high levels in the testes, particularly compared to chemerin and its other receptors, however CCRL2 protein levels in the testes were relatively low. CCRL2 mRNA expression increases in expression in rat development from neonate to adult (Li et al., 2014).

1.3.3 Function of CCRL2

As an atypical receptor, CCRL2 would be expected to bind and internalise its ligands, in order to establish a concentration gradient. A report has suggested that CCRL2 is internalised and then readily re-expressed on the cell surface, a phenotype that is indicative of the receptor acting as an ACKR (Leick et al., 2010). However, this report remains controversial due to others showing no ligand dependent nor ligand independent endocytosis of CCRL2 (Zabel et al., 2008).

Although not a chemokine, CCRL2 still functions as an atypical receptor when bound to chemerin; it does not appear to signal, but instead captures the adipokine for presentation to cells expressing ChemR23 (Zabel et al., 2008, Gonzalvo-Feo et al., 2014). Chemerin regulation by CCRL2 has also been seen *in vivo*, with plasma levels of chemerin being higher in CCRL2 deficient mice, and this is even more pronounced after injection of LPS (Monnier et al., 2012).

1.3.3.1 Effect of CCRL2 deficiency in the mouse

To date, there have been four studies published which utilise CCRL2 deficient mice to assess the role of CCRL2 *in vivo*. $CCRL2^{-/-}$ mice are fertile, with expected male-female ratios of offspring (Zabel et al., 2008, Otero et al., 2010). A brief summary of the four studies is given here.

CCRL2 deficient mice were first studied in 2008, where a role of CCRL2 was identified on mast cells (Zabel et al., 2008). In this study, Zabel and colleagues examined passive cutaneous anaphylaxis (PCA) which is a mast cell-dependent model of allergy. This IgE-dependent model causes local inflammation of the ear. Tissue swelling was not significantly altered between WT and CCRL2 deficient mice, however when the original sensitising dose of antigen was administered at lower levels swelling was highly reduced in CCRL2$^{-/-}$ mice. When mast cell deficient mice were engrafted with either WT or CCRL2 deficient cells, and these mice were then challenged with the PCA model, mice receiving CCRL2$^{-/-}$ mast cells had a reduction in ear swelling, but no difference in total numbers of mast cells. There was, however, a reduction in neutrophils and mononuclear cells. Therefore, CCRL2 expression on mast cells enhances tissue swelling and leukocyte infiltration in the PCA model of allergy (Zabel et al., 2008).

CCRL2 expression at an mRNA level in the macrophage and bronchial epithelium was first described in OVA-induced airway inflammation in 2004 (Oostendorp et al., 2004), however a functional role of CCRL2 in OVA-induced inflammation of the lung was not described until 2010 (Otero et al., 2010). In this study, Otero *et al.* show that OVA-immunised CCRL2 deficient mice have a reduction in the number of leukocytes, particularly eosinophils and lymphocytes, recovered from bronchoalveolar lavage. Upon challenge of CCRL2 deficient mice with OVA, there was no difference in the migration of any DC subset to the lung compared with WT mice. Yet FITC-OVA immunised CCRL2$^{-/-}$ mice had a reduction in the numbers of FITC^{+} DCs within the mediastinal draining LNs at two and three days post immunisation. This is not due to CCRL2 deficient DCs having abnormal expression of other chemokine receptors nor due to the inability of these cells

to migrate. Therefore, CCRL2 has a role in the trafficking of antigen-loaded DCs to the mediastinal LN, and lack of CCRL2 expression protects against OVA-induced airway inflammation (Otero et al., 2010).

Monnier and colleagues have shown a role for CCRL2 on endothelial cells (Monnier et al., 2012). CCRL2 is expressed during steady state conditions on both mouse and human endothelial cells – and injection of LPS causes an upregulation of CCRL2 expression in liver endothelial cells too. CCRL2 expressed on the endothelial cell surface binds and concentrates chemerin, and regulates chemerin levels in the plasma of mice. After induction of lung inflammation, the numbers of infiltrating NK cells in CCRL2 deficient mice was reduced; although the NK cells do not express CCRL2, they do express another chemerin receptor, ChemR23. The authors proposed that CCRL2-expressing endothelial cells capture chemerin, concentrating it on the cell surface, so it is available for detection by and recruitment of ChemR23^{+} NK cells (Monnier et al., 2012).

Finally, the most recent paper with CCRL2 deficient mice assessed its role in ischemic brain injury (Douglas et al., 2013). Analysis of cortical slides incubated with ischemic solution revealed a reduction in cell death in CCRL2 deficient mice compared to WT. To assess this further, mice underwent a procedure known as “transient middle cerebral artery occlusion”, a mouse stroke model in which the artery is blocked for 30 minutes. CCRL2 deficient mice presented with significantly smaller brain lesions and lower neurological scores post procedure relative to WT mice. Together, this suggests that the absence of CCRL2 allows for an improved functional recovery in mice that have undergone ischemic brain injury (Douglas et al., 2013).

The above studies all use CCRL2 deficient mice to determine the role of CCRL2 in either innate immune cells or the brain. However, no study has yet described the role of CCRL2 in activation of the adaptive immune system. This study uses CCRL2$^{-/-}$ mice to study B cell activation and differentiation in the spleen.

1.4 Splenic architecture

The spleen is the largest secondary lymphoid organ in the body and has two broad functions; initiating an immune response against blood borne antigens and filtering the blood. These two functions are carried out in two distinct areas of the spleen, the former in the white pulp, and the latter in the red pulp. These areas are different in both cellular composition and microarchitecture (figures 1.2, 1.3 and 3.2). As this study focusses on the immune response generated within the spleen of immunised mice, the red pulp is not discussed here. For a comprehensive review of overall spleen and red pulp structure and function, see (Cesta, 2006).

1.4.1 The marginal zone and marginal sinus

The marginal zone (MZ) is a layer of cells that surrounds the B cell follicles and the T zone (TZ). The MZ is made up mainly of B cells (Kumararatne and MacLennan, 1981) and macrophages (Humphrey, 1979). The MZ macrophages are essential for the trapping of blood-borne antigens, and without them the early control of infection is impaired (Aichele et al., 2003). In between the rest of the white pulp and the MZ is a thin band of cells known as the marginal sinus, which is where the smallest arterial branches terminate (Kraal et al., 1995, Mebius and Kraal, 2005). Both T and B lymphocytes as well as antigen-loaded DCs enter the splenic white pulp from the blood through the marginal

sinus, due to the marginal sinus cells expressing MadCAM-1, a lymphocyte homing molecule (Kraal et al., 1995, Streeter et al., 1988, Nieuwenhuis and Ford, 1976). After entering the splenic white pulp, the majority of T cells migrate to the TZ, whereas most B cells migrate to the follicle (Nieuwenhuis and Ford, 1976).

1.4.2 The T zone

The TZ, also known as the periarteriolar lymphoid sheath (PALS), is located in the centre of the white pulp. The TZ acts as an area for T cell activation; recirculating T cells enter the TZ and may interact with peptide presenting DCs for priming (Inaba et al., 1990) (Stoll et al., 2002). If the T cell receptor specifically recognises the peptide, the T cell can be primed. Primed T cells subsequently migrate to the T cell zone – B cell follicle (T-B) border by reducing their expression of CCR7 (required for TZ localisation) and increasing their expression of CXCR5 (required for follicular localisation (Hardtke et al., 2005)). Once arrived at the T-B border, T cells can interact with activated B cells and provide costimulatory signals required to fully activate the B cells.

1.4.3 The follicle

The TZ is partially surrounded by follicles; areas which are mainly made up of follicular B cells, as well as follicular DCs (FDCs) (Tew et al., 1997). B cells recirculate throughout follicles of secondary lymphoid organs in search of foreign antigen (Nieuwenhuis and Ford, 1976). Upon thymus dependent (TD) B cell activation (and in some instances thymus independent (TI) activation (de Vinuesa et al., 2000)), B cells can differentiate into germinal centre (GC) B cells, with GCs forming within the follicle.

1.5 A brief introduction to mature B cell subsets

There are two subtypes of B cells, namely B1 and B2. Upon activation, other B cell subsets arise; GC B cells, antibody producing cells (plasmablasts and plasma cells) and memory B cells. A brief overview of B1 and B2 cells is described here, with differentiation upon activation discussed later.

The differentiation of B cells into either B1 or B2 cells has been extensively studied for many years. In a study 15 years ago, Lam and Rajewsky showed that B1 and B2 cell fate in mouse B cells can be manipulated by altering the heavy chain variable region; suggesting that B cell receptor (BCR) specificity can determine B cell fate (Lam and Rajewsky, 1999). As well as BCR specificity, BCR signalling has also been hypothesised to induce either B1 or B2 phenotypes; mice deficient in BCR signalling molecules have reduced B1 cell populations (reviewed in (Berland and Wortis, 2002)).

1.5.1 B1 cells

B1 cells, originally designated Ly-1 B cells, are the predominant B cell subset detected within the peritoneal cavity. These cells mainly develop in the foetal liver, (Hayakawa et al., 1985) and although the adult spleen and bone marrow were originally shown to be unable to reconstitute B1 cells (Hayakawa et al., 1985), more recent studies have detected precursors in the spleen that are able to replenish B1 cells (Rosado et al., 2009).

B1 cells can be further subdivided by their expression of CD5; B1a $CD5^+$ cells, and B1b $CD5^-$. Peritoneal cavity B1a and B1b cells can also be distinguished by CD11b expression, with $CD11b^-$ B1 cells able to reconstitute both $CD11b^-$ and $CD11b^+$ B1 cells, yet $CD11b^+$ cells can only reconstitute themselves (Ghosn et al., 2008).

B1a B cells are able to constitutively produce vast amounts of "natural antibody" (Baumgarth et al., 1999), which is antibody present in unimmunised and germ-free mice, under steady state conditions. B1b cells are activated upon antigen administration, with long lasting antibody production occurring from activated B1b cells in response to the thymus independent antigen 4-hydroxy-3-nitrophenylacetyl (NP)-Ficoll (Hsu et al., 2006). As well as NP-Ficoll, B1b cells have also been shown to play an important role in the response to *Borrelia hermsii* (Alugupalli et al., 2004) and to systemic *Salmonella* infection (Gil-Cruz et al., 2009, Marshall et al., 2012).

1.5.2 B2 cells

B2 cells constitute the major B cell population of the spleen. B2 cells are split by phenotype and anatomical location into MZ and follicular B cell subsets.

1.5.2.1 Marginal zone B cells

Marginal zone B cells are the first line of defence against blood-borne pathogens. As stated previously, the MZ lies between the marginal sinus and the red pulp, allowing near instant access of MZ cells to blood flowing into the spleen. Immature DCs capture and transport antigen to the spleen and present it to MZ B cells (Balazs et al., 2002). These DCs then provide survival signals to MZ B cells and promote their differentiation into plasmablasts (Balazs et al., 2002). Interestingly, MZ B cells are not fully confined to the MZ, and are able to shuttle between the MZ and follicular areas (Cinamon et al., 2008).

MZ B cells can be activated to induce early antibody responses to both TD and TI antigens (Martin et al., 2001, Song and Cerny, 2003) and are also able to contribute to the GC response (Song and Cerny, 2003).

1.5.2.2 Follicular B cells

Follicular B cells are the largest B cell population in adult mice. These cells are phenotypically distinguishable from MZ B cells due to their expression of Krüppel-like factor 2 (KLF2), which prevents expression of MZ factors (Winkelmann et al., 2011). Follicular B cells are constantly migrating between the follicles of secondary lymphoid organs surveying for foreign antigen. Follicular B cells respond to TD antigen, and take part in both extrafollicular and GC responses. Follicular B cells, however, are unable to respond to TI type II (TI-II) antigens (Lane et al., 1986).

Direct visualisation of antigen encounter by follicular B cells has been observed using two-photon microscopy, where B cells associated with antigen-loaded FDCs (Suzuki et al., 2009). Antigen is located on FDCs for more than 1 week post immunisation, allowing rare follicular B cells an opportunity to detect the antigens (Suzuki et al., 2009).

1.6 B cell activation

The mounting of a successful humoral response against foreign antigens requires B cell activation. Upon activation, B cells can differentiate into antibody secreting plasma cells, GC cells or memory cells. As already alluded to, B cell activation can be broadly split into two types; thymus dependent, and thymus independent.

1.6.1 Thymus dependent responses

As would be expected by the name, TD B cell activation involves the collaboration of B and T cells. TD B cell activation is specifically confined to protein antigens. Two signals are required for full B cell activation. The first is recognition of antigen by the B cells, which enables the B cells to take up the protein and display component peptides via

major histocompatibility complex (MHC) on the cell surface. Upon activation, B cells migrate to the T-B border, with antigen-specific B cells detectable in the outer T zone by 4 hours post immunisation (Sze et al., 2000, Okada et al., 2005, Zhang, 2010, Marshall, 2009) (figure 1.2). T cells of the TZ provide the second, costimulatory signals which fully activate the B cells. The requirement for T cell priming before full B cell activation causes a delayed B cell response, as sufficiently primed T cells are only available three days post immunisation (Toellner et al., 1998), with B cell proliferation and GC formation not evident until day 5 (Toellner et al., 1998).

Immunoglobulin (Ig) switching in the TD response is dependent on the antigen and on the type of T cell response this antigen induced during T cell priming. For example, immunisation with the haptenated protein NP-CGG (4-hydroxy-3-nitrophenylacetyl-chicken γ globulin) causes T cells to produce Th2 type cytokines and B cells to switch to IgG1, yet immunisation with Swiss type mouse mammary tumour virus is associated with Th1 priming and IgG2a production (Toellner et al., 1998).

1.6.1.1 The germinal centre

Germinal centres were defined by I.C.M. MacLennan as structures which "develop in the B cell follicles of secondary lymphoid tissues… where B cells undergo massive clonal expansion and activate a site-directed hypermutation mechanism on Ig-variable region genes" (MacLennan, 1994). Thus, during a GC response the affinity of antibody to antigen increases. GCs are made up of distinct areas and zones which aid this process, with B cell migration between the zones being required for optimal mutation and affinity maturation (Bannard et al., 2013). The dark zone (DZ) contains large B cells known as

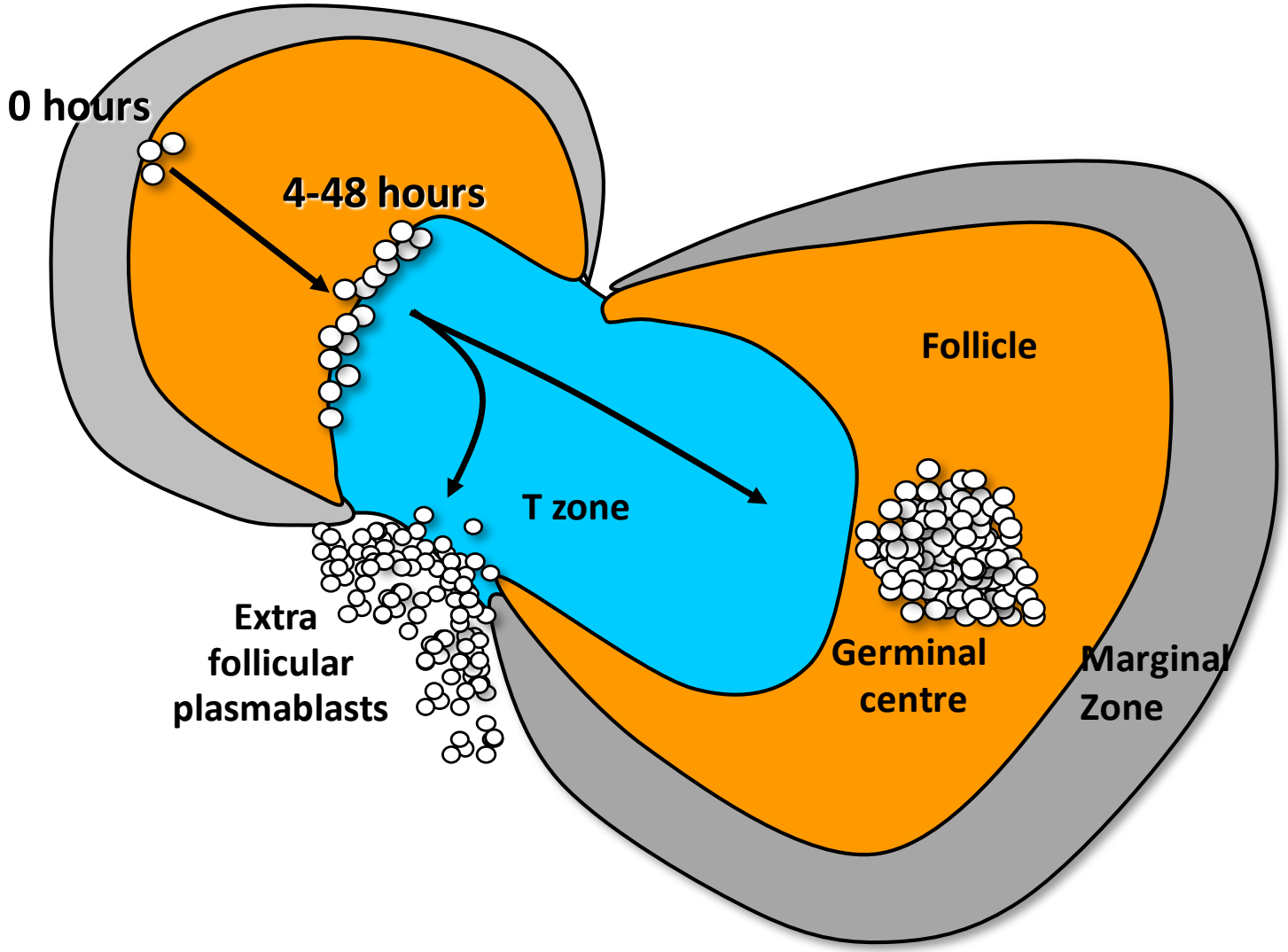

Figure 1.2. B cell migration post antigen encounter. Upon antigen encounter, antigen-specific B cells migrate to the T-B border within a few hours. Here, they undergo rounds of proliferation, before either differentiating into plasmablasts and exiting the white pulp via bridging channels, or re-entering the follicle and differentiating into germinal centre B cells to undergo further rounds of mutation and proliferation. For references, see text.
Picture kindly provided by Dr. J. Marshall

centroblasts, which rapidly proliferate. While proliferating, these centroblasts undergo somatic hypermutation of the immuglobulin heavy and light chain variable region (Zubler, 2001). Somatic hypermutation occurs by single nucleotide changes or microdeletions (Berek et al., 1991) which causes either enhanced or reduced affinity for the receptor to antigen.

Within the light zone (LZ) are smaller centrocytes that appear to be less proliferative, derived from the larger centroblasts (Allen et al., 2007, Gitlin et al., 2014, Bannard et al., 2013). The LZ can itself be split into two areas; the inner LZ which contains FDCs and the T helper cell-rich outer LZ (MacLennan, 1994). These smaller centrocytes compete to bind antigen which is presented on the surface of FDCs (Allen et al., 2007), with high affinity B cells out-competing those of a lower affinity and so enabling their survival. Recent data from our laboratory has shown that secreted IgM can enter the GC and bind FDCs; therefore limiting antigen access over the course of the GC response. This enables selection of increasingly higher affinity GC B cells (Zhang et al., 2013). The remaining B cells die via apoptosis due to lack of stimulation from the B cell receptor-antigen complex or because they were unable to interact with T cells (Shih et al., 2002, Shokat and Goodnow, 1995). If B cells are unable to displace high affinity antibody bound to antigen on FDCs, the GC reaction terminates (Zhang et al., 2013). Successfully selected B cells can differentiate into plasma or memory cells in the LZ (MacLennan, 1994). The GC response, including somatic hypermutation and class switch recombination, is discussed further in chapter 4.

1.6.1.2 Plasmablasts and plasma cells

Antibody secreting cells include plasmablasts and both short- and long-lived plasma cells. Unlike terminally differentiated plasma cells, plasmablasts are still highly proliferative and secrete antibody at lower levels. Studies in spleens have shown individual plasmablasts typically divide five times before differentiating into plasma cells (Sze et al., 2000). Plasmablasts and plasma cells differentially express at least 800 genes (Tarte et al., 2003), showing a surprisingly large difference between the two populations.

Differentiation into plasmablasts can occur directly after activation outside the follicular environment, preceding the follicular GC response and producing rapid, low affinity antibody (figure 1.2). GCs also produce plasma cells that may have undergone affinity maturation. The master regulator of plasma cell differentiation is BLIMP-1, a transcriptional repressor. Without BLIMP-1, short lived, GC-derived and memory response derived plasma cells are absent in the mouse (Shapiro-Shelef et al., 2003). A full analysis of the role of BLIMP-1 in plasmablast fate is discussed in chapter 3.

During a TD response, extrafollicular plasmablasts gradually proliferate and therefore increase, peaking at 96 hours post immunisation (Sze et al., 2000). Extrafollicular plasmablasts are located primarily at the junction of the TZ and red pulp (Sze et al., 2000) (figure 1.2). Plasma cell numbers reduce by day 7 post immunisation, and remain at the same low levels in the red pulp at three weeks (Sze et al., 2000).

1.6.2 Thymus independent responses

Non-protein antigens, such as polysaccharides, glycolipids and nucleic acids, cannot be processed by the B cell and presented in the context of MHC molecules. Therefore B cell

activation by these antigens does not occur with the aid of T cell help. Nude mice, which lack a thymus, are able to induce B cell immune responses to these antigens, giving them the title "thymus-independent". They are split into two types: TI-I and TI-II, depending on whether the response can occur in CBA/N mice. CBA/N mice are deficient in the kinase Btk, found downstream in the BCR signalling pathway. TI-I antigens are able to bypass downstream BCR signalling, and therefore CBA/N mice are able to mount a response to TI-I antigens (Mosier et al., 1976). However, TI-II antigens, which require BCR and therefore Btk signalling, are not able to induce a B cell response in CBA/N mice (Mosier et al., 1977), reviewed in (Vinuesa and Chang, 2013).

Like in TD responses, TI B cell activation can lead to class switching in the absence of T cell derived signals (Marshall et al., 2011). Importantly, TI activation can induce memory B cell formation (Obukhanych and Nussenzweig, 2006) as well as long lived plasma cells which reside in the bone marrow (Taillardet et al., 2009, Bortnick et al., 2012). In mice where the majority of B cells are specific for a single TI antigen, GCs can be formed in the absence of T cells, however these GCs disappear synchronously at day 5 post immunisation due to the lack of T follicular helper cell signals required to sustain them (de Vinuesa et al., 2000).

1.6.2.1 Thymus independent type I responses

Thymus independent type I antigens can activate B cells by signalling through Toll-like receptors (TLRs). These antigens are common microbial constituents, for example viral RNA, lipopeptides and LPS. LPS binds to CD14 on the B cells, which associates with TLR-4; signalling through both receptors causes an upregulation in CD69, CD79a phosphorylation and calcium mobilisation (Minguet et al., 2008, Pone et al., 2012) leading to B cell

activation. TI immunoglobulin class switching can occur; in this instance activation induced cytidine deaminase (AID), the protein responsible for somatic hypermutation and class switch recombination, is induced through NFκB signalling. IgG1 secretion is enhanced by LPS-activated B cells due to cross talk between TLR4 and Dectin-1 (Pone et al., 2012, Seo et al., 2013). For more information on AID, see chapter 4.

1.6.2.2 Thymus independent type II responses

TI-II antigens are multivalent, enabling cross linking of multiple BCRs, which transmit activating signals to the B cell (reviewed in (Mond et al., 1995)). MZ B cells are highly reactive to TI-II antigens. A full response to TI-II antigens does not occur until the age of 5 years, with no response detected until several months after birth (Murray and Lopez, 1997). TI-II antigens are found in the capsules of *Neisseria meningitides*, *Streptococcus pneumonia, Haemophilus influenza* type b and *Salmonella*. These organisms are associated with a high risk of death in children between 6 months and 5 years of age (Murray and Lopez, 1997), correlating with a reduced response to TI-II antigens in children.

In mice, 4 hours after immunisation with TI-II antigen, B cells have migrated from the MZ of the spleen to the T-B border (Lopes-Carvalho and Kearney, 2004). By 8 hours, the activated B cells are rapidly dividing, and by 3 days post immunisation clusters of plasma cells are formed in the red pulp (Liu et al., 1991, Lopes-Carvalho and Kearney, 2004). As previously stated, TI antigens can induce class switching, with plasma cells produced in a TI-II response preferably switching to IgG3 (Garcia de Vinuesa et al., 1999b). B blasts of mice immunised with the TI-II antigen NP-Ficoll express *Aicda*, the AID producing mRNA,

which is downregulated upon plasmablast differentiation (Marshall et al., 2011). Class switching in TI-II responses is dose-dependent (de Vinuesa et al., 2000); with higher amounts of antigen inducing *Aicda* expression (Marshall et al., 2011).

TI-II responses have previously been shown to induce the formation of GCs (de Vinuesa et al., 2000); a process which was originally thought to only be induced by TD antigens. Confirming the TD dependence, TI-II induced GCs spontaneously involute 5 days post immunisation; probably due to the lack of T follicular helper (Tfh) cell help (de Vinuesa et al., 2000). Supporting this, immunisation of CCR7-deficient mice with NP-Ficoll results in long-lived GCs, probably due to the presence of T cells within these GCs (Achtman et al., 2009).

1.6.3 Newly defined modes of B cell activation

A recent review by Vinuesa and Chang has suggested updated classification of antibody responses, with two new groups defined: TD-II and TI-III (Vinuesa and Chang, 2013). The antibody responses from these two groups are driven by innate cells; thymus-derived invariant NKT (iNKT) cells for the TD-II response, and B cell helper neutrophils for TI-III (Vinuesa and Chang, 2013). B cell activation by iNKT cells and B helper neutrophils are beyond the scope of this study, and will not be discussed further here.

1.7 Control of splenic B cell localisation

The positioning of B cells within the splenic white pulp during responses is controlled by the expression of receptors on the cell surface. These bind specifically located ligands and subsequently cause an attraction to (or repulsion from) that area. The control of B cell positioning within the spleen is summarised here and within figure 1.3.

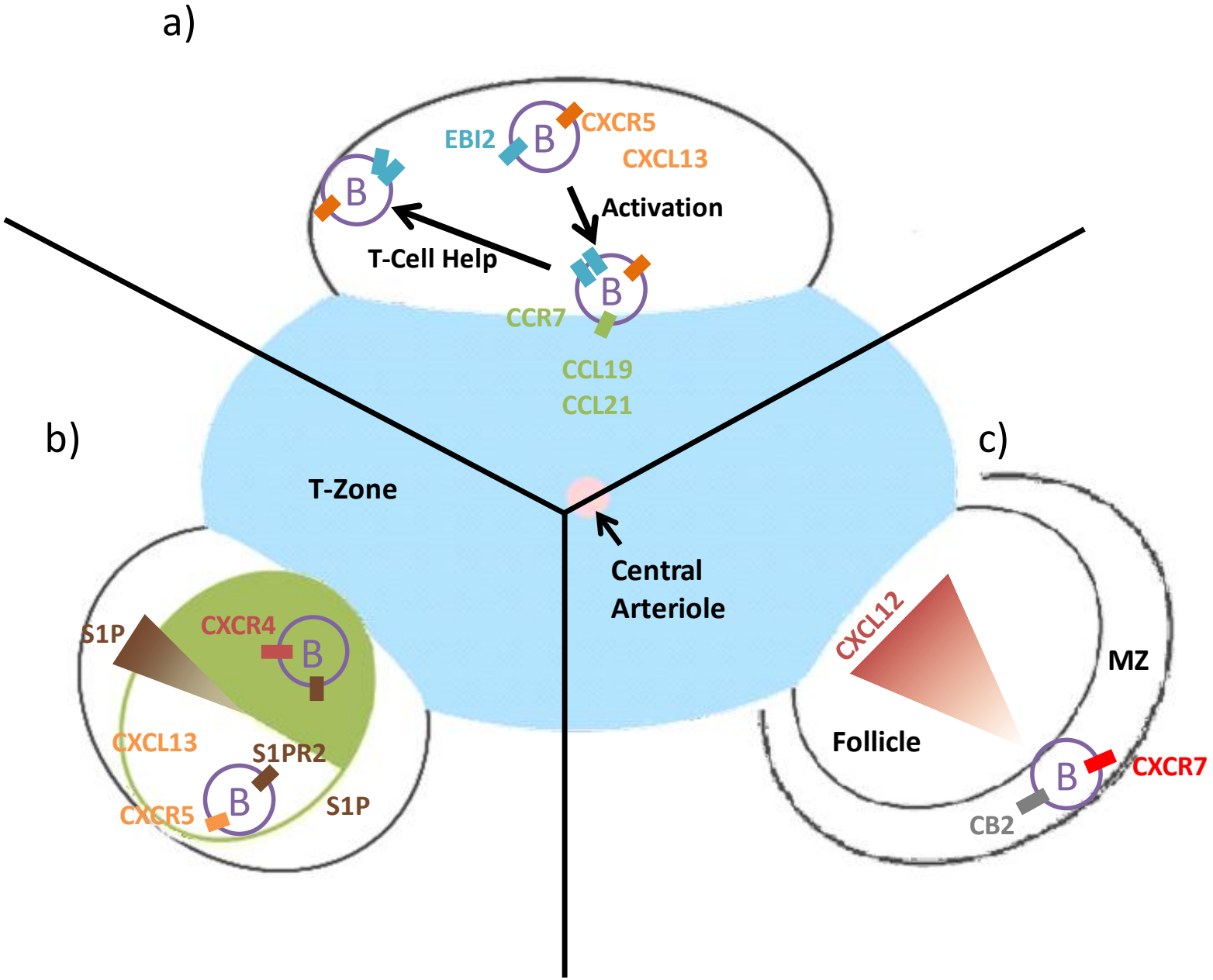

Figure 1.3.
Expression of ligand-receptor pairs involved in B cell migration.
a) follicular homing and early activation; b) GC organisation; c) MZ positioning. For references, see text. Receptors and their ligands are displayed with the same colour.
Triangles indicate a ligand concentration gradient.

1.7.1 Steady state homing of B cells

Naïve B cells express low levels of the chemokine receptor CCR7, and, along with $CCR7^{hi}$ T cells, use this receptor to enter lymphoid tissues; a process that is severely disrupted in CCR7 deficient mice (Forster et al., 1999). Upon splenic entry, B cells are guided to the follicle by expression of the chemokine receptor CXCR5, which binds the chemokine CXCL13**.** CXCL13 is expressed within the B cell follicles by stromal cells (Green and Cyster, 2012) causing B cells home to the follicular area. Conversely, T cells are guided to the TZ through their high expression of CCR7, whose ligands CCL19 and CCL21 are expressed at high levels in the TZ (Forster et al., 1999, Gunn et al., 1999).

B cells localise to the MZ due to their expression of sphingosine-1-phosphate receptor 1 (S1PR1), the GPCR cannabinoid receptor 2 (CB2) and their lack of Krüppel-like factor 2 (KLF2) expression (Muppidi et al., 2011, Winkelmann et al., 2011, Cinamon et al., 2004). This may seem surprising, as in T cells S1PR1 is downregulated without KLF2, showing differential regulatory pathways between the two lymphocyte subsets (Winkelmann et al., 2011). Interestingly, over-expression of CB2 localises B cells to the MZ, yet overexpression of S1PR1 distributes B cells throughout the red pulp (Muppidi et al., 2011). A recent paper by Wang *et al. h*as suggested that MZ B cells can also be defined by their expression of ACKR3 (Wang et al., 2012), an atypical chemokine receptor which binds the CXCR4 ligand, CXCL12. The authors proposed that internalisation of CXCL12 by ACKR3-expressing MZ B cells causes a gradient of the chemokine along the B cell follicle (Wang et al., 2012); a higher concentration of CXCL12 close to the TZ, to which centroblasts are attracted during the GC response, and a lower concentration at the outer follicle (Wang et al., 2012).

MZ B cells are not confined to the MZ, and are able to shuttle between MZ and follicular areas (Cinamon et al., 2008). Unsurprisingly, migration into the follicle by MZ B cells requires expression of CXCR5, whilst migration back to the MZ required S1PR1 and S1PR3 (Cinamon et al., 2008).

1.7.2 B cell migration post activation

Homing of B cells to the correct niche allows access to antigen via FDC processes and subsequent activation. By 6 hours post activation, B cells migrate to the T-B border due to an upregulation in the expression of CCR7, yet their expression of CXCR5 remains constant (Reif et al., 2002). Although CXCR5 deficient B cells do not enter B cell follicles, they do migrate to the T-B border upon activation (Reif et al., 2002), showing that CXCR5 is not required for this initial migration. However, distribution along the T-B border does require CXCR5; $CXCR5^{-/-}$ activated B cells cluster at bridging zones (Reif et al., 2002). Migration to the T-B border enables B cells to interact with activated T cells that have also migrated to this area, which provide constimulatory signals to allow full B cell activation and differentiation into either GC B cells or plasmablasts. Yet this migration is also observed upon B cell activation as part of a TI response (Garcia de Vinuesa et al., 1999b, Vinuesa et al., 2001), indicating this process is an intrinsic B cell response to activation.

Epstein-Barr virus-induced GPCR 2 (EBI2) is also upregulated upon B cell activation and prevents the CCR7 expressing B cells from fully entering the TZ; activated EBI2 deficient cells are found within the TZ (Pereira et al., 2009, Glynne et al., 2000, Gatto et al., 2009).

1.7.3 Plasmablast and plasma cell migration

Interestingly, after migration to the T-B border, EBI2 causes B cell migration around the follicular perimeter (Gatto et al., 2009). It is proposed that migration to this microenvironment is essential for plasmablast differentiation and survival (Gatto et al., 2009). Once differentiated into antibody secreting cells, B cells can migrate to the bone marrow where they can survive for long periods of time. Antibody secreting cells of the bone marrow express CXCR4 and are highly attracted to its ligand CXCL12 (Hauser et al., 2002). These cells do not respond to CXCL13 (Hauser et al., 2002), the chemokine that enables their location to B cell follicles. Interestingly, a proportion of these cells also migrate towards the CXCR3 ligand CXCL9 (Hauser et al., 2002). CXCR3 can be upregulated on antibody secreting cells through signalling by interferon (IFN)-γ and the transcription factor T-box expressed in T cells (T-bet) (Serre et al., 2012), with CXCR3 expression allowing recruitment of cells to sites of infection (Rosas et al., 2005). Mice unable to express CXCR3 are unable to control *Leishmania major* infection (Rosas et al., 2005), showing the importance of this chemokine receptor in the recruitment of cells to the site of infection during an immune response.

1.7.4 Germinal centre formation, orientation and migration

Post activation, some B cells migrate back to the centre of the follicle in order to form GCs. Interestingly, GCs of CCR7 deficient mice are located within the T cell depleted PALS (Achtman et al., 2009). However, as CCR7 is required for the positioning of multiple cell types under steady state conditions (Forster et al., 1999), the exact cause of GC positioning in the model is unclear. To re-enter the follicle, EBI2 expression is reduced (Pereira et al., 2009, Gatto et al., 2009), which is unsurprising as EBI2$^{-/-}$ B cells transferred

into WT hosts are observed within the follicle, co-localising with FDCs (Gatto et al., 2009). Reduction in EBI2 is probably B cell lymphoma (Bcl)-6 dependent; a thorough computational and ChIP-on-chip analysis implicated the promoter region of EBI2 as a Bcl6 target in GC B cells (Basso et al., 2010).

The GCs themselves are organised into distinct areas and zones. In 2004, Allen *et al*. showed that the light and dark zone organisation of a GC is mainly controlled by the two chemokine receptors CXCR4 and CXCR5, and their ligands (Allen et al., 2004). CXCR4 expression on centroblasts attracts these cells to the DZ, due to the expression of CXCL12 by reticular cells in this area of the GC (Allen et al., 2004, Bannard et al., 2013). Interestingly, $Aicda^{-/-}$ (AID deficient) GC B cells express lower levels of CXCR4 and so accumulate as centrocytes within the GC (Boulianne et al., 2013). The expression of CXCR4 on B cells also enables them to regulate the position of FDCs and CXCL13; there is no FDC and CXCL13 polarity when $CXCR4^{-/-}$ B cells are transferred into B cell deficient mice (Allen et al., 2004). Over the course of the GC response, LZ restricted $CXCR4^{-/-}$ GC B cells are gradually outcompeted by WT cells, showing DZ access is essential for optimal GC B cell responses (Bannard et al., 2013). Using GFP-fusion, GC B cells have also been shown to express Regulator of G protein Signalling (RGS) 13 (Shi et al., 2002). RGS13 is able to reduce the responsiveness of CXCR4-transfected cells to CXCL12 (Shi et al., 2002), and so may have a role in regulating GC B cell migration between dark and light zones.

On the other hand, CXCR5 attracts B cells to the LZ. In the spleen, the LZ of the GC is always next to the marginal sinus, where blood-borne antigens enter. CXCR5 and its ligand dictate this orientation of the GC; $CXCL13^{-/-}$ mice have a GC with FDCs located in

the centre, surrounded by a ring of centroblasts (Allen et al., 2004). In addition to CXCR4 and CXCR5, both centroblasts and centrocytes express the GPCR S1PR2 which binds the sphingolipid sphingosine-1-phosphate (S1P) (Green et al., 2011). This interaction is required for the retention of GC B cells within the GC; interestingly, S1PR2 has since been detected in Tfhs and also retains these cells within the GC (Moriyama et al., 2014). GC retention is caused by stromal cells outside of the follicle producing S1P, which degrades as it travels through the follicle, causing a gradient of S1P to the follicular centre (Green et al., 2011). Binding of S1P via S1PR2 prompts turning and migration, therefore providing a GC association for the S1PR2 expressing cells (Green et al., 2011). It should be noted, however, that S1PR2 deficient GC B cells are not able to colonise the whole follicle (Green et al., 2011), and so other signals must also dictate GC B cell association with the GC. One such signal is CXCL13, as a double KO of S1PR2 and CXCL13 increases GC B cell dispersion (Green et al., 2011). Tfh cells deficient in both CXCR5 and S1PR2 are unable to support GC responses (Moriyama et al., 2014).

1.8 The role of CCRL2 on B cells

CCRL2 was shown to be expressed on most human hematopoietic cells, but was not initially detected on B cells (Migeotte et al., 2002). However, B cell expression was later shown to be maturation stage dependent (Hartmann et al., 2008). In the latter study, CCRL2 was originally found to be expressed on the pre-B acute lymphoblastoid leukaemia cell line Nalm6, and this was confirmed with a similar cell line, G2. Furthermore, CCRL2 expression on B cell subsets from adult bone marrow showed expression on subpopulations of pro- and mature- B cells, and all pre-B cells; however no CCRL2 was detectable on immature B cells (Hartmann et al., 2008). Upon challenge of WT and

CCRL2 deficient mice with OVA, there was no difference in IgE production (Otero et al., 2010). However, no study has yet explored the role of CCRL2 in B cell migration, nor plasmablast and GC responses in depth.

1.9 Aims of project

The purpose of this project is to assess the role of the atypical chemoattractant receptor CCRL2 in the B cell response. For this purpose, CCRL2 deficient mice are immunised with a variety of antigens and the response assessed; cellular location determined by immunohistology, plasma cell and GC cell levels assessed by both flow cytometry and immunohistochemistry and antibody output determined by enzyme-linked immunosorbent assay (ELISA).

Chapter 2. Materials and Methods

2.1 Mice

All mice used in this study were housed in specific pathogen free conditions at the Biomedical Services Unit (BMSU) at University of Birmingham, UK and treated in accordance to guidelines set out by The Home Office. The Mouse Genome Informatics (MGI) accession number for each mouse strain used in this study is summarised in table 2.1.

Strain	MGI Accession Number(s)	
QM	MGI:3045610	MGI:1857188
$CCRL2^{-/-}$	MGI:3604544	
$ACKR4^{-/-}$	MGI:2449041	MGI:4847614
$CCR7^{-/-}$	MGI:2180679	

Table 2.1. MGI Accession Numbers for all Genetically Modified Mouse Strains used in this Study.

C57BL/6 mice were either purchased from Harlan Laboratories or bred within BMSU from CCRL2 heterozygous ($CCRL2^{+/-}$) parents. These mice were used as wild type (WT) controls in experiments involving CCRL2 knock out ($CCRL2^{-/-}$) mice. They express the CD45.2 variant of the CD45 allele.

BoyJ (B6.SJL-Ptprc^{a}Pepc^{b}/BoyJ) mice were purchased from BMSU, University of Birmingham, UK or Charles River Laboratories. These WT mice express the CD45.1 variant of the CD45 allele and were used in the generation of bone marrow chimeras or in adoptive transfer experiments.

Quasi-monoclonal (QM) mice are B cell receptor knock in mice, in which approximately 60% of the mouse B cells are specific for the hapten 4-hydroxy-3-nitrophenyl (NP). This mouse was developed by Wabl *et al* (Cascalho et al., 1996) and is summarised here. The mouse heavy chain was rearranged to V_HDJ_H 17.2.25 (for NP-specificity), and these mice crossed with mice unable to express Ig heavy and κ light chains, as antibodies against NP are mainly formed of a λ light chain. QM mice were bred with mice deficient in CCR7, ACKR4 and CCRL2 to generate NP-specific B cells deficient in these receptors. QM mice are on a C57BL/6 background, and so express the CD45.2 variant of the CD45 allele.

CCRL2$^{-/-}$ mice (strain B6.129-*Ccrl2*^{tm1Dgen}/J) were purchased from The Jackson Laboratory, ME, USA. These mice were used to study to effect of removing CCRL2 on the B cell response. CCRL2$^{-/-}$ mice are on a C57BL/6 background, and so express the CD45.2 variant of the CD45 allele.

ACKR4$^{-/-}$ mice were a gift from R. Nibbs (University of Glasgow), generated as described in (Comerford et al., 2010). These mice were used as control mice in experiments involving CCL19 uptake and binding by cells.

CCR7$^{-/-}$ mice (stain B6.129P2(c)-Ccr7^{tm1Rfor}/J) were purchased from The Jackson Laboratory, ME, USA. These mice were used as control mice in experiments involving CCL19 uptake and binding by cells.

2.2 Immunisations and injections

2.2.1 Thymus dependent antigens

For the primary response, NP was conjugated to chicken gamma globulin (CGG, Sigma) by Mrs. Chandra Raykundalia, Division of Immunity and Infection, University of Birmingham to form NP-CGG. Before injection, NP-CGG was prepared by alum precipitation (mixing with 9% aluminium potassium sulphate and adjusting pH to 6.5) and kept agitated in the dark for 1hr. After centrifugation (5min, 2000rpm), NP-CGG was washed twice in Phosphate Buffered Saline (PBS). For splenic responses, NP-CGG was resuspended in PBS to a value of 50µg/200µl per mouse with 10^7 *Bordetella pertussis* (Dako), and injected intraperitoneally (*i.p.*). For the lymph node response, NP-CGG was resuspended in PBS to 20µg/20µl per mouse with 10^7 *Bordetella pertussis*, and injected in the footpad.

To initiate a memory response, mice were primed *i.p.* with 50µg of alum precipitated CGG (Jackson Immuno Research, West Gove, PA, USA) in 200µl PBS with 10^7 *Bordetella pertussis*. Five weeks later, a boost injection *i.p.* of NP-CGG (50µg in 200µl PBS) was administered.

2.2.2 Thymus independent antigens

Trinitrophenyl-lipopolysaccharide (TNP-LPS, Sigma) is a thymus independent type I (TI-I) antigen. It was dissolved in PBS at 30µg/200µl per mouse and injected *i.p.*

NP-Ficoll (Biosearch Technologies, Novato, CA) is a thymus independent type II (TI-II) antigen. It was dissolved in PBS at 30µg/200µl per mouse and injected *i.p* or intravenally (*i.v.*). A fluorescent version, NP-FITC-Ficoll (Biosearch Technologies), is prepared and injected by the same protocol.

2.2.3 Infection model, Salmonella Typhimurium

To assess the role of CCRL2 upon B cell activation as part of a response to an infection, a model of Salmonella infection was used. Mice underwent primary infection with a non-virulent Salmonella Typhimurium (STm) strain, SL3261 (Hoiseth and Stocker, 1981). STm was prepared by overnight growth of a single bacterial colony in sterile LB medium at 37°C. Bacteria were harvested by centrifugation at 6000g for 5mins once optical density (OD) at 600nm measured 0.8-1.0, as this indicated the mid-exponential growth phase. STm were washed twice in 1ml sterile PBS before being resuspended in PBS. The OD was measured at 600nm and the number of bacteria/ml was assessed using a standard growth curve. STm were then diluted in sterile PBS to $5x10^5$ bacteria/200µl/mouse and administered *i.p.*

2.2.4 EdU injections

EdU (5-Ethynyl-2'-deoxyuridine) (Molecular Probes by Life Technologies) was dissolved in sterile PBS to a concentration of 0.5mg/200µl/mouse and injected *i.p.* 2 hours prior to culling.

2.3 Bone marrow chimeras

Isolated bone marrow cells (section 2.5.4) were counted using a haemocytometer and resuspended in PBS to a final concentration of $1.5x10^7$cells/ml.

Recipient mice had two doses of irradiation at 4.5G, before *i.v.* injection of 200µl of the donor cell suspension ($3x10^6$cells/mouse). Success of transfer was determined by tail bleed and flow cytometry (see sections 2.5.1 and 2.10) 42 days post cell transfer. Mice

were immunised with NP-Ficoll (as described in section 2.2.2) 65 days post cell transfer (figure 2.1).

2.4 Adoptive cell transfer

2.4.1 Thymus dependent responses

BoyJ mice were primed with 50µg CGG as described in section 2.2.1. Five weeks later, splenocytes from QM mice were prepared (section 2.5.3) and B cells were enriched by magnetic-activated cell sorting (MACS, Miltenyi Biotec) using CD43 (Ly48) Microbeads or B cell isolation cocktail (Miltenyi Biotec) as per the manufacturer's protocol. Cells were counted, and their purity was verified using flow cytometry (section 2.10). Cells were diluted to $5x10^4$ NP-binding cells/mouse in 200µl PBS and injected *i.v.* into BoyJ hosts. Host mice were immunised one day later with NP-CGG (50µg/mouse in 200µl PBS) *i.p.*

2.4.2 Thymus independent responses

Splenocytes from QM mice were prepared, sorted and purity confirmed as described in section 2.4.1. Cells were diluted to $5x10^5$ NP-binding cells/mouse in 200µl PBS and injected *i.v.* into either BoyJ or C57BL/6 hosts. Host mice were immunised one day later with NP-Ficoll (section 2.2.2)

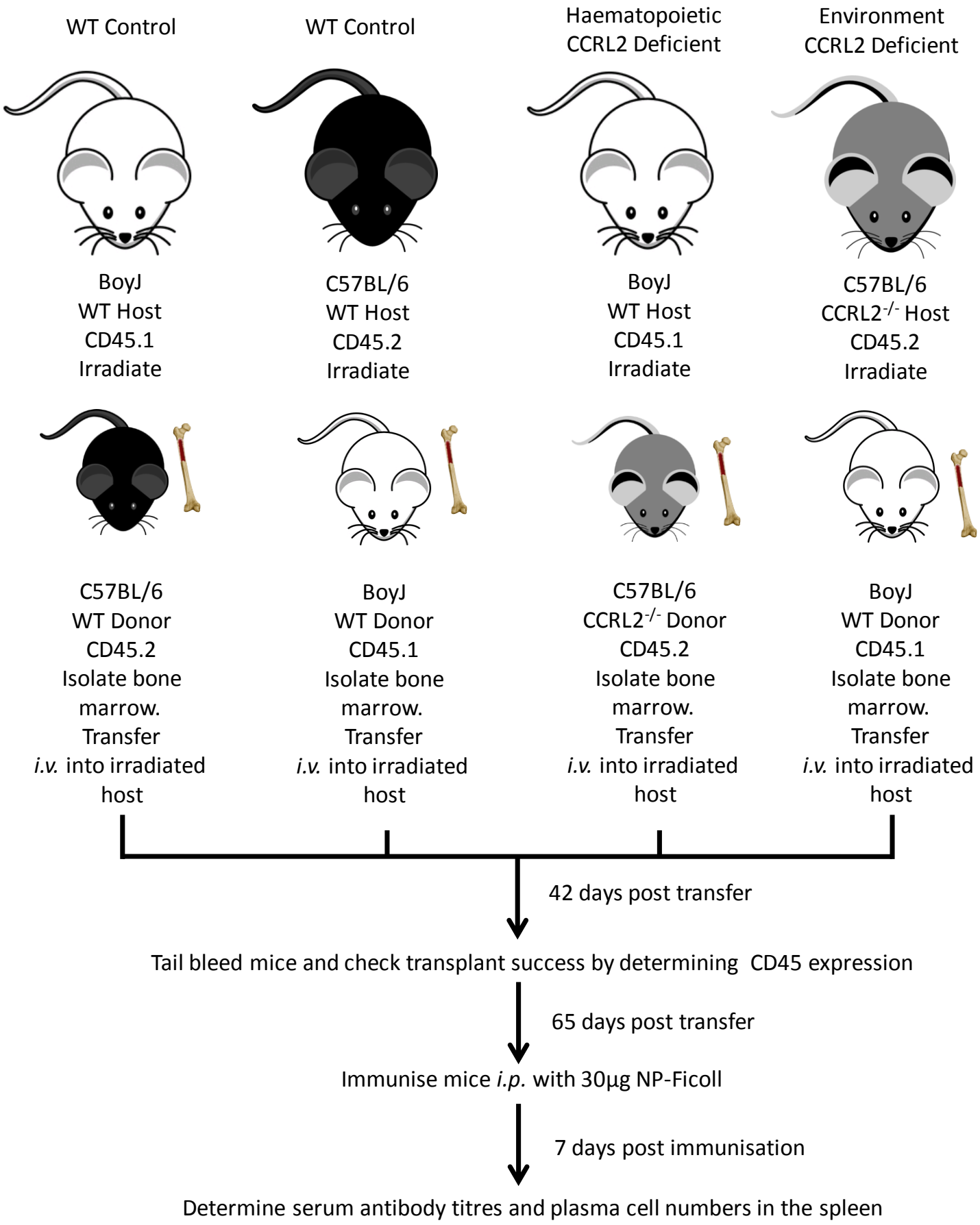

Figure 2.1. Bone marrow chimera protocol

2.5 Sample preparation

2.5.1 Blood

For flow cytometry blood was collected in Ethylenediaminetetraacetic acid (EDTA) and transferred to a 96-well plate. The blood was repeatedly incubated for 1min with 100µl of ACK Lysing Buffer (Gibco Invitrogen Compounds) to lyse red blood cells and stained for specific markers for flow cytometry analysis (section 2.10).

For serum isolation, blood was collected and incubated at 37°C for at least 2 hours to enable clotting. The blood was then spun at 10 000rpm, 10mins and serum (supernatant) was taken.

2.5.2 Peritoneal cell harvest

Peritoneal cells were collected by injection of 5ml of ice cold PBS into the peritoneal cavity. This was then re-collected and stored on ice. The cell suspension was spun (1400rpm, 4mins) and transferred into a 96-well plate. If required, cells were red cell lysed and stained for specific markers for flow cytometry analysis (section 2.10).

2.5.3 Spleen

Spleens were disrupted by mashing through a cell strainer (BD Biosciences, NJ, USA) and cells were collected into complete media (RPMI 1640 media supplemented with 10% fetal calf serum [FCS] and 1% penicillin and streptomycin [penicillin 10000units/ml and streptomycin 10000µg/ml in PBS], all from Invitrogen). If required, splenocytes were red cell lysed and then cells counted using a haemocytometer. Cells were subsequently stained for specific markers for either fluorescent activated cell sorting (FACS), flow cytometry analyses, or B cells enriched for *in vitro* cell culture or adoptive transfer

(sections 2.11, 2.10, 2.6 and 2.4 respectively). For immunohistology (section 2.7), spleens were snap frozen in liquid nitrogen or on dry ice and stored at -80°C.

2.5.4 Bone marrow

Bone marrow cells were isolated in PBS and put through a cell strainer. Red cells were lysed by multiple incubations in ACK Lysing Buffer (Gibco Invitrogen Compounds).

2.6 *In vitro* culture and stimulation

2.6.1 Culture of non-QM B cells

Spleens of unimmunised mice were prepared and enriched for B cells as described in section 2.5.3. To determine proliferation of cells over time, cells were labelled with CellTrace™ Violet Cell Proliferation Kit (Invitrogen) as per the manufacturers' instructions. B cells were seeded in triplicate into sterile 96 well plates at $1x10^5$ cells/well and grown in complete media (section 2.5.3) supplemented with HEPES (10mM), 2-mercaptoethanol (50µM) and sodium pyruvate (1mM) (all from Sigma-Aldrich). Cells were stimulated with carrier free IL-4 (6.25ng/ml, R&D Systems) and LPS (12.5µg/ml, Sigma-Aldrich) as described in (Sciammas et al., 2006). If required, media was also supplemented with 310pM of CCL5, CCL19 or chemerin (All from R & D Systems). Stimulated cells were analysed by flow cytometry (section 2.10).

2.6.2 Culture of QM B cells

QM B cells were prepared as described in section 2.6.1. Numbers of NP-specific cells were quantified using flow cytometry (section 2.10) and $1x10^5$ NP-specific B cells were seeded into 96 well plates and supplemented with media as described in section 2.6.1. However, cells were stimulated with 2µg/well of NP-Ficoll with IL-4 (6.25ng/ml).

2.6.3 Culture of total splenocytes

Spleens were red cell lysed and analysed by flow cytometry to determine levels of B cells (non-QM) or NP^+ B cells (QM). Splenocytes were seeded into wells so each well contained $1x10^5$ B cells or NP-specific B cells, and cells were stimulated as described in either section 2.6.1 or 2.6.2.

2.7 Immunohistology

2.7.1 Immunohistochemistry

2.7.1.1 Immunohistochemical staining

Spleens were cut onto glass slides using a cryostat, to a thickness of 6µm. Slides were fixed in acetone (20min at 4°C) and kept at -20°C until required. Slides were washed for 10min in Tris (pH 7.6, Appendix A) and subsequently stained with primary antibody for 1hr (Appendix B). Secondary antibody was incubated for 1hr with 10% normal mouse serum (Dako, Ely, UK) to block unspecific binding. Slides were washed as before and incubated with secondary antibody for 45mins prior to another wash step. Slides were incubated for 40mins with Vectastain ABC-AP kit (Vector Laboratories, Burlingame, CA, USA) before undergoing a further wash step. Brown staining was developed by incubation for approximately 5min with the horseradish peroxidase substrate 3,3 diaminobenzidine tetrahydrochloride (DAB, Sigma). Slides were washed as described, and blue staining developed by incubation for approximately 10min with the alkaline phosphate substrate Fast Blue (Sigma). Slides were washed as before, rinsed in distilled water, and mounted using Glycerol Gelatin (Sigma). Pictures were taken using a DM6000

microscope (Leica Microsystems) coupled to a micropublisher 5.ORTV camera and using Q Capture software.

2.7.1.1 Quantification of NP-specific plasmablasts and germinal centres

Quantification is as described in (Zhang, 2010), but summarised here. Antigen specific germinal centres were detected as NP^+ IgD^- regions within IgD^+ B cell follicles. Antigen specific plasmablasts were identified as NP^{high} cells within the red pulp and in the white pulp exit zones. To quantify the area of spleen taken up by GC and plasmablasts, the area of GC and plasmablasts was calculated, relative to the area of total spleen. The area of spleen was calculated by counting the number of intercepts in a $100mm^2$ eyepiece graticule at x4 magnification (Weibel, 1963). Antigen-specific GC and plasmablast areas were counted by the same method, but at x25 magnification.

2.7.1.2 Quantification of antigen within splenic sections

Mice were immunised with NP-FITC-Ficoll and the antigen was detected in the spleen by $FITC^+$ fluorescence staining. A threshold of $FITC^+$ staining was set and the area of $FITC^+$ staining was measured, all using ImageJ software. As previous studies have shown NP-Ficoll is located on marginal zone macrophages {Vinuesa, 2000 #406}, spleens were also stained for CD169 and the area of $CD169^+$ staining was determined by ImageJ, as described for antigen. The area of antigen was divided by the area of macrophage for the whole spleen section and the data was represented as a percentage.

2.7.2 Immunofluorescence

Tissue sections were cut and fixed as described in section 2.7.1. Slides were blocked with 10% horse serum for 10mins at room temperature (RT) before addition of primary

antibodies. For intracellular stains, slides were incubated for 15mins and RT with 0.2% Triton-100. All other steps as section 2.7.1, however the wash buffer used is PBS, the antibody diluent was PBS with 1% bovine serum albumin (PBS-1%BSA). All steps after addition of fluorochrome-conjugated antibodies were carried out in the dark. If required after the final antibody addition, slides were stained with DAPI and washed 3 times in cold PBS. Slides were mounted using ProLong Gold antifade reagent (Invitrogen). Pictures were taken using a DM6000 microscope coupled to a DF350FX camera (Leica Microsystems).

2.8 Enzyme linked immunosorbent assay (ELISA)

2.8.1 NP-, CGG-, OMP-, LPS- and FliC- specific antibody detection by ELISA

Immuno 96 MicroWell solid plates (Nunc, Thermo Scientific) were coated with 5µg/ml of either CGG (Jackson Immuno Research), NP_2-BSA (for detection of high affinity antibody) or NP_{15}-BSA (for detection of total antibody - both conjugations prepared by Mrs. Chandra Raykundalia, Division of Immunity and Infection, University of Birmingham). For the Salmonella infection model, plates were coated with either outer membrane protein (OMP) (prepared in house (Bobat, 2011)), LPS from Salmonella typhimurium S-form (Enzo Life Sciences) or FliC (prepared in house (Bobat, 2011)) in coating buffer (Na_2CO_3 15mM, $NaHCO_3$ 35mM) and incubated overnight at 4°C. Plates were washed in wash buffer (PBS 100mM, 0.05% Tween 20, at pH 6.8) and subsequently blocked for 1.5hr at 37˚C with PBS-1%BSA before another wash step. Mouse serum was serially diluted 1/3 in PBS-1%BSA within the plate and incubated for 1.5hr at 37˚C. After washing, 100µl of isotype specific alkaline phosphatase-conjugated antibody was added (Appendix B) and

incubated for 1hr at 37˚C. To visualise the detected antibody, after a final wash step 100µl of p-nitrophenyl phosphate (N2770, Sigma-Aldrich) was added to the plate. The plate was incubated at 37˚C and, upon appearance of colour, the plate was read at 405nm using EMax Endpoint ELISA Microplate Reader (Molecular Devices, CA, USA).

2.8.2 Allotype NP-specific antibody detection by ELISA

Allotype specific secondary antibodies were used in order to differentiate between antibody secreted by donor QM cells and antibody secreted by host mice within an adoptive transfer experiment (section 2.4). Method as section 2.8.1**,** however serum was incubated overnight at 4°C and biotin-conjugated secondary antibodies (Appendix B) were incubated for 2 hours at 37°C. After washing as directed in section 2.8.1, Alkaline Phosphatase Streptavidin (Vector Laboraories) was added for 1 hour at 37°C before plates were developed as in section 2.8.1.

2.9 Enzyme linked immunosorbent spot (ELISpot)

96 well nitrocellulose microtiter plates (Merck Millipore, MA, USA) were coated overnight at 4°C with NP_{15}-BSA in sterile PBS (5µg/ml) and blocked for 2hr at 37°C with RPMI 1640 medium (Sigma-Aldrich) containing FCS (10%, heat inactivated). Bone marrow or splenic cells were prepared (sections 2.5) and resuspended in RPMI 1640-10%FCS. $2.5x10^5$ cell were added to each well before overnight incubation (37˚C). Plates were washed with wash buffer (section 2.8) and incubated with isotype specific alkaline phosphatase-conjugated antibody (Appendix B) diluted in PBS-1%BSA for 2 hours at RT. Plates were washed in wash buffer and PBS, before addition of Sigma Fast BCIP/NBT alkaline phosphatase substrate (Sigma-Aldrich) dissolved in distilled water. The reaction was

stopped with addition of distilled water, and plates were air dried. Spots were counted using an AID ELISPOT reader (Autoimmun Diagnostika GmbH, Strassburg, Germany) with Eli4 software (Autoimmun Diagnostika GmbH). Each sample was conducted in triplicate, with the median number of spots taken.

2.10 Flow cytometry

Prepared cells (section 2.5) were resuspended in flow cytometry media (PBS supplemented with 1% FCS and 0.5M EDTA) and transferred to a 96-well plate. All wash steps and antibody dilutions were made with flow cyometry media.

The plate was centrifuged at 4˚C, 1400rpm for 4mins and cells incubated with anti-CD16/CD32 antibody (20mins, 4˚C), in order to block Fc receptors. Plates were washed and cells were incubated with fluorescently-conjugated antibody (Appendix B). After washing, cells were resuspended in flow cytometry media, unless intracellular staining is required.

For intracellular staining, cells were incubated with Cytofix/Cytoperm (BD Biosciences) for 25mins at 4˚C and were subsequently washed with Permwash (BD Biosciences). Cells were stained with intracellular antibodies (20mins 4˚C) diluted in Permwash. Cells were washed with, and subsequently resuspended in, Permwash and stored at 4˚C until analysis.

If required, cells were detected for incorporation of EdU using Click-iT EdU flow cyometry assay kit (Molecular Probes) as per the manufacturer's protocol.

Cells were analysed using a CyAN FACS Analyser (Beckman Coulter, UK) controlled by Summit v4.3 software or BD Fortessa Analyser using FACSDiva6.2 software (BD Biosciences) and offline analysis was conducted by FlowJo software version 9.2.

2.11 Fluorescence activated cell sorting (FACS)

Cells were isolated, Fc receptors blocked and stained for extracellular antigens as described in section 2.10. Subsequently, cells were stained with Hoechst nuclear dye to enabling exclusion of dead cells and before resuspension in flow cytometry media. Cells were filtered using Partec CellTrics sterile filters (Partec, Germany) and sorted into populations using MoFlo High Speed Sorter (Beckman Coulter) controlled by Summit v4.3 software. Sorted cell samples were tested for purity using CyAN FACS Analyser and Summit v4.3 software. Sorted cells were washed in PBS, snap frozen in liquid nitrogen and subsequently stored at -80˚C.

2.12 Taqman reverse transcription-quantitative real-time PCR (RT-qPCR)

2.12.1 mRNA preparation

mRNA was prepared from sorted cell populations (section 2.11) using QIAshredder columns with either RNeasy Mini or Micro kits (all from Qiagen). The mRNA in all cases was eluted in RNase free water and stored at -80˚C.

2.12.2 cDNA preparation

cDNA was prepared by addition of random primer (Promega) to mRNA, and the sample denatured at 70˚C for 10mins. This was shock cooled on ice, after which reverse transcription mix was added, Appendix A. The sample was incubated at 41˚C for 1hr and then 90˚C for 10mins. All cDNAs were stored at -20˚C until required.

2.12.3 RT-qPCR

For RT-qPCR, either 0.5µl or 1µl of the cDNA preparation was added to a 384 well plate (Applied Biosystems, CA, USA). Taqman Universal PCR Master Mix (Applied Biosystems) was added, along with the desired primers and probes (Appendix C) at previously defined optimal concentrations. The plate was covered with Optical Adhesive Film (Applied Biosystems), mixed, and then centrifuged before being loaded onto an ABI 7900 real-time PCR machine (Applied Biosystems). The temperature cycle was as follows: 50˚C for 2mins, 95˚C for 10mins, then 40 cycles of 95˚C 15s, 60˚C 1min. Fluorescence analysis was performed using SDS 2.2.2 software (Applied Biosystems), where the threshold was set manually to the logarithmic phase. The quantification cycle (Cq) was recorded for each sample and the relative quantity of the target gene was deduced by taking the ΔCq (Cq-target gene minus Cq-housekeeping gene) and calculating $2^{-\Delta Cq}$.

2.13 Ligand uptake assay

2.13.1 CCL19 uptake assay

Alexa Fluor 647 conjugated CCL19 ($CCL19^{AF647}$, Almac) was kindly provided by Chris Hansell, The University of Glasgow. Chemokine uptake assay was performed as stated in (Hansell et al., 2011), but is summarised briefly here. Splenic cells were prepared and $2x10^6$ cells were cultured at 37°C for 60mins in complete medium (section 2.5.3) supplemented with 4mM L-glutamine, 20mM HEPES and 12.5nM $CCL19^{AF647}$. To ensure any detected fluorescence was specific for chemokine uptake, control samples were incubated with 250nM of unlabelled CCL19 (R & D systems). Cells were then stained for specific markers and analysed by flow cytometry (section 2.10).

2.13.2 Chemerin uptake assay

Chemerin was coupled to Cy5 using the Lightning-Link™ Rapid Cy5 conjugation kit (Innova Biosciences) as per the manufacturers' instructions. Uptake of chemerin was then conducted as 2.14.1.

2.14 Statistical analysis

Data was plotted in GraphPad Prism version 6. Data was analysed by Mann Whitney U to determine statistical significance. Statistical significance was accepted for p values smaller than 0.05 in a two-tailed test, which does not give a preconception that one test group will be different to another.

Chapter 3. Effect of CCRL2 Deficiency during the Plasmablast Response

3.1 Introduction

3.1.1 NP-specific responses

Throughout this study the response of mice to NP-conjugated antigens is described. NP-specific responses have been utilised for decades to assess the action of antigen administration in B cell activation and differentiation (Bothwell et al., 1981, Imanishi and Makela, 1974).

Here, to further assess the B cell response, quasi-monoclonal (QM) mice are used (Cascalho et al., 1996), in which the majority of B cells are specific for NP. Due to >95% of anti-NP antibodies containing the lambda light chain (Jack et al., 1977), including upon immunisation with NP-Ficoll (Smith et al., 1985), QM mice are deficient for the kappa light chain (Cascalho et al., 1996). Interestingly, unlike a traditional NP-response, immunisation of mice with NP-LPS generates an antibody response dominated by kappa light chains (Smith et al., 1985). As the main focus of this study is immunisation of mice with NP-Ficoll, a short summary of the NP-Ficoll response is detailed below.

3.1.1.1 The NP-Ficoll response of C57BL/6 mice

Characterisation of the response in C57BL/6 mice to NP-Ficoll was a subject of multiple papers in the last couple of decades. In the spleen, one day post intraperitoneal (*i.p.*) immunisation, NP-specific B cells migrate to the T-B border, with the majority of these cells being 5-bromo-2'-deoxyuridine ($BrdU^+$) and thus already proliferating (Garcia de

Vinuesa et al., 1999b). From day 1 there is an exponential increase in the levels of NP-specific B cells, which peak at day 5 (Garcia de Vinuesa et al., 1999b). This early phase of the B cell response to NP-Ficoll is dependent on antigen receptor affinity; in competition experiments, B cells with a higher affinity for NP expand to a much greater extent than their lower affinity counterparts (Shih et al., 2002). On day 5 post immunisation with NP-Ficoll, NP-specific B cells decline in the spleen, with no $BrdU^+$ B cells detected later than day 10 post immunisation (Garcia de Vinuesa et al., 1999b).

Interestingly, NP-Ficoll immunisation results in a large extrafollicular plasmablast response, with red pulp resident plasmablasts detectable in the spleen from day 3 onwards, which peak at day 5 (Garcia de Vinuesa et al., 1999b). The antibody response to NP-Ficoll is long-lasting, with antibody still detectable at 90 days post immunisation. Also, injection of BrdU on day 90 indicates 8% of NP-specific splenic plasmablasts are still actively proliferating (Garcia de Vinuesa et al., 1999b, Hsu et al., 2006). Immunisation of RAG-1 deficient mice reconstituted with peritoneal cells suggests that the sustained antibody response is due to activation of B1b cells (Hsu et al., 2006).

3.1.2 B cell response to attenuated *Salmonell*a Typhimurium infection

Infection of mice with an attenuated strain of *Salmonella* Typhimurium (STm) *i.p.* causes a large bacterial burden in the spleen, with STm detectable at high levels 4 days post infection (Cunningham et al., 2007). Bacterial burdens remains elevated a week post infection and begin to decline at 20 days post infection (Cunningham et al., 2007). By day 35 there is minimal bacterial presence in the spleen (Cunningham et al., 2007). Infection

is accompanied by a marked splenomegaly which peaks at day 20, before a reduction to near baseline levels a week later (Cunningham et al., 2007).

Unlike T cell deficient mice which have a high mortality to attenuated STm infection (Hess et al., 1996, Pie et al., 1997), B cell deficient mice do not succumb to primary STm infection (McSorley and Jenkins, 2000). This study focuses on the early antibody response to STm, up to one week post infection. STm initially induces a huge extrafollicular response, with initial IgM production against outer membrane proteins (Omp) being T cell independent before production of anti-Omp IgG2c switched antibody in a T cell dependent manner (Cunningham et al., 2007). Further characterisation of the antibody response against Omp identified OmpD as the main target, with OmpD being a B1b antigen (Gil-Cruz et al., 2009). B1b cells also being the major cell type to respond to the polysaccharide Vi antigen of Salmonella (Marshall et al., 2012). At this early stage of infection germinal centres are not present, and they do not appear until day 35 (Cunningham et al., 2007), once the infection has largely resolved.

3.1.3 Plasmablast differentiation

Upon activation, B cells can differentiate into plasmablasts which are proliferative antibody secreting cells. Following proliferation, some plasmablasts can differentiate into non-dividing antibody secreting plasma cells. Differentiation into plasmablasts involves the expression of multiple genes, including Blimp-1 (B-lymphocytes induced maturation protein-1) and IRF4 (Interferon Regulatory Factor 4).

3.1.3.1 Blimp-1 is required for plasmablast differentiation

Blimp-1 was first described by Turner and colleagues in 1994 (Turner et al., 1994) as a transcription factor that induces B cell differentiation into the early plasma cell stage. It has since been shown to be essential and sufficient for differentiation into plasmablasts and plasma cells both *in vivo* and *in vitro* (Soro et al., 1999, Shapiro-Shelef et al., 2003, Shaffer et al., 2002). Analysis of Blimp-1 binding identified an optimal consensus sequence of (A/C)AG(T/C)GAAAG(T/C)(G/T) (Kuo and Calame, 2004).

As a transcriptional repressor, Blimp-1 acts on a variety of genes to prevent their expression. Bcl-6 (Shaffer et al., 2000), c-Myc (Lin et al., 1997) and Pax5 (Nera et al., 2006) are downregulated due to Blimp-1 expression. As well as repressing the transcription of various genes, Blimp-1 can also act as an activator. For example, a series of papers by Shaffer and colleagues showed that XBP-1 expression is dependent on Blimp-1 (Shaffer et al., 2002) and that plasma cell differentiation is dependent on XBP-1 expression (Shaffer et al., 2004). This is due to XBP-1 inducing the expression of genes involved in the secretory pathway (Shaffer et al., 2004). Induction of Blimp-1 is regulated by the high expression of another transcription factor, IRF4.

3.1.3.2 High expression of IRF4 is required for plasma cell differentiation

IRF4 is a transcription factor that is highly expressed in multiple mature lymphocyte cell lines, but is particularly highly expressed in plasma cells (Matsuyama et al., 1995). Conditional deletion of IRF4 in germinal centre B cells indicates that, although GCs can form normally, plasma cells do not form in these mice (Klein et al., 2006). This lack in

plasma cell differentiation is due to the failure to transcribe mRNA for AID and Blimp-1 (Sciammas et al., 2006, Klein et al., 2006).

IRF4 deficient mice have severely reduced class switch recombination, as do mice in which IRF4 is deficient only in GC B cells (Klein et al., 2006, Sciammas et al., 2006), even though the latter have normal GC formation. It was later established that IRF4 acts as a "molecular switch" in germinal centre and plasma cell fate; low IRF4 levels induce GC B cell fate, whilst high IRF4 expression drives plasma cell fate (Ochiai et al., 2013); indicating that normal GC formation in the conditional knockout study was due to residual levels of IRF4 still present in the GC B cells.

3.1.4 The BAFF/APRIL system

TNF family ligands APRIL (A Proliferation Induced Ligand) and BAFF (B Cell Activating Factor of the TNF Family, also known as BLγS, B Lymphocyte Stimulator) and their receptors are a major family of proteins involved in B cell biology. BAFF and APRIL interact with the TNFR family members TACI (Transmembrane Activator and Calcium Modulator and Cyclophilin Ligand Interactor), BCMA (B Cell Maturation Antigen) and, in the case of BAFF only, BAFFR (figure 3.17a). BAFFR and BCMA are involved in B cell survival through NFκB signalling (reviewed by (Bossen and Schneider, 2006)).

3.1.4.1 Role of BAFF/APRIL system in the germinal centre response

On day 14 post immunisation of mice with NP-CGG, BAFF can be detected in the follicle and GC light zone, but not in the DZ (Goenka et al., 2014). Expression of BAFF receptors alternates between the cell types; BAFFR is present on GC and follicular B cells, TACI only present on follicular, and BCMA is absent on both cell types (Goenka et al., 2014). A

decade ago, BAFF was shown to have a key role in setting thresholds for B cell receptor mediated selection (Cancro, 2004) in naïve B cells, suggesting it may play a similar role in the GC response. Supporting this, the GC response in BAFF- or BAFFR- deficient mice terminates early (Rahman et al., 2003), with the presence of BAFF in the GC required for affinity maturation to occur (Goenka et al., 2014).

Although data suggests TACI is present only on follicular B cells (Goenka et al., 2014), TACI has also been shown to play a role in the germinal centre response. Immunisation of TACI deficient mice with a TD antigen causes an increase in both GC B and T follicular helper (Tfh) cell numbers (Ou et al., 2012).

3.1.4.2 Role of BAFF/APRIL system in the plasmablast response

TACI is expressed at high levels on B1b cells (Dickinson et al., 2014) and upon thymus independent B cell activation, TACI is required for plasmablast differentiation. NP-Ficoll (Mantchev et al., 2007) and TNP-LPS (Ozcan et al., 2009) immunised TACI deficient mice have a huge reduction in both IgM and switched NP-specific responses. TACI signalling promotes sustained BLIMP-1 expression by B cells (Tsuji et al., 2011) and ligation of TACI *in vitro* enhances the number of $CD138^{+}$ cells as well as antibody secretion (Castigli et al., 2007). B cells of newborn mice have a severe reduction in TACI expression and stimulation with TACI ligands *in vitro* does not induce CD138 expression, unlike in adult mice (Kanswal et al., 2008). This indicates that a poor childhood response to TI-II antigens (Murray and Lopez, 1997) may be due to impaired TACI expression. APRIL enables B cell proliferation of LPS-stimulated B cells *in vitro* in a TACI-dependent manner (Ozcan et al., 2009) and APRIL deficient mice have a slight reduction in antibody

responses to both NP-Ficoll and NP-LPS (Hardenberg et al., 2008), indicating that TACI may act through APRIL to initiate plasmablast differentiation. However, as the reduction in the antibody response is not as dramatic as that seen in TACI deficient mice, there is likely to be some redundancy within the system.

Interestingly, TACI is not required for thymus-independent IgM and IgG production against *Borrelia hermsii*, which requires both B cell receptor and TLR2 signalling (Dickinson et al., 2014). BAFFR is also present on B1b cells, and BAFF and BAFFR are required to control this infection (Dickinson et al., 2014), indicating a complex set of interactions and mechanisms regarding the role of BAFF/APRIL and their receptors in the thymus independent plasmablast response.

Although the above reports the role of TACI in TI-II responses, TACI has also been shown to have a role in TD plasmablast responses (Ou et al., 2012). Upon immunisation with a TD antigen, $TACI^{-/-}$ plasma cells are unable to downregulate the pro-apoptotic factor BIM (B-cell lymphoma 2 interacting mediator of cell death) causing a defective antibody response (Ou et al., 2012).

However, TACI is not required for activation nor proliferation of B cells ($TACI^{-/-}$ B cells stay in the cell cycle longer) (Mantchev et al., 2007). *In vitro* activation studies indicate that interleukin (IL)-21 prevents TACI, but not BAFFR, upregulation in activated B cells (Goenka et al., 2014), with IL-21 being a critical cytokine in the generation of virus-specific long lived plasma cells (Rasheed et al., 2013).

3.1.5 Aims of chapter

Previous data has shown that CCRL2 mRNA is upregulated within plasmablasts post immunisation with NP-Ficoll. This study aims to assess whether there is a role of CCRL2 in plasmablast and B cell function by;

1. Assessing the role of CCRL2 pre-immunisation in the spleen and peritoneal cavity
2. Further examining the expression pattern of CCRL2 in plasmablasts
3. Assessing plasmablast and antibody output of CCRL2 deficient mice to both TI and TD antigens
4. Characterising the early extrafollicular response to STm in CCRL2 deficient mice

3.2 Assessment of CCRL2 deficient mouse spleen and peritoneal cavity cells

This study analyses the splenic response of WT and CCRL2$^{-/-}$ mice to both TI and TD antigens. The majority of experiments test the effect of CCRL2 deficiency during the splenic immune response after *i.p.* immunisation. To determine whether CCRL2 deficiency has an effect pre-immunisation, splenic and peritoneal cells were analysed by immunohistology and flow cytometry.

3.2.1 CCRL2 deficiency does not obviously affect the microarchitecture of, nor B cell subpopulations in, the spleens of unimmunised mice

Throughout this study, WT, CCRL2$^{+/-}$ and CCRL2$^{-/-}$ mice are immunised and the splenic response studied. To determine if there are intrinsic differences pre-immunisation, the spleen mass of unimmunised mice was measured. Interestingly, although the mass of WT and CCRL2$^{+/-}$ spleens are similar, CCRL2$^{-/-}$ spleens are on average 27% heavier than WT counterparts and 19% heavier than CCRL2$^{+/-}$ ($p<0.001$ and $p<0.05$, respectively, figure 3.1a). WT and CCRL2$^{-/-}$ splenic B cell populations were analysed by flow cytometry. Figure 3.1b shows the gating strategy applied for different B cell populations. B cells were subdivided into marginal zone, follicular and B1 cells using the markers CD21 and CD23. No differences were observed between WT and CCRL2$^{-/-}$ mice in the proportions of these B cell subsets (figure 3.1c). B1 cells were further subdivided into B1a and B1b cells based on CD5 expression. The majority (>95%) of B1 cells in both WT and CCRL2$^{-/-}$ mice were B1b, and there was no significant difference between the genotypes (figure 3.1d). B1b cells were further subdivided according to CD11b expression. Again, although the majority of cells were CD11b^{-}, this was true for both WT and CCRL2$^{-/-}$ mice and there was no difference between the genotypes (figure 3.1e).

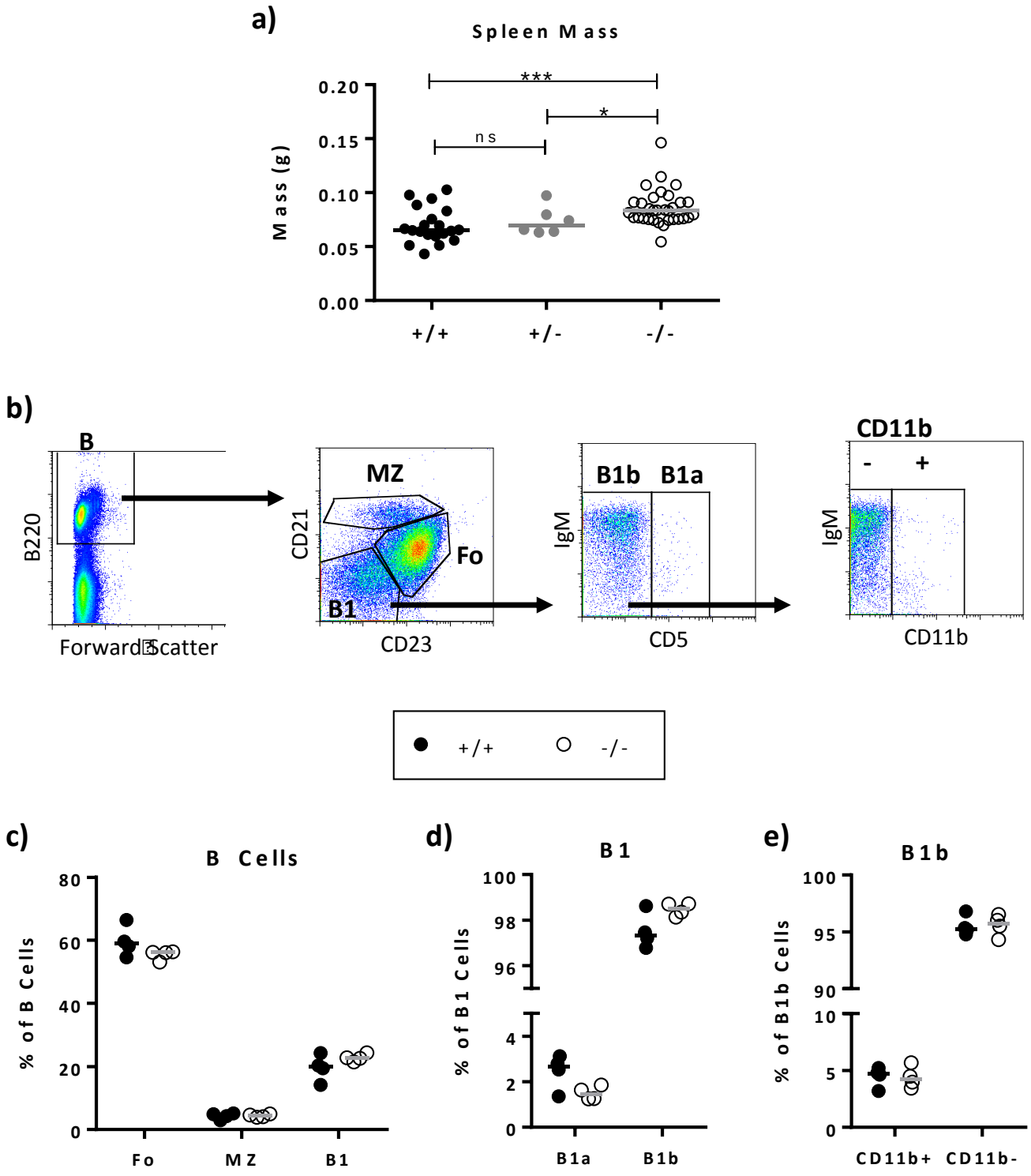

Figure 3.1. CCRL2$^{-/-}$ spleens are larger, but splenic B cell populations are similar to WT mice. a) Spleen masses of unimmunised mice; b-e) Spleens of WT and CCRL2$^{-/-}$ mice were extracted and analysed by flow cytometry for B populations b) Flow cytometric gating strategy; c) B cell subsets; d) B1 subsets; e) B1b CD11b^{+} and CD11b^{-} B1b cells.
Key: Fo – Follicular; MZ – Marginal Zone
B cell data from single experiment. Bars indicate median
***p<0.001, *p<0.05

To test whether splenic microarchitecture is affected by CCRL2 deficiency, WT and CCRL2 deficient spleens were sectioned and stained for markers representing cells resident in the T zone, follicle, marginal zone and the red pulp. The splenic white pulp in CCRL2$^{-/-}$ mice is split into CD3^{+} T cell zones surrounded by IgD^{+} B cell follicles, as seen in WT mice (figure 3.2a). B cell follicles are surrounded by the marginal zone, detected using CD169, a marker for marginal zone metallophilic macrophages (MZM) (figure 3.2b). In both WT and CCRL2$^{-/-}$ sections, this thin layer of cells protrude into the follicle, but do not fully enter either the follicle, or the red pulp. Finally, the white and red pulp are distinct areas, with F4/80^{+} macrophage confined to the red pulp (figure 3.2c). In all staining protocols (figures 3.2a-c), there were no detectable differences in the microarchitecture of the spleens of unimmunised CCRL2 deficient mice relative to WT mice, with no obvious differences in the size of these compartments. All cells were confined to their own compartment, with clearly defined zones and borders. Together, this shows that although the CCRL2$^{-/-}$ have larger spleens than both WT and CCRL2$^{+/-}$ mice, splenic B cell subpopulations and microarchitecture are not affected by CCRL2 deficiency.

3.2.2 Different proportions of innate cells are present within the peritoneal cavity of WT and CCRL2$^{-/-}$ mice

Throughout this study, CCRL2$^{-/-}$ mice were challenged *i.p.* with different antigens. To test whether there are intrinsic differences in peritoneal cell subpopulations, cells were harvested from the peritoneum of unimmunised WT, CCRL2$^{+/-}$ and CCRL2$^{-/-}$ mice and analysed by flow cytometry via two previously published protocols (Ghosn et al., 2010, Gil-Cruz et al., 2009) (figures 3.3a and 3.4a).

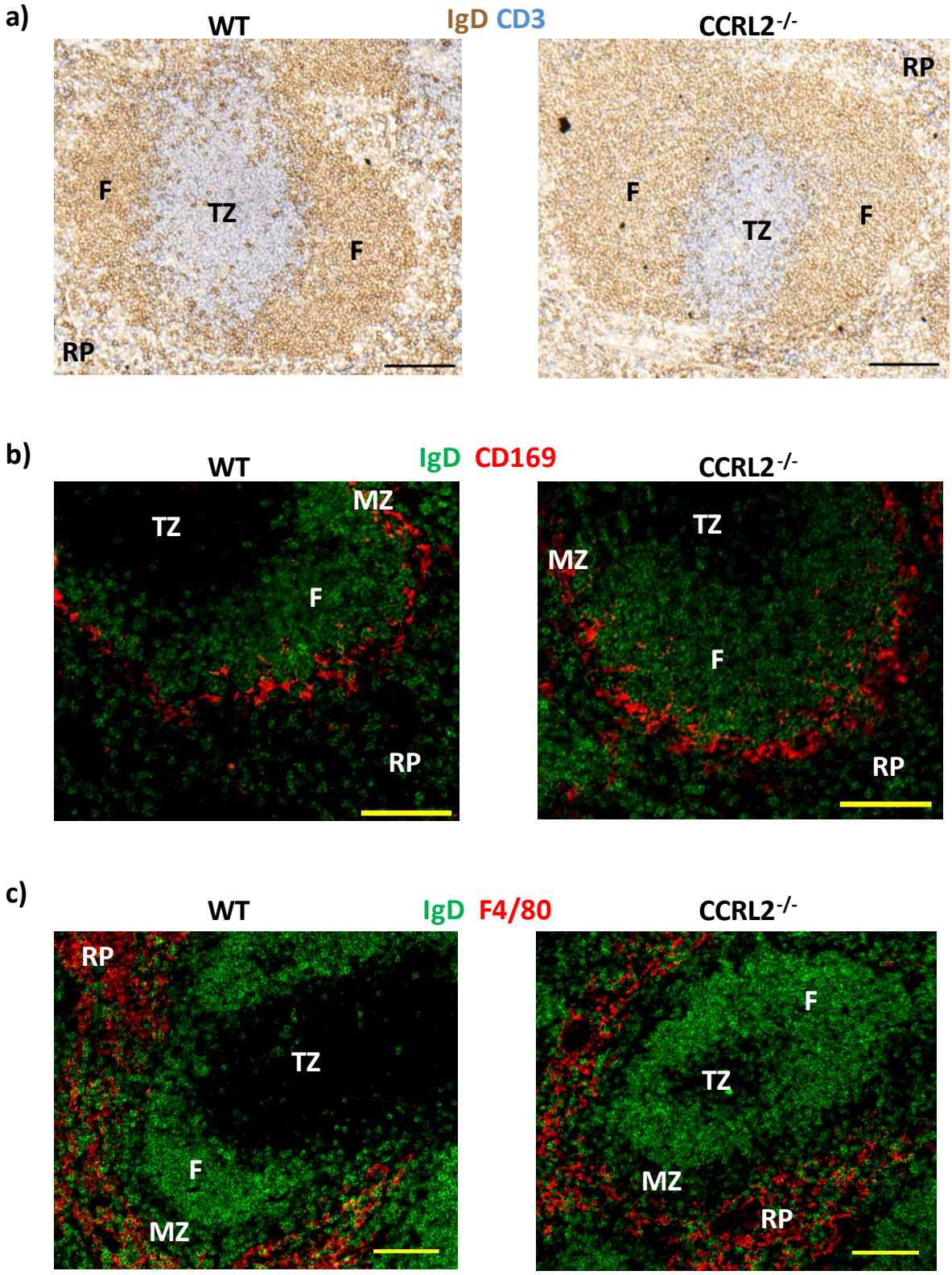

Figure 3.2. CCRL2 deficiency does not affect splenic microarchitecture of unimmunised mice. Spleens of unimmunised WT and CCRL2$^{-/-}$ mice were sectioned and stained for stated markers to visualise defined zones and cells a) White pulp showing CD3^{+} T cell zone (blue) surrounded by IgD^{+} B cell follicles (brown); b) Marginal zone metallophils (red) separate IgD^{+} B cell follicles (green) and red pulp; c) Red pulp macrophages (red) outside the MZ and IgD^{+} B cell follicles (green).
Representative images taken from 4 mice per group
Key: F – Follicle; MZ- Marginal Zone; RP – Red Pulp; TZ – T-Zone; Scale Bar – 100µm

The frequency of B cells detected in the peritoneum of all genotypes was similar (figure 3.3b), and no significant changes were detected in the proportions of both B1 and B2 subsets (figure 3.3c). Unlike the spleen, the peritoneum contains a higher proportion of B1a than B1b cells; and the proportions of each B1 subset was similar across all genotypes (figure 3.3d). Finally, B1b cells were analysed for their expression of CD11b, which has been shown to define two distinct subsets of peritoneal B1 cells (Ghosn et al., 2008). CD11b expression was highly variable, however there was no significant difference between WT, CCRL2$^{+/-}$ and CCRL2$^{-/-}$ mice (figure 3.3e).

Levels of innate immune cells in the peritoneal cavity were analysed using a protocol published by Ghosn and colleagues (Ghosn et al., 2010) with the gating strategy shown in figure 3.4a. It could be argued that CCRL2 deficient mice have a reduction in peritoneal cavity resident CD11c^{+} dendritic cells (DCs), however this change is not significant (figure 3.4b). Mast cells, neutrophils, eosinophils and small peritoneal macrophages are all minor populations in the peritoneal cavity, each being <5% of the total population. No difference in levels of any of these subsets between WT and CCRL2$^{-/-}$ mice was observed, despite peritoneal mast cells being shown to express CCRL2 (Zabel et al., 2008). Like DCs, there was a small reduction in large peritoneal macrophage and T/NKT cells in CCRL2 deficient mice, however this was not significant in either case. Conversely, NK cells appear higher in proportion in CCRL2$^{-/-}$ mice, but again this is not significant.

Together, this data shows that CCRL2 deficiency does not significantly affect the proportion of cells within the peritoneal cavity. B cell subsets appear unaffected and although there are minor changes in the frequency of

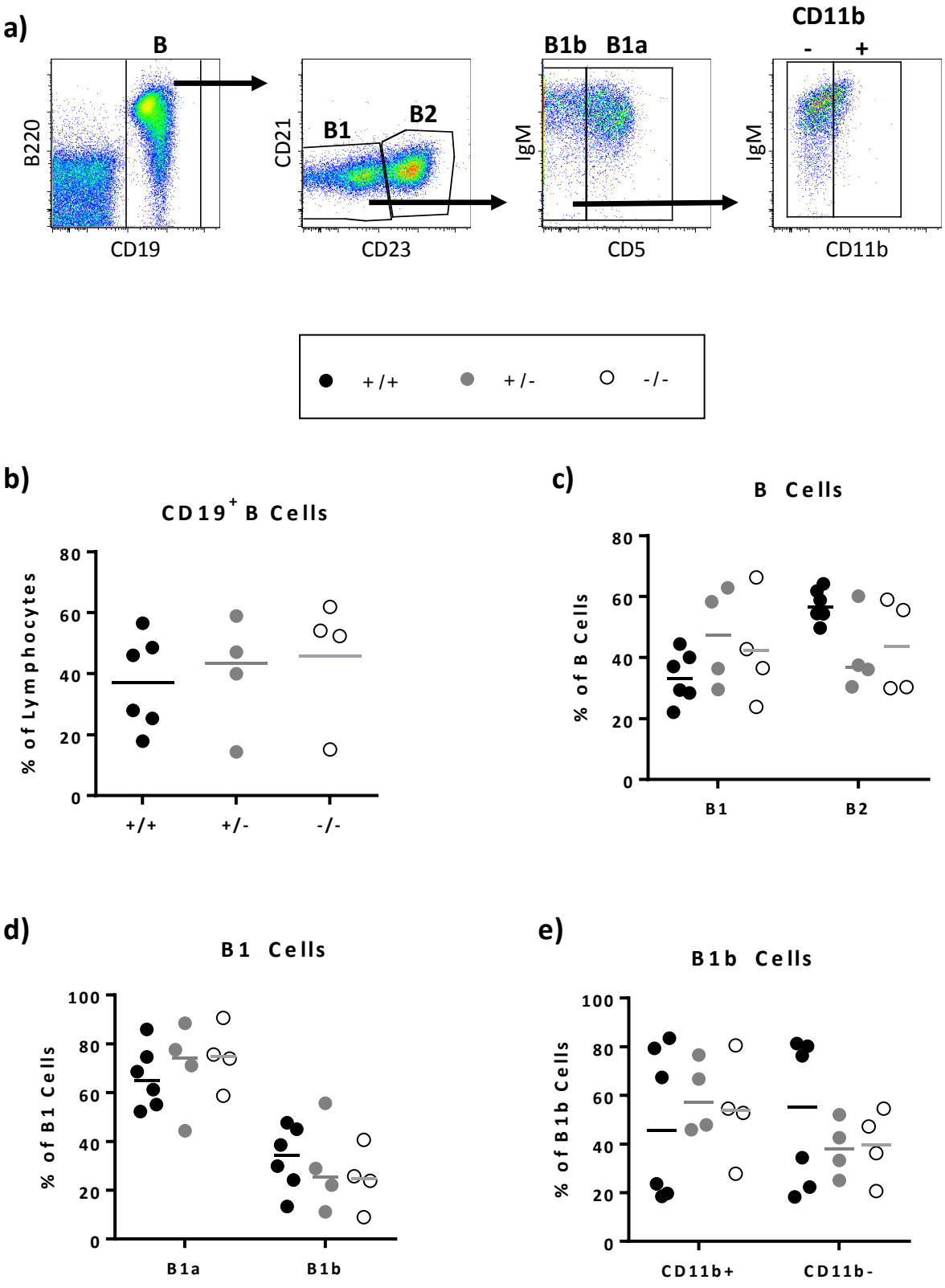

Figure 3.3. Analysis of B cells within the peritoneum of CCRL2 deficient mice. PeC cells of WT, CCRL2$^{+/-}$ and CCRL2$^{-/-}$ mice were extracted and analysed by flow cytometry according to a previously published protocol (Gil-Cruz et al., 2009); a) Flow cytometric gating strategy; b) PeC B cells; c) PeC B1 and B2 cells; d) PeC B1a and B1b cells; e) PeC CD11b^{+} and CD11b^{-} B1b cells.
Data pooled from two independent experiments. Bars indicate median
Key: PeC – Peritoneal cavity

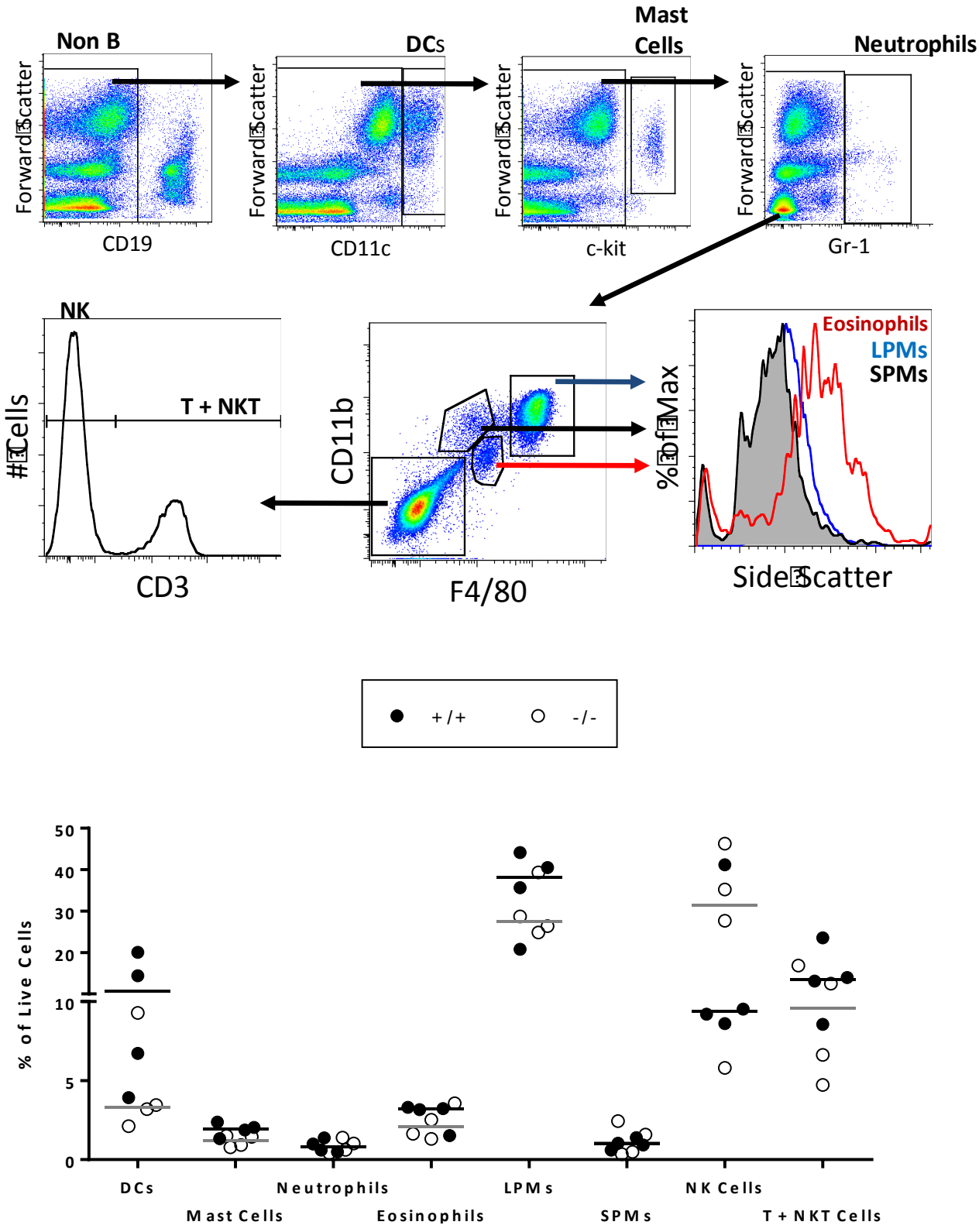

Figure 3.4. Analysis of innate cells within peritoneum of CCRL2 deficient mice. Peritoneal cells of WT and CCRL2$^{-/-}$ mice were extracted and analysed by flow cytometry according to a previously published protocol (Ghosn et al., 2010); a) Flow cytometric gating strategy; b) Proportions of stated cell types in peritoneum of mice.
Key: DCs – Dendritic Cells; LPMs – Large Peritoneal Macrophages; NK – Natural Killer; SPMs – Small Peritoneal Macrophages
Data from single experiment. Bars indicate median

DCs, large peritoneal macrophage and NK cells, a repeat of the experiment is required for this change to be significant.

3.3 CCRL2 mRNA is upregulated upon differentiation into plasmablasts

Previous data from our laboratory ((Cook, 2011) reprinted here – figure 3.5a) showed that CCRL2 mRNA is upregulated in plasmablasts 4 days post immunisation with NP-Ficoll, and remains at high levels on day 7. To confirm this, WT mice with NP-specific B cell receptors were immunised with NP-Ficoll and cells were sorted on day 3 into germinal centre (GC) B cells and plasmablasts (for purity see figure 3.16a). In concurrence with previous results, CCRL2 is upregulated approximately ten-fold in plasmablasts ($p<0.05$, figure 3.5b). In order to understand why CCRL2 is upregulated, the MAPPER database was utilised to determine which transcription factors may bind the promoter region of CCRL2 (Marinescu et al., 2005), although further experiments would be required to confirm binding. Interestingly, BLIMP-1, the master regulator of plasma cell fate, is predicted to bind the CCRL2 promoter region (figure 3.5c). BLIMP-1 has the fourth lowest E-value, after Oct-1, IRF and NIT2. A member of the IRF family of transcription factors, IRF4, is required for expression of Blimp-1 and therefore also required for plasmablast fate. Together, this suggests that CCRL2 mRNA is upregulated when transcriptional regulation towards a plasmablast phenotype is activated, and this could be due to binding of BLIMP-1 or IRF4 to the CCRL2 promoter.

a)

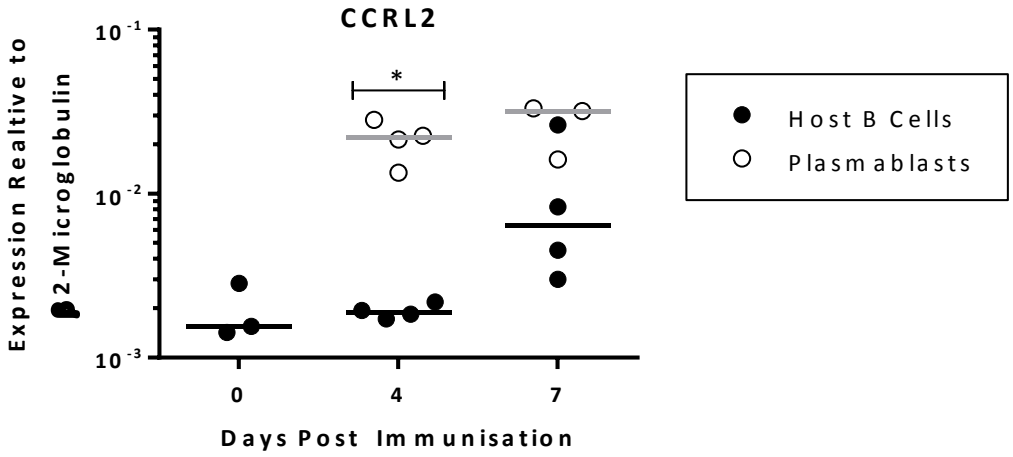

b)

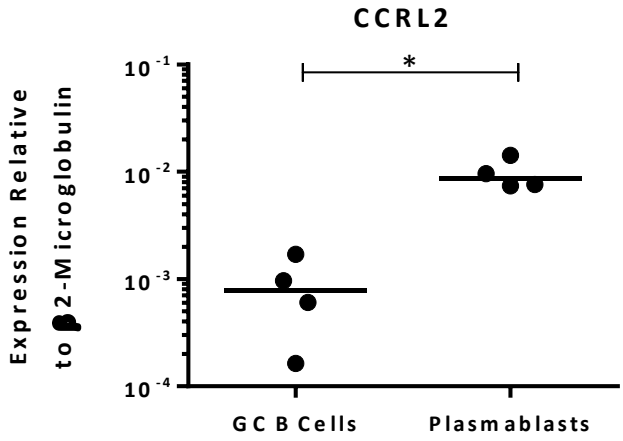

c)

Transcription Factor	DNA Strand	Chromosome	Binding Region	E-value
Oct-1	-	chr9	Promoter	0.61
IRF	+	chr9	Promoter	1.3
NIT2	-	chr9	Promoter	1.4
Blimp-1	-	chr9	Promoter	1.8

Figure 3.5. CCRL2 is expressed on plasmablasts at the mRNA level. a) NP-specific eYFP$^+$ cells were transferred into WT hosts and a day later mice were immunised with NP-Ficoll. eYFP$^+$ CD138$^+$ plasmablasts were sorted by FACS and CCRL2 mRNA expression was determined by RT-qPCR. cDNA was kindly provided by Dr. Laura George, data republished with permission from (Cook, 2011), b) WT mice with B cells specific for NP were immunised with NP-Ficoll and plasmablasts and GC B cells were sorted by FACS on day 3 and CCRL2 mRNA expression was determined by RT-qPCR, c) List of transcription factors most likely to bind CCRL2 promoter regions according to the MAPPER database (Marinedcu et al., 2005).
Data from single experiments. Bars indicate median
*p<0.05

3.4 Immunisation of CCRL2 deficient mice with the thymus independent antigen NP-Ficoll

In order to understand the role of CCRL2 in plasmablast responses, WT and CCRL2$^{-/-}$ mice were immunised with the TI-II antigen NP-Ficoll, which generates a strong extrafollicular plasmablast response, independent of T cell help.

3.4.1 Antigen specific antibody titres increase in CCRL2 deficient mice post TI-II immunisation

To analyse the effect of CCRL2 deficiency on the NP-Ficoll response, mice were immunised *i.p.* with Ficoll coupled to the hapten NP. Spleens were taken 3, 5, 7 and 10 days post immunisation and the blood analysed for NP-specific antibodies.

Previous studies have shown that in the WT mouse, antigen-specific IgM is detectable from day 5 and peaks at day 10 (Garcia de Vinuesa et al., 1999b). In agreement with this, figure 3.6a shows that WT mice have detectable NP-specific IgM at day 5, which increases through days 7 and 10. Similarly, antigen-specific IgM is detectable in CCRL2$^{-/-}$ mice at day 5, and titres increase up to day 10 post immunisation. On day 5, there are ten-fold higher levels of IgM in CCRL2$^{-/-}$ mice compared to WT mice ($p<0.001$). At days 7 and 10 post immunisation IgM titres are still three-fold greater in CCRL2$^{-/-}$ mice, however on day 7 this increase is not significant, possibly due to low sample numbers.

The main IgG isotype induced during a TI-II immune response is IgG3 (Garcia de Vinuesa et al., 1999b). IgG3 was detectable from day 7 post immunisation (figure 3.6b) and levels increased further by day 10. Although there were slightly higher titres of IgG3 at day 7 of

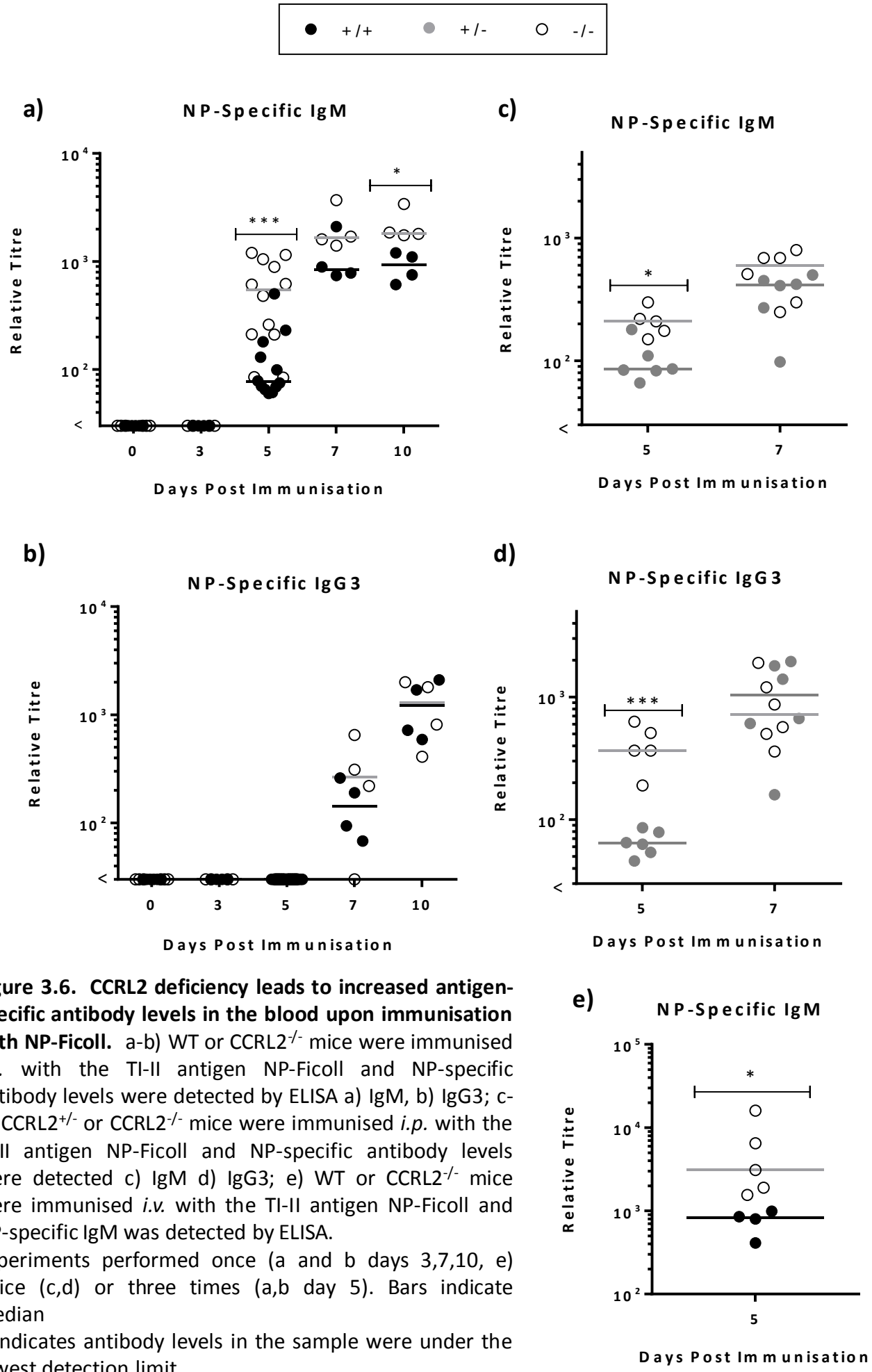

Figure 3.6. CCRL2 deficiency leads to increased antigen-specific antibody levels in the blood upon immunisation with NP-Ficoll. a-b) WT or CCRL2$^{-/-}$ mice were immunised *i.p.* with the TI-II antigen NP-Ficoll and NP-specific antibody levels were detected by ELISA a) IgM, b) IgG3; c-d) CCRL2$^{+/-}$ or CCRL2$^{-/-}$ mice were immunised *i.p.* with the TI-II antigen NP-Ficoll and NP-specific antibody levels were detected c) IgM d) IgG3; e) WT or CCRL2$^{-/-}$ mice were immunised *i.v.* with the TI-II antigen NP-Ficoll and NP-specific IgM was detected by ELISA.

Experiments performed once (a and b days 3,7,10, e) twice (c,d) or three times (a,b day 5). Bars indicate median

< indicates antibody levels in the sample were under the lowest detection limit

***p<0.001, *p<0.05

the response in CCRL2 deficient mice, this was not significant, and by day 10 no difference in the levels of serum antigen-specific IgG3 was detectable.

The WT mice used in this study were purchased from an external company (Harlan, UK), while CCRL2$^{-/-}$ mice were bred in-house at the University of Birmingham Biomedical Services Unit. To ensure that the phenotype observed here was not an artefact of using commercial mice relative to in-house mice (i.e. due to different endogenous flora), CCRL2$^{+/-}$ mice were generated in-house, and antibody titres compared to CCRL2$^{-/-}$ mice. As figure 3.6c-d shows, CCRL2$^{-/-}$ mice have a significant increase in both unswitched ($p<0.05$) and IgG3 ($p<0.001$) antibody titres compared to CCRL2$^{+/-}$ mice on day 5 post NP-Ficoll immunisation. Interestingly, as seen in WT versus CCRL2$^{-/-}$ experiments, the difference in antibody levels is no longer apparent at day 7 for both IgM and switched antibody. It is possible that these apparent discrepancies between WT and CCRL2$^{+/-}$ responses are due to the expression of a single CCRL2 allele.

Finally, it was tested whether the observed phenotype is due to the injection route of the antigen. This is due to the differences detected in innate cells between WT and CCRL2$^{-/-}$ mice pre-immunisation. WT and CCRL2$^{-/-}$ mice were immunised with NP-Ficoll *i.v.*, as opposed to *i.p.* in the previous experiments. As figure 3.6e shows, even after *i.v.* immunisation, CCRL2$^{-/-}$ mice have higher levels of NP-specific IgM on day 5 of the response, compared to WT mice.

Together, this shows that CCRL2 deficient mice have increased levels of antigen-specific antibody post TI-II immunisation. Larger differences are detected with IgM than switched

antibody, suggesting this is a phenotype affecting early plasmablast responses. This phenotype is not an artefact of sourcing WT mice externally, nor injection route.

3.4.2 Increased antibody in CCRL2 deficient mice post TI-II immunisation is due to an increase in plasmablasts

Changes in the level of antigen-specific IgM could be the result of two factors: increased production of plasma cells, or higher amounts of antibody secreted by individual plasma cells. To determine the cause of the observed phenotype, the numbers of NP-specific plasma cells in the spleen of WT and CCRL2$^{-/-}$ mice were determined by immunohistology and flow cytometry.

Immunohistochemical analysis showed that antigen-specific splenic plasma cells (NP^{hi}) were detectable from day 3 post immunisation (figure 3.7b), and at this early stage CCRL2 deficient mice had significantly higher numbers of plasma cells ($p<0.05$). NP-specific plasma cell numbers massively increased in the spleen at day 5 (figure 3.7a and b), with CCRL2 deficient mice having much higher levels of plasmablasts than WT mice, and this was also apparent on day 10 post immunisation ($p<0.01$ and $p<0.05$ respectively). In support of the immunohistochemical data, flow cytometry analysis also revealed significantly higher levels of antigen-specific plasmablasts in the spleen on days 5 and 10 post immunisation ($p<0.001$ and $p<0.05$ respectively figure 3.7d). Interestingly, both flow cytometry and immunohistochemistry found no differences in NP-specific splenic plasma cells on day 7 post immunisation, which correlates with antibody data. Together, this data shows that the increase in antibody titres post NP-Ficoll immunisation

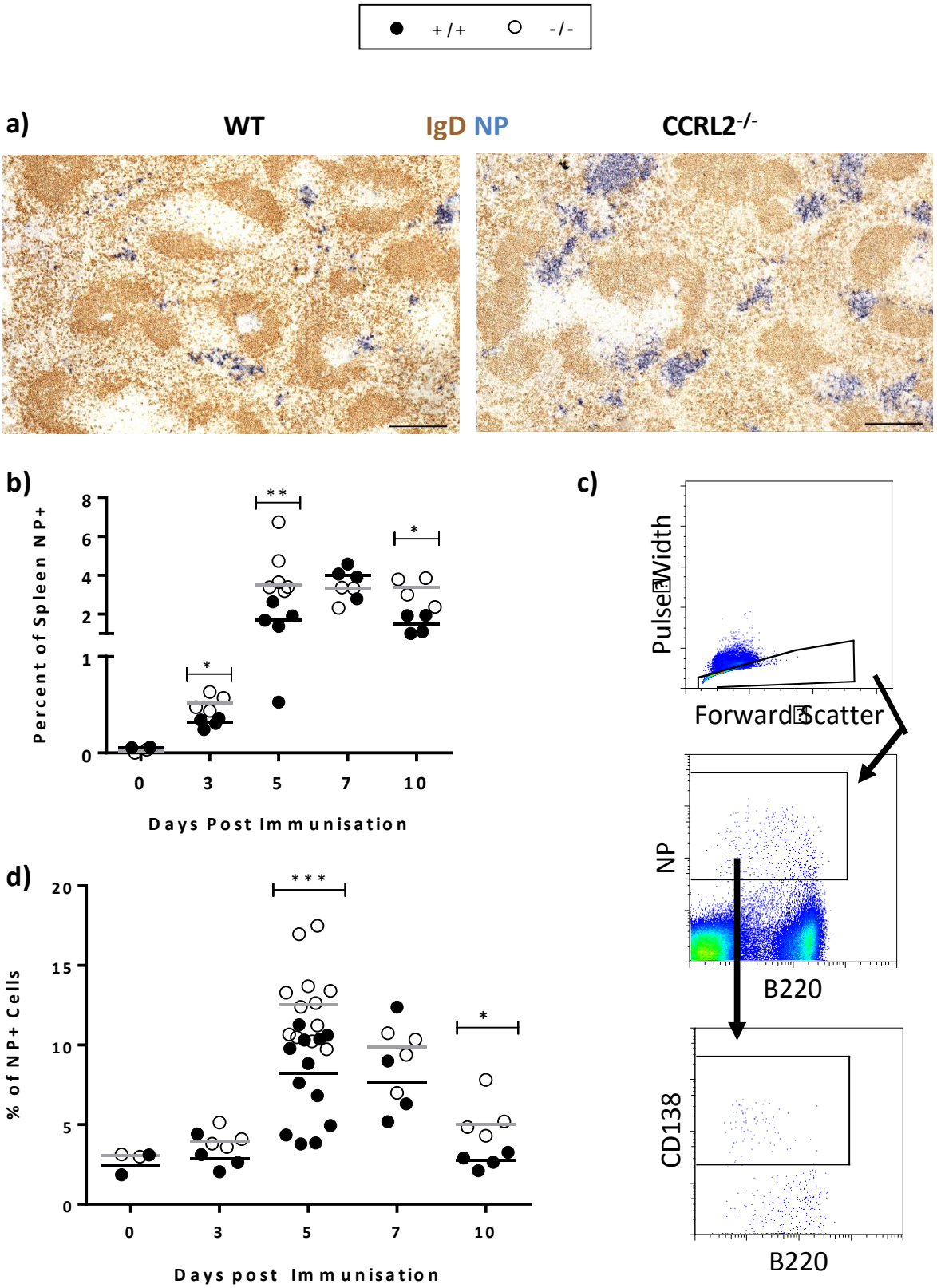

Figure 3.7. CCRL2 deficiency leads to increased plasma cell numbers in the spleen upon immunisation with NP-Ficoll. WT or CCRL2$^{-/-}$ mice were immunised with the TI-II antigen NP-Ficoll and spleens were processed to determine the plasma cell response; a) Spleens were sectioned and stained for NP-specific plasma cells (blue), representive image taken from day 5 of the response; b) The percentage of NP^{+} plasma cells over the whole spleen section was quantified (also see figure 3.15); c-d) Flow cytometric analysis of plasma cell levels upon NP-Ficoll immunisation c) Example gating; d) Flow cytometry results.
Experiments performed once (b and d days 3,7,10) twice (b day 5) or three times (d day 5). Bars indicate median
Scale bar - 250µm; ***p<0.001, **p<0.01, *p<0.05

69

of CCRL2 deficient mice is due to an increase in the levels of NP-specific plasmablasts in these mice.

3.4.3 CCRL2 deficiency does not affect the response to NP-Ficoll in quasimonoclonal mice

"Quasimonoclonal" (QM) mice are mice with a targeted insertion of an unmutated rearranged immunoglobulin heavy chain VDJ combination from an NP-specific BALB/c plasma cell (Cascalho et al., 1996). These mice are also kappa light chain deficient, as anti-NP antibodies are produced with the heavy chain in combination with the lambda light chain (Cascalho et al., 1996). Due to the high number of NP-specific cells, these mice have a rapid and strong response to NP-Ficoll. WT or CCRL2$^{-/-}$ QM mice (hereafter known as QM^{WT} and QM^{KO} respectively) were immunised with NP-Ficoll and the response analysed at 4 hours and 2, 3, 4 and 5 days post immunisation. Levels of NP-specific IgM (figure 3.8a) and IgG3 (figure 3.8b) were determined by ELISA. In some cases, low levels of IgM were detectable from 2 days post immunisation, however large amounts of IgM were detectable from day 3. Unsurprisingly, IgM then increased to day 5, however there was no difference in IgM levels between QM^{WT} and QM^{KO} mice at any time point. Conversely, NP-specific IgG3 was only detectable at 5 days post immunisation. As with IgM, there was no difference in IgG3 levels between QM^{WT} and QM^{KO} immunised mice.

Upon immunisation with NP-Ficoll, CCRL2 deficient mice have increased plasmablast levels in the spleen compared to WT mice (figure 3.7). Therefore, although no difference in antibody titres was detected, splenic levels of plasmablasts in QM^{WT} and QM^{KO} mice was measured by flow cytometry (days 2, 3 and 5) and antibody secreting cells measured by ELISpot (day 5 only) (figures 3.8c and 3.8d, respectively). At each time point, there

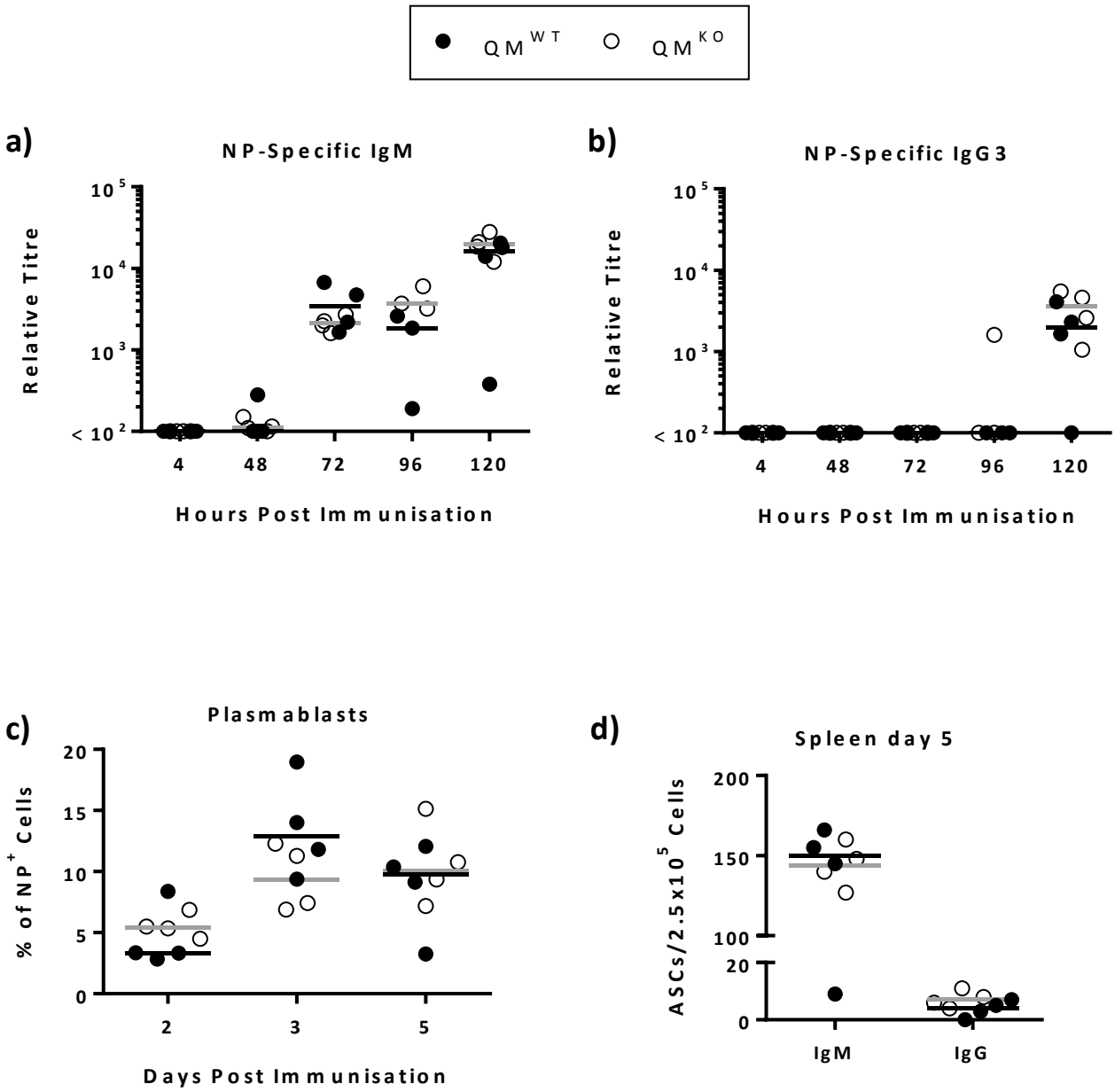

Figure 3.8. The NP-Ficoll response in QM mice is unaffected by a loss of CCRL2. WT or CCRL2$^{-/-}$ QM mice (QM^{WT} and QM^{KO}, respectively) were immunised with NP-Ficoll and the NP-specific response analysed over time; a-b) Levels of NP-specific a) IgM and b) IgG3 in the blood of immunised mice; c) splenic plasmablasts number as determined by flow cytometry; d) Splenic antibody secreting cells as determined by ELISpot.
Data from single experiment. Bars indicate median
< indicates antibody levels in the sample were under the lowest detection limit

was a large spread in the proportion of plasmablasts as determined by flow cytometry, however there was no difference in the proportions between QM^{WT} and QM^{KO} mice. On day 5, the levels of both IgM and IgG secreting cells in the spleen was also consistent between QM^{WT} and QM^{KO} mice. Therefore, there is no difference in the NP-Ficoll response of QM^{WT} and QM^{KO} mice, despite an improved IgM response detected between WT and $CCRL2^{-/-}$ mice.

3.4.4 Determining the cell type responsible for increased antigen-specific antibody post TI-II immunisation in CCRL2 deficient mice

3.4.4.1 Increased levels of NP-specific antibody in $CCRL2^{-/-}$ mice is haematopoietic cell intrinsic

As shown earlier (figure 3.5), CCRL2 is upregulated on plasma cells, however the receptor is also highly expressed on multiple cell types including macrophage – CCRL2 is also known as CRAM, Chemokine Receptor on Activated Macrophage. Furthermore, a recent publication has shown a functional presence of the receptor on endothelial cells (Monnier et al., 2012). To determine whether the increase in serum antibody is due to CCRL2 deficiency on haematopoietic cells, or whether it is caused by CCRL2 deficiency within the cellular microenvironment (including endothelial cells), bone marrow chimeras were generated. Four groups of mice were created (Methods figure 2.1), with two WT control groups to ensure any differences detected in antibody titre is an effect of CCRL2 deficiency, and not inherent differences in the antibody response between the two mouse strains used (C57BL/6 and BoyJ). BoyJ mice were used as controls in this experiment due to the expression of the CD45.1 allele, compared to CD45.2 in C57BL/6 mice; this congenic marker can be used to identify transferred cells. To ensure the

success of the irradiation and transplant, mice were tail bled 6 weeks post-transplant and the blood was analysed by flow cytometry for B cell markers along with the two CD45 alleles. As figure 3.9a shows, the transplant was successful for all mice in each group - the B cells in the blood were all of the donor CD45 allele and no host B cells survived. Therefore, ten weeks post-transplant the mice were immunised with NP-Ficoll and the antibody response analysed on day 7.

Transfer of cells from C57BL/6 mice into BoyJ hosts produced higher IgM antibody levels than transfer of BoyJ into C57BL/6 hosts, regardless of CCRL2 genotype (figure 3.9b). This indicates that B cells of mice on a C57BL/6 background have better antibody responses to NP-Ficoll than B cells from mice of a BoyJ background. Transfer of CCRL2$^{-/-}$ cells into BoyJ hosts caused a small increase in NP-specific IgM compared to C57BL/6 cell transfer, although this was not significant. Likewise, there was no difference in NP-specific IgM when BoyJ cells were transferred into BoyJ or CCRL2$^{-/-}$ hosts. As with NP-specific IgM, there were no differences in NP-specific IgG1 when either the environment or the haematopoietic cell populations were CCRL2 deficient (figure 3.9c).

Unlike IgM, NP-specific IgG3 titres significantly increased when CCRL2$^{-/-}$ cells were transferred into BoyJ hosts, compared to C57BL/6 cell transfer (figure 3.9d). Interestingly, in comparison to BoyJ transfer into a C57BL/6 environment, BoyJ transfer into a CCRL2$^{-/-}$ environment slightly reduced NP-specific IgG3 levels, even though there was no difference in IgG3 levels upon immunisation of WT and CCRL2$^{-/-}$ mice (figure 3.6b). The reason for this discrepancy could be the response levelling out when both environment and haematopoietic cells are CCRL2 deficient. As seen previously, flow cytometric analysis showed an increase in NP-specific antibody levels correlated with a

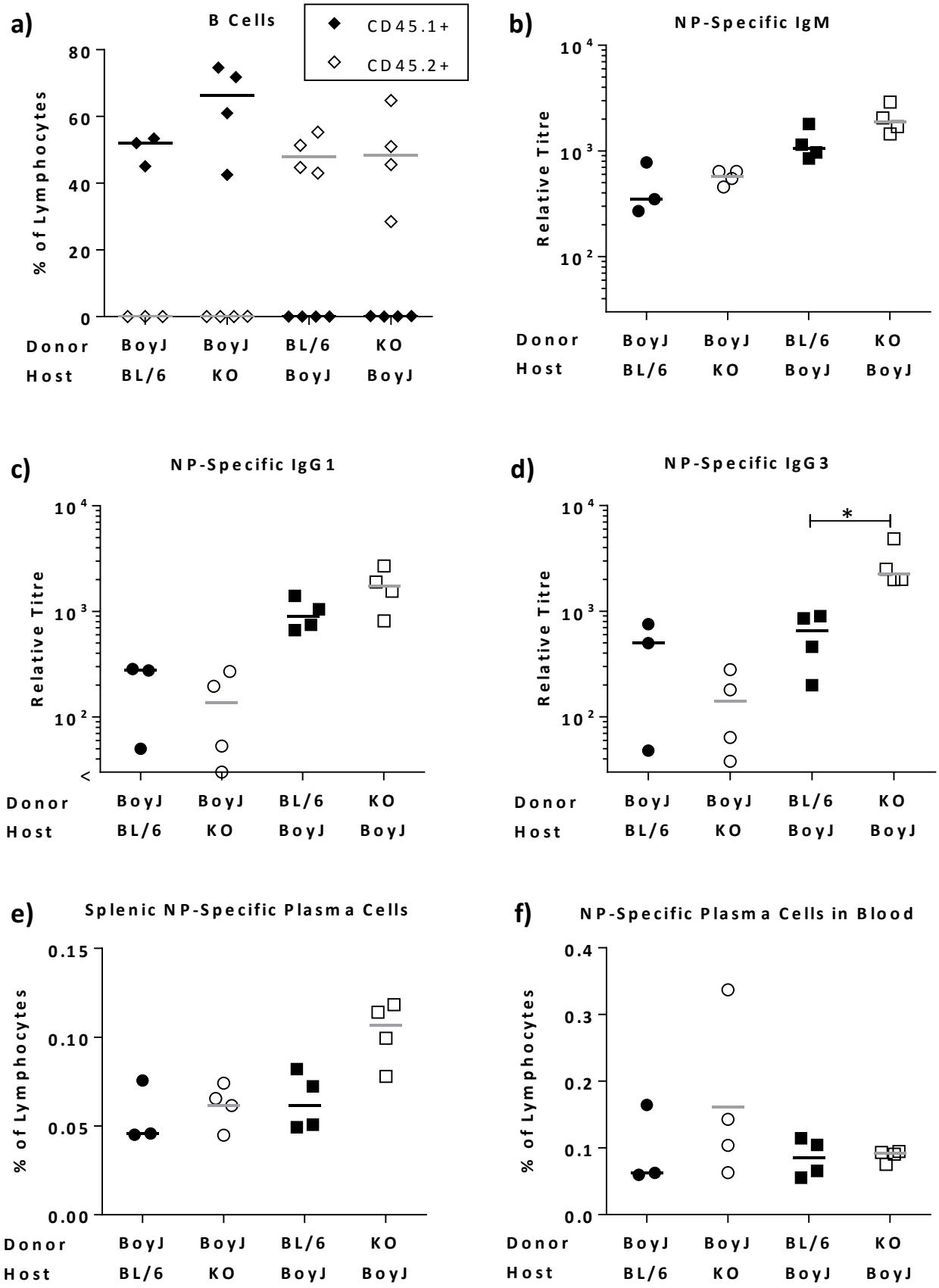

Figure 3.9. Increased NP-specific antibody levels in CCRL2 deficient mice is haematopoietic cell intrinsic. Generated bone marrow chimeras were immunised with NP-Ficoll and the antibody response analysed on day 7; a) Analysis of B cells by flow cytometry indicates bone marrow transplant successful; b-d) Levels of antigen specific b) IgM, c) IgG1 and d) IgG3 in blood of immunised chimeras; e-f) Flow cytometric analysis of antigen specific plasma cell levels in e) Spleen and f) Blood of immunised chimeric mice.
Key: BL/6 – C57BL/6 WT; BoyJ – BoyJ WT; KO- CCRL2$^{-/-}$; *p<0.05; Bars indicate median
< indicates antibody levels in the sample were under the lowest detection limit
Data from single experiment.

74

slight increase in splenic antigen-specific plasma cells, however this was not significant (figure 3.9e). There was also no difference in the numbers of antigen-specific plasma cells within the blood between any of the groups (figure 3.9f).

3.4.4.2 Increased levels of NP-specific antibody in CCRL2$^{-/-}$ mice is B cell intrinsic

Bone marrow chimeras of WT and CCRL2 deficient mice suggest that increased levels of antigen-specific antibody upon immunisation of CCRL2 deficient mice with NP-Ficoll is a haematopoietic cell effect. As CCRL2 is upregulated upon plasmablast differentiation (figure 3.5), it was examined whether the phenotype is B cell intrinsic. For this purpose, CD45.2^{+} WT or CCRL2 deficient NP-specific B cells (hereafter known as QM^{WT} and QM^{KO}, respectively) were isolated by MACS and adoptively transferred into CD45.1-expressing WT BoyJ mice, to enable the transferred cells to be distinguished from the host. One day later the mice were immunised with NP-Ficoll and the response was assessed at day 4 (figure 3.10). BoyJ mice which received QM^{KO} B cells had 9-fold greater levels of NP-specific IgM in the blood compared to BoyJ mice which received QM^{WT} B cells ($p<0.05$ figure 3.10a). Due to allotypic variation, NP-specific antibody produced by QM cells (IgM^{a}) can be distinguished from the antibody produced by the host (IgM^{b}). As with total IgM, levels of NP-specific IgM^{a}, were also greater in mice which had received QM^{KO} B cells ($p<0.01$ figure 3.10b). Surprisingly, this difference was less pronounced than the difference seen in total IgM; mice receiving QM^{KO} cells only having approximately 3 fold higher levels of IgM^{a}. This variation is likely to reflect alternative ELISA protocols for the detection of the two antibodies. However, the discrepancy may also be due to variation in host-produced IgM^{b}. To assess whether host IgM was altered in QM^{KO} recipients, IgM^{b} was also measured (figure 3.10c). Surprisingly, levels of IgM^{b} were higher in mice that

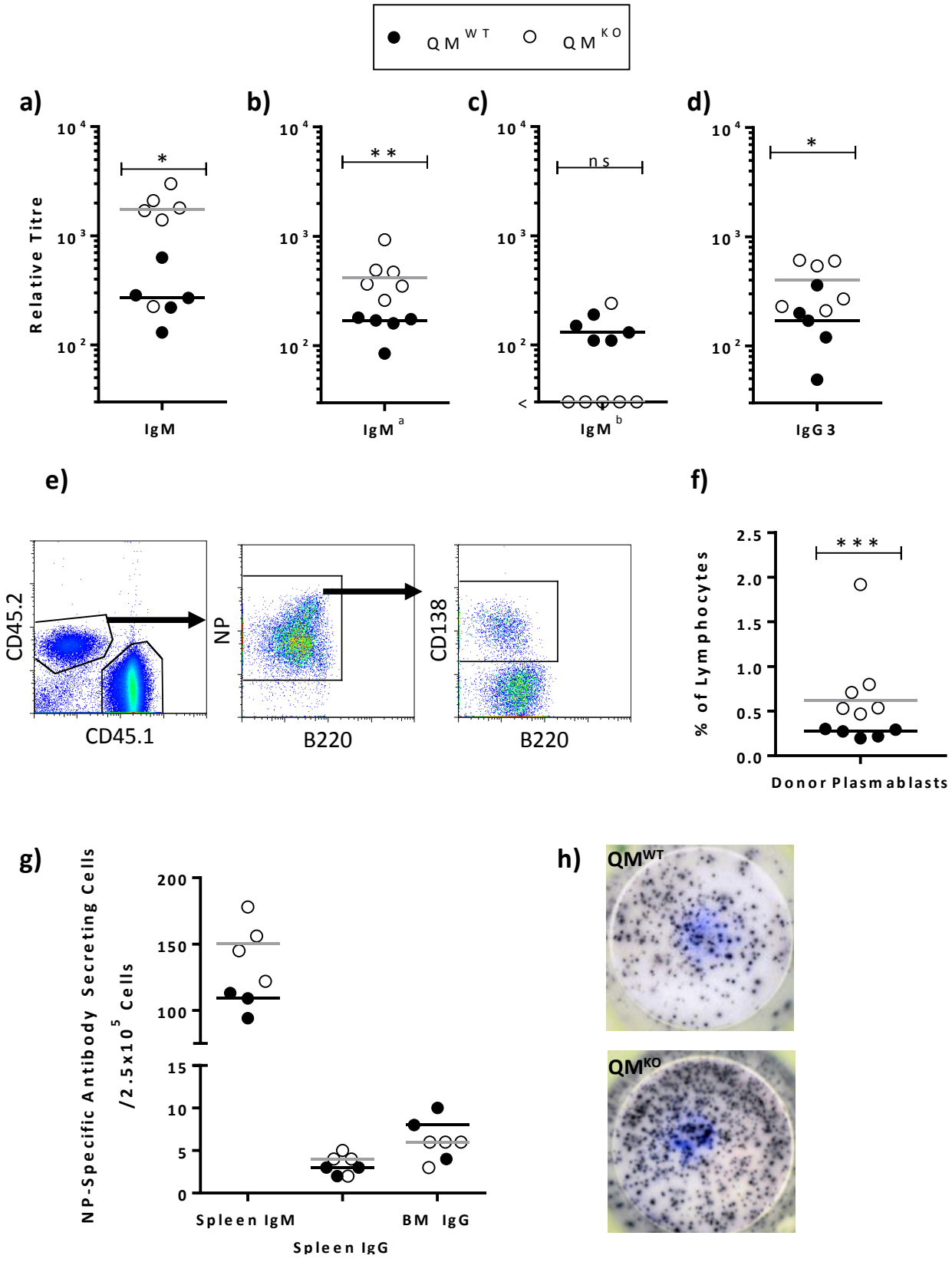

Figure 3.10. Increased NP-specific antibody levels in CCRL2 deficient mice is B cell intrinsic. NP-specific QM^{WT} or QM^{KO} B cells were transferred into BoyJ (WT) hosts and the response to NP-Ficoll analysed on day 4; a-d) Levels of NP-specific a) IgM, b) IgM^a, c) IgM^b and d) IgG3 in blood of immunised mice; e-f) Numbers of NP-specific antibody secreting cells in spleen as determined by flow cytometry, e) Example gating; f) Flow cytometry results; g) Levels of antibody secreting cells in the spleen and bone marrow (BM) as determined by ELISpot; h) Example of wells from splenic IgM ELISpot.
Data pooled from two independent experiments (a-f) or from one experiment (g-h). Bars indicate median
***p<0.001, **p<0.01, *p<0.05
< indicates antibody levels in the sample were under the lowest detection limit

76

received QM^{WT} cells than those which received QM^{KO} cells, with IgM^b largely not detected in the latter. This suggests that CCRL2 deficiency in some B cells negatively affects the performance of other, CCRL2 sufficient cells. As with IgM, levels of IgG3 switched antibody was three-fold greater in mice that received QM^{KO} cells ($p<0.05$, figure 3.10d). This increase in NP-specific antibody correlated with more than double the levels of NP-specific plasmablasts in the spleens of QM^{KO} recipient mice, as determined by flow cytometry ($p<0.001$, figure 3.10f). The flow cytometry data was supported by ELISpot as more IgM secreting cells were detected in QM^{KO} recipients, however this was not significant due to low sample numbers (figure 3.10g). However, splenic and bone marrow IgG secreting cells were similar amongst QM^{WT} and QM^{KO} recipients.

The transfer of QM^{WT} and QM^{KO} cells into WT hosts indicates that CCRL2-expressing plasmablasts are responsible for the increased antibody observed in $CCRL2^{-/-}$ mice upon immunisation with NP-Ficoll. Moreover, it is possible that CCRL2-deficient plasmablasts are able to suppress, or out-compete, CCRL2 sufficient plasmablasts.

3.4.4.3 CCRL2 deficiency in non-B cells does not affect the NP-specific antibody response in $CCRL2^{-/-}$ mice

Although data from the previous section indicated that the increase in antigen-specific antibody in $CCRL2^{-/-}$ mice is B cell intrinsic, it could be argued that bone marrow chimeras show that a deficiency of CCRL2 in the environment is detrimental to the response (figure 3.9). To determine whether CCRL2 deficiency in non-B cells affects the observed phenotype, QM^{WT} or QM^{KO} NP-specific B cells were transferred into either $CCRL2^{+/-}$ or

CCRL2$^{-/-}$ littermates, and the NP-specific antibody response analysed on day 4 post immunisation with NP-Ficoll.

As observed in section 3.4.4.2, in both CCRL2$^{+/-}$ and CCRL2$^{-/-}$ host mice, transfer of QM^{KO} B cells leads to a significant increase in NP-specific IgM (6-fold), IgG3 (10-fold) and IgM^{a} (5-fold) compared to the transfer of QM^{WT} B cells ($p<0.05$, figure 3.11). However, there is no difference in the NP-specific antibody response upon transfer of QM^{WT} into either CCRL2$^{+/-}$ or CCRL2$^{-/-}$ mice. Likewise, there is no difference when comparing the NP-specific antibody response of CCRL2$^{+/-}$ and CCRL2$^{-/-}$ mice that have received QM^{KO} B cells. This data confirms that any minor differences detected in the bone marrow chimera experiment are an artefact, and there is no role for CCRL2 in non-B cells upon NP-Ficoll immunisation in either a positive or negative manner.

3.4.5 Kinetics of the CCRL2 deficient response to NP-Ficoll

CCRL2 mRNA is upregulated in plasmablasts (figure 3.5), and previous data from J. Marshall suggests that CCRL2 mRNA is upregulated early within plasmablast differentiation (Marshall, 2009). To determine at what stage in the response there are detectable positive effects of CCRL2 deficiency in B cells, QM^{WT} or QM^{KO} cells were transferred into congenic hosts, which were immunised with NP-Ficoll one day later. The response was then analysed on days 2-4 post immunisation. NP-specific IgM was detectable in most samples at day 3 post immunisation, and even at this early time point QM^{KO} recipients appeared to have a slight advantage (figure 3.12a). However, significantly higher levels of NP-specific IgM in QM^{KO} recipients was not observed until

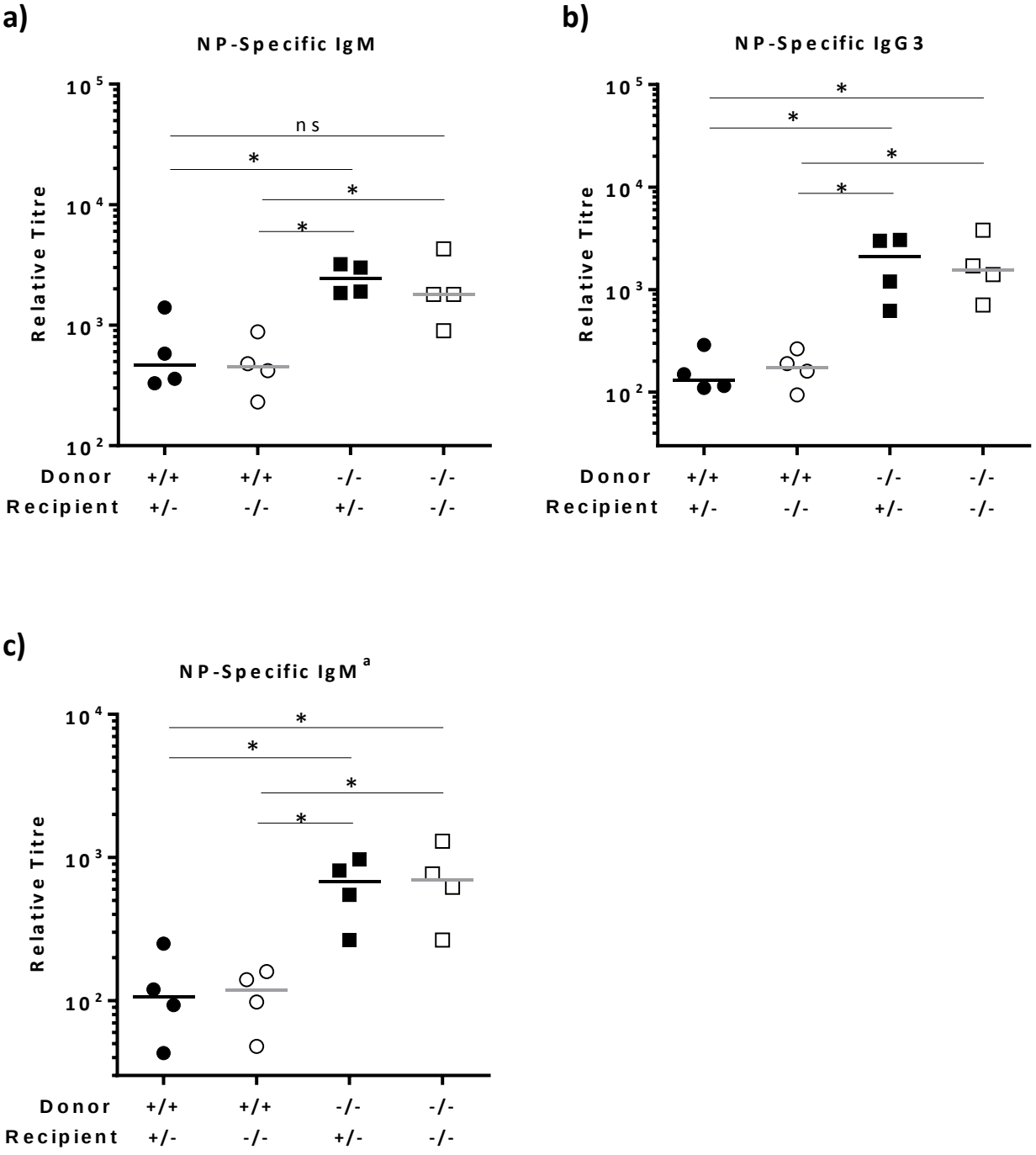

Figure 3.11. CCRL2 deficiency in non-B cells does not affect the antibody response. QM^{WT} or QM^{KO} B cells were transferred into either $CCRL2^{+/-}$ or $CCRL2^{-/-}$ hosts. A day later, the hosts were immunised with NP-Ficoll and the response was analysed on day 4; a-c) Levels of NP-specific a) IgM, b) IgG3 and c) IgM^a in blood of immunised mice as determined by ELISA.
Data from single experiment. Bars indicate median
*$p<0.05$

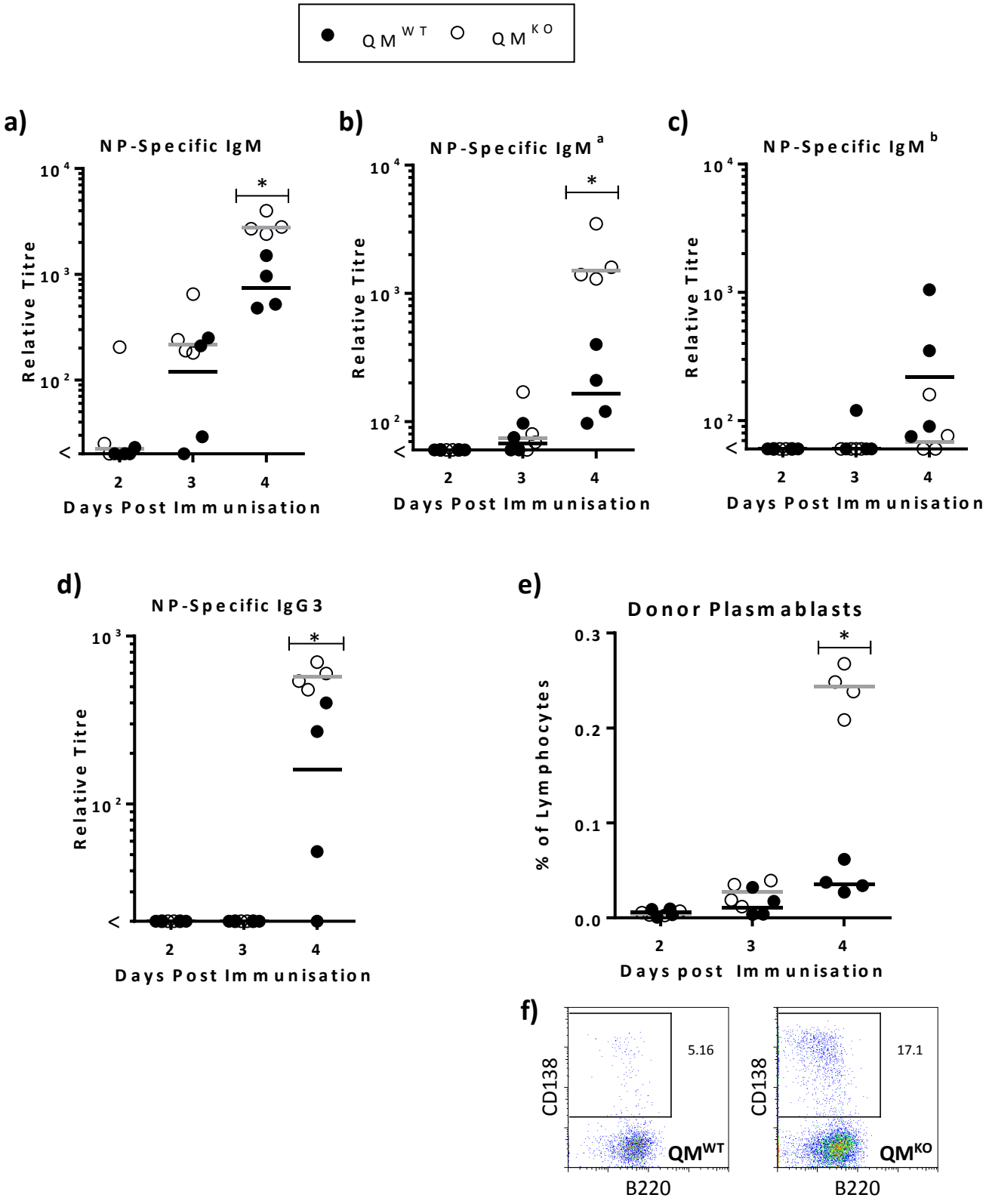

Figure 3.12. Kinetics of early NP-Ficoll response by WT and CCRL2 deficient B cells. NP-specific B cells from QM^{WT} or QM^{KO} mice were isolated and transferred into WT BoyJ hosts. A day later hosts were immunised with NP-Ficoll and the response analysed on days 2, 3 and 4 post immunisation; a-c) Levels of NP-specific a) IgM, b) IgM^a, c) IgM^b and d) IgG3 in blood of immunised mice; e-f) Flow cytometric analysis of donor NP-specific plasmablasts, e) Donor specific plasmablasts over time, f) Day 4 donor plasmablasts flow cytometry example.
Data from single experiment. Bars indicate median
*p<0.05
< indicates antibody levels in the sample were under the lowest detection limit

day 4 ($p<0.05$). Interestingly, unlike IgM, IgM^a was not detectable at high levels in most samples until day 4 post immunisation (figure 3.12b), with no advantage in QM^{KO} transferred cells detectable at day 3. However, as observed previously, at day 4 QM^{KO} cells produced 10x more IgM^a ($p<0.05$). Previous experiments suggested that QM^{KO} transferred cells out compete host plasmablasts, with little detectable IgM^b in mice that received CCRL2 deficient cells. In agreement with this, mice which received QM^{WT} cells do have a slight, but not significant, advantage on day 4 post immunisation but there is no detectable host antibody at earlier time points (figure 3.12c). NP-specific IgG3 switched antibody was not detectable until day 4, and at this time point 3-fold higher levels were observed in QM^{KO} recipients ($p<0.05$, figure 3.12d). Correlating with this, NP-specific plasmablasts were 2-fold, but not significantly higher in the spleens of QM^{KO} recipients at day 3 which increased to 5 times higher at day 4 post immunisation ($p<0.05$, figure 3.12e-f). Together, this shows that CCRL2 deficiency affects the plasmablast response at low levels from day 3, at the point of plasmablast differentiation. However, large effects in the response are detectable at day 4 post immunisation, when plasmablasts have expanded to greater levels.

3.5 Investigation into the mechanism of increased antibody levels in CCRL2 deficient mice upon NP-Ficoll immunisation

3.5.1 Antigen location to, and within, the spleen is unaffected by CCRL2 deficiency

In 2010, Otero *et al.* showed that $CCRL2^{-/-}$ mice have defects in trafficking of antigen loaded dendritic cells to the mediastinal lymph node (Otero et al., 2010). To determine whether CCRL2 deficiency affects antigen transport, WT and $CCRL2^{-/-}$ mice were

immunised with NP-FITC-Ficoll, a fluorescent version of the NP-Ficoll antigen, and after 4 hours its location within the spleen was analysed by immunofluorescence. Previous work has shown that in WT mice, 4 hours post immunisation the antigen is located within marginal zone macrophages (MZM, $CD169^{+}$ (Vinuesa, 2000)). Analysis of antigen deposition 4 hours post injection showed no obvious differences between WT and CCRL2 deficient mice in the location of NP-FITC-Ficoll in the splenic marginal zone (figure 3.13a). As antigen location was not affected by CCRL2 deficiency, it was determined whether the amount of antigen transported to the spleen was altered in the $CCRL2^{-/-}$ mouse. A semiquantitative fluorescent microscopic analysis of the $FITC^{+}$ signal per area of MZM across the entire spleen section showed that the amount of antigen within the spleen was similar between WT and $CCRL2^{-/-}$ mice (figure 3.13b). Unfortunately, WT control mice showed a large variability in the amount of marginal zone antigen deposition. Consequently, there is no evidence that the amount of antigen which is entering the spleen is affected by CCRL2 deficiency. This supports evidence from previous sections, which suggest that CCRL2 does not influence the NP-Ficoll response until the appearance of plasmablasts and therefore after the appearance of antigen in the spleen of immunised mice.

3.5.2 Splenic location of CCRL2 deficient activated B cells and plasmablasts

CCRL2 is an atypical chemoattractant receptor. Therefore it is possible that without CCRL2, the location of plasmablasts within the spleen is affected which may explain the increase in plasmablasts in CCRL2 deficient mice. To address this, the location of CCRL2 deficient cells in the spleen of mice was determined by immunohistology.

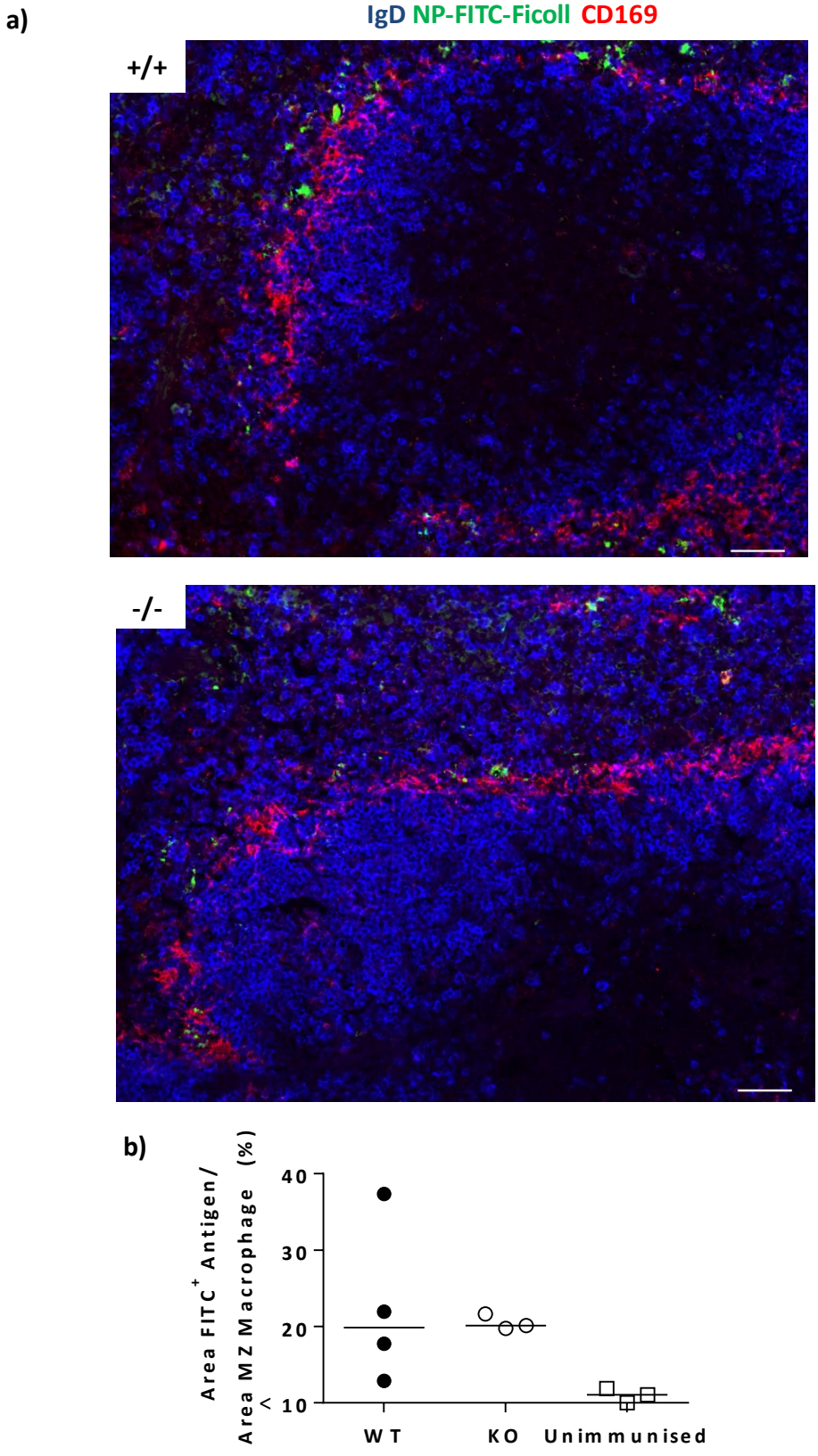

Figure 3.13. Antigen location to, and within, the spleen is not affected by CCRL2 deficiency. WT and CCRL2$^{-/-}$ mice were immunised with NP-FITC-Ficoll and antigen location was determined by immunohistology 4 hours post immunisation; a) Immunohistology examples, b) Quantification of antigen in spleen from immunohistology sections.
Representative sections from at least 3 mice per group. Data from single experiment.
Bars indicate median
Scale Bar - 25µm

83

3.5.2.1 Location of splenic activated B cells early in the response is not affected by CCRL2 deficiency

To determine the location of CCRL2 deficient cells early in the NP-Ficoll response, $CD45.2^+$ NP-specific WT or $CCRL2^{-/-}$ B cells (hereafter known as QM^{WT} and QM^{KO}, respectively) were isolated by MACS and transferred into WT $CD45.1^+$ BoyJ hosts. One day later, hosts were immunised with NP-Ficoll and spleens were sectioned on days 2, 3 and 4 post immunisation. Donor cell location was determined by staining for $CD45.2^+$ cells relative to IgD^+ B cell follicles and $CD11c^+$ dendritic cells (figure 3.14). The latter was chosen due to the association between dendritic cells and plasmablast survival (Garcia De Vinuesa et al., 1999a).

On day 2 post immunisation activated B cells were resident along the B cell follicle-T zone border (T-B border). Some cells were located amongst $CD11c^+$ areas, whilst a few cells were detected within the red pulp. Each individual donor cell is isolated and there was no evidence of donor cells interacting with each other. CCRL2 deficiency did not affect the location of the cells at this time point, as all of these locations were seen within spleens of both QM^{WT} and QM^{KO} recipients.

By day 3 there had been an expansion of donor cells in both QM^{WT} and QM^{KO} recipients. As on day 2 of the response, these cells were all isolated and they were largely clustered at the T-B border, whilst some cells were still located within $CD11c^+$ areas. Unlike the response at day 2, a large number of donor cells had migrated back inside the follicle whilst a smaller number are found in the centre of the TZ. As at day 2, very small

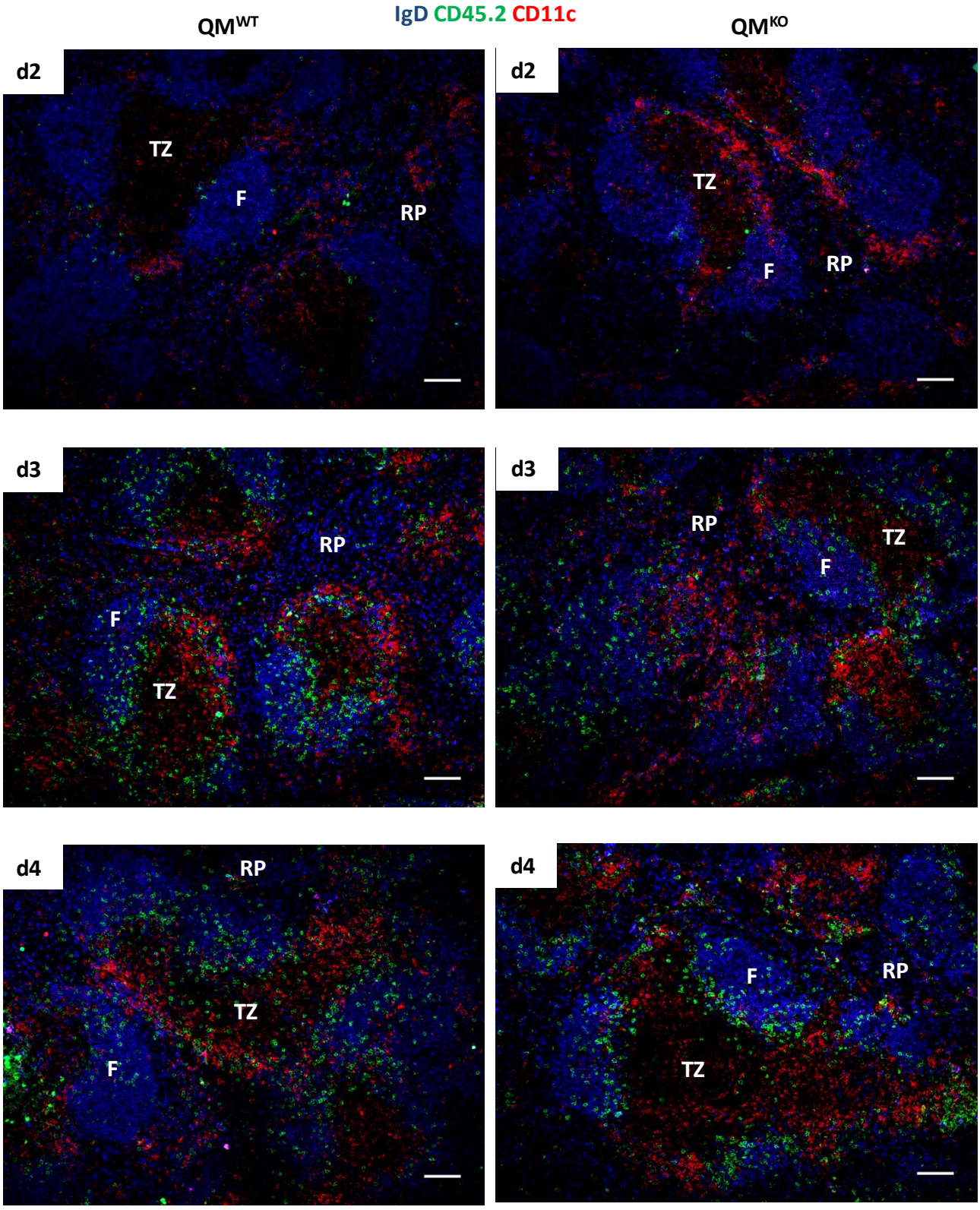

Figure 3.14. Early B cell migration is not affected by CCRL2 deficiency. CD45.2$^+$ QM^{WT} or QM^{KO} B cells were transferred into CD45.1$^+$ WT BoyJ hosts, and a day later hosts were immunised with NP-Ficoll. Spleens were sectioned days 2, 3 and 4 post immunisation and stained for IgD$^+$ B cell follicles (blue) CD11c$^+$ monocytes (red) and CD45.2$^+$ donor cells (green).
Key: d – Day; F – Follicle; RP – Red Pulp; TZ – T Zone.
Representative sections from 4 mice per group.
Scale Bar - 100µm

numbers of cells were also located within the red pulp. There are no obvious differences in the location of donor cells between QM^{WT} and QM^{KO} recipient mice.

Finally, on day 4 of the response, donor cells were at similar locations as seen on day 3. A large accumulation of B cells was apparent along the T-B border, with some cells within the follicle and a small number in the centre of the TZ. In both QM^{WT} and QM^{KO} samples plasmablast foci were visible, where large clusters of plasmablasts were detected amongst the red pulp.

Together, this suggests that the early migration of activated cells is not affected by CCRL2 deficiency.

3.5.2.2 Location of CCRL2 deficient plasmablasts in the spleen is not affected by CCRL2 deficiency

In order to determine the location of CCRL2 deficient plasmablasts, WT and $CCRL2^{-/-}$ mice were immunised with NP-Ficoll and the spleens were sectioned and stained for plasmablast markers by immunohistochemistry (figure 3.7a and 3.15).

As shown by quantitative techniques (figure 3.7b), few plasmablasts are detectable in the spleen on day 3 post immunisation (figure 3.15). As expected, those that are present are mainly clustered together within the red pulp (black arrows). However some individual cells are present near white pulp "exit sites", between the follicles (blue arrows). This is true for both WT and $CCRL2^{-/-}$ mice. On day 5 plasmablast location is similar to that seen on day 3, where the majority are still resident within the red pulp or migrating out of white pulp exit sites (figure 3.7a). Although at day 5 plasmablasts have undergone

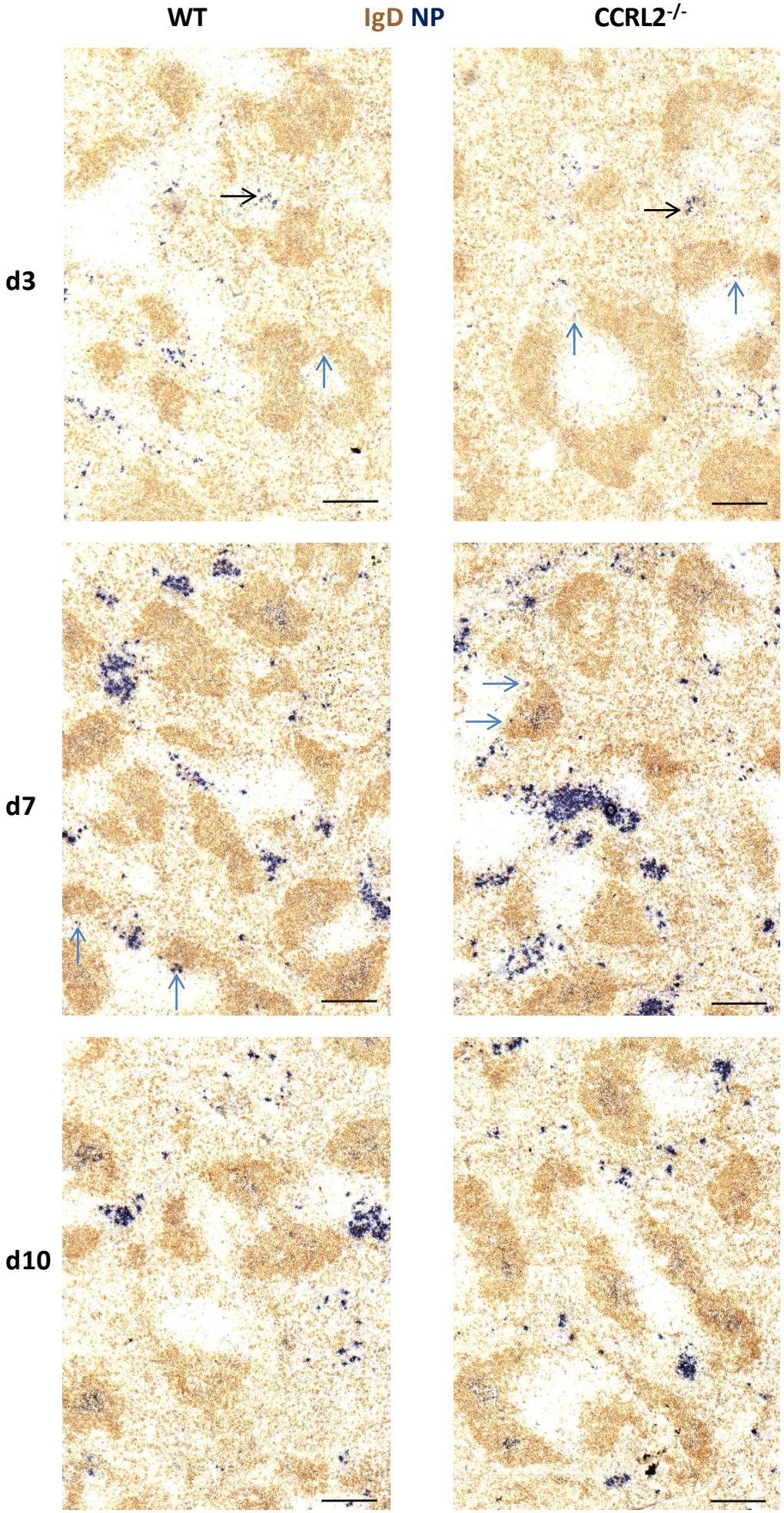

Figure 3.15. CCRL2 deficiency does not affect plasma cell location in the spleen. WT or CCRL2$^{-/-}$ mice were immunised with the TI-II antigen NP-Ficoll. Spleens were sectioned and stained for NP-specific plasma cells (blue) and IgD^{+} B cell follicles (brown) on days 3, 5, 7 and 10 post immunisation. Day 5 spleens are in figure 3.7. Black arrows indicate red pulp plasmablasts, blue arrows indicate cells at the T-B border.

Representative sections from 4 mice per group.

Key: d - Day
Scale bar – 200µm

extensive expansion, particularly in CCRL2 deficient mice, meaning that there are now large clusters of cells within the red pulp.

By day 7, although the plasmablast pool begins to contract, the location remains unchanged (figure 3.15). Foci of plasmablasts are detectable leaving the white pulp within interfollicular sites, with other clusters of plasmablasts within the red pulp itself. Interestingly plasmablasts are also detectable along the T-B border of the white pulp (blue arrows), but this is true in both WT and CCRL2 deficient spleens.

Finally, at day 10, plasmablasts levels are reduced further. Although the large cellular clusters detected at day 5 are still present, they are much smaller. Furthermore, they are generally located at the white pulp interfollicular sites rather than in the red pulp, which now contains many individual cells instead of large foci. At this time point, plasmablasts are no longer detectable along the T-B border.

3.5.3 mRNA analysis of CCRL2 deficient plasmablasts

As the increase in antibody levels in CCRL2 deficient mice is B cell intrinsic, whether this is due to intrinsic changes in the transcriptome of CCRL2$^{-/-}$ plasmablasts was examined. In order to address this, WT or CCRL2$^{-/-}$ NP-specific mice (hereafter known as QM^{WT} or QM^{KO}, respectively) were immunised with NP-Ficoll and NP-specific GC B cells (NP^{+}B220^{+}CD138^{-}CD38^{-}Fas^{+}) or NP-specific plasmablasts (NP^{+}B220$^{mid\text{-}lo}$ CD138^{+}) were sorted by FACS on day 3. cDNA prepared from the sorted cells was then analysed by RT-qPCR for expression of the plasmablast-associated genes BLIMP-1 and IRF4, and the ligands and receptors of the BAFF/APRIL system (figures 3.16c-d and 3.17).

First, to ensure the purity of sorted cells, some cells were run on a flow cytometer post sorting. Singlets were first gated, then NP^+ cells were selected before $CD138^+$ plasmablasts were taken. GC B cells were then sorted from the remaining $CD138^-$ B cells, as $GL7^+Fas^+$ (figure 3.16a). As shown in figure 3.16b, for both GC B cells and plasmablast samples, >92% of singlets were NP^+. Likewise, for purified plasmablasts, >91% of singlets were $CD138^+$, whereas less than 0.2% of cells in the GC B cell samples were $CD138^+$. The GC samples purity was slightly less, between 71 and 88%. cDNA was prepared from these purified samples and the various factors (listed below) analysed by RT-qPCR.

BLIMP-1 is a transcriptional repressor, and the master regulator of plasma cell fate. As shown in figure 3.16c, BLIMP-1 is not detectable in GC B cells, as expected. Interestingly however, BLIMP-1 expression appears slightly reduced in QM^{KO} plasmablasts compared to QM^{WT} plasmablasts, although this is not significant. IRF4 is a transcription factor which is also required for plasma cell differentiation and class switch recombination. IRF4 is expressed at high levels in both GC B cells and plasmablasts (figure 3.16d), however there are no differences in IRF4 expression between QM^{WT} and QM^{KO} cells.

BAFF and APRIL are ligands within the TNF superfamily that have multiple roles within B cell development and function. BAFF and APRIL bind to the receptors TACI and BCMA, with BAFF also binding BAFFR (figure 3.17a). Neither of the ligands are detectable at an mRNA level in either GC B cells or plasmablasts (figure 3.17b and c). Supporting this, BAFF is expressed within the GC, but GC BAFF is derived from T follicular helper cells not GC B cells (Goenka et al., 2014). Expression of BAFFR is relatively high in both GC B cells and plasmablast samples (figure 3.17d), however there is no difference in mRNA

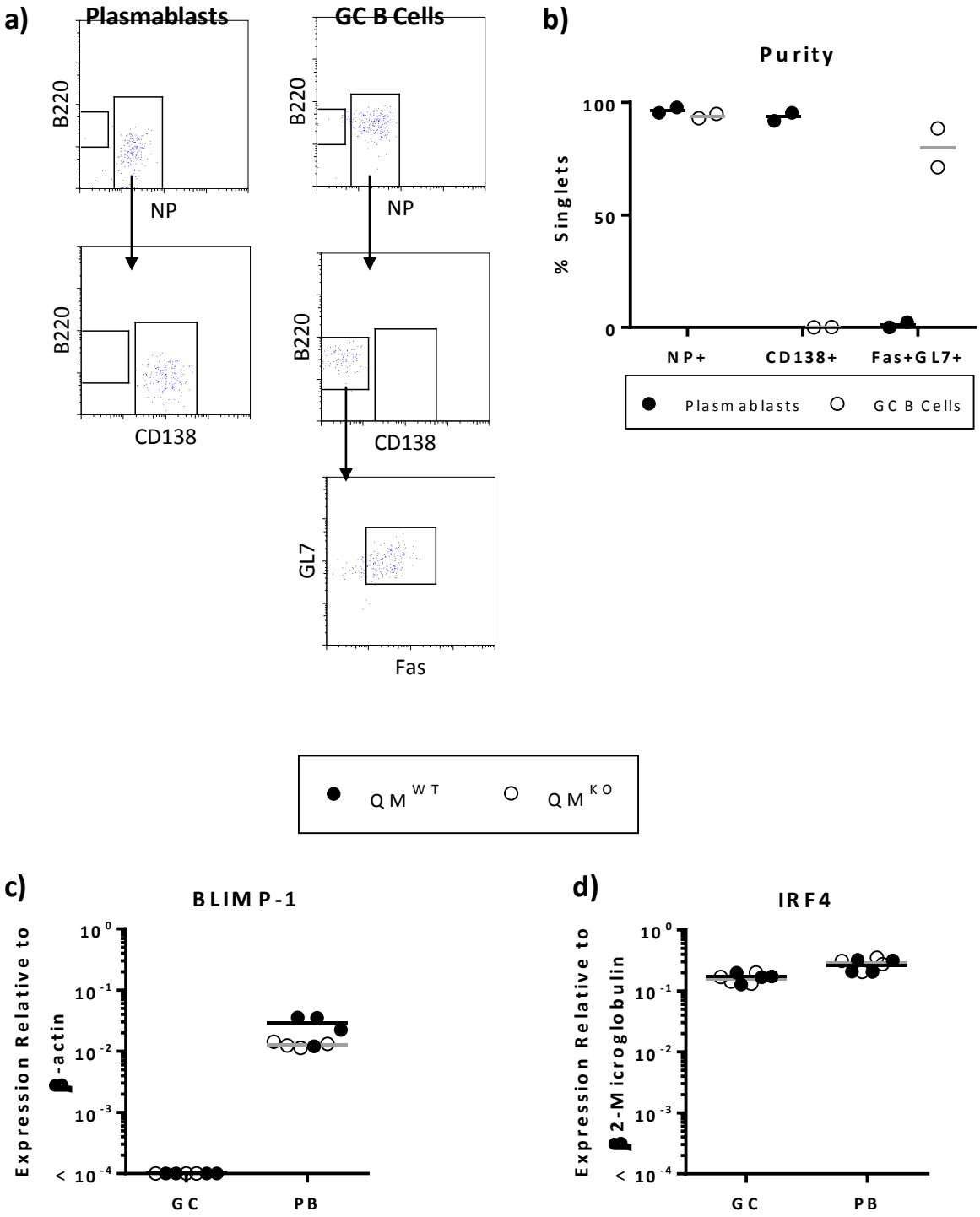

Figure 3.16. Purity of sorted cell samples and expression of plasmablast associated genes in WT and CCRL2 deficient B cells. QM^{WT} or QM^{KO} mice were immunised with NP-Ficoll and activated B cells were sorted on day 3 of the response; a-b) purity of sorted samples as determined by flow cytometry a) Gating strategy, b) Purity; c-d) After preparation of cDNA, expression of plasmablast associated mRNAs was determined by RT-qPCR, c)BLIMP-1 d) IRF4.
Key: GC – GC B Cells; PB – Plasmablasts
Data from single experiment. Bars indicate median
< indicates antibody levels in the sample were under the lowest detection limit

90

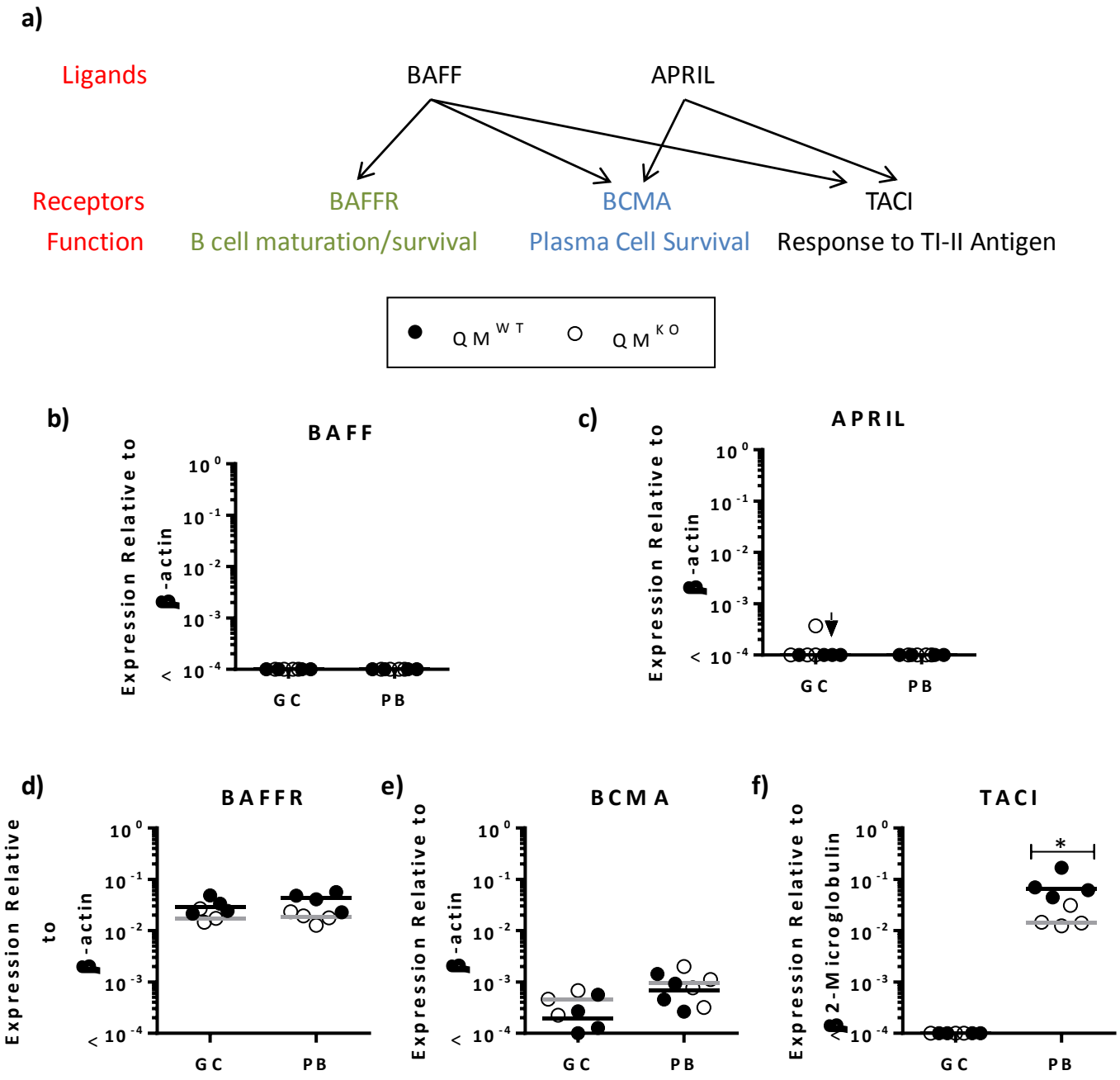

Figure 3.17. Expression of genes within the BAFF-APRIL system in WT and CCRL2 deficient B cells. a) Pictorial representation of the BAFF-APRIL system; b-f) QM^{WT} or QM^{KO} mice were immunised with NP-Ficoll and activated B cells were sorted on day 3 of the response and analysed for the mRNA expression of b) BAFF, c) APRIL, d) BAFFR, e) BCMA and f) TACI, by RT-qPCR.
Key: GC – GC B cells; PB – Plasmablasts
*$p<0.05$
Data from single experiment. Bars indicate median
< indicates mRNA levels in the sample were under the lowest detection limit

expression between QM^{WT} and QM^{KO} cells. In comparison, expression of BCMA mRNA is low in both samples, although it is slightly higher in plasmablasts than GC B cells (figure 3.17e). Again, the expression of BCMA is not affected by CCRL2 deficiency. Expression of the final receptor, TACI, was also determined by RT-qPCR. TACI was undetectable in both QM^{WT} and QM^{KO} GC B cells, but expressed at very high levels in plasmablasts (figure 3.17f). Interestingly, TACI levels were 3-fold higher in QM^{WT} plasmablasts compared to QM^{KO} plasmablasts ($p<0.05$).

Due to the role of TACI during thymus independent type 2 responses, protein levels of TACI were examined using immunohistology and flow cytometry (figure 3.18). Spleens were taken from QM^{WT} and QM^{KO} mice on day 3 of the NP-Ficoll response, and were sectioned and stained for TACI and NP (figure 3.18a). In the large plasmablast foci that have formed, TACI expression was more readily detectable in QM^{WT} spleens than QM^{KO}. Flow cytometry was conducted to quantitate TACI protein in the QM^{WT} and QM^{KO} plasmablasts. As expected, GC B cells from both genotypes had low TACI expression (figure 3.18b). However, TACI mean fluorescence intensity (MFI) of plasmablasts was equal in both QM^{WT} and QM^{KO} mice, on both day 3 and day 4 post immunisation. In order to determine whether this is true amongst protocols, TACI levels were determined on plasmablasts from cell transfer experiments, where QM^{WT} or QM^{KO} NP-specific cells were transferred into WT hosts, and hosts immunised a day later with NP-Ficoll. Again, protein levels of TACI were equal at each time point, irrespective of the plasmablast genotype (figure 3.18c).

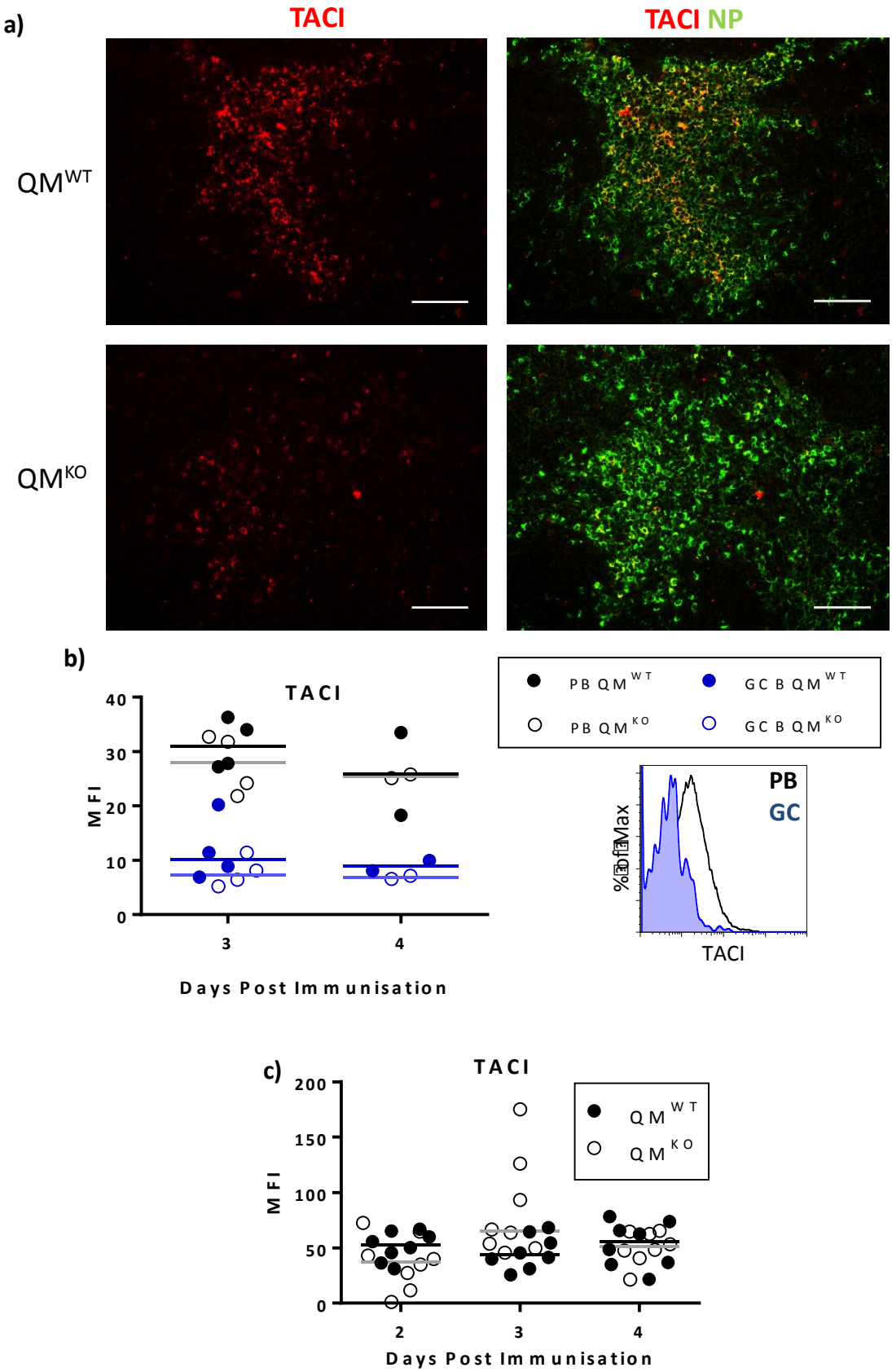

Figure 3.18. Expression of TACI at the protein level. a-b) QM^{WT} or QM^{KO} mice were immunised with NP-Ficoll and spleens were taken on day 3 of the response. TACI expression on NP^{hi} plasmablasts was detected by a) Immunohistology (Representative sections from 4 mice per group) and b) Flow cytometry; c) QM^{WT} or QM^{KO} NP-specific B cells were transferred into WT hosts and 24h later recipient mice were immunised with NP-Ficoll. TACI expression was determined by flow cytometry. Data pooled from single experiment (a-b) or two independent experiments (c). Bars indicate median
Key: PB – Plasmablasts. Scale bar - 100µm.

93

Together, this suggests that a reduction in TACI in QM-deficient plasmablasts post NP-Ficoll immunisation at the mRNA level is not reflected at the protein level by flow cytometry.

3.5.4 CCRL2$^{-/-}$ plasmablasts proliferate more and undergo less apoptosis than CCRL2 sufficient plasmablasts

To determine why there are greater numbers of plasmablasts in CCRL2 deficient mice, sections of spleens from WT or CCRL2$^{-/-}$ mice immunised with NP-Ficoll were stained for the proliferation marker Ki67 at day 5 post immunisation. Ki67 is a protein expressed in all active phases of the cell cycle, but it is not present in G0 (resting cells) (Scholzen and Gerdes, 2000). Day 5 post immunisation was chosen as this is when the difference in the response was at its highest (figure 3.6). Proliferating plasmablasts, which are double positive for NP^{hi} and Ki67, were counted and related to non-proliferating NP^{hi} plasmablasts (figure 3.19a). Approximately 25% of CCRL2$^{-/-}$ plasmablasts were Ki67^{+}, nearly two-fold higher than the WT average of 13%, however due to low sample numbers this difference was not significant (figure 3.19b).

To further assess plasmablast proliferation, EdU incorporation into proliferating plasmablasts was assessed *in vivo*. EdU is a thymidine analogue, and upon injection into mice, EdU is incorporated into cells which are undergoing DNA synthesis during the S phase of the cell cycle. An adoptive transfer was conducted where NP-specific WT or CCRL2$^{-/-}$ cells (hereafter known as QM^{WT} or QM^{KO}, respectively) were transferred into congenic hosts, and recipient mice were immunised a day later with NP-Ficoll. Previous reports have shown that during a primary splenic response to NP-Ficoll, small numbers of

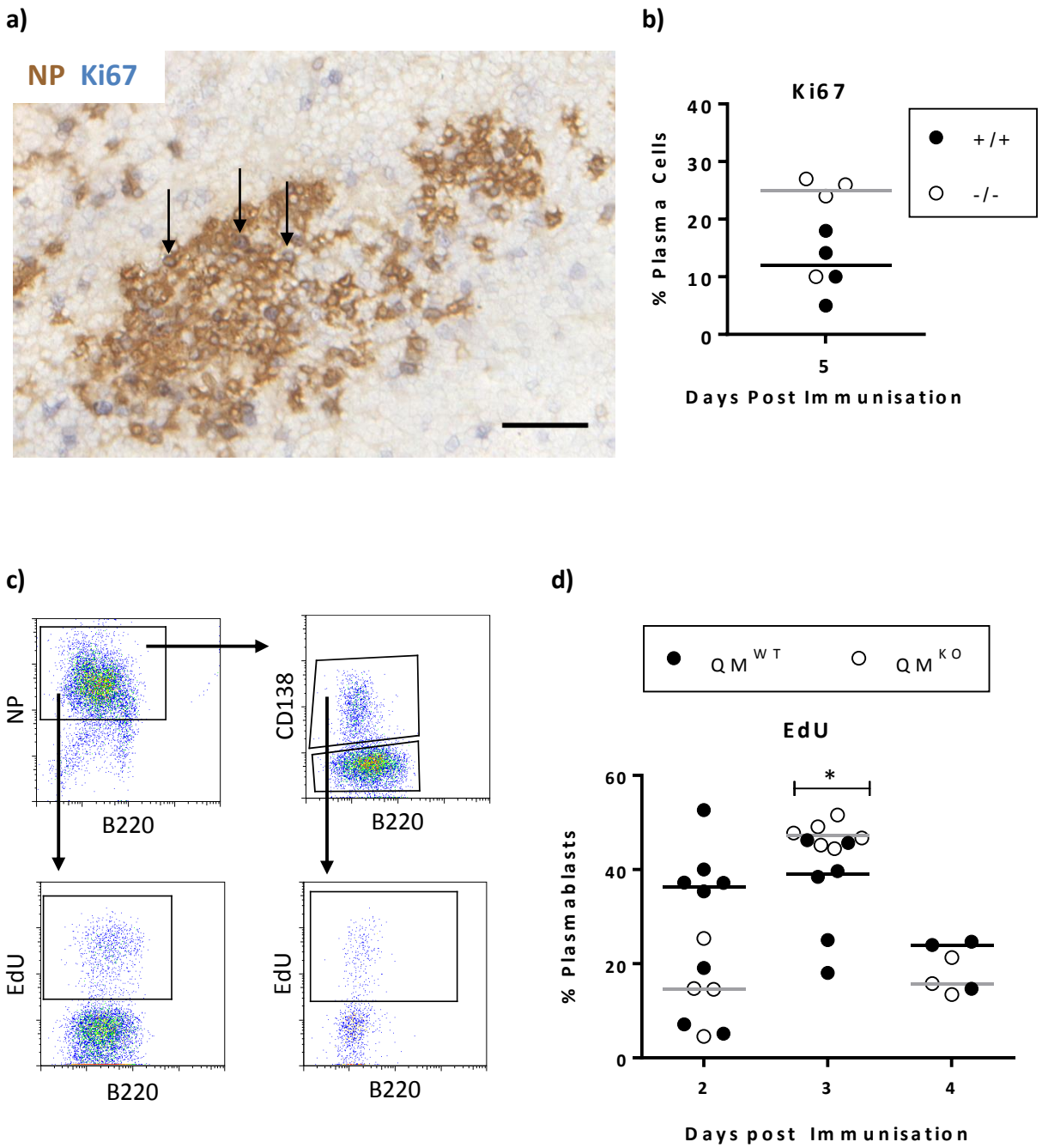

Figure 3.19. CCRL2$^{-/-}$ plasmablasts proliferate more than CCRL2 sufficient plasmablasts. a-b) WT and CCRL2$^{-/-}$ mice were immunised with NP-Ficoll and on day 5 post immunisation spleens were sectioned and stained for NP^{hi} plasmablasts and Ki67 a) Arrows indicate examples of NP^{hi} Ki67 positive plasmablasts; b) Percentage of NP^{hi} plasmablasts Ki67^{+}; c-d) QM^{WT} or QM^{KO} B cells were transferred into WT BoyJ hosts and a day later hosts were immunised with NP-Ficoll. 2h prior to culling, mice were injected with EdU and incorporation was assessed by flow cytometry; c) Flow cytometry gating, d) EdU^{+} plasmablasts.
Data from single experiment (b) or pooled from two experiments (d). Bars indicate median
Scale bar - 75µm
*p<0.05

95

antigen-specific B cells have already entered the S phase as early as 24 hours (Garcia de Vinuesa et al., 1999b). Therefore, on days 2, 3 and 4 post immunisation, two hours prior to culling, mice were injected with EdU and its incorporation into cellular DNA was analysed by flow cytometry (gating strategy shown in figure 3.19c). Unexpectedly, on day 2 post immunisation, a much higher proportion of QM^{WT} cells had incorporated EdU than QM^{KO} cells (~38% and ~18%, respectively, figure 3.19d), however this has not reached statistical significance. On day 3, there was an increase in the proportion of plasmablasts that were proliferating. Interestingly, there was a small, but significant increase in the proportion of EdU^{+} QM^{KO} plasmablasts relative to EdU^{+} QM^{WT} plasmablasts (50% to 40%, respectively, $p<0.05$), showing a greater proportion of QM^{KO} plasmablasts were actively proliferating. However, by day 4 the proportion of plasmablasts which were proliferating declined dramatically for both genotypes, however, there are too few samples for any accurate conclusions to be made at this time point.

Although this data shows a greater propensity for proliferation by plasmablasts deficient in CCRL2, at days 2 and 4 a greater proportion of QM^{WT} cells were actively proliferating. To determine whether apoptosis also plays a role in the greater proportion of QM^{KO} plasmablasts, the apoptotic capacity of transferred cells was also assessed by flow cytometry. It has previously been shown that $CCRL2^{-/-}$ cells may also be less prone to cell death (Douglas et al., 2013). Splenic plasmablasts were stained for Annexin V and 7-Aminoactinomycin D (7-AAD) for flow cytometry analysis on days 2, 3 and 4 (figure 3.20a). Annexin V is a probe which binds phosphatidylserine (PS) and phosphatidylethanolamine (PE).

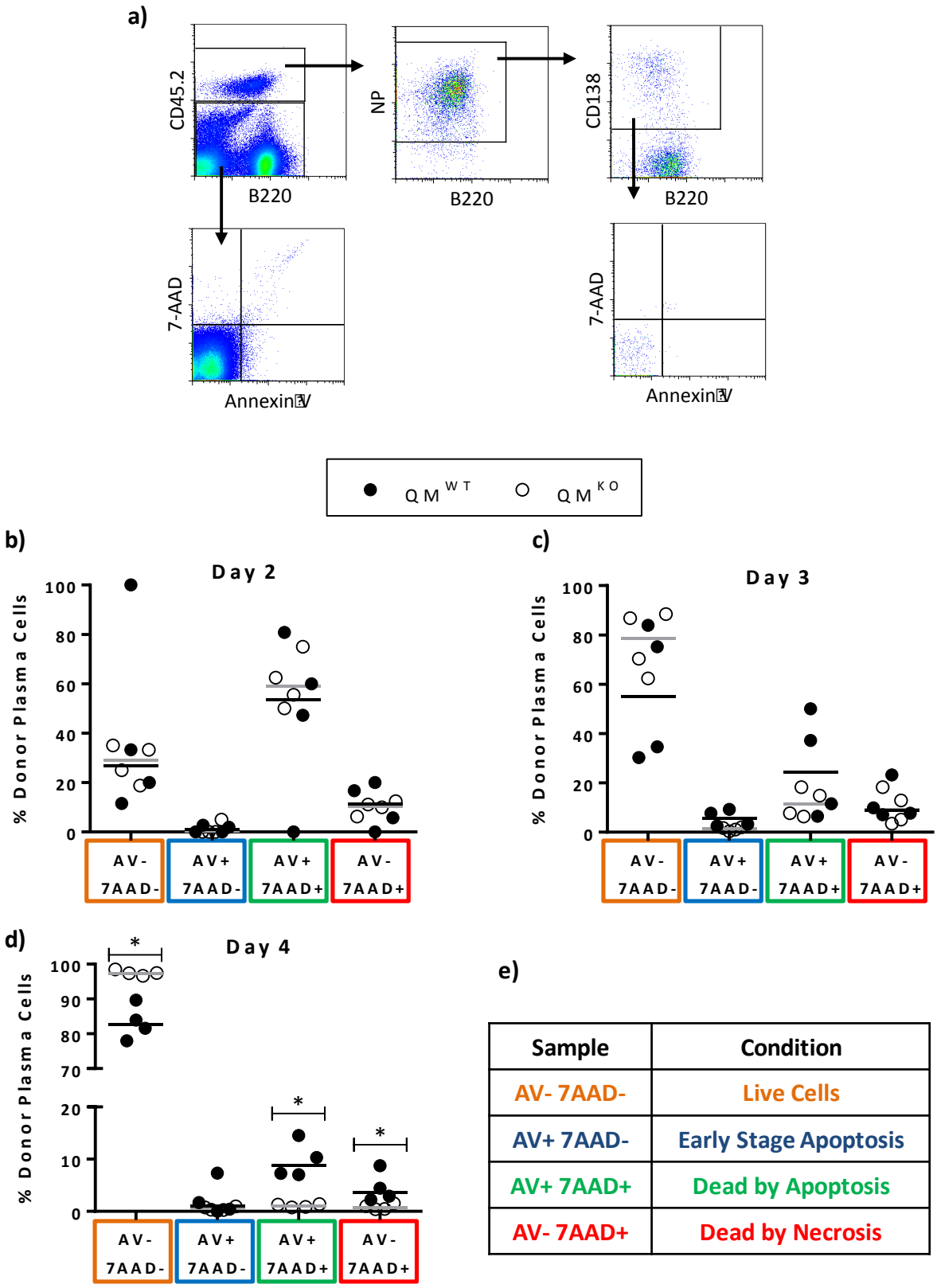

Sample	Condition
AV- 7AAD-	Live Cells
AV+ 7AAD-	Early Stage Apoptosis
AV+ 7AAD+	Dead by Apoptosis
AV- 7AAD+	Dead by Necrosis

Figure 3.20. CCRL2$^{-/-}$ plasmablasts are less prone to apoptosis than CCRL2 sufficient plasmablasts. QM^{WT} or QM^{KO} B cells were transferred into WT BoyJ hosts and a day later hosts were immunised with NP-Ficoll. Splenocytes were analysed by flow cytometry for 7-AAD and Annexin V binding; a) flow cytometry gating, b-d) Plasmablast apoptotic fate on b) Day 2, c) Day 3 and d) Day 4 post immunisation; e) Table indicating colour code of graphs.
Data from single experiment. Bars indicate median
Key: AV – Annexin V. *p<0.05

PS and PE are phospholipids found on the cytosolic side of the cell membrane in live cells, but flip to the outside of the membrane once a cell is undergoing apoptosis. PS and PE are then detected by macrophages, which then dispose of the dead cells. 7-AAD, on the other hand is able to bind to DNA and thus can be used to distinguish apoptotic cells and cells that are dead due to necrosis.

On day 2 post immunisation, more than half of the donor plasmablasts were undergoing apoptosis, with only approximately 30% of plasmablasts alive (figure 3.20b). There was no difference in the proportion of apoptotic plasmablasts between QM^{WT} and QM^{KO} plasmablasts at this early time point. By day three, the majority of plasmablasts were alive. Interestingly, the median living cells for QM^{KO} is 80%, whereas for QM^{WT} plasmablasts the median is only 55%, however this difference is not significant (figure 3.20c). This was not due to cellular death by necrosis, but due to apoptotic cell death. By day 4 >80% of QM^{WT} plasmablasts were alive, however significantly higher proportions (>95%) of QM^{KO} plasmablasts were alive ($p<0.05$, figure 3.20d). A higher proportion of QM^{WT} plasmablasts were undergoing apoptosis, with approximately 10% of QM^{WT} plasmablasts being apoptotic, compared to ~1% of QM^{KO} plasmablasts ($p<0.05$). Interestingly, although most plasmablasts were undergoing cell death, on day four 3% of QM^{WT} plasmablasts were also dying through necrosis, compared to only 0.5% of QM^{KO} plasmablasts ($p<0.05$). At each time point, only a few cells were in the early stage of apoptosis, suggesting that once apoptosis is initiated, the DNA is soon detectable.

3.5.5 Increased antibody titres are not due to reduced uptake of CCL19 in CCRL2 deficient plasmablasts

CCL19 is a chemokine which has been shown to bind the receptor CCR7, as well as ACKR4 (CCRL1). In 2009, human CCRL2 was also proposed to bind CCL19 (Leick et al., 2010) with a similar affinity to which CCR7 binds CCL19. However, this has never been shown for mouse CCRL2. To address whether CCL19 binds plasmablasts via CCRL2, a chemokine uptake assay was conducted, in which fluorescently conjugated CCL19 ($CCL19^{AF647}$, a kind gift from Chris Hansell, The University of Glasgow) was incubated with WT and $CCRL2^{-/-}$ cell populations and fluorescence analysed by flow cytometry, as per a previously published protocol (Hansell et al., 2011). To ensure specific uptake of CCL19 in this assay, spleen cells from WT, $CCR7^{-/-}$, $ACKR4^{-/-}$ and $CCRL2^{-/-}$ mice were isolated and stained for the T cell marker, CD3. Splenic T cells express high levels of CCR7, which enables their localisation to the T-Zone (Forster et al., 1999, Gunn et al., 1999). Uptake of $CCL19^{AF647}$ into T cells was analysed by flow cytometry (figure 3.21a). WT, $ACKR4^{-/-}$ and $CCRL2^{-/-}$ T cells gave a high CCL19 signal, each with a mean fluorescence intensity (MFI) of approximately 1000 (figure 3.21b). However, upon the addition of excess unconjugated CCL19, the MFI for each of these genotypes is reduced to approximately 500. However, $CCL19^{AF647}$ binding is abolished in CCR7 deficient T cells, with an MFI lower than 500. Together, this shows that CCL19 binding in this assay is specific.

In order to determine if plasmablasts are able to uptake CCL19 in a CCRL2-dependent manner, mice of each genotype were bred with QM mice to generate mice deficient in either CCRL2, ACKR4 or CCR7 with NP-specific B cell receptors. These mice were immunised with NP-Ficoll to generate high numbers of NP-specific plasmablasts, and

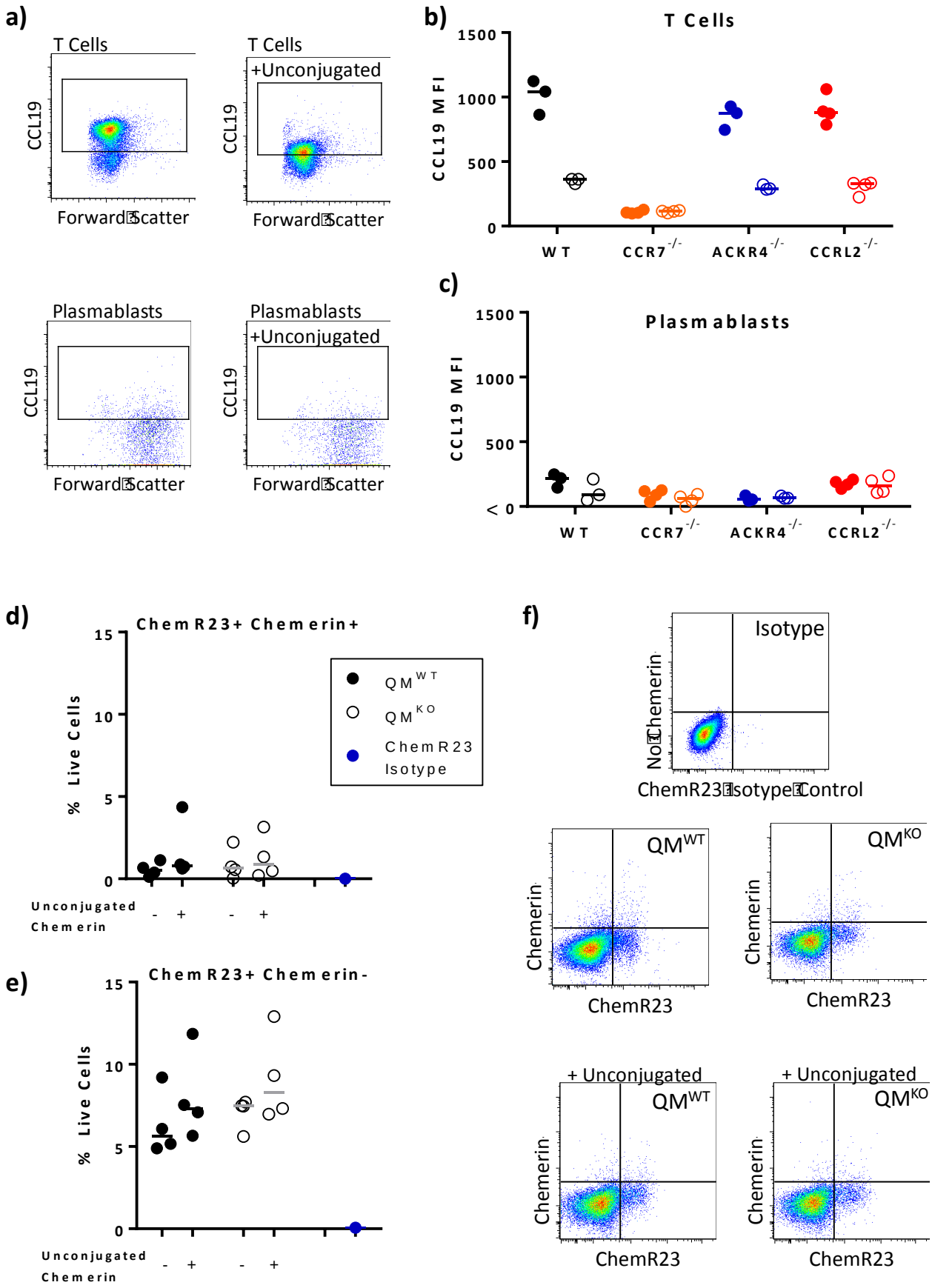

Figure 3.21. Uptake of fluorescently conjugated CCL19 and chemerin. WT, CCR7$^{-/-}$, ACKR4$^{-/-}$ or CCRL2$^{-/-}$ QM mice were immunised with NP-Ficoll and splenic cells isolated and incubated with CCL19^{AF647}; a) Flow cytometry gating; b-c) Chemokine uptake was analysed in b) CD3^{+} T cells and c) CD138^{+} plasmablasts. Closed circles indicate CCL19^{AF647} incubation only, open circles indicate addition of unlabelled CCL19. d-f) Chemerin was conjugated to Cy5 and uptake measured in whole splenocytes d) ChemR23^{+}Chemerin^{+} splenocytes, e) ChemR23^{+}Chemerin^{-} splenocytes, f) Flow cytometric gating strategy. Data from single experiment. Bars indicate median

100

CCL19 uptake determined by flow cytometry using the plasmablast marker CD138. As figure 3.21c shows, CCL19 MFI values were very low (MFI of <250) for each genotype. Addition of an excess of unconjugated CCL19 did not have any effect on CCL19 uptake with any genotype. Therefore, plasmablasts are unable to bind CCL19 in either a CCRL2 – dependent nor –independent manner.

3.5.6 Preliminary experiments are unable to detect fluorescent chemerin uptake

Chemerin is an adipokine, and proposed to be a specific ligand of CCRL2 (Zabel et al., 2008). In order to determine whether plasmablast are able to bind chemerin via CCRL2, a preliminary experiment in which chemerin was coupled to Cy5 and uptake assessed by flow cytometry was conducted. WT or CCRL2 deficient mice with NP-specific B cell receptors (QM^{WT} and QM^{KO}, respectively) were immunised with NP-Ficoll to generate high numbers of plasmablasts. Three days post immunisation splenocytes were incubated with chemerin-Cy5 either with or without an excess of unconjugated chemerin. As a positive control, ChemR23, another specific receptor for chemerin, was stained for and chemerin binding was assessed on $ChemR23^{+}$ cells. As shown in figure 3.21d-f, in both QM^{WT} and QM^{KO} samples, $ChemR23^{+}$ cells are rarely $chemerin^{+}$. Also, $ChemR23^{+}$ cells that have bound chemerin do not have a reduction in chemerin positivity upon the addition of unconjugated chemerin (figure 3.21d). This preliminary experiment suggests that the prepared chemerin-Cy5 is not specifically taken up by cells, with potential reasons for this described in the discussion.

3.5.7 Published ligands of CCRL2 do not affect NP-Ficoll induced plasmablast differentiation *in vitro*

An increase in antibody levels in CCRL2 deficient mice is B cell intrinsic. To further assess the role of B cells in the observed phenotype, B cells were isolated by MACS and stimulated in triplicate, *in vitro*, with NP-Ficoll and IL-4. Plasmablast differentiation was then assessed by flow cytometry, with the median of the three samples taken. B cells were isolated from the spleens of WT and CCRL2$^{-/-}$ QM mice, due to the proportion of NP-specific B cells. After sorting, B cells were at least 86% pure (figure 3.22a). Flow cytometry was used to detect the proportion of NP-specific B cells in each sample, thus ensuring the same number of NP-specific B cells were stimulated in each sample.

Flow cytometry was used to assess the differentiation of cells post stimulation. The percentage of live cells on day 4 was equal amongst QM^{WT} and QM^{KO} samples (figure 3.22b). Similarly, the percentage of live cells that had differentiated into plasmablasts (CD138^{+}) was equal amongst QM^{WT} and QM^{KO} B cells (figure 3.22c). To determine whether other splenic cells effect *in vitro* differentiation of B cells into plasmablasts, a preliminary experiment in which whole splenocytes were also stimulated with NP-Ficoll was conducted. As figure 3.22d shows, there is no difference in CD138^{+} plasmablast differentiation between QM^{WT} and QM^{KO} stimulated splenocytes.

To test whether described ligands of CCRL2 affect plasmablast differentiation *in vitro*, isolated B cells were stimulated with NP-Ficoll and IL-4, with the addition of either chemerin, CCL19 or CCL5. Cellular differentiation was then related to the same sample without ligand. Therefore, if the ligand had no effect, the sample would be plotted at 1; a

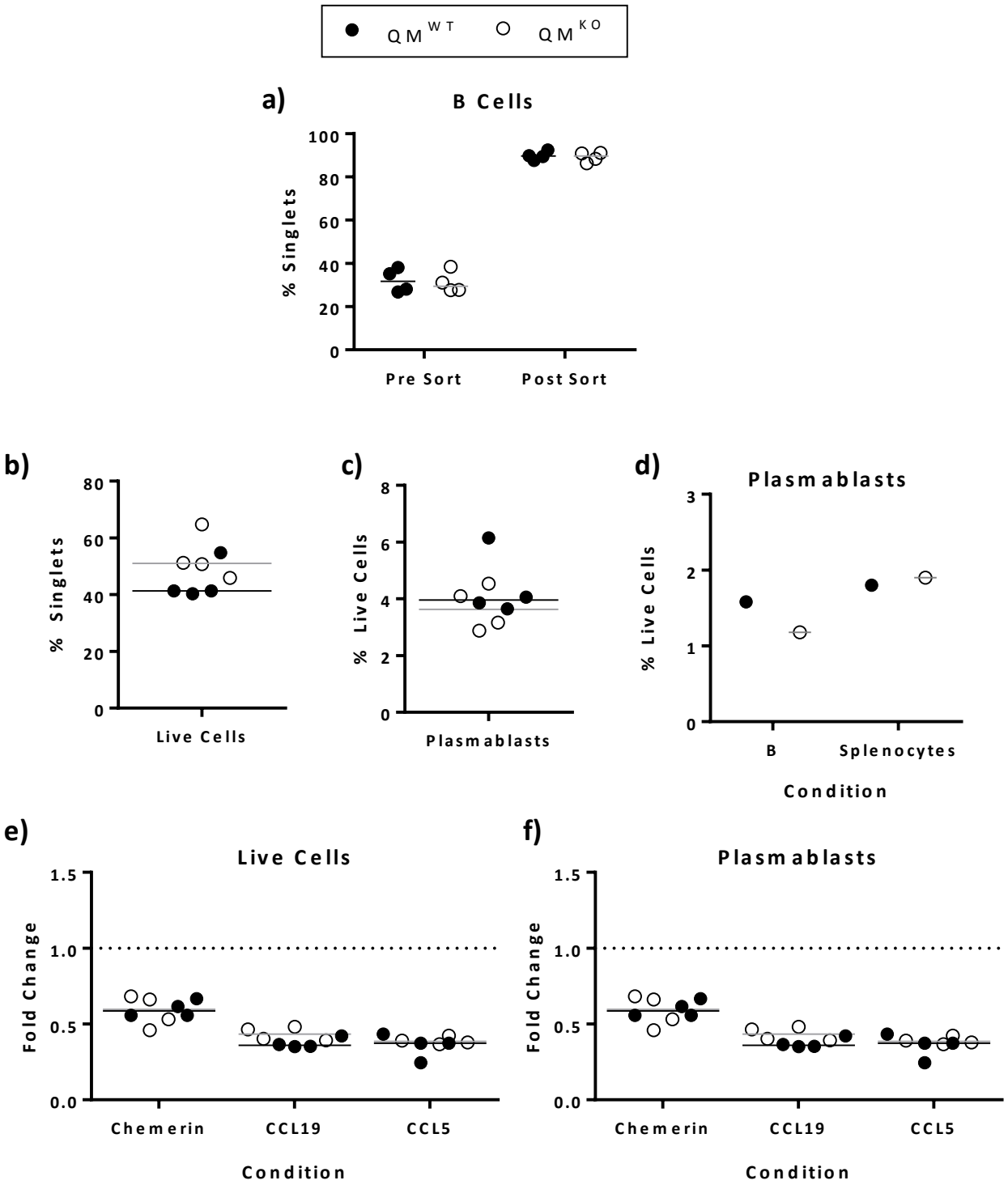

Figure 3.22. No difference in plasmablast differentiation of QM^{WT} or QM^{KO} cells stimulated *in vitro* with IL-4 and NP-Ficoll. B cells from QM^{WT} and QM^{KO} mice were isolated and 1x10^5 NP-specific cells were stimulated in triplicate *in vitro* with IL-4 and NP-Ficoll; a) B cell purity post MACS; b) % of cells alive 4 days post stimulation; c) % of cells differentiated into plasmablasts day 4 post stimulation; d) Comparison of plasmablast differentiation with isolated B cells and whole splenocytes; e-f) Effect of addition of proposed ligands of CCRL2 on e) Cell survival, f) Plasmablast differentiation, upon *in vitro* culture.
Data from single experiment. Bars indicate median

positive effect of the ligand would be >1, and a negative effect <1. Interestingly, addition of each ligand was detrimental to the cells; fold change being <1 for each condition, in both the amount of live cells and plasmablast differentiation (figure 3.22 e and f, respectively). However, there was no difference between QM^{WT} and QM^{KO} cells.

All cells were incubated with Cell Trace™ in order to monitor proliferation and Cell Trace™ plots were gated so that the percentage of plasmablasts within each gate could be calculated (figure 3.23a). As figure 3.23b shows, <5% of QM^{WT} plasmablasts have undergone 0 or only one division. However, the number of QM^{WT} plasmablasts that have undergone 2 to 4 divisions gradually increased from approximately 15% (2 divisions) to ~35% (4 divisions). Then there was a huge reduction to only 5% of QM^{WT} plasmablasts undergoing 5+ divisions. The proportion of QM^{KO} plasmablasts that had undergone each of these divisions is similar to QM^{WT} plasmablasts. There is a minor increase in the proportion of QM^{KO} cells that have undergone 5+ divisions, however this is not significant.

To assess the role of described ligands of CCRL2 during *in vitro* plasmablast proliferation, the number of divisions plasmablasts underwent with ligand was deduced relative to the same sample without ligand. As figure 3.23c shows, for the most part, the addition of chemerin did not affect the number of divisions plasmablasts underwent. There was a small increase in the proportion of cells which did not divide and cells that underwent 5+ divisions, however this was irrespective of the genotype. A similar pattern was detected with the addition of CCL19 (figure 3.23d) and CCL5 (figure 3.23e), but as with chemerin, small increases occurred irrespective of genotype.

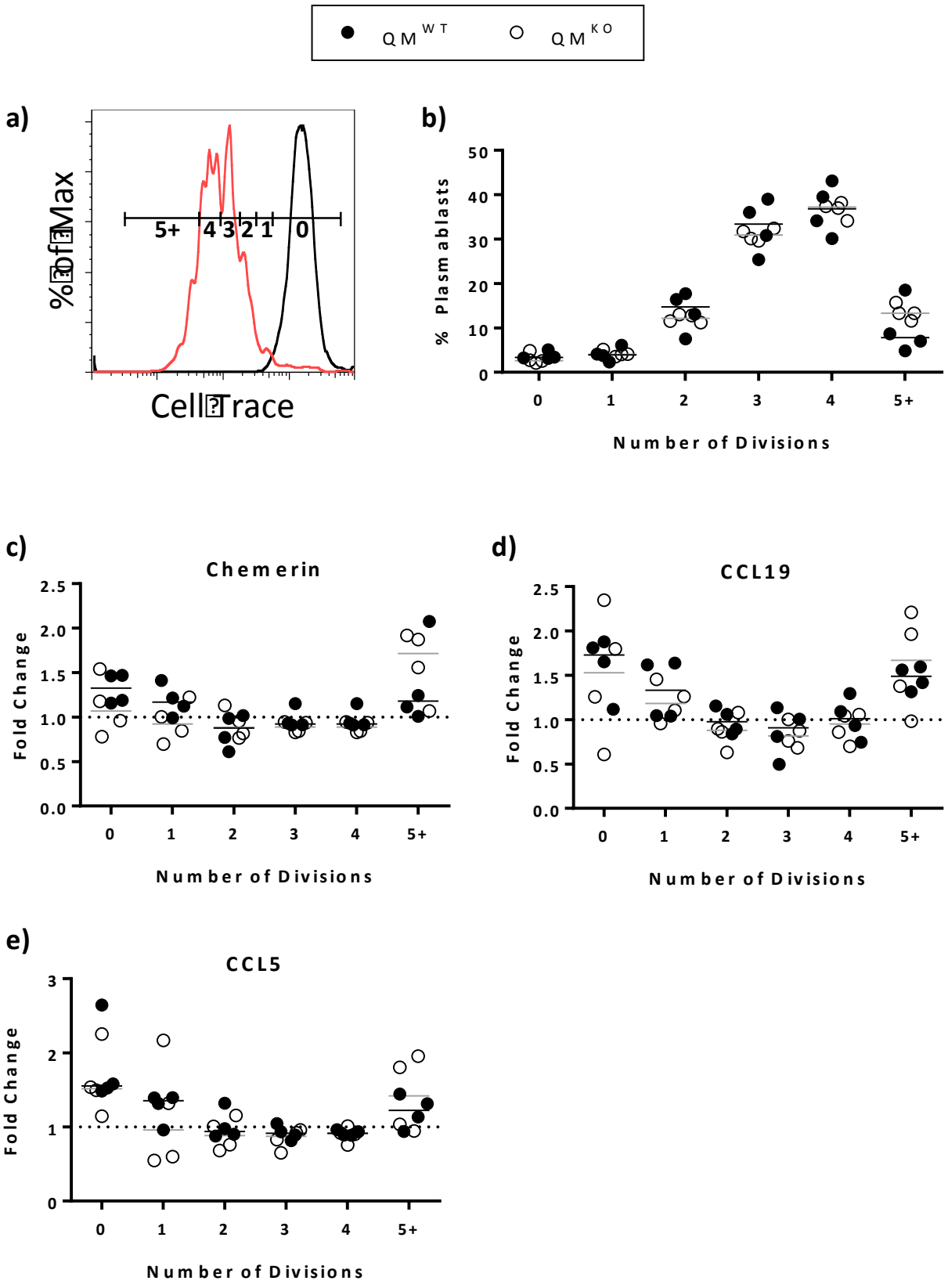

Figure 3.23. No difference in plasmablast proliferation of QM^{WT} or QM^{KO} cells stimulated *in vitro* with IL-4 and NP-Ficoll. B cells from QM^{WT} and QM^{KO} mice were isolated and 1x10^5 NP-specific cells were incubated with Cell Trace^{TM} and subsequently stimulated in triplicate *in vitro* with IL-4 and NP-Ficoll; a-b) Proliferation was monitored by dilution of Cell Trace^{TM}; a) example flow cytometry gating, b) Percentage of plasmblasts that had undergone stated number of cell divisions; c-e) Cells were incubated with addition of c) Chemerin, d) CCL19, e) CCL5 and plasmablast proliferation related to same samples without ligand addition.
Data from single experiment. Bars indicate median

105

Together, this indicates that CCRL2 deficiency does not affect plasmablast differentiation nor proliferation upon *in vitro* stimulation of B cells with NP-Ficoll. However, there was very little plasmablast differentiation, suggesting that the stimulation technique should be optimised further. Nevertheless, the data here indicates that cellular interactions *in vivo* are required for the observed phenotype within CCRL2 deficient mice.

3.6 Immunisation of CCRL2 deficient mice with the thymus independent type I antigen TNP-LPS

Thus far all results have stemmed from immunisation with the thymus independent type II antigen, NP-Ficoll. In order to assess the role of CCRL2 during a response to other antigens, mice were also immunised with TI-I and TD antigens as well as an infection model of STm.

3.6.1 CCRL2 deficient mice have a reduced antibody response to TNP-LPS

TI-I antigens are common microbial constituents, which activate B cells through Toll-like receptors. In this case, mice were immunised with (tri)NP-lipopolysaccharide (TNP-LPS) and the plasmablast response was assessed by ELISA and flow cytometry on days 5, 7 and 10 post immunisation. These immunisations were conducted in two batches, with day 5 first, and then days 7 and 10 at later dates. As figure 3.24a shows, the different experiments resulted in different response strengths, with the first immunisation resulting in a superior response compared to the second. Although WT and CCRL2 deficient mice have similar levels on NP-specific IgM on day 5, there is a small reduction in NP-specific IgM in CCRL2$^{-/-}$ mice on day 7 of the response and a two-fold reduction on day 10. However, due to a small sample size this is not significant.

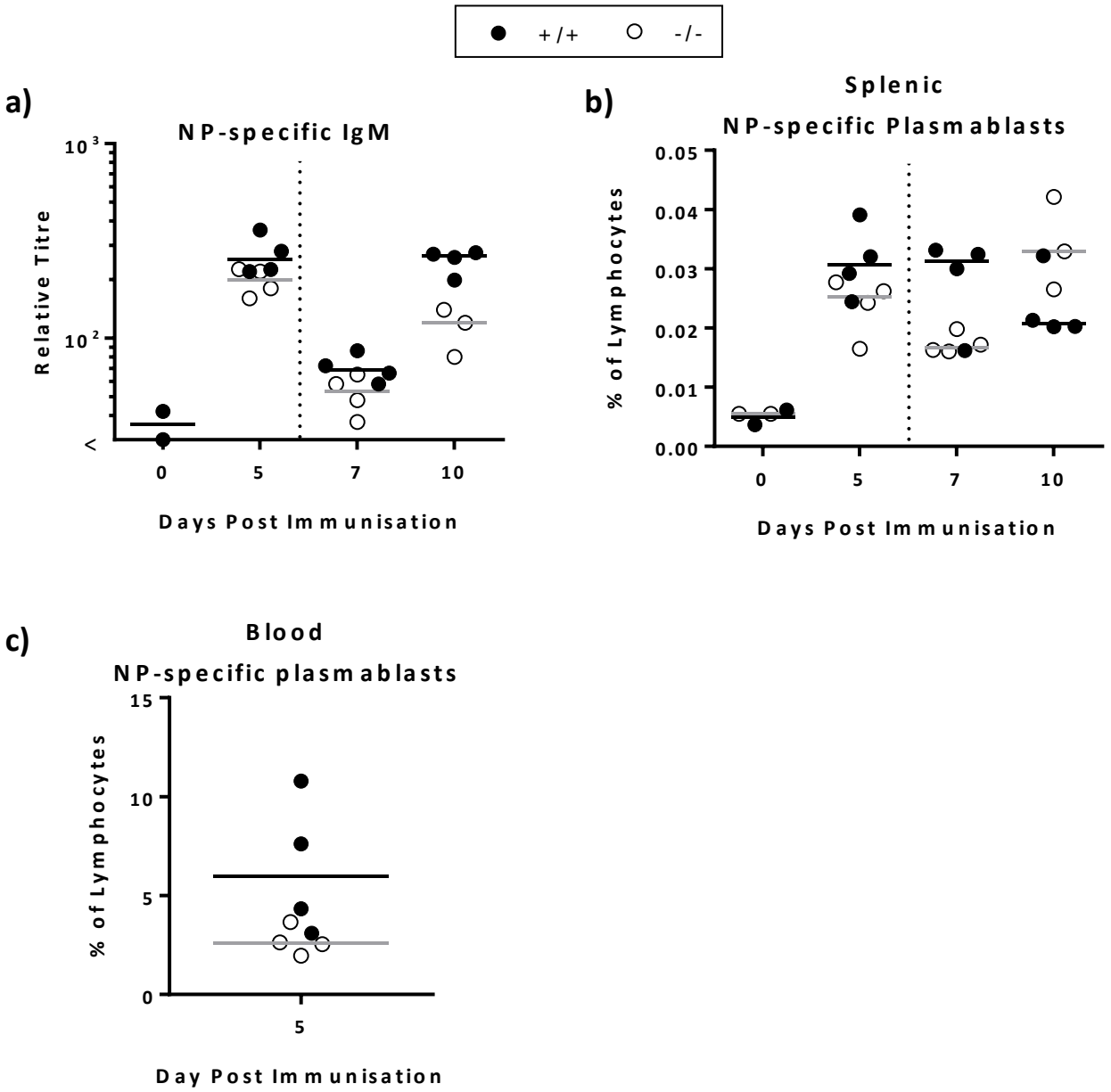

Figure 3.24. Upon TI-I immunisation, CCRL2 deficient mice have a reduced antibody response. WT and CCRL2$^{-/-}$ mice were immunised with the TI-I antigen TNP-LPS and NP-specific a) IgM and b-c) NP-specific plasmablasts in the b) Spleen and c) Blood were detected using flow cytometry.
Dotted line separates different immunisation experiments (see text).
Bars indicate median
< indicates antibody levels in the sample were under the lowest detection limit

Analysis of plasmablasts present in the spleen (figure 3.24b) and blood (figure 3.24c) of immunised mice by flow cytometry also shows a consistent reduction in NP-specific plasmablasts on days 5 and 7 post immunisation. However, unlike antibody titres, there is a slight increase in CCRL2$^{-/-}$ NP-specific plasmablasts on day 10 of the response.

3.6.2 LPS-induced plasmablast differentiation *in vitro* is not affected by CCRL2 deficiency

Immunisation of CCRL2 deficient mice with NP-Ficoll induces a B cell intrinsic phenotype. To determine whether there is a B cell specific response upon LPS stimulation, B cells were isolated from WT, CCRL2$^{+/-}$ and CCRL2$^{-/-}$ mice and stimulated *in vitro* with IL-4 and LPS for 1 through to 4 days to generate plasmablasts, as per a previously published protocol (Sciammas et al., 2006). Cells were then assessed by flow cytometry for plasmablast differentiation and proliferation (figure 3.25a). The purity of isolated B cells was always >95%, even though pre-sorting B cells were only approximately 60% of the isolated splenocytes (figure 3.25b). For all genotypes post stimulation, the majority of cells were alive days 1 through 3, with live cells not dropping below 60% at these time points (figure 3.25c). However, by day 4 cells had started to die, with only 20-40% of cells still alive at this time point, irrespective of genotype.

Plasmablast differentiation was monitored by CD138^{+} expression on the stimulated cells. Day 1 post stimulation, CD138 expression was not detectable (figure 3.25d). By day 2, approximately 5% of live cells were CD138^{+}, and although this slightly increased on days 3 and 4 of stimulation, the median was ~7% at its highest. Although at day 4 post

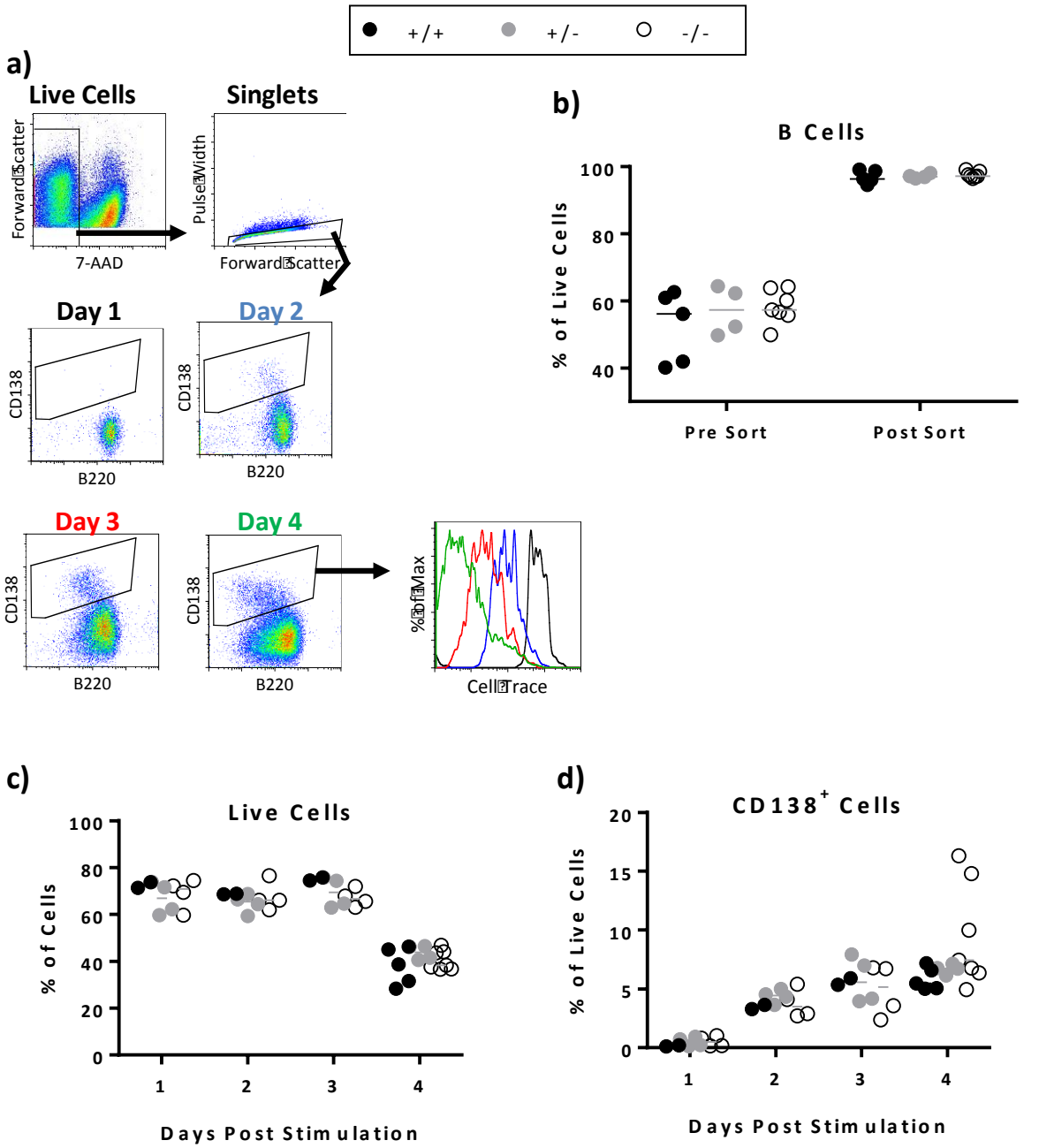

Figure 3.25. CCRL2 deficiency does not affect LPS-induced plasmablast differentiation *in vitro*. B cells from WT, CCRL2$^{+/-}$ and CCRL2$^{-/-}$ mice were isolated and stimulated in triplicate *in vitro* with IL-4 and LPS; a) Example flow cytometry gating; b) B cell purity post MACS; c) % of cells alive 1-4 days post stimulation; d) % of cells differentiated into plasmablasts 1-4 days post stimulation; e) Comparison of plasmablast differentiation with isolated B cells and whole splenocytes.
Data from single experiment. Bars indicate median

109

stimulation some CCRL2 deficient samples had slightly higher percentages of plasmablast differentiation, the majority were similar to WT and CCRL2$^{+/-}$ samples. To determine whether plasmablast differentiation *in vitro* requires whole splenocytes, a preliminary experiment in which isolated B cells or whole splenocytes were stimulated with IL-4 and LPS was conducted. As figure 3.25e shows, whole splenocytes did not influence plasmablast differentiation, irrespective of genotype.

3.6.2.1 Proposed ligands of CCRL2 do not affect LPS induced plasmablast differentiation in vitro

In order to assess the role of the proposed ligands of CCRL2 in plasmablast differentiation upon stimulation of cells with IL-4 and LPS, cells were stimulated with either chemerin, CCL19 or CCL5, and results related to the same sample without ligand addition. As before, B cells were sorted by MACS and purity assessed by flow cytometry (figure 3.26a). Post B cell isolation, all samples were >90% B cells, except a single WT group which was approximately 80% pure. Cells were stimulated for 2 to 4 days in triplicate with or without the stated ligands. The median proportion of live cells was calculated for each sample, and this result divided by the median proportion of live cells from the same sample without ligand addition.

Although there was no effect on day 2, addition of chemerin slightly increased the proportion of live cells on days 3 and 4 post stimulation (figure 3.26b). However, this increase in viability occurred irrespective of the genotype. Similar results were observed with the addition of both CCL19 (figure 3.26c) and CCL5 (figure 3.26d). Therefore,

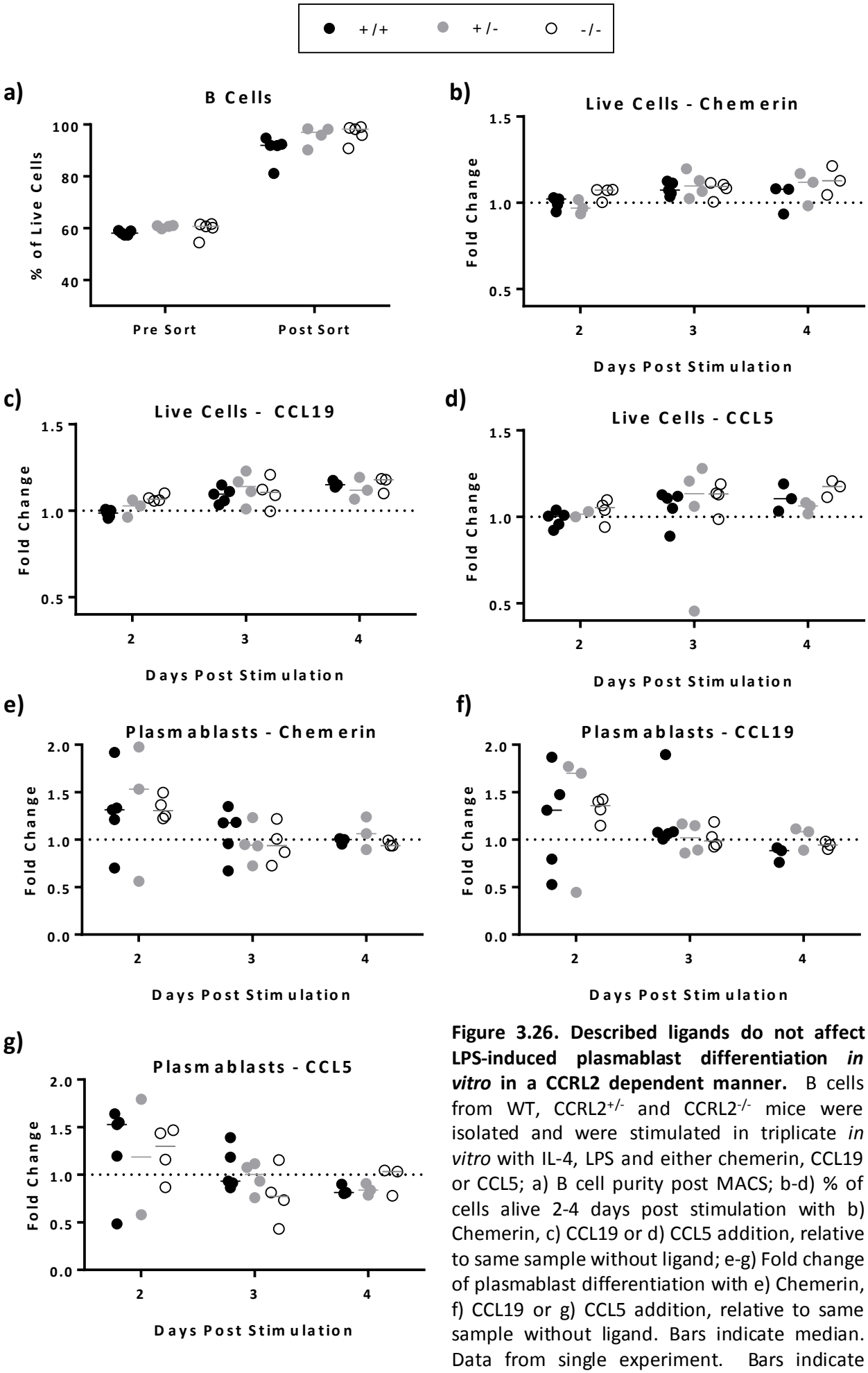

Figure 3.26. Described ligands do not affect LPS-induced plasmablast differentiation *in vitro* in a CCRL2 dependent manner. B cells from WT, CCRL2$^{+/-}$ and CCRL2$^{-/-}$ mice were isolated and were stimulated in triplicate *in vitro* with IL-4, LPS and either chemerin, CCL19 or CCL5; a) B cell purity post MACS; b-d) % of cells alive 2-4 days post stimulation with b) Chemerin, c) CCL19 or d) CCL5 addition, relative to same sample without ligand; e-g) Fold change of plasmablast differentiation with e) Chemerin, f) CCL19 or g) CCL5 addition, relative to same sample without ligand. Bars indicate median. Data from single experiment. Bars indicate median

111

although the proposed ligands of CCRL2 increase the proportion of live cells post IL-4 and LPS stimulation, this is not CCRL2 dependent.

Finally, the role of these ligands in plasmablast differentiation was subsequently assessed. As with the viability assessment, the proportion of differentiated plasmablasts as determined by flow cytometry upon the addition of ligand was divided by the result from the same sample without ligand addition. For all ligands at day 2 post stimulation there was a high degree of variation (figure 3.26a-c), possibly due to there being minimal plasmablast differentiation at this time point (figure 3.25d). Chemerin had no effect on plasmablast differentiation for any genotype on both days 3 and 4 (figure 3.26e). Likewise, CCL19 and CCL5 addition did not significantly affect plasmablast differentiation on either days 3 or 4 (figures 3.26f-g).

3.6.3 LPS-induced plasmablast proliferation *in vitro* is not affected by CCRL2 deficiency

In order to monitor the proliferation of plasmablasts, cells were incubated with Cell Trace^{TM} prior to stimulation, which was diluted as the cells divided. The proportion of plasmablasts which had undergone a set number of cell divisions was then determined by flow cytometry (figure 3.27a). As shown in figure 3.27b, on the second day of stimulation the majority of plasmablasts were either undivided, or had undergone only 1 or 2 divisions. A smaller proportion, approximately 10%, had undergone three divisions, however very few samples had plasmablasts that had 4 or more divisions. Interestingly, there was a small increase in the proportion of CCRL2$^{-/-}$ plasmablasts that had undergone

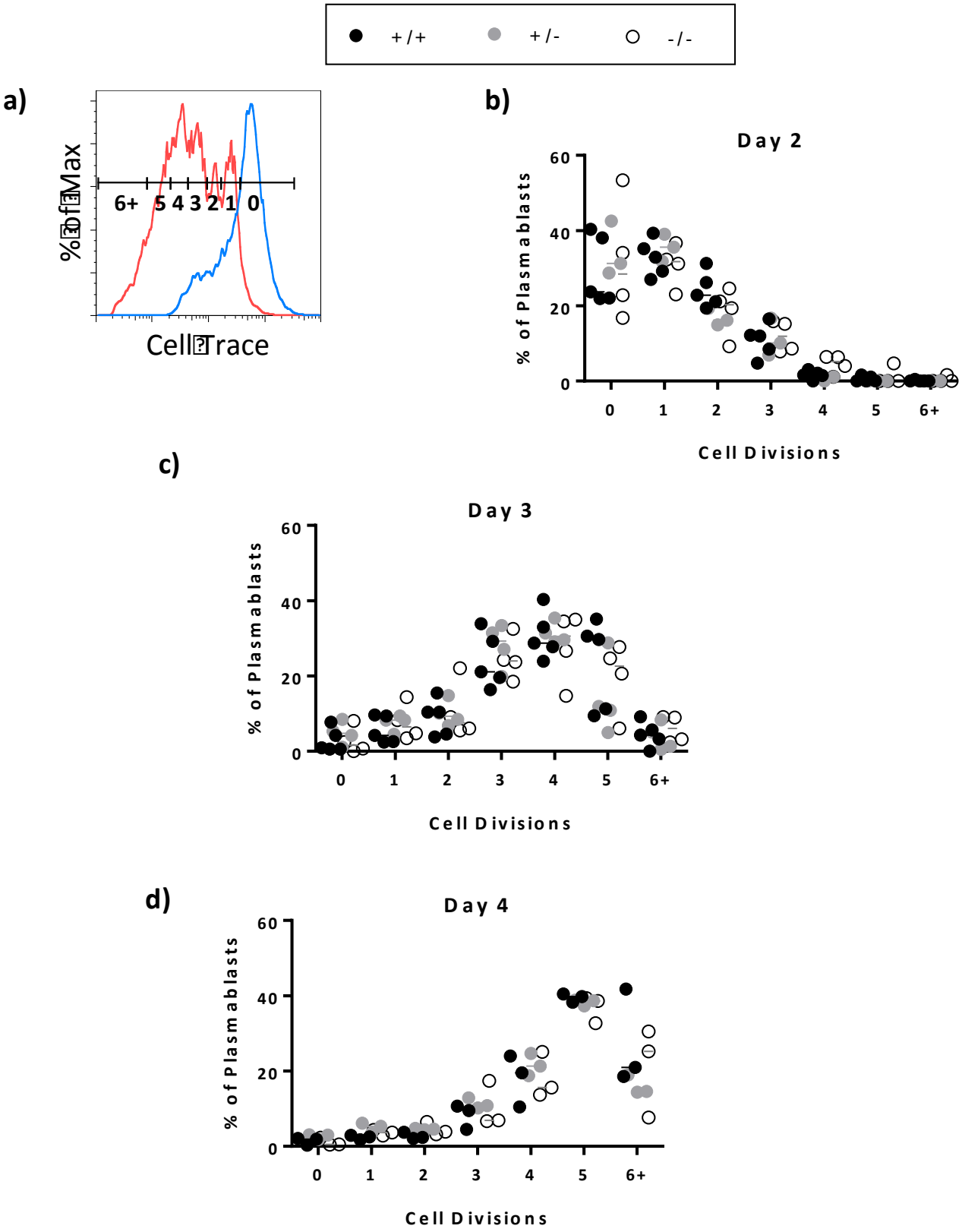

Figure 3.27. CCRL2 deficiency does not affect LPS-induced proliferation of plasmablasts *in vitro*. B cells from WT, CCRL2$^{+/-}$ and CCRL2$^{-/-}$ mice were isolated and incubated with Cell Trace™ and were subsequently stimulated in triplicate *in vitro* with IL-4 and LPS, proliferation was then monitored by flow cytometry; a) Flow cytometry gating of plasmablast proliferation; b-d) Number of cell divisions plasmablasts have undergone b) Two, c) Three, d) Four days post stimulation.
Data from single experiment. Bars indicate median

4 divisions, compared to WT and CCRL2$^{+/-}$, however this was not significant due to low sample numbers. At all other time points, the proportion of plasmablasts that had undergone each number of divisions was equal irrespective of genotype

By day three, plasmablasts had undergone more rounds of proliferation (figure 3.27c), with undivided cells now being <5% of the total. There was a gradual increase in the number of plasmablasts that had undergone 1-3 divisions, with a peak at 4. Although some cells had undergone 5 divisions, only 5% had undergone 6 or more. As with day 2, there were no differences in the number of divisions plasmablasts had undergone between any of the genotypes.

Finally, by day 4 there had been another shift in the number of divisions each plasmablast has undergone. Less than 10% of plasmablasts had undergone 0, 1 or 2 divisions (figure 3.27d). The proportion of cells that had undergone 3 to 5 divisions increased from 10 to approximately 40%, with 5 being the peak number of divisions. The proportion of plasmablasts that had undergone 6 or more divisions dropped to approximately 20%. There were no differences in the number of cell divisions plasmablasts had undergone between the genotypes.

3.6.2.1 Proposed ligands of CCRL2 do not affect LPS-induced plasmablast proliferation in vitro

In order to assess whether the proposed ligands of CCRL2 affect plasmablast proliferation upon stimulation with LPS, B cells were stimulated in the presence of either chemerin, CCL19 or CCL5. The number of divisions plasmablasts have undergone was then related to the same sample without the addition of ligand. As figure 3.28b shows, on day 3 the

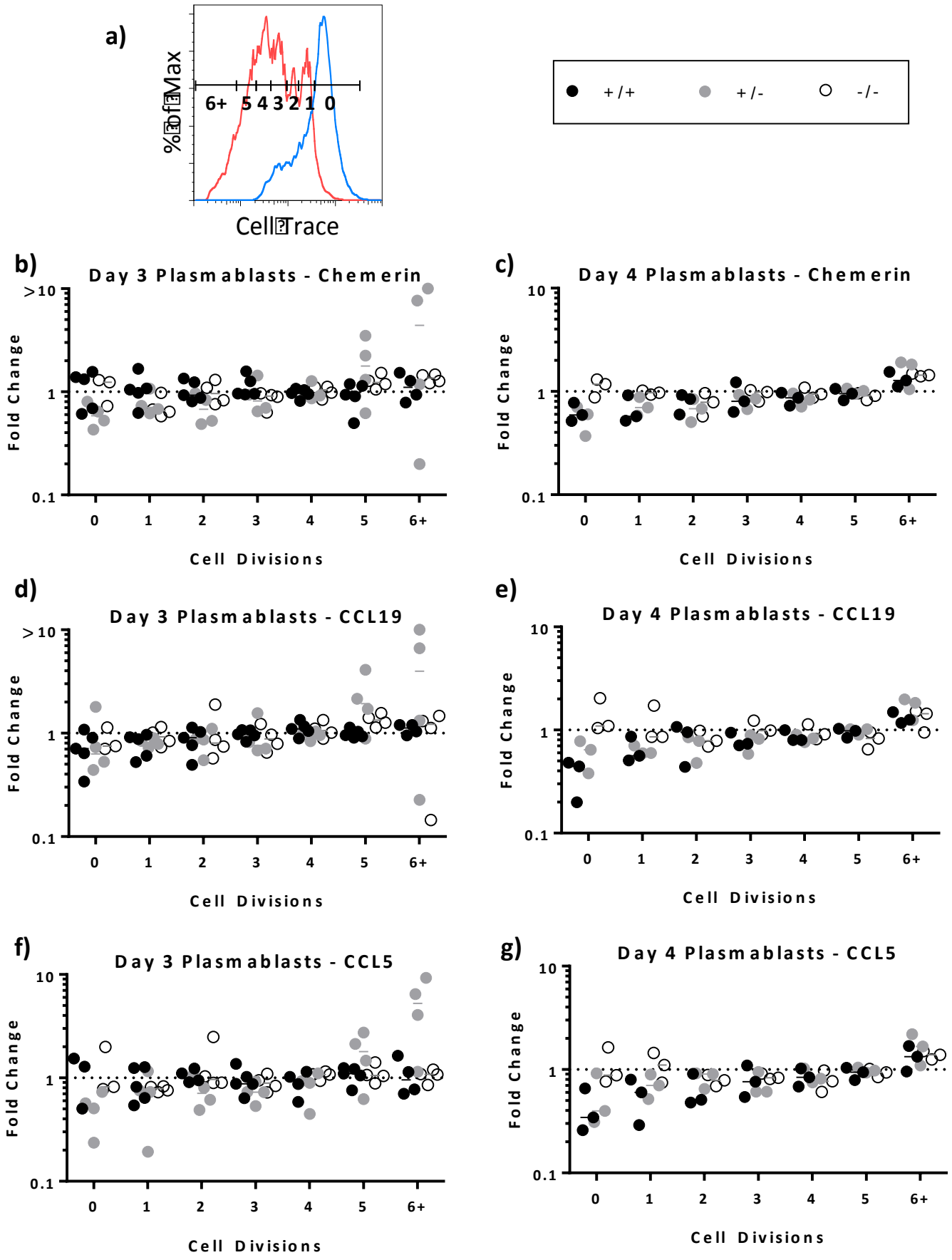

Figure 3.28. Described ligands do not affect LPS-induced plasmablast proliferation *in vitro* in a CCRL2 dependent manner. B cells from WT, CCRL2$^{+/-}$ and CCRL2$^{-/-}$ mice were isolated and incubated with Cell Trace™ and were subsequently stimulated in triplicate *in vitro* with IL-4, LPS and either chemerin, CCL19 or CCL5. Proliferation was then monitored by flow cytometry; a) Flow cytometry gating of plasmablast proliferation; b-g) Fold change in proliferation compared to sample without ligand b-c) Chemerin, b) Day 3, c) Day 4; d-e) CCL19 d) Day 3 e) Day 4; f-g) CCL5 f) Day 3 and g) Day 4 post stimulation. Data from single experiment. Bars indicate median

addition of chemerin did not have any major effects on plasmablast proliferation. Although the proportion of cells that had undergone 5 or more rounds of proliferation did increase slightly, this was irrespective of the genotype. An increase in the proportion of cells that had undergone 6 or more divisions was also detectable on day 4 (figure 3.28c), but once again this was observed in all genotypes. Interestingly, on day 4 a higher proportion of CCRL2$^{-/-}$ cells had not divided compared to the other genotypes, but due to the low sample number this was not significant.

As observed with chemerin, addition of CCL19 did not affect the proliferation of plasmablasts on day 3 post stimulation (figure 3.28d). Interestingly, like chemerin, addition of CCL19 increased the proportion of plasmablasts that had undergone 6 or more divisions on day 4 post stimulation (figure 3.28e), and there was an increase in undivided CCRL2$^{-/-}$ cells.

Addition of CCL5 did not affect the proliferation of plasmablasts on day 3 of the response (figure 3.28f). On day 4 there was a decrease in the proportion of undivided plasmablasts, and also plasmablasts that had only undergone 1 or 2 divisions. This correlated with an increase in the proportion of cells that had undergone 6 or more divisions. However, this was not CCRL2 dependent, as it was apparent in all genotypes (figure 3.28g).

3.7 Immunisation of CCRL2 deficient mice with the thymus dependent antigen NP-CGG

Unlike the thymus independent antigens discussed above, B cell activation with TD antigens requires the collaboration of both B and T cells. Consequently, B cell activation during a TD response is slower than activation during a TI response.

3.7.1 CCRL2 deficiency causes minor effects during the primary TD B cell response within the spleen and lymph node

To assess the role of CCRL2 in TD B cell activation, WT and CCRL2 deficient mice were immunised with NP-chicken gamma globulin (NP-CGG) and the antibody response was examined on days 5, 8 and 14 post immunisation. NP-specific IgM gradually increased in WT mice days 5 through 14 (figure 3.29a). Although early in the response at day 5 there was a minor (but not significant) advantage for CCRL2 deficient mice, this had evened out by day 8. By day 14, CCRL2$^{-/-}$ mice had a slightly reduced response in comparison to WT mice, but this was also not significant. NP-specific IgG1 switched antibody was detectable from day 8 (figure 3.29b) and increased on day 14. As with NP-specific IgM, there was a small advantage in IgG1 production by CCRL2 deficient mice on day 8, but these minor differences evened out by day 14.

As with the TI-II response, NP-specific plasmablasts were detected by immunohistology and flow cytometry (figure 3.29c and d, respectively). Plasmablasts were detectable at very low levels on day 5 post immunisation by immunohistology, with the peak plasmablast response in the spleen apparent at day 8. By day 14, plasmablast levels had returned to levels observed at day 5. Although at each time point CCRL2 deficient mice had slightly higher median plasmablast levels compared to WT mice (up to 5x more at day 8), at no time point was this significant. Interestingly, flow cytometry analysis indicated different results on plasmablast appearance in the spleen. On day 5 of the response, levels of NP-specific plasmablasts were not detectable above background levels seen in unimmunised mice. Splenic plasmablasts increased in proportion on day 8 of the response, and the splenic plasmablasts further increased at day 14. However, as with the

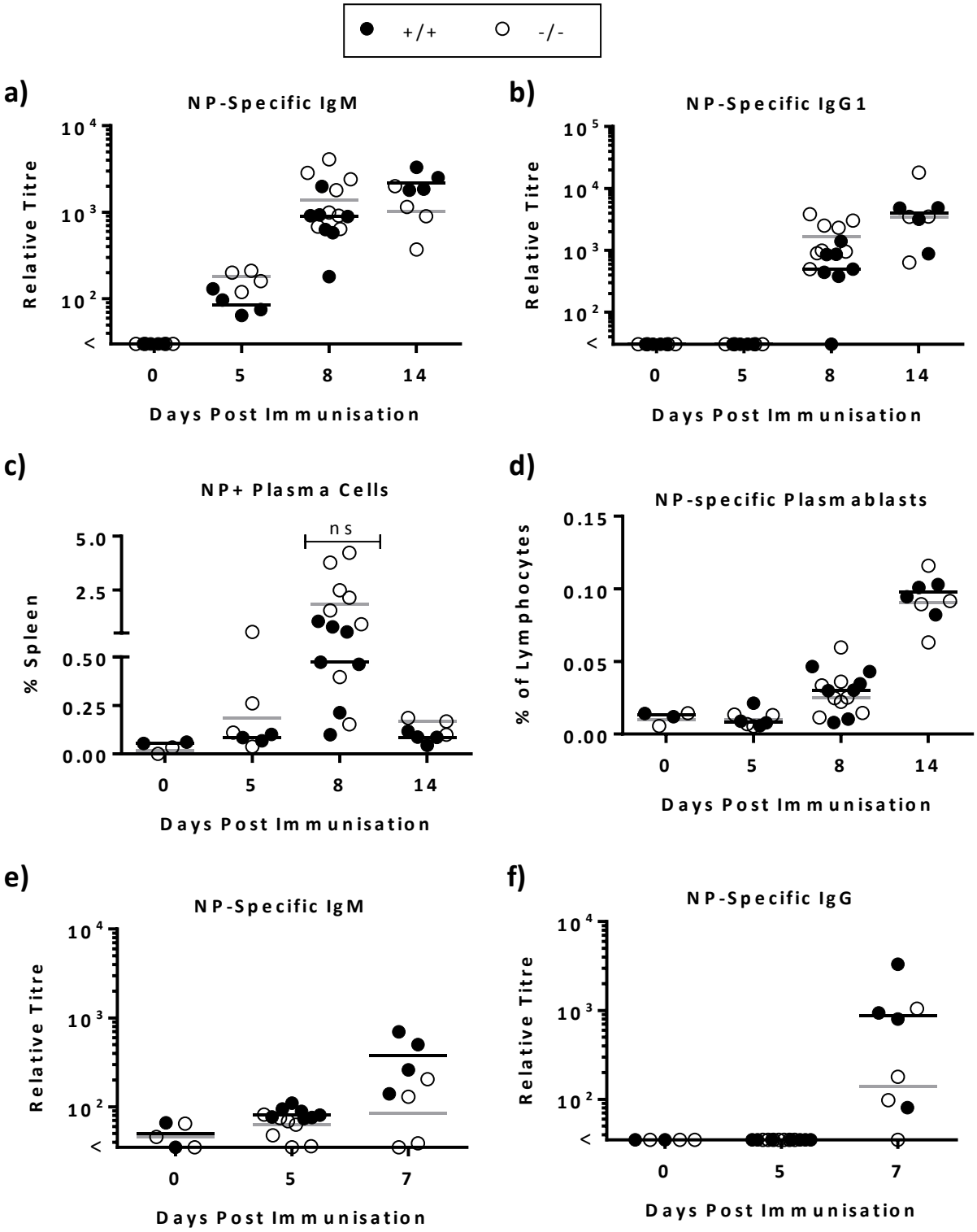

Figure 3.29. In response to the TD antigen NP-CGG, CCRL2 deficient mice do not have significantly higher antibody responses compared to WT mice. a-d) WT and CCRL2$^{-/-}$ mice were immunised with NP-CGG and the NP-specific response was analysed at the stated time points; levels of NP-specific a) IgM and b) IgG1 in the blood of immunised mice; NP-specific plasma cells in spleens of immunised mice as determined by c) Histology and d) Flow cytometry; e-f) WT and CCRL2$^{-/-}$ mice were immunised in the footpad with NP-CGG to activate B cells of the popliteal lymph node and the NP-specific response was analysed at the stated time points, levels of NP-specific e) IgM and f) IgG in the blood of immunised mice.

Data pooled from two independent experiments. Bars indicate median

< indicates antibody levels in the sample were under the lowest detection limit

immunohistology data, there were no differences in the proportion of WT and CCRL2$^{-/-}$ plasmablasts in the spleen throughout the primary TD response.

In order to assess the difference between the TD splenic and the TD lymph node response, mice were immunised with NP-CGG in the footpad to activate B cells of the popliteal lymph node. NP-specific IgM was detectable at low levels on day 5 of the response and this increased further on day 7 (figure 3.29e). Even though CCRL2$^{-/-}$ mice had a 3-fold reduction in IgM levels on day 7, there were no significant differences between WT and CCRL2 deficient mice. Unlike IgM, NP-specific IgG was only detectable on day 7 post immunisation (figure 3.29f). As with IgM, the levels of IgG were lower in CCRL2 deficient mice, in this instance approximately 10-fold, but this is not significant.

3.7.2 Improved antibody titres are detected in CCRL2 deficient mice upon naïve B cell activation as part of a secondary TD response

TD activation of B cells generates both memory B and memory T cells. Upon reactivation, the response is stronger and faster than the primary TD response. Also, due to the recruitment and activation of memory T cells, the kinetics of naïve B cell activation is similar to a TI response.

Mice were primed with CGG, to generate CGG-specific T and B cells. Five weeks later, these mice were boost immunised with NP-CGG. In this case, naïve NP-specific B cells were activated by memory CGG-specific T cells. Memory CGG-specific B cells are also activated by the CGG present within NP-CGG.

NP-specific IgM was detectable one day post boost immunisation, and this increased ten-fold by day 5 (figure 3.30a). Levels of IgM were comparable between CCRL2$^{-/-}$ and WT

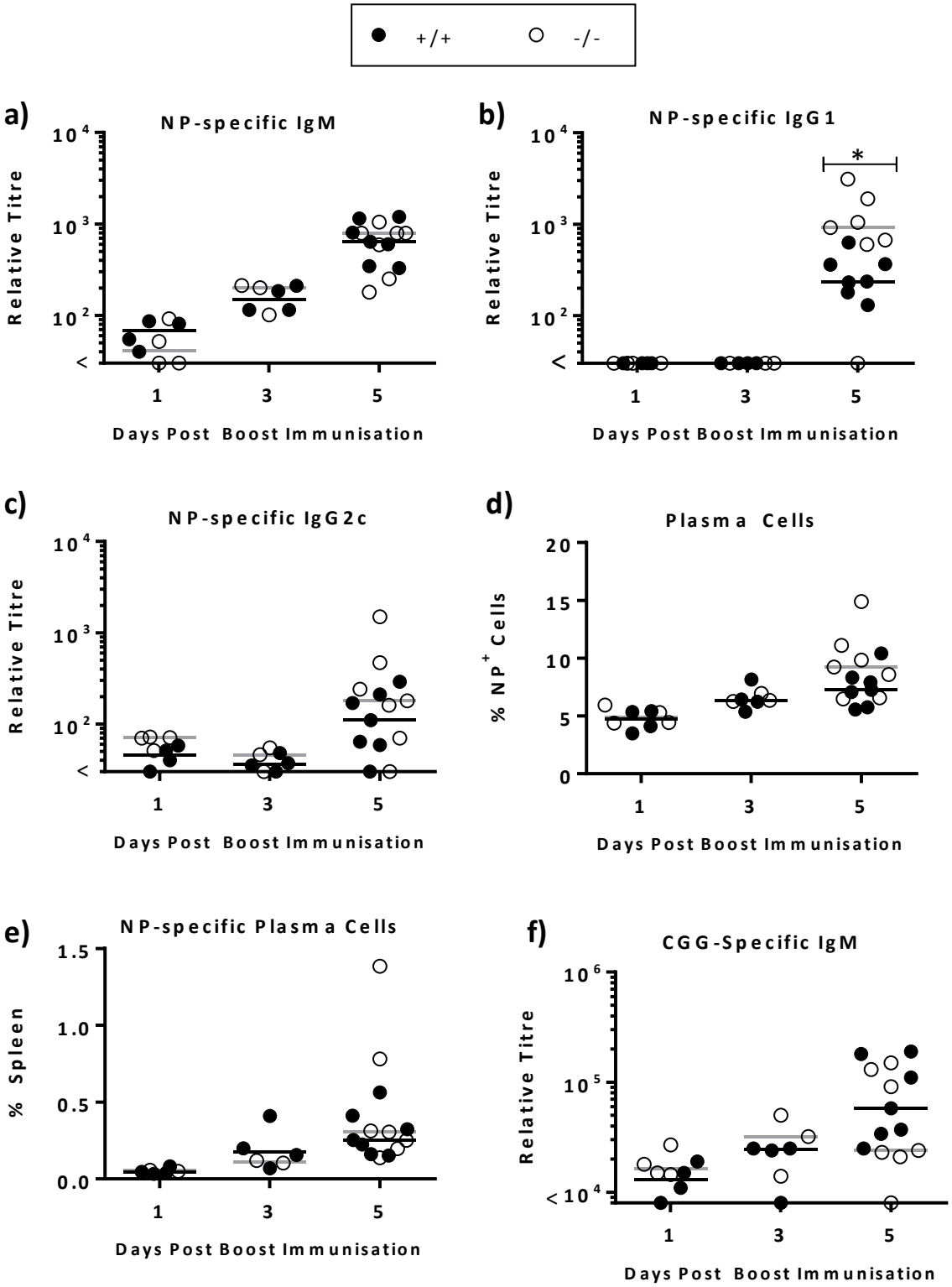

Figure 3.30. CCRL2 deficient mice have improved IgG1 switched responses to TD antigens upon boost immunisation. WT mice were immunised with CGG and five-weeks later boost immunised with NP-CGG, and the CGG- or NP-specific response was analysed at the stated time points; a-c) Levels of NP-specific a) IgM, b) IgG1 and c) IgG2c in the blood of immunised mice; d-e) Splenic NP-specific plasma cells as determined by d) Flow cytometry e) Immunohistochemistry; f) CGG-specific IgM in blood of immunised mice.
Data pooled from two individual experiments.
Bars indicate median
< indicates antibody levels in the sample were under the lowest detection limit

mice throughout. Conversely, NP-specific IgG1 was only detectable on day 5 post boost immunisation in both WT and CCRL2 deficient mice (figure 3.30b). Interestingly, 5-fold higher levels of IgG1 were detected in CCRL2 deficient mice ($p<0.05$). This increase is reminiscent of the elevated IgM response observed on day 5 post NP-Ficoll immunisation (figure 3.6a). IgG2c levels also increased by day 5, although background levels on day 1 were relatively high (figure 3.30c). However, there were no differences in the levels of IgG2c between WT and CCRL2 deficient mice, showing that the increase in switched NP-specific antibody is specific for IgG1.

The frequency of plasmablasts was then assessed by both flow cytometry and immunohistology. As is suggested by the IgM and IgG2c levels on day 1 post boost, background levels of NP-specific plasmablasts by flow cytometry were quite high at this time point – around 5% of NP-specific cells (figure 3.30d). There was a slight increase in the proportion of plasmablasts on day three, and a further increase on day 5. On day 5 there was a small increase in plasmablasts within $CCRL2^{-/-}$ mice (8% in $CCRL2^{-/-}$ mice compared to 5% in WT), however this was not significant. Likewise, NP-specific plasma cells, as calculated using immunohistology sections, showed the same pattern, with increased plasma cell numbers at day 3 and then further at day 5 (figure 3.30e). As with flow cytometry, no observable differences in the levels of these cells were found between $CCRL2^{-/-}$ and WT mice.

Finally, the memory response was assessed by calculating levels of CGG-specific antibody production (figure 3.30f). Unsurprisingly, high levels of CGG-specific IgM were detected on day 1 post boost, with IgM gradually increasing on day 3 and day 5. Although there

was a slight reduction in CGG-specific IgM in CCRL2$^{-/-}$ mice on day 5 post boost, this was not significant due to the high variability.

3.8 Infection of CCRL2 deficient mice with Salmonella

The previous immunisations within this study were all single antigens. To assess the role of CCRL2 in an infection model, where multiple antigens are available to activate B cells, mice were infected with the attenuated STm strain, SL3261. CCRL2$^{+/-}$ and CCRL2$^{-/-}$ littermates were infected with STm and the early extrafollicular B cell response was analysed on days 3, 4 and 7. Upon infection, splenomegaly occurs, with the biggest increase being in erythroid cells (Jackson et al., 2010). To monitor splenomegaly, spleens were weighed at each time point. As figure 3.31a shows, an increase in spleen size is already apparent at day 3 post infection in both CCRL2$^{+/-}$ and CCRL2$^{-/-}$ mice, although there was no difference between the groups, which was also observed on day 4. However, on day 7 post infection the size of the spleens had more than doubled compared to day 4, but there was still no difference between the two genotypes.

In order to monitor bacterial clearance, spleen and blood cultures were incubated overnight and the number of colonies formed were calculated at each time point (figure 3.31b and c, respectively). For the spleen, bacterial counts were approximately 10^6-10^7 both days 3 and 4 post infection, with no differences between CCRL2$^{+/-}$ and CCRL2$^{-/-}$ mice. However, by day 7 the counts were 10-fold lower, to between 10^5 and 10^6, with again, no difference between the two genotypes. Bacterial counts within the blood of the mice were highly variable. Although some bacteria were detected at each time point, there was no difference in bacterial counts between time point nor genotypes.

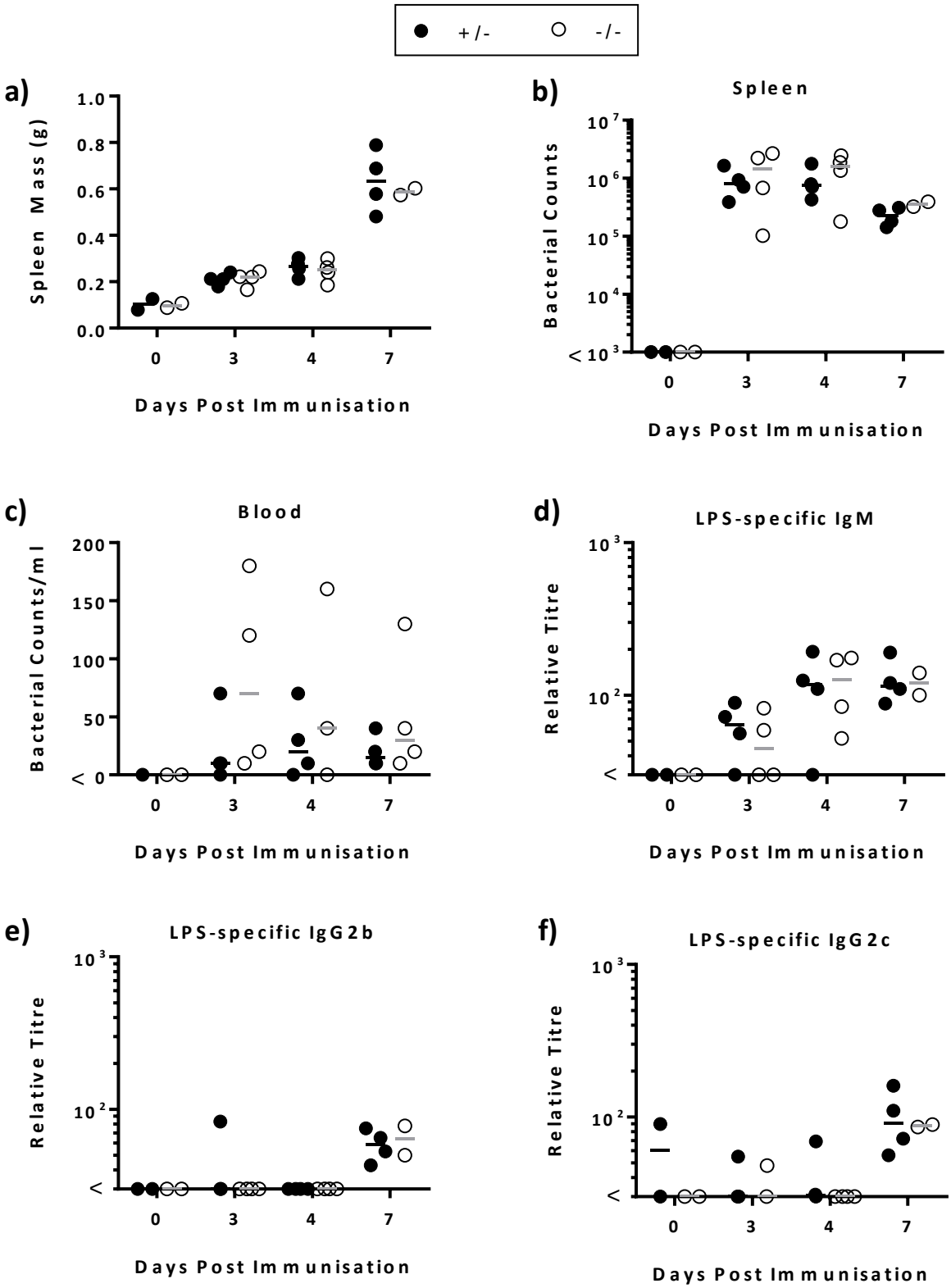

Figure 3.31. CCRL2 deficiency does not affect the early plasmablast response to Salmonella (1). CCRL2$^{+/-}$ or CCRL2$^{-/-}$ mice were infected with Salmonella and the response analysed on days 3, 4 and 7; a) Spleen masses; b-c) Bacterial numbers in the b) Spleen and c) Blood; d-f) LPS-specific antibody response was measured by ELISA, d) IgM, e) IgG2b and f) IgG2c.
LPS-specific IgG3 was not detectable at anytime point (data not shown).
Data pooled from three individual experiments. Bars indicate median
< indicates antibody levels in the sample were under the lowest detection limit

To determine the effectiveness of the antibody response, LPS- OMP- and FliC- specific antibody was analysed by ELISA. LPS specific IgM was detectable from day 3 post infection, with titres increasing on day 4, but staying level at day 7. There were no differences in the levels of LPS-specific IgM between either genotype (figure 3.31d). Both IgG2b and IgG2c LPS-specific switched antibody was only detectable at low levels on day 7 post infection and there were no differences between $CCRL2^{+/-}$ and CCRL2 deficient mice (figure 3.31e-f). IgG3 switched antibody was not detectable at any time point (data not shown).

There were high background (uninfected) levels of OMP-specific IgM (figure 3.32a), but nevertheless, the antibody increased day-on-day. Again, no differences between the two genotypes were detected. OMP-specific IgG2c and IgG3 were only detectable on day 7 post infection (figure 3.32b and c), but OMP-specific IgG2b was not detectable at any time point (data not shown). There were no differences in OMP-specific IgG2c between $CCRL2^{+/-}$ and $CCRL2^{-/-}$ mice. Interestingly, OMP-specific IgG3 appeared at lower levels in CCRL2 deficient mice, however, due to low sample numbers and a wide spread in $CCRL2^{+/-}$ mice, this was not significant.

Finally, FliC-specific IgM was only detectable above baseline levels from day 4 post infection, with an increase in antibody on day 7 (figure 3.32d). Again, IgG2b and IgG2c switched antibody was only detectable on day 7 (IgG3 switched was not detectable at any time point – data not shown), but only at very low titres (figure 3.32 e and f). Neither IgM, IgG2b nor IgG2c FliC-specific antibody titres were altered between $CCRL2^{+/-}$ and $CCRL2^{-/-}$ mice.

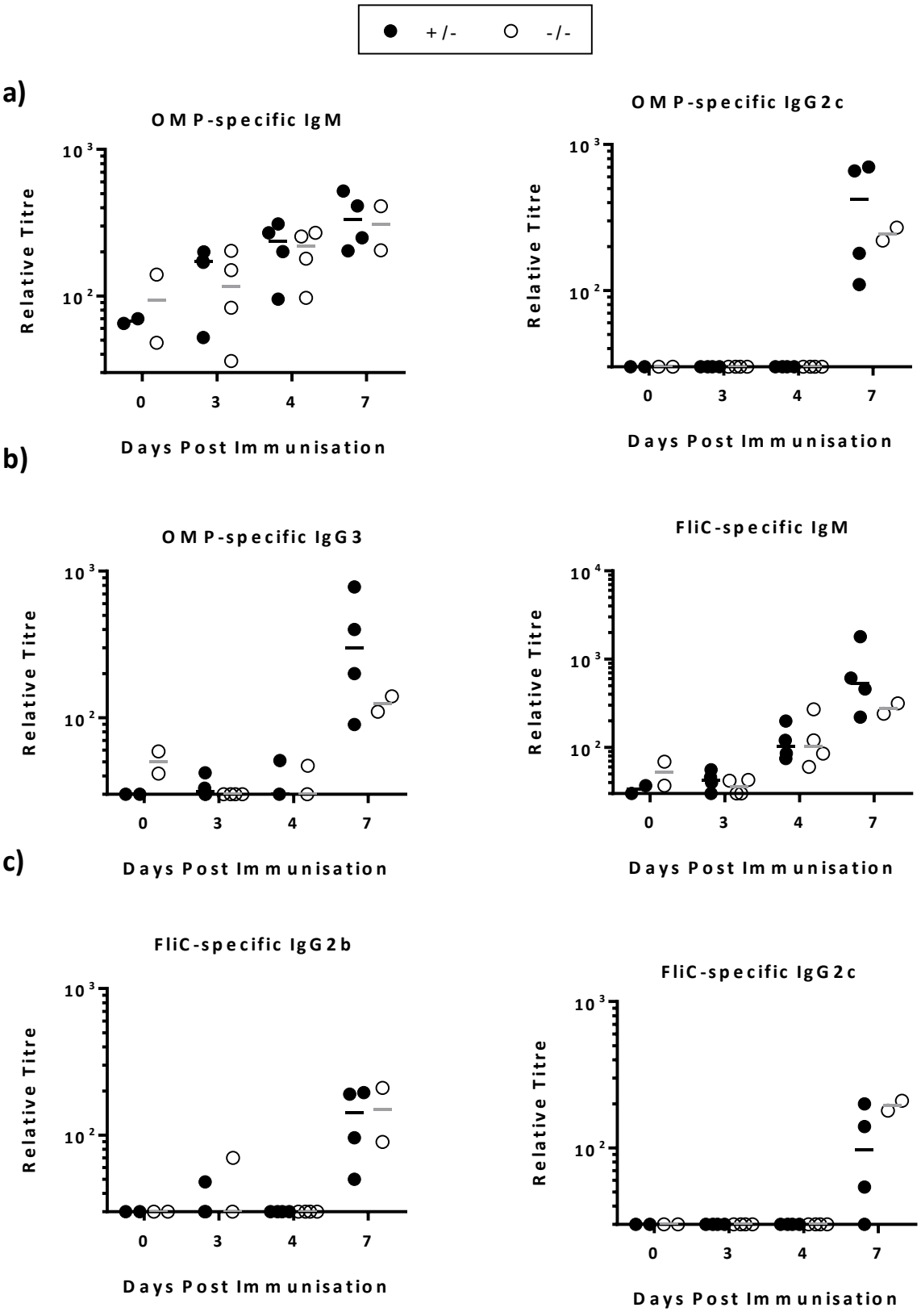

Figure 3.32. CCRL2 deficiency does not affect the early plasmablast response to Salmonella (2). CCRL2$^{+/-}$ or CCRL2$^{-/-}$ mice were infected with Salmonella and the response analysed on days 3, 4 and 7; a-c) OMP-specific antibody response was measured by ELISA, a) IgM, b) IgG2c and c) IgG3. d-f) FliC-specific antibody response was measured by ELISA, d) IgM, e) IgG2b and f) IgG2c.
OMP-specific IgG2b was not detectable at any time point (data not shown).
FliC-specific IgG3 was not detectable at any time point (data not shown).
Data pooled from three individual experiments. Bars indicate median
< indicates antibody levels in the sample were under the lowest detection limit

In order to relate antibody titres to plasmablast production, plasmablast levels were assessed by flow cytometry (for example gating see figure 3.33a). As would be expected due to the late induction of germinal centres in this model, GC B cells were not detectable above baseline levels at any time point (figure 3.33b), showing that the antibody produced was from the extrafollicular response. Upon calculation of total plasmablasts (figure 3.33c), day 3 post infection showed levels similar to those detected in unimmunised mice, but plasmablast numbers increased at a steady rate days 4 and 7 post infection. There were no differences between $CCRL2^{+/-}$ and $CCRL2^{-/-}$ mice at any time point studied.

In order to break down plasmablast differentiation into the antibody isotypes, spleens were stained for IgM-, IgG2b- and IgG2c- specific plasmablasts. The level of IgM-specific plasmablasts was highly distributed amongst samples (figure 3.33d). However, as with total plasmablasts, levels only increased above baseline from day 4 and increased to higher levels again on day 7. There were no difference in numbers of IgM specific plasmablasts between genotypes at any time point. IgG2b and IgG2c specific plasmablasts had lower background levels than IgM (figure 3.33e and f). $IgG2b^{+}$ plasmablasts were detectable above background levels on day 4, with even higher numbers on day 7, however there were no differences in the levels of $IgG2b^{+}$ plasmablasts at any time point between $CCRL2^{+/-}$ and CCRL2 deficient mice. As with $IgG2b^{+}$ plasmablasts, $IgG2c^{+}$ plasmablasts were detectable above background on day 4, and increased again approximately 10-fold on day 7. Again, no significant differences were detectable between the two mouse genotypes.

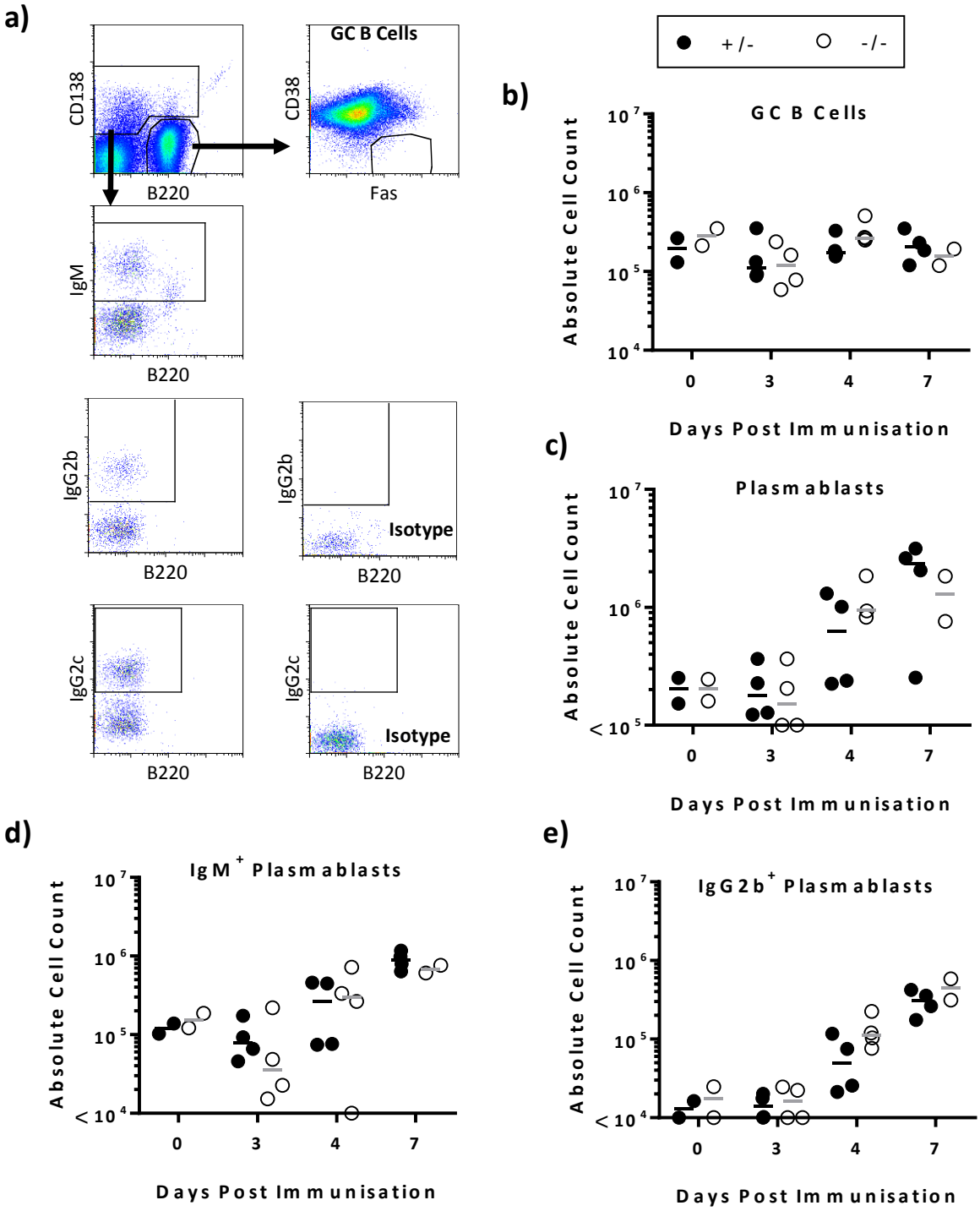

Figure 3.33. CCRL2 deficiency does not affect the early plasmablast response to Salmonella (3). CCRL2$^{+/-}$ or CCRL2$^{-/-}$ mice were infected with Salmonella, spleens were stained for GC and PB markers and analysed by flow cytometry on days 3, 4 and 7, a) Flow cytometry gating example; b-g) Splenic levels of b) GC B cells, c) PBs, d) IgM^{+} PBs, e) IgG2b-switching PBs, f) IgG2b^{+} PBs and g) IgG2c^{+} PBs. Data pooled from three individual experiments.
Key: PB – Plasmablast
Bars indicate median
< indicates cell counts were under 10^4 for that sample

127

Together, this data indicates that CCRL2 deficiency does not affect the early extrafollicular response to STm infection. Neither antibodies against STm components, nor plasmablast levels were altered between $CCRL2^{+/-}$ and $CCRL2^{-/-}$ mice, and both mice were able to control early infection with similar kinetics. Together, this indicates a different role in CCRL2 regulation of the antibody response against single antigen challenge and models of infection.

3.9 Discussion

3.9.1 CCRL2 is expressed by plasmablasts, however there was no detectable binding of chemerin nor CCL19

Expression of CCRL2 on B cells was originally detected by Hartman and colleagues, who used various B cell lines to deduce B cell expression of CCRL2 at different maturation stages (Hartmann et al., 2008). However, this study did not determine the expression of CCRL2 in B cells upon activation and differentiation into plasmablasts. Previous studies from our laboratory have detected CCRL2 as one of the first genes upregulated at an mRNA level upon differentiation into plasmablasts (Marshall, 2009, Cook, 2011), which is confirmed within this study. To confirm the presence of CCRL2 at a functional protein level, uptake of fluorescently labelled chemokine was assessed by flow cytometry using a previously published protocol (Hansell et al., 2011). Two different conjugates were used; fluorescently labelled CCL19 (Almac) and chemerin, which was conjugated to Cy5 using a Lightning Link kit (Innova Biosciences).

Plasmablast uptake of both CCL19 and chemerin was not detected in either instance. CCL19 has been suggested to bind human CCRL2 (Leick et al., 2010), but this has not been

independently confirmed, nor has any laboratory shown the ability of mouse CCRL2 to bind CCL19. As human CCRL2 has two transcript variants, it is possible that CCL19 binds human CCRL2A, and therefore no binding would be detectable in the mouse, whose single transcript variant is most similar to CCRL2B (Del Prete et al., 2013). Due to the preliminary nature of the chemerin uptake assay, further optimisation is required. It is possible that the assay was unsuccessful at numerous stages; the original conjugation of chemerin to Cy5 may have been insufficient, or conversely, the conjugation may have disrupted the site at which CCRL2 and ChemR23 bind to chemerin. Due to time constraints, there was no optimisation of the assay, therefore an insufficient concentration of chemerin may have been used.

3.9.2 Expression of CCRL2 on plasma cells negatively regulates the antibody response to NP-Ficoll

CCRL2 deficient mice immunised with the TI-II antigen NP-Ficoll have greater levels of NP-specific plasmablasts and NP-specific antibody than WT mice. This phenotype is B cell intrinsic, with no obvious contribution from CCRL2 deficiency in other cells.

From the histological observations made within this study, CCRL2 deficient plasmablasts appear in greater amounts, but within the same microanatomical compartments as CCRL2 sufficient plasmablasts. This was surprising, as CCRL2 deficiency has been shown to affect the migration of cells, including NK cells, neutrophils and dendritic cells (Zabel et al., 2008, Monnier et al., 2012, Otero et al., 2010). Also, defects in cellular migration is a common attribute in general to ACKR deficiency (Ulvmar et al., 2014, Dona et al., 2013, Venkiteswaran et al., 2013, Nibbs and Graham, 2013). However, it is possible that minor

differences in cellular location have not been detected, as well as plasmablast interactions with other cells of the spleen.

To further establish the role of CCRL2 in plasmablast function, the levels of apoptosis and proliferation were assessed. CCRL2 deficient plasmablasts incorporated reduced levels of Annexin V and 7-AAD, indicating these cells undergo lower levels of apoptosis. This is not the first time that CCRL2 deficiency has been associated with reduced cell death. In fact, cortical slides of CCRL2 deficient mice have reduced cellular death compared to their WT counterparts after incubation with ischemic solution (Douglas et al., 2013). In that study, Douglas and colleagues suggest that CCRL2 initiates an inflammatory cascade to induce apoptosis and necrosis; both of which are seen at higher levels here (Douglas et al., 2013). If CCRL2 initiates an apoptotic cascade, it would be due to ligand binding. However, this could be due to direct initiation of the cascade by CCRL2, or indirect initiation due to CCRL2 presenting the ligand to an accessory cell, and the accessory cell providing the death signal. The latter is more likely, as 1) CCRL2 does not appear to internalise its ligand, but present it on the cell surface for other cells to detect (Zabel et al., 2008) and 2) although chemerin has been shown to promote phagocytosis of apoptosing cells (Cash et al., 2010), it has not been shown to induce apoptosis itself.

Unlike apoptosis, chemerin has been implicated in causing the proliferation of cells (Yang et al., 2012). Here, CCRL2 deficient plasmablasts appear to proliferate more than CCRL2 sufficient plasmablasts in both immunised CCRL2$^{-/-}$ mice and in the adoptive transfer model. As CCRL2 deficiency has been shown to cause an increase in plasma levels of chemerin, it could be argued that plasmablast deficiency in CCRL2 could increase local

chemerin concentrations and lead to enhanced proliferation. However, this is unlikely, as an increase in local chemerin concentrations would positively affect all plasmablasts; yet transfer of QM^{KO} cells into WT hosts appears to repress the host response. Also, incubation of cells with chemerin or other ligands *in vitro* does not affect cellular proliferation.

If not through the ligand, how are CCRL2 deficient plasmablasts proliferating to greater extent than WT? Data here suggests that CCRL2 deficient plasmablasts express lower levels of TACI mRNA compared to CCRL2 sufficient plasmablasts. At first this was surprising, as a loss of TACI has a severe negative impact on both TI-II and TD responses due to the inability of cells to survive (Mantchev et al., 2007, Ou et al., 2012). However, a closer look at the data reveals that before the mass death of TACI deficient plasmablasts, they undergo a much greater amount of proliferation (Mantchev et al., 2007). Moreover, $TACI^{-/-}$ mice develop lymphoproliferation, leading to infiltration of lymphocytes in the liver and kidney and enlarged spleen and LNs (Seshasayee et al., 2003). Therefore, a reduction in the expression of TACI may result in more proliferation, without the detrimental factor of cellular death due to TACI not being completely absent.

Although plausible, the involvement of TACI remains unclear; the above is based on TACI being reduced at an mRNA level, but TACI expression at a protein level gave conflicting data. Although immunofluorescence data shows a reduction in TACI fluorescence in CCRL2 deficient plasmablasts, more accurate quantitation by flow cytometry did not indicate a difference in TACI at the protein level. Flow cytometry indicates equal levels of TACI protein between WT and $CCRL2^{-/-}$ plasmablasts. Although not proven here, it is

possible that this discrepancy is due to the intracellular stores of TACI, which would show up in the histology but not in the flow cytometry data. The other BAFF and APRIL receptor, BCMA, is highly expressed inside the Golgi apparatus (Gras et al., 1995) and therefore it is possible that TACI is also present inside the cell. To assess intracellular TACI levels and therefore determine whether this is the reason for the histology and flow cytometry discrepancy, intracellular staining by flow cytometry could be conducted.

To further assess the role of CCRL2 on plasmablasts in the response to NP-Ficoll, B cells were stimulated *in vitro* with the antigen. Differentiation into $CD138^{+}$ cells was minimal, and addition of whole splenocytes did not aid this process. Cells were stimulated with the addition of β-Mercaptoethanol, as this chemical was shown nearly 40 years ago to improve *in vitro* B cell differentiation into antibody secreting cells by NP-Ficoll (Chused et al., 1976). However, the study also showed that addition of macrophage to the culture increases the formation of antibody secreting cells to an even greater extent (Chused et al., 1976), which may be due to MZ macrophages binding NP-Ficoll (figure 3.13). This implies that, to further improve on the response from *in vitro* stimulation of B cells, addition of macrophage may be required.

Surprisingly, immunisation of CCRL2 deficient QM mice with NP-Ficoll did not induce an advantage in the response in comparison to immunisation of WT QM mice. A previous study (Hsu et al., 2006) has shown that spleens can only sustain a limited amount of plasmablasts. Due to the sheer volume of antigen-specific B cells in the QM mouse, the peak of plasmablast levels is reached much sooner than in conventional WT and CCRL2 mice. Therefore, it is likely that the sheer strength of the response in both WT and CCRL2

deficient QM mice cancelled out the positive effect of CCRL2 deficiency detected in non-QM mice.

3.9.3 The role of CCRL2 in the response to TD-, TI-I- and Salmonella- immunised CCRL2 deficient mice is less clear

Although CCRL2 deficient mice had a slightly improved response to the TD antigen NP-CGG, the increase was not at the level seen in response the NP-Ficoll, and was not significant at any time point. A previous study from Otero and colleagues deduced that the amount of IgE in response to OVA was similar between WT and CCRL2 deficient mice (Otero et al., 2010). IgE levels were measured 23 days after the original immunisation with OVA and the levels of other antibody isotypes are not deduced (Otero et al., 2010). Here, the IgG1 switched response is level between WT and CCRL2 deficient mice by day 14, which concurs with the late TD response being level amongst WT and CCRL2$^{-/-}$ mice.

Unlike during the primary TD response, CCRL2 deficient mice had an improved response to secondary immunisation, where naïve B cells were activated by memory T cells, compared to WT. This data is similar to that seen in response to NP-Ficoll, suggesting that the slow B cell response to primary immunisation, ie. the need for T cell activation also, impedes the positive effect of CCRL2 deficiency.

The increases in antibody and plasmablast levels detected upon NP-Ficoll and secondary TD immunisation was not observed upon immunisation with the TI-I antigen, TNP-LPS. In fact, in this instance, CCRL2 deficiency appeared to negatively affect the response; with reduced antibody levels detected, although this was not significant at any time point. Although these minor changes in the LPS phenotype is opposite to that detected with NP-

Ficoll, the phenotype is not necessarily surprising. LPS is an inflammatory mediator and four studies have shown that CCRL2 deficient mice are protected in response to inflammatory models (Monnier et al., 2012, Zabel et al., 2008, Otero et al., 2010, Douglas et al., 2013), showing that CCRL2 has an important role in inflammation. Therefore, a reduced response to TNP-LPS in CCRL2 deficient mice would concur with previous reports. Also, the apparent discrepancy between the NP-Ficoll and TNP-LPS responses could be explained by the expression of CCRL2 upon LPS stimulation. As described in the introduction, CCRL2 is upregulated upon LPS stimulation of macrophage, neutrophils and endothelial cells (Shimada et al., 1998, Galligan et al., 2004, Monnier et al., 2012). Conversely, in the NP-Ficoll response it is likely that CCRL2 is only upregulated on plasmablasts upon their differentiation. To specifically differentiate the role of CCRL2 in B cells upon injection of LPS, similar experiments to the ones used in this study with NP-Ficoll should be conducted, where only B cells are deficient in CCRL2. However, as the primary response to NP-LPS is dominated by kappa light chain antibodies (Smith et al., 1985) QM mice could not be used, due to these having a non-functional kappa allele (Cascalho et al., 1996). Therefore, in this instance transfer of WT or CCRL2$^{-/-}$ B cells into RAG-1$^{-/-}$ mice (which are unable to produce mature B and T lymphocytes (Mombaerts et al., 1992)), would be more appropriate. This would establish the role of CCRL2 deficiency in B cells only, without the effect of other cells inducing CCRL2 due to LPS injection.

Surprisingly, in response to the TI-II antigen OMP, in the context of Salmonella infection, there is no difference in the early plasmablast response between CCRL2$^{+/-}$ and CCRL2 deficient mice. In this instance, CCRL2$^{+/-}$ and CCRL2$^{-/-}$ littermates were used due to previous experiments indicating CCRL2$^{+/-}$ mice act as WT. Littermates also ensure the

mice had all been exposed to similar endogenous bacterial flora pre-infection. To more accurately assess the role of CCRL2 deficiency on the extrafollicular Salmonella response, WT and CCRL2$^{-/-}$ littermates should be used; however, due to time constraints this was not possible here. Nevertheless, in all parameters assessed, CCRL2$^{+/-}$ and CCRL2$^{-/-}$ mice gave similar results. It is possible that any positive effect of CCRL2 deficiency on the antibody response to OMP is neutralised by the negative, inflammatory effect of LPS, as observed in the experiments with individual immunisations of TI-II and TI-I antigens. Immunisation with isolated OMP would enable assessment of the role of CCRL2 to the protein individually, and therefore determine whether immunisation with multiple antigens affects the antibody response to OMP.

Altogether, this chapter shows a novel role of CCRL2 in the regulation of the plasmablast response. In response to NP-Ficoll, the NP-specific antibody and plasmablast response in CCRL2 deficient mice is increased compared to WT. Moreover, antigen-specific antibody produced by naïve B cells activated by primed T cells is also increased in CCRL2 deficient mice. The increase in plasmablasts is due to improved proliferation and reduced apoptosis of CCRL2 deficient plasmablasts. However, as CCRL2 may positively regulate the B cell response to LPS, further analysis of the exact mechanisms are required to fully understand the role of CCRL2 in plasmablast biology.

Chapter 4. Effect of CCRL2 Deficiency on GC Responses

4.1 Introduction

B cells activated by thymus dependent (TD) antigen may enter into various differentiation stages: extrafollicular plasmablasts, follicular germinal centre (GC) B cells and from the GC into memory B cells or plasma cells. As discussed in the previous chapter, CCRL2 deficiency in plasmablasts is positive for the response, suggesting CCRL2 acts as a negative regulator. This chapter will explore the role of CCRL2 in GC B cell differentiation and function.

4.1.1 The germinal centre

The GC is a structure that forms within the B cell follicles of secondary lymphoid organs. It is made up of several cell types, GC B cells (which differentiate into centroblasts and centrocytes), T follicular helper cells (T_{FH}) follicular dendritic cells (FDCs) and tingible body macrophages. These cells interact, resulting in affinity maturation of B cell receptors (BCRs) expressed by GC B cells and enabling the production of high affinity plasma cells and memory B cells. For an overview of the GC response, see Chapter 1, section 1.6.1.1.

4.1.1.1 GC B cell differentiation; a role for Bcl6

B cell lymphoma 6 (Bcl6) is a transcriptional repressor that allows GC B cell fate. Bcl6 is also involved in the development of $CD4^+$ T_{FH} cells, which is discussed in detail in (Choi et al., 2013)). GC B cells are highly proliferative and express mutagenic enzymes, therefore expression of Bcl6 is highly regulated. Interestingly, Bcl6 binds its own 5' regulatory region, and mutations in Bcl6 which prevent it from binding this region have been implicated in GC-derived lymphomas (Pasqualucci et al., 2003).

As a transcriptional repressor, Bcl6 suppresses genes responsible for plasma cell differentiation and function. Tunyaplin *et al.* showed that one gene repressed by Bcl6 is *prdm1* (which encodes Blimp1, the transcriptional repressor that has a central role in plasma cell differentiation). The authors found that two intronic regions of mouse *prdm1* are able to undergo Bcl6-dependent repression, with one of these sites being conserved between mice and humans. Subsequently, $Bcl6^{-/-}$ mice have elevated levels of $Blimp1^{+}$ plasma cells *in vivo* (Tunyaplin et al., 2004).

As well as repressing the transcription of protein-coding genes, Bcl6 has also been shown to regulate the expression of micro (mi)RNAs. Using ChIP-on-chip data along with miRNA expression, Basso and colleagues identified Bcl6 binding of 15 miRNAs, including miR-155 and miR-361; two miRNAs which modulate the expression of activation-induced cytidine deaminase (AID) (Basso et al., 2012).

4.1.1.2 Increasing antibody affinity; somatic hypermutation and AID

Somatic hypermutation (SHM) is the process in which dark zone resident centroblasts mutate their genes to increase the specificity of their B cell receptor for foreign antigen. Point mutations are introduced to the variable ("V") region of both the heavy and light chains of immunoglobulin genes; the frequency of mutation is ~10^{-5} to 10^{-3}/base pair/generation (the base level of mutation being approximately 10^{-9}) (reviewed by (Peled et al., 2008)). Mutations are not always positive; affinity to antigen may be reduced in the mutated cell, resulting in apoptosis.

One of the key elements of this process is AID, a mutagenic enzyme whose expression is restricted to GC B cells. The function of AID is to convert deoxycytidines (dC) to

deoxyuridine (dU). These mutations then undergo error-prone repair, causing permanent mutations within the V region (reviewed by (Peled et al., 2008)). The importance of AID in SHM was confirmed by Revy and colleagues, who noted that patients with mutations in AID have hyper-IgM syndrome type 2 (HIGM2) and lack immunoglobulin somatic hypermutations. Similarly, $AID^{-/-}$ mice have HIGM2, resulting in large TD GCs, but little SHM and class switch recombination (CSR) (Revy et al., 2000).

4.1.1.3 Changing antibody effector function; class switch recombination and AID

Class switch recombination is the process by which B cells alter their immunoglobulin isotype, by changing the heavy chain constant region. Unlike SHM, CSR does not increase antibody affinity, but alters the effector function of the antibody.

Naïve B cells express either IgM or IgD, due to expression of heavy chain constant regions Cμ or Cδ. Upstream of the different constant regions (except Cδ) are switch (S) regions, through which CSR occurs. AID converts dC to dU within two of these S regions, which leads to breaks within the DNA, excision of the intervening regions and subsequently switching (reviewed by (Stavnezer et al., 2008) and (Xu et al., 2012)).

CSR can occur by B cell-expressed CD40 binding CD40L (CD154) and/or B cell-expressed Toll-like receptor 4 (TLR4) binding LPS. However, the isotype to which cells switch is influenced by the type of response. For example, T_H1 responses, in which interferon (IFN)-γ is produced, cells primarily switch to IgG_{2a}. Yet interleukin (IL)-4 producing T_H2 responses induces switching to IgG1 and IgE (Toellner et al., 1998). Isotype switching can also occur in extrafollicular thymus independent (TI) responses; as observed in the previous chapter. TI-II antigens, such as NP-Ficoll, induce switching predominantly to

IgG3, however TI-I antigens mainly cause switching to IgG_{2b} (Perlmutter et al., 1978, Marshall et al., 2011).

4.1.2 Aims of chapter

1. Determine the expression of CCRL2 within GC B cells
2. Determine the effect of CCRL2 deficiency on GC microarchitecture
3. Determine the effect of CCRL2 deficiency on GC B cell phenotype
4. Determine the effect of CCRL2 deficiency on GC output

4.2 Results

4.2.1 CCRL2 expression within GCs

4.2.1.1 CCRL2 mRNA is present in the GC, but CCRL2 is not expressed in GC B cells

CCRL2 mRNA is upregulated early in plasmablast differentiation (figure 3.5) and previous data from our laboratory has shown that microdissected GCs have higher levels of CCRL2 mRNA expression than in the T-Zone (TZ) (Cook, 2011). To determine whether CCRL2 mRNA is specifically upregulated in B cells of the GC, CCRL2 expression was determined on GC B sorted cells. cDNA was kindly provided by Dr. Yang Zhang, in an experiment where WT mice were immunised with NP-Sheep Red Blood Cells and GC B cells sorted on days 4, 5, 8 and 10 post immunisation. However, CCRL2 expression was not detectable at any time point (data not shown).

4.2.1.2 ACKR4 binds CCL19 on GC B cells

TZ expressed CCL19 has been shown to bind the receptors CCR7 and ACKR4, however it has also been proposed to bind CCRL2 (Leick et al., 2010) (for full details see chapter 3, section 3.5.5). To test whether GC B cells are able to bind CCL19 via CCRL2, WT and CCRL2$^{-/-}$ mice with NP-specific BCRs were immunised with NP-Ficoll to generate GCs. Spleen cells were isolated and the cells were incubated with fluorescently conjugated CCL19 (a kind gift from Chris Hansell, The University of Glasgow). Fluorescence was detected by flow cytometry, as per a previously published protocol (Hansell et al., 2011). As CCRL2 was not present at the mRNA level (section 4.2.1.1) CCL19 binding was not expected to be any different between WT and CCRL2 deficient samples. As a control,

CCR7$^{-/-}$ and ACKR4$^{-/-}$ mice with NP-specific BCRs were also analysed, due to these receptors also binding CCL19.

Germinal centre cells were gated as B220^{+} CD138^{-}, Fas^{+} CD38^{-} (figure 4.1a) (Oliver et al., 1997). As shown in figure 4.1, WT GC B cells have detectable binding of CCL19, with an MFI of 752 similar to that seen in T cells (chapter 3, figure 3.21b). Addition of excess amounts of unconjugated CCL19 did not reduce CCL19 binding (figure 4.1c). CCR7$^{-/-}$ cells had a similar CCL19 MFI compared to WT cells. ACKR4$^{-/-}$ GC B cells were unable to efficiently bind CCL19, with a reduction of median MFI to 277 (figures 4.1b and 4.1c). The MFI detected in ACKR4 deficient cells was at as low a level as that seen in CCR7$^{-/-}$ cells with addition of unconjugated CCL19. This suggests that CCL19 binds GC B cells via ACKR4. Unsurprisingly, as CCRL2 was not present at an mRNA level on GC B cells, CCRL2$^{-/-}$ GC B cells bind CCL19 at a similar level to that seen in WT GC B cells, with a CCL19 MFI of 604.5. Together, this shows that ACKR4, but not CCRL2 nor CCR7, binds CCL19 on GC B cells.

Therefore, CCRL2 is expressed within GCs, however it is not expressed on GC B cells. It is possible that CCRL2 is present on other cells of the GC – T_{FH} cells or FDCs. However, ACKR4 can bind CCL19 via GC B cells, suggesting that this atypical receptor has a role in GC B cell function.

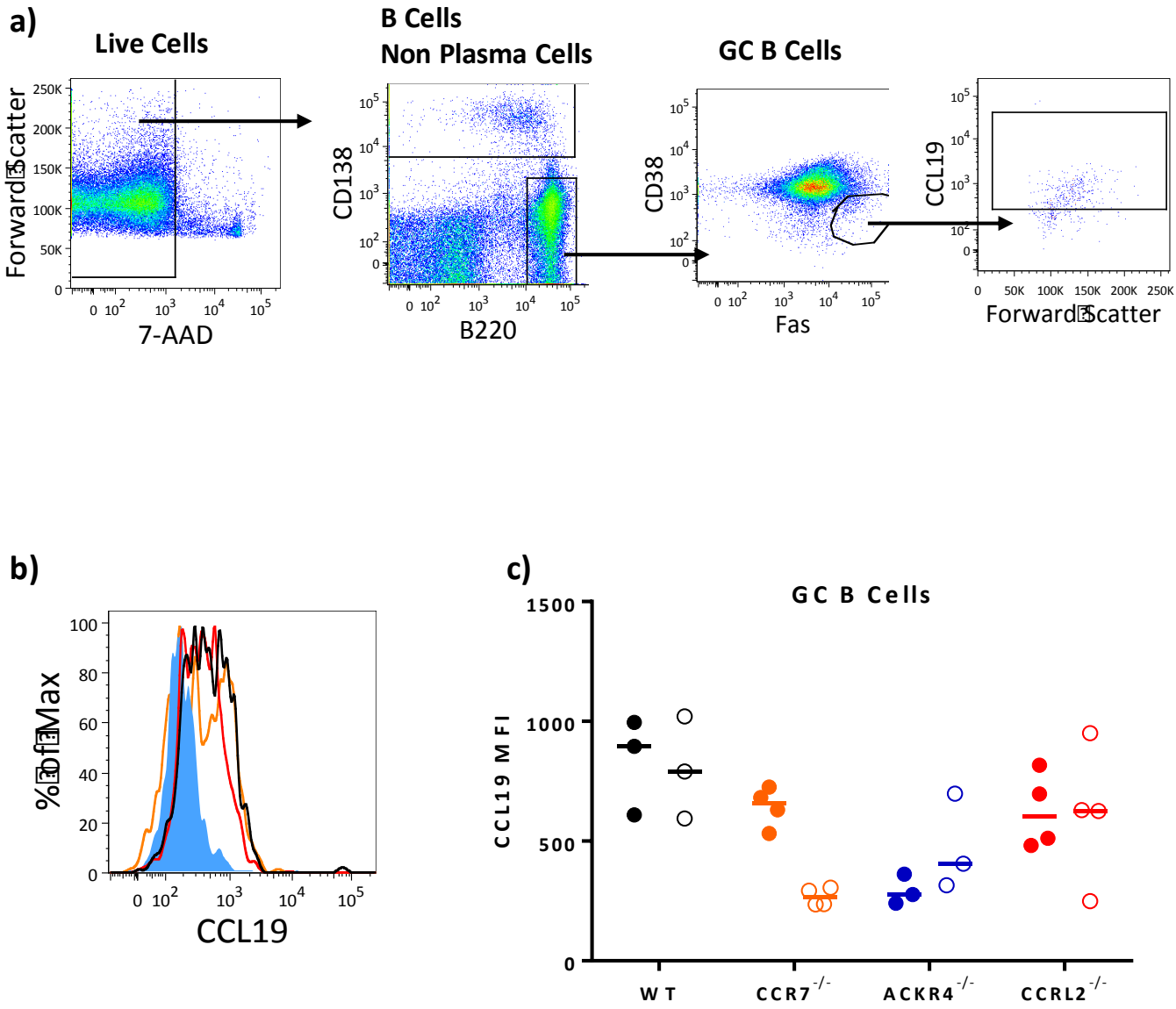

Figure 4.1. GC B cells bind CCL19 via ACKR4 and not CCRL2. WT, CCR7$^{-/-}$, ACKR4$^{-/-}$ and CCRL2$^{-/-}$ mice with NP-specific B cells were immunised with NP-Ficoll to generate GC B cells. Splenocytes were incubated with CCL19^{AF647} with or without unconjugated CCL19 and CCL19 binding analysed by flow cytometry; a) Flow cytometric gating; b-c) CCL19 binding on GC B cells by genotype, b) Histogram representation of CCL19 binding, c) CCL19 MFI of GC B cells.
Key: Closed circles with CCL19^{AF647} only. Open circles CCL19^{AF647} with unconjugated CCL19. MFI – Mean Fluorescence Intensity.
Data from single experiment. Bars indicate median.

4.2.2 GC microarchitecture is unaffected by CCRL2 deficiency

GCs are microstructures within the B cell follicles of secondary lymphoid organs. Although there was no detectable differences in splenic microarchitecture by the methods used in this study (figure 3.2), it is not known whether GC microarchitecture is disturbed due to a lack of CCRL2. Although CCRL2 mRNA was not detected in GC B cells (section 4.2.1.1), it is present in higher levels in GCs than in the TZ (Cook, 2011). To assess whether CCRL2 has a role in GC organisation or microarchitecture, WT and CCRL2$^{-/-}$ mice were immunised with NP-CGG to induce GC formation in the spleen, and spleens were sectioned and stained for B cell, follicular dendritic cell and stromal cell markers in order to visualise GC microarchitecture (figure 4.2).

GCs are identified as IgD^{-} structures that form within IgD^{+} B cell follicles in the spleens of WT mice, with GCs induced by NP-CGG immunisation being NP^{+}. As shown in figure 4.2a, GCs formed within both WT and CCRL2$^{-/-}$ mice, with no obvious difference in GC shape, size nor location between the genotypes.

GCs contain two main regions; the dark and light zones (DZ and LZ, respectively). In order to determine whether GC formed in CCRL2 deficient mice contain both DZ and LZs, spleens were stained for CD35 (also known as complement receptor 1), which is highly expressed in LZ resident FDCs, but absent in the DZ. Staining of WT GCs with CD35 revealed a similar LZ-DZ separation in both WT and CCRL2$^{-/-}$ mice (figure 4.2b), with CD35^{+} FDCs of the LZ towards the red pulp, and CD35^{-} DZ closer to the TZ. FDCs are not just resident within the IgD^{-} areas of the B cell follicle, but also extend within the IgD^{+} B cell areas .

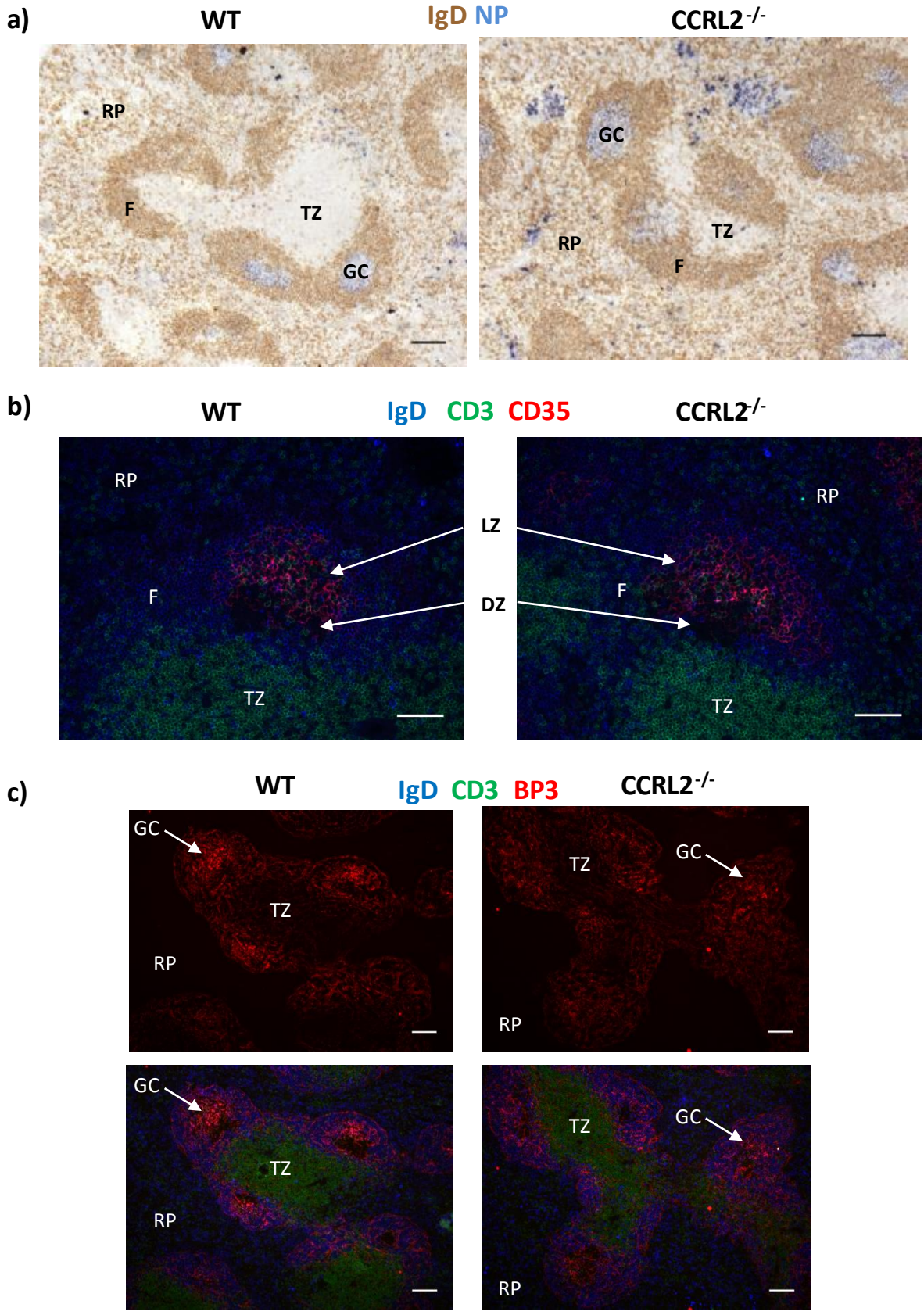

Figure 4.2. CCRL2 deficiency does not affect germinal centre microarchitecture. WT and CCRL2$^{-/-}$ mice were immunised with NP-CGG and spleens were sectioned and stained for stated markers to visualise defined zones and cells of the GC; a) Immunohistochemistry showing NP-specific GCs formed in B cell follicles of splenic white pulp; b) CD35^{+} follicular dendritic cells (red) located within the light zone of the GC; c) BP3^{+} FDCs and follicular stromal cells present in both WT and CCRL2$^{-/-}$ GCs.
Sections representative of 4 mice per group.
Key: F– Follicle; GC – Germinal Centre; RP – Red Pulp; TZ – T-Zone
Scale Bar – 100µm (a,c); 75µm (b)

144

It could be argued that FDCs from the CCRL2 deficient spleen section extended further into the follicle than in the WT section, however this appears to be an artefact of CD35 staining, as staining of the FDCs with BP3 (figure 4.2c) does not indicate this phenotype. Further assessment of FDCs with other markers, such as FDCM2, would clarify this potential phenotype.

FDCs also express BP3 (CD157), which is also a marker for follicular stromal cells. To determine if CCRL2 deficiency affects the organisation of the stromal compartment as a whole, NP-CGG immunised WT and CCRL2$^{-/-}$ spleens were stained for BP3 (figure 4.2c). The highly organised stromal network is present in the follicles of both WT and CCRL2 deficient spleens, with stronger BP3 expression on FDCs in both WT and CCRL2$^{-/-}$ mice. A thin layer of BP3^{+} cells form a border around the follicles, separating the white and red pulps. BP3^{+} areas were also present within the TZ of both WT and CCRL2 deficient mice, but this is a much weaker staining compared to that of the follicles. Therefore, this shows that CCRL2 deficiency does not obviously affect the organisation of the stromal network, even post GC formation. Altogether, there are no obvious differences in GC organisation in the spleens of CCRL2 deficient mice, as detected using the markers, IgD, CD35 and BP3. Further analysis using other markers such as FDC-M1 and FDC-M2 would allow a more thorough analysis of the FDC phenotype observed here.

4.2.3 Phenotype of GC B cells formed as part of a thymus independent response

Traditionally, GCs were thought to form only in response to thymus TD antigens (MacLennan, 1994). However, QM mice, which have a high frequency of B cells with an NP-specific receptor, are able to form GCs in response to NP-Ficoll. These GCs are short

lived, and often collapse day 5 post immunisation due to a lack of T cell help (de Vinuesa et al., 2000). In order to analyse the effect of CCRL2 deficiency on GCs, WT and CCRL2$^{-/-}$ QM mice (known hereafter as QM^{WT} and QM^{KO}, respectively) were immunised with NP-Ficoll and GC B cell formation was followed by flow cytometry (figure 4.3a). Although low levels of GC B cells were present on day 2 post immunisation, in QM^{WT} mice the levels double by day 3, and remain at this high level on day 5 post immunisation. However, the proportions of GC B cells in QM^{KO} mice remain at the day 2 levels on day 3, and increase slightly on day 5. The proportion of GC B cells in QM^{KO} mice never reached the levels seen in QM^{WT} ($p<0.05$).

To determine if there are any intrinsic differences in QM^{WT} and QM^{KO} GC B cells, on day 3 post NP-Ficoll immunisation NP-specific GC B cells were sorted by FACS (NP^{+}B220^{+}CD138^{-} Fas^{+}CD38^{-}) and prepared cDNA was tested by RT-qPCR for GC-associated genes. NP-specific plasmablasts (NP^{+}B220^{+}CD138^{+}) were used as controls. For information on purity see chapter 3 figure 3.16.

AID is a protein involved in both SHM and CSR. Expression of AID was reduced 10-fold in QM^{KO} B cells compared to their WT counterparts ($p<0.05$, figure 4.3b). As expected, AID was not detectable in the plasmablast sample. Bcl6 is a transcription repressor, and the master regulator of GC B cell fate. Expression of Bcl6 was approximately 100 fold less in QM^{KO} GC B cells compared to QM^{WT} GC B cells ($p<0.05$, figure 4.3c). Unsurprisingly, plasmablast samples did not have detectable levels of Bcl6 mRNA expression.

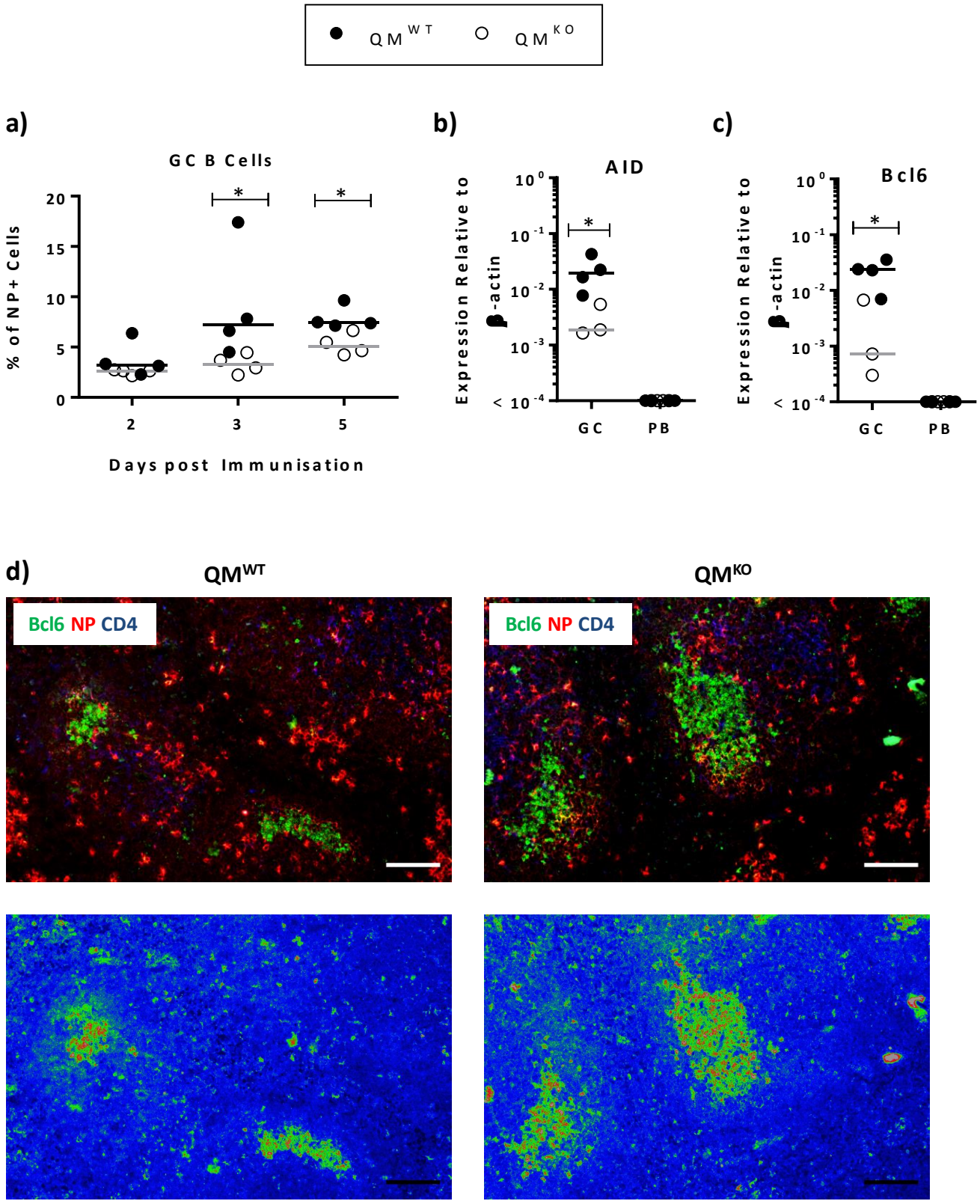

Figure 4.3. Phenotype of TI-II induced GC B cells in WT and CCRL2 deficient mice. QM^{WT} or QM^{KO} mice were immunised with NP-Ficoll and a) GC B cells were analysed by flow cytometry; b-c) Activated B cells were sorted on day 3 of the response and b) AID mRNA expression, c) Bcl6 mRNA expression was determined by RT-qPCR; d) Bcl6 protein expression by immunofluorescence on day 3 of the response.
Sections representative of 4 mice per group. Data from single experiment. Bars indicate median
Scale bar - 100µm
Key: GC – Germinal Centre B cells; PB - Plasmablasts
< indicates mRNA levels in the sample were under the lowest detection limit
*p<0.05

In order to determine whether altered Bcl6 expression is also reflected at the protein level, GC B cells were stained for Bcl6 by both flow cytometry and immunohistology (figures 4.3d and 4.4). QM^{WT} and QM^{KO} mice were immunised with NP-Ficoll and spleens were sectioned and Bcl6 expression examined by immunofluorescence (figure 4.3d). There were no detectable differences between QM^{WT} and QM^{KO} mice, with high Bcl6 expression observed in the GCs of both mice, particularly when pictures are studied in "heat map" form.

To further assess Bcl6 protein expression in GC B cells of immunised QM^{WT} and QM^{KO} mice, levels of Bcl6 were determined by flow cytometry (figure 4.4). As shown in figure 4.4a, Bcl6 MFI was higher in GC B cells than NP^- B cells. However, on day 3 of the response there was no difference in Bcl6 expression in GC B cells of QM^{WT} and QM^{KO} mice. To determine whether it takes time for changes in Bcl6 mRNA levels to have an effect at the protein level, mice were also tested for Bcl6 expression on day 4 of the response by flow cytometry. As figure 4.4a shows, there is a small, but not significant, reduction in MFI of Bcl6 in GC B cells of QM^{KO} mice at day 4. In order to establish whether an alternate immunisation regimen shows any effect in Bcl6 protein levels, QM^{WT} and QM^{KO} B cells were isolated and transferred into WT BoyJ mice. Recipient mice were immunised with NP-Ficoll 24 hours later. Flow cytometry gating is shown in figure 4.4b. Host B cells had a much smaller Bcl6 MFI than GC B cells derived from transferred cells. At the start of the response (days 2 and 3) there were no differences in Bcl6 levels, with the MFI in both QM^{WT} and QM^{KO} derived GC B cells being level.

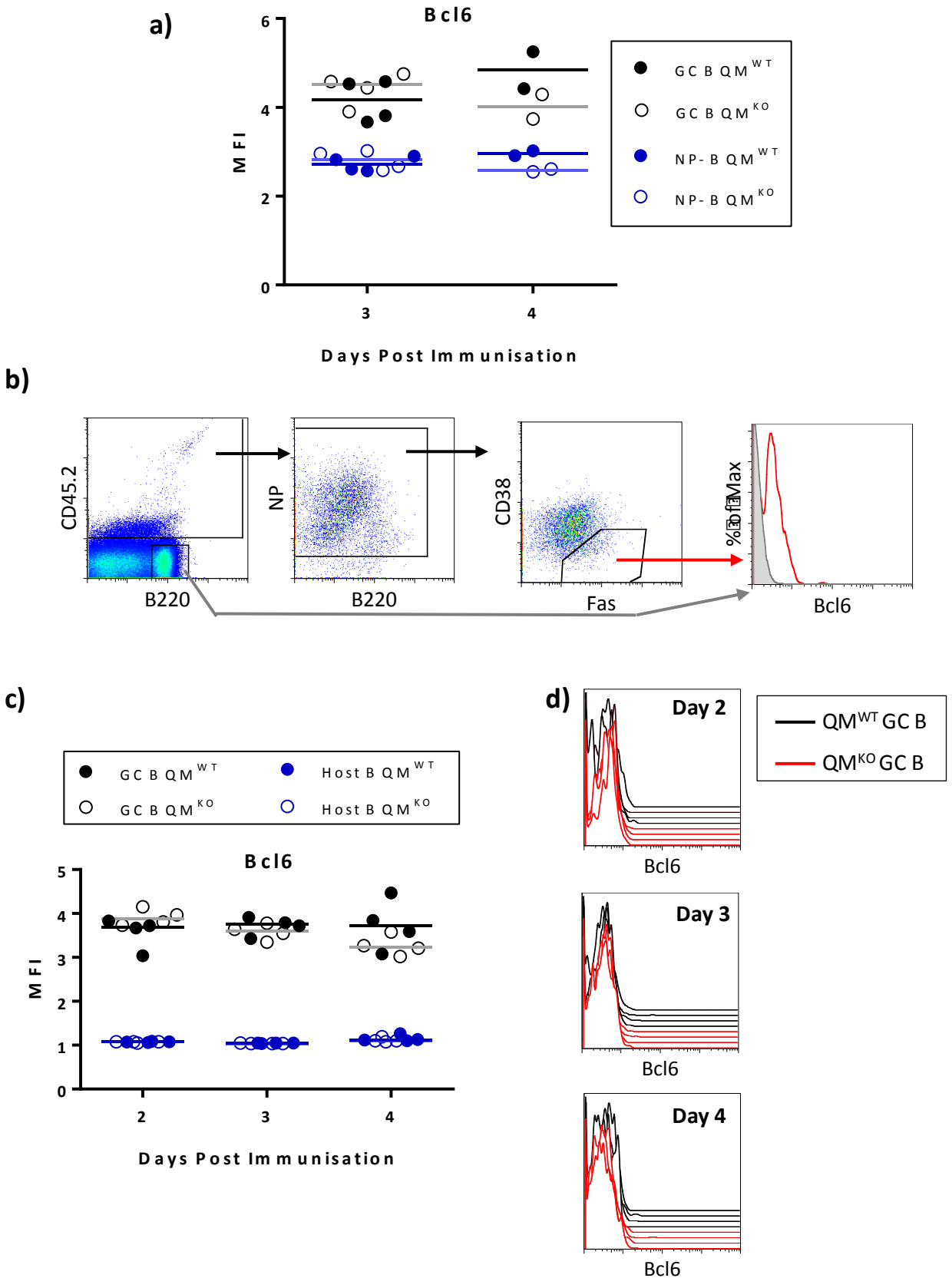

Figure 4.4. Flow cytometry analysis of Bcl6 expression in GC B cells of WT and CCRL2 deficient mice. a) QM^{WT} or QM^{KO} mice were immunised with NP-Ficoll and GC B cells were analysed for Bcl6 expression on day 3 of the response; b-d) QM^{WT} or QM^{KO} NP-specific B cells were transferred into WT and hosts and 24h later recipient mice were immunised with NP-Ficoll, Bcl6 expression was determined by flow cytometry on days 2, 3 and 4 post immunisation, b) Flow cytometry gating strategy, c) Bcl6 MFI, d) Histogram representation of Bcl6 expression in GC B cells
Data from single experiments. Bars indicate median.

However, on day 4 of the response QM^{KO} cells had a small decrease in Bcl6 expression (from an MFI of approximately 4 in QM^{WT} to 3.5 in QM^{KO}), but this small decrease is not significant, nor does it reflect the large difference detected at an mRNA level (figures 4.4c and 4.4d).

Altogether, QM^{KO} mice immunised with NP-Ficoll are altered in their GC B cell phenotype compared to QM^{WT}, however results gained are inconsistent. CCRL2 deficient mice have a reduction in the proportions of GC B cells as well as a reduction in AID and Bcl6 mRNA production. Although the reduction in Bcl6 is not obviously affected at the protein level, whether changes at an mRNA have an effect in the production or affinity of antibody of CCRL2 deficient GCs is determined in the following sections through TD responses.

4.2.4 CCRL2 deficient thymus dependent GCs

Although there are no obvious differences in GC microarchitecture, CCRL2 deficient GC B cells formed as part of a TI response have a reduction in the mRNA expression of 2 key factors, AID and Bcl6. In order to determine whether these changes have an effect in TD GC function, time courses of primary and secondary immunisations in WT and CCRL2 deficient mice were conducted and GC output assessed.

4.2.4.1 Primary thymus dependent GC responses

To deduce whether GC output is affected in primary TD responses, WT and $CCRL2^{-/-}$ mice were immunised with NP-CGG, and the response analysed on days 5, 8 and 14 so that the early, peak and late GC response is assessed.

GC B cell levels of the spleen were analysed by flow cytometry. The number of GC B cells increased from day 0 (unimmunised) through day 5 and to day 8, in both WT and $CCRL2^{-/-}$

mice (figure 4.5b). On day 14, GC B cells decreased by about half, although not to background levels in either genotype. Unlike with the TI GCs, there were no differences in GC B cell levels in WT and CCRL2$^{-/-}$ immunised mice at any time point.

Although there is no difference in GC microarchitecture, the size and numbers of GCs over the spleen section has not been assessed. GCs, as a percent of spleen size, increased on days 5 through 8, before a reduction at day 14 as seen with GC B cells by flow cytometry (figure 4.5c). Interestingly, on day 8 of the GC response 2.5% of the spleen was taken up by GCs in CCRL2$^{-/-}$ mice compared to only 1% in WT ($p<0.05$, figure 4.5c), even though there were no differences in GC B cell levels by flow cytometry. The percentage of spleen taken up by GC was not different between WT and CCRL2$^{-/-}$ mice on other days of the response. Therefore, although flow cytometry indicates no difference in the percentage of GC B cells between WT and CCRL2$^{-/-}$ mice, a larger proportion of the spleen in the latter is taken up by GCs. This would indicate an expansion in a non-B GC population, possibly FDCs as suggested by immunofluorescence staining (figure 4.2b).

To determine whether GC output is affected by CCRL2 deficiency, the affinity of antibody in the blood of immunised mice was assessed by ELISA. High affinity NP-specific antibody was detected by coating plates with NP_2-BSA; high affinity antibody out competes antibody of lower affinity due to the limited availability of NP. Conversely, total NP-specific antibody is detected by coating plates with NP_{15}-BSA; the high amount of NP available enables binding of all NP-specific antibodies.

High affinity IgG1 was only detectable on day 14 of the response (figure 4.5d), and there was no difference in the amount of high affinity IgG1 between WT and CCRL2$^{-/-}$ mice. In

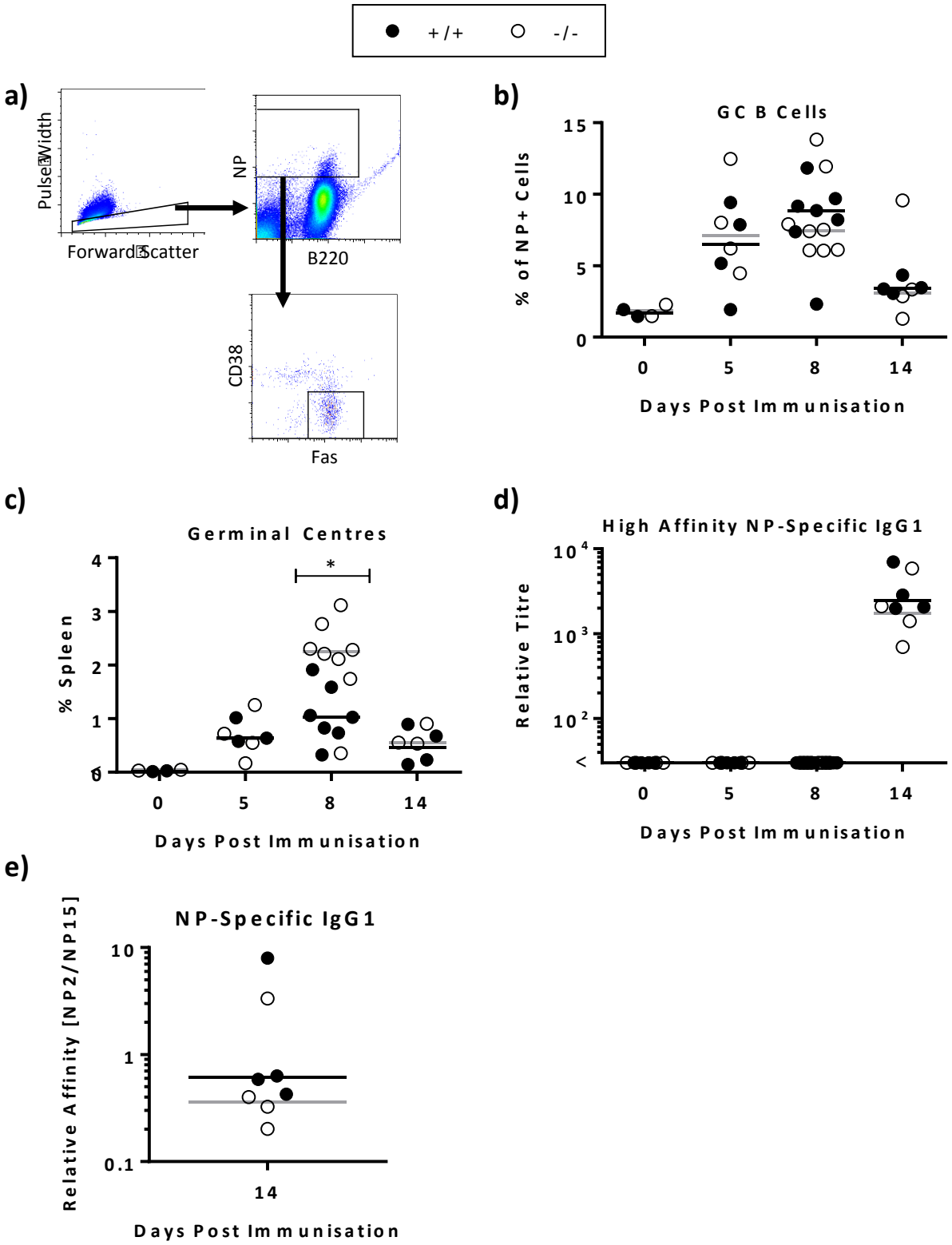

Figure 4.5. Minor differences in NP-specific GCs in CCRL2$^{-/-}$ mice do not affect NP-specific antibody affinity. WT and CCRL2$^{-/-}$ mice were immunised with NP-CGG and the GC response analysed at days 5, 8 and 14 post immunisation; a-b) Flow cytometry analysis of GC B cells in the spleen of immunised mice, a) Example gating of NP-specific GC B cells, b) NP-specific GC B cells; c) GC size as determined by immunohistology; d) High affinity NP-specific IgG1 in the blood of mice; e) Relative affinity of NP-specific IgG1.
Data pooled from two individual experiments.
Bars indicate median
< indicates antibody levels in the sample were under the lowest detection limit

order to relate the amount of high affinity antibody produced to total NP-specific antibody (chapter 3, figure 3.29), the relative affinity of antibody was calculated (figure 4.5e). There was a high variability in the relative affinity of IgG1, with no observable difference between WT and CCRL2$^{-/-}$ mice.

Although the thymus independent response showed a reduction in GC B cells and levels of AID and Bcl6 in GC B cells, no such differences are detected in the TD response. There was no differences between GC B cells from WT and CCRL2$^{-/-}$ mice, and the affinity of GC-derived antibody was not altered amongst WT and CCRL2 deficient mice, suggesting that the protein functions of Bcl6 and AID were not affected. Interestingly, the proportion of spleen sections taken up by GCs was much greater in CCRL2 deficient mice compared to WT, which is likely to reflect a non-B cell role of this receptor in GC biology.

4.2.4.2 Secondary thymus dependent GC response

As primed T cells are readily available in secondary antibody responses, there is not a delay due to T cell priming. This enables a much faster B cell response with kinetics more closely resembling TI B cell activation. Here, mice are primed with CGG and 5 weeks later boost immunised with NP-CGG.

Within the memory response, NP-specific GC B cells were detectable by flow cytometry as early as day 3 post immunisation (figure 4.6a). On both days 3 and 5, the proportions of NP-specific GC B cells were level amongst WT and CCRL2 deficient mice, although there was a high variability in GC B cell proportions on day 5. Within the primary GC response, the size of NP-specific GCs in CCRL2$^{-/-}$ mice was larger than in WT, therefore to assess GC size changes over time, NP^{+} GCs stained by immunohistochemistry were quantified

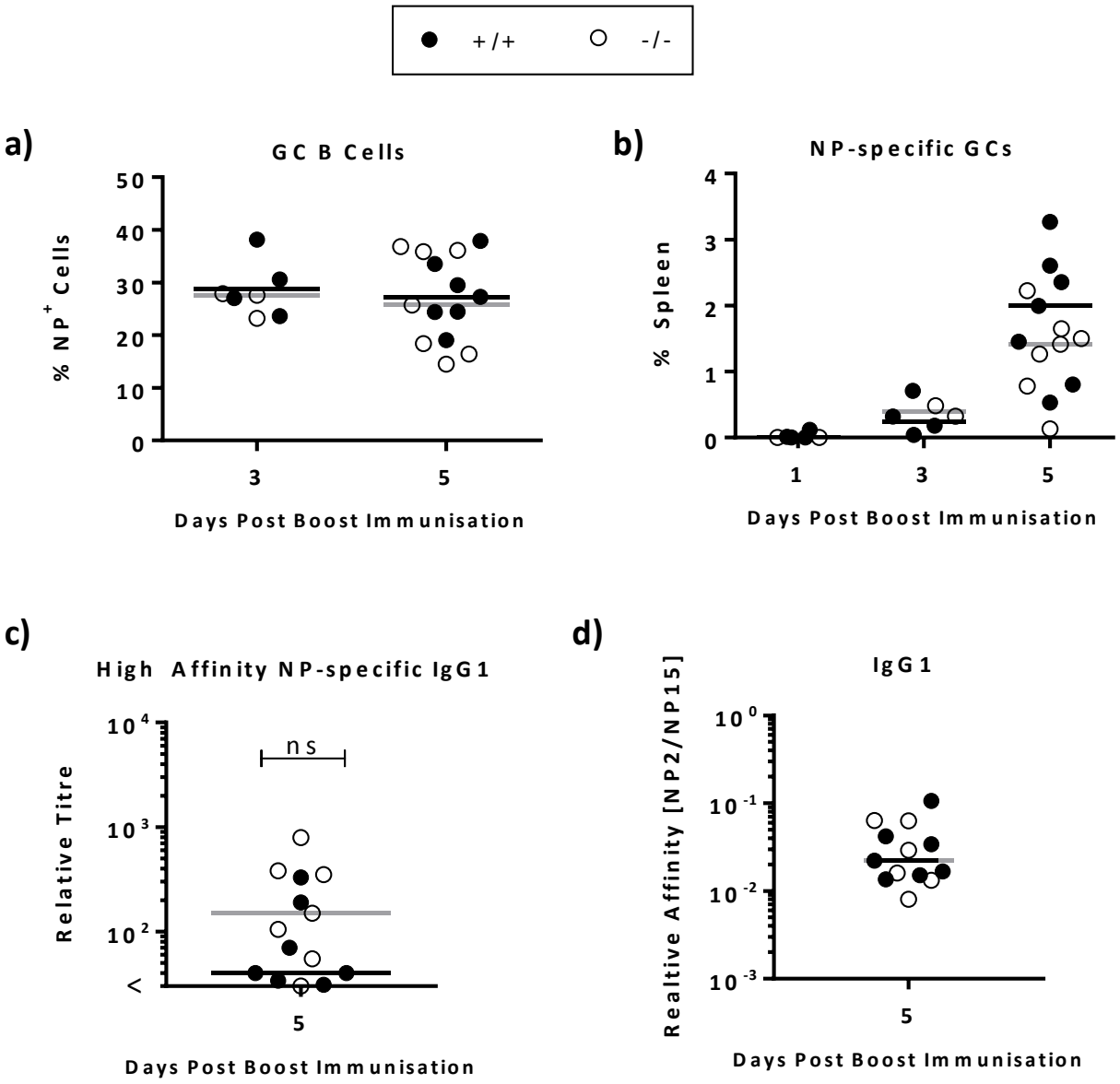

Figure 4.6. No difference in NP-specific GCs of WT and CCRL2 deficient mice as part of a secondary response. WT and CCRL2$^{-/-}$ mice were primed with CGG and boost immunised with NP-CGG and the GC response analysed at the stated time points; a) Flow cytometry analysis of GC B cells in the spleen of immunised mice; b) GC size as determined by immunohistology; c) High affinity NP-specific IgG1 in the blood of mice; d) Relative affinity of NP-specific IgG1.
Data pooled from two individual experiments. Bars indicate median
< indicates antibody levels in the sample were under the lowest detection limit

(figure 4.6b). The proportion of spleen taken up by GCs increased over time from days 1 to 5. However, unlike the primary TD response, there was no difference in the percentage of spleen taken up by NP-specific GCs between WT and CCRL2$^{-/-}$ mice. Indeed, there is a slight reduction in GC size in CCRL2 deficient mice (2% in WT and 1.5% in CCRL2$^{-/-}$ mice). However, like GC B cells by flow cytometry, the variability of GC size at day 5 was very high.

To determine whether CCRL2 deficiency affects the affinity of antibody produced in the memory TD response, high affinity IgG1 was measured using ELISA plates coated with NP_2-BSA. Even though immunohistology indicated CCRL2 deficient mice have reduced proportions of NP-specific GCs in the spleen, levels of high affinity NP-specific IgG1 were five-fold higher in CCRL2 deficient mice, although this increase was not significant (figure 4.6c). To assess whether the relative affinity of the antibody is altered, the levels of high affinity IgG1 was divided by levels of total IgG1. As with the primary TD response, the relative affinity of NP-specific antibody produced by the mice was the same, irrespective of genotype (figure 4.6d).

Together, this data suggests that, although there are minor differences in the GC phenotype between WT and CCRL2$^{-/-}$ mice, GC output in the form of high affinity antibody is not affected by a deficiency in the atypical chemoattractant receptor. As CCRL2 is not being expressed by GC B cells, it is likely that CCRL2 affects other components of the GC; for example FDCs or Tfhs.

4.3 Discussion

4.3.1 CCRL2 deficiency does not overtly affect GC size, architecture or antibody output

CCRL2 was previously shown to be expressed in the GC (Cook, 2011), however it was established in this study that it is not specifically GC B cells that express CCRL2. Nevertheless, expression of CCRL2 by other cells of the GC may affect GC B cell function, and so this study aimed to establish the role of CCRL2 in the GC B cell response.

CCRL2 deficient GCs are similar to CCRL2 sufficient GCs in microarchitecture, with correct positioning within the follicle and LZ and DZ orientation. This phenotype is vastly different to both deficiency in other chemokine receptors, such as CXCR4, CXCR5 and CCR7 (Allen et al., 2004, Achtman et al., 2009).

Although GC microarchitecture is similar amongst WT and CCRL2$^{-/-}$ mice, the amount of spleen taken up by GCs appeared greater in CCRL2 deficient mice by immunohistology. However, this was not reflected in GC B cell numbers by flow cytometry. It is possible that deficiency causes an expansion in another cell type not assessed here; FDCs or Tfh cells, for example. This is supported by CD35^{+} FDCs of the GC appearing to spread further into the follicle in CCRL2 deficient mice. However, high BP3 staining on FDCs does not corroborate with this phenotype, and so further investigation into FDCs is required. The FDC-specific marker FDC-M2 could also be used to investigate FDC-specific location and distribution within the follicle (Taylor et al., 2002). Another cell type, not studied here, are GC-resident tingible body macrophages. This macrophage subset scavenges apoptotic lymphocytes, and they have also been proposed to downregulate the GC reaction (Smith et al., 1998). As CCRL2 is highly expressed on macrophage (Shimada et

al., 1998, Oostendorp et al., 2004), it could be these cells which are increasing GC size. Nevertheless, this slight increase in size does not affect the longevity of the GC response, with GCs still reducing by day 14 in CCRL2 deficient mice.

Finally, GC output was assessed by measuring high affinity antibody. Unlike antibody produced as part of the TI-II extrafollicular response, this was not altered between WT and CCRL2$^{-/-}$ mice. This reflects that GCs formed within CCRL2 deficient mice are fully functional with no explicit phenotype.

4.3.2 CCRL2 deficiency affects Bcl6 and AID Expression in TI induced GC B cells

CCRL2 is not expressed in GC B cells at any time point post immunisation. Therefore it is interesting that CCRL2 deficiency had such a large effect on mRNA expression within GC B cells. However, as CCRL2 appears to be expressed within the GC (Cook, 2011), it is possible that this causes the altered expression of mRNA in GC B cells. For example, lack of expression of CCRL2 within the GC may cause an increase in ligand concentration, which subsequently affects mRNA expression within GC B cells. However, for Bcl6 at least, the altered mRNA expression does not appear to affect the protein level of the transcription factor. Furthermore, the altered mRNA was detected within GC B cells derived from a TI response. If Bcl6 is also reduced at an mRNA level within TD GC B cells, the reduction does not affect the ability of CCRL2 deficient B cells to differentiate into GC B cells. Also, if AID is reduced in GC B cells of a TD response, the ability for these cells to produce high affinity antibody is also not affected. Therefore, altered expression of mRNAs in GC B cells does not obviously affect GC B cell function.

Altogether, this chapter indicates a minimal role for CCRL2 in GC biology. There were no obvious effects on GC B cell function, including production of high affinity antibody. It is possible that CCRL2 deficiency expands FDCs further into follicles, but additional investigation into this is required to conclusively demonstrate the phenotype.

Chapter 5. Concluding Discussion

This study assesses the role of CCRL2 upon B cell activation and differentiation into plasmablasts and GC B cells. Although a previous study has established the expression of CCRL2 on B cells (Hartmann et al., 2008), this is the first study ascertaining a functional role of CCRL2 in B cell activation.

CCRL2 is upregulated in plasmablasts upon their differentiation. CCRL2 negatively regulates the early plasmablast response to thymus independent (TI) type II antigen NP-Ficoll, in a B cell intrinsic manner. The presence of CCRL2 causes cellular apoptosis, although the exact mechanisms are not yet fully established. The idea that CCRL2 regulates the early plasmablast response is supported by thymus dependent responses where naïve B cells are activated by primed T cells. Conversely, the response of B cells to LPS is positively regulated by CCRL2. The opposite effect of CCRL2 deficiency during the TI-I response may be due to the increased expression of CCRL2 on other, non-B cells upon LPS immunisation.

Although CCRL2 is expressed in GCs, it is not expressed by GC B cells. This may be the reason why CCRL2 deficiency has no obvious effect on GC B cell function. Nevertheless, there is a minor increase in the proportion of spleen taken up by GCs in CCRL2 deficient mice, which is probably caused by CCRL2 deficiency in a different GC-resident cell.

5.1 Mechanisms of CCRL2 action on plasmablasts

CCRL2 deficient mice immunised with NP-Ficoll show increased antigen-specific plasmablast and antibody levels compared to WT mice. Further, immunisation of WT mice that have received either WT or CCRL2 deficient NP-specific B cells (known as QM^{WT}

or QM^{KO}, respectively) results in two effects: the first is that QM^{KO} cells show increased plasmablast differentiation and antibody responses compared to QM^{WT}, the second is that QM^{KO} B cell transfer "represses" the hosts B cell antibody response. Taken together, these results lead to two possible models, compatible with the data and the previously described functions of CCRL2 (figure 5.1).

5.1.1 Model 1: CCRL2 as a ligand scavenger

Previous studies have shown that CCRL2 deficient mice have higher plasma chemerin levels than CCRL2 sufficient mice (Monnier et al., 2012). Therefore, CCRL2 on plasmablasts may be acting as a scavenger. According to this model, CCRL2-expressing plasmablasts scavenge their ligand, reducing the concentration within the foci. However, QM^{KO} cells are unable to scavenge CCRL2 ligand, generating plasmablast foci of high ligand concentration. The ligand could then inhibit the plasmablast response.

A complication of this model is the fact that CCRL2 must be both scavenging and signalling upon ligand binding. CCRL2 must be signalling upon ligand binding because if the higher ligand concentration is acting through another receptor, both WT and CCRL2 deficient cells would be affected by the higher ligand concentration. Although this is possible, it is unlikely, as previous studies indicate that chemerin binding to CCRL2 does not induce signal transduction (Zabel et al., 2008). Therefore, it is unlikely that there is a direct inhibition of CCRL2-expressing plasmablasts through ligand binding, irrespective of ligand concentration.

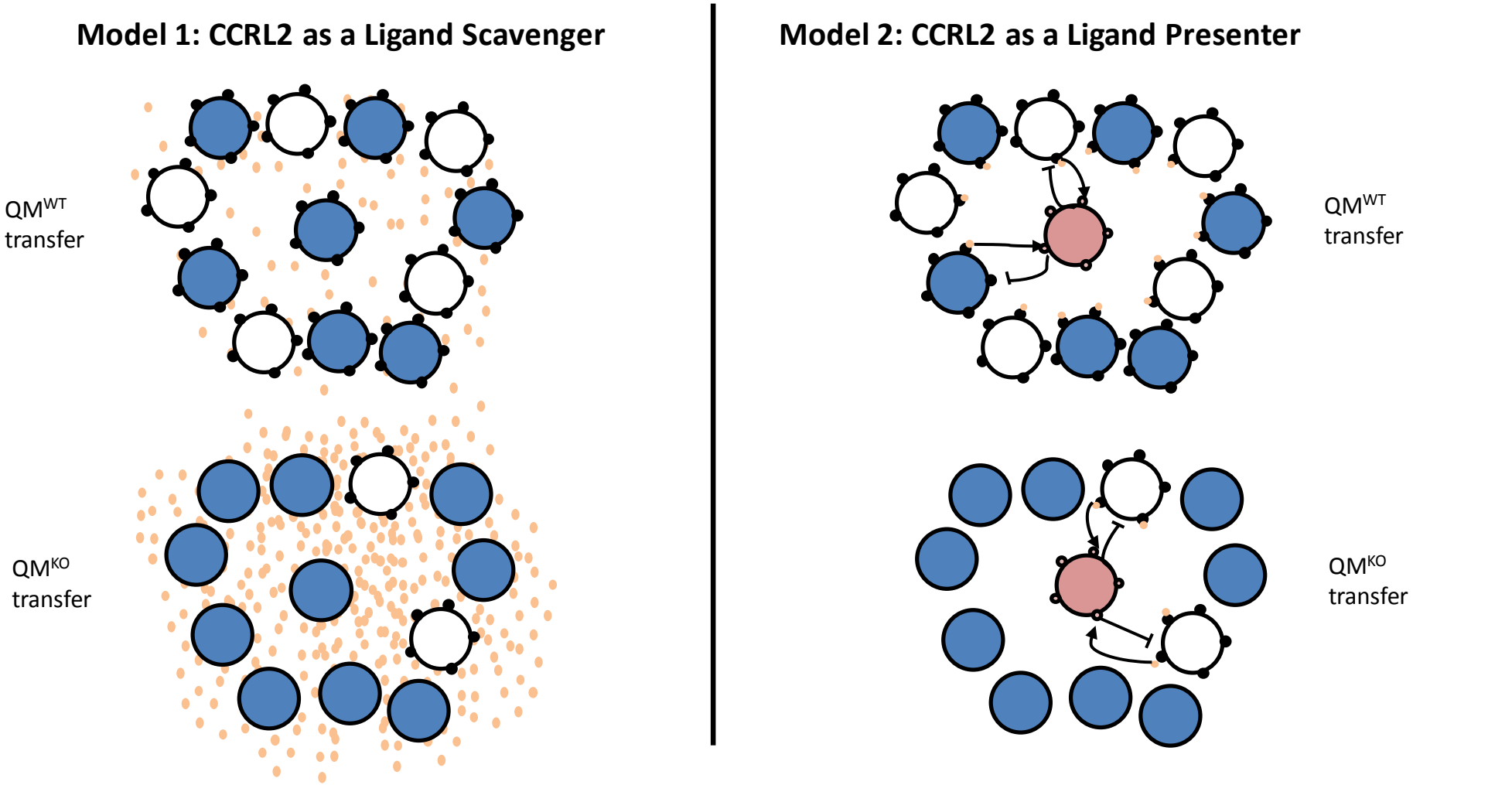

Figure 5.1. Pictorial representation of two proposed models of the mechanism of CCRL2 action on plasmablasts.

Model 1. CCRL2$^+$ PBs scavenge ligand, reducing its concentration. However, QM^{KO} PBs are unable to scavenge the ligand, increasing its concentration in PB foci. The ligand then inhibits the response of CCRL2$^+$ PBs.

Model 2. Ligand binds to CCRL2$^+$ PBs, which present the ligand to accessory cells. Accessory cells then direct a negative signal to the WT PBs. However, QM^{KO} PBs do not bind ligand, and therefore do not receive the negative signal.

Key: PB - Plasmablast

5.1.2 Model 2: CCRL2 as a presenter of ligand

Previous publications have suggested that CCRL2-expressing cells can bind and present chemerin on surface to cells expressing another chemerin receptor, ChemR23 (Zabel et al., 2008, Monnier et al., 2012). Therefore, CCRL2-expressing plasmablasts could be binding ligand, and presenting it to other cells expressing an alternate receptor. According to this model, CCRL2 ligand binds to CCRL2-expressing WT cells, which in turn present the ligand to other, accessory cells. These accessory cells could subsequently direct a negative signal to the WT cells. However, QM^{KO} cells are unable to bind CCRL2 ligand, and therefore do not receive the negative signal.

What could this accessory cell be?

First, plasmablasts are associated in large extrafollicular foci, indicating that the accessory cell could be other plasmablasts. If this is the case, the presentation is unlikely to be of chemerin to ChemR23-expressing plasmablasts, as flow cytometry data indicated <2% of plasmablasts are $ChemR23^{+}$ (data not shown).

Second, it has been reported that $CD11c^{high}$ dendritic cells interact with plasmablasts in both the spleen (Garcia De Vinuesa et al., 1999a) and lymph node (Mohr et al., 2009). However, association with these DCs is associated with plasmablast survival, not apoptosis, which is opposite to the model proposed here (Garcia De Vinuesa et al., 1999a). Therefore, unless $CD11c^{high}$ DCs have a dual role in plasmablast survival, they are unlikely to be the accessory cell.

Third, previous studies have shown that neutrophils and monocyte/macrophage populations co-localise with plasma cells in the LN (Mohr et al., 2009). These monocytes/macrophages are a source of high levels of APRIL (Mohr et al., 2009), which binds TACI, the receptor found to be reduced in CCRL2 deficient plasmablasts in this study. However, as *in vivo* studies have indicated that APRIL is essential for plasmablast survival (Belnoue et al., 2008) it is unlikely that production of this factor by macrophage/monocytes is the cause of the reduced response of ligand-presenting CCRL2 sufficient plasmablasts. Therefore if monocytes/macrophage are the accessory cell, they must produce another factor to negatively regulate the response.

Fourth, within the bone marrow plasma cells associate with eosinophils, which produce survival factors essential for plasma cell maintenance and retention (Chu et al., 2011). Although plasmablast association with eosinophils has not been shown in the spleen, eosinophils are also required for IgA plasma cell production in the gut (Chu et al., 2014), showing that this plasma cell-eosinophil association is at other sites as well as the bone marrow. However, as discussed with other cell types above, if eosinophils are the accessory cell described in this model they must have an alternate role in CCRL2-regulated plasmablast survival.

Finally, plasmablasts may be interacting with stromal cells of the spleen. Human red pulp stromal cells have been shown to be associated with plasma cells in the spleen, and are proposed to contribute to plasma cell retention (Ellyard et al., 2005), although there has been no studies relating to the role of these cells in plasmablast survival.

5.2 Conclusion

Although first described more than 15 years ago, there is still relatively little known about the atypical receptor, CCRL2. There has been wide debate about both its ligands and its biochemical function, with contradictory reports on both (Biber et al., 2003, Hartmann et al., 2008, Galligan et al., 2004, Zabel et al., 2008). This study provides insight into the role of CCRL2 in the regulation of the antibody response, in which CCRL2 expression on plasmablasts reduces plasmablast proliferation, survival and therefore antibody production. This provides a novel role for the receptor in B cell biology, but further study into the exact mechanisms is required to fully establish the behaviour of CCRL2 on plasmablasts.

Appendix A - Buffers

Tris Buffer pH 7.6

For 4L

1.5L of Physiological NaCl
1.5L of 0.1M HCl
1.0L of 0.2M Tris (base)

0.1M HCl: 10mls 10M HCl in 1L dH_2O
0.2M Trizma base (MW 121.14g): 24.228g, in 1L H_2O
Pysiological NaCl: 42.5g in 5L dH_2O

Tris Buffer pH 9.2

As above but pH to 9.2 with HCl

Peroxidase Substrate

Dissolve 1 tablet of 3, 3'-diaminobenzidine tetrahydrochloride (DAB) (Sigma) in 15mls of Tris Buffer pH 7.6. Filter to 10mls and add 1 drop of hydrogen peroxide (Sigma).

Alkaline Phosphate Substrate

Dissolve 8mgs of levamisole (Sigma) in 10mls of Tris Buffer pH 9.2
In a fume hood dissolve 4mg of Napthol AS-MX-phosphate (Sigma) in 380µl of dimethyl formamide in a glass bottle. Add this to the middle of the levamisole solution. Add 10mg of Fast Blue BB salt (Sigma). Filter.

PBS

10x: 425g NaCl)
53.5g Na_2HPO_4) in 5L dH_2O
19.5g NaH_2PO_4)

RT-qPCR Reverse Transcription Mix

For a typical 30µl mRNA sample
12µl 5x first strand buffer (Invitrogen)
6µl DTT 0.1M (Invitrogen)
3µl dNTP (10mM) (Invitrogen)
3µl Moloney murine leukemia virus reverse transcriptase (Invitrogen)
1.5µl RNasin RNase inhibitor (Promega)
1.5µl RNase free water

Appendix B – Antibody Listing

Specificity	Isotype	Clone	Source	Conjugation
7AAD	N/A	N/A	eBioscience	N/A
Alexa488	Rabbit IgG	Polyclonal	Molecular Probes	Purified
B220	Rat IgG2a, κ	RA3-6B2	eBioscience	eFluor450
B220	Rat IgG2a, κ	RA3-6B2	BD PharMingen	FITC
B220	Rat IgG2a, κ	RA3-6B2	BD PharMingen	PE-Texas Red
Bcl6	Mouse	K112-91	BD PharMingen	Alexa488
CD3	Rat	KT3	AbD serotec	Purified
CD4	Mouse IgG1, κ	GK1.5	BD PharMingen	PE
CD4	Rat IgG2a, κ	RM4-5	BD PharMingen	PerCP-Cy5.5
CD5, Ly.1	Rat IgG2a, κ	53-7.3	BD Biosciences	PE-Cy5
CD11b	Rat IgG2b, κ	M1/70	eBioscience	APC
CD11b	Rat IgG2b, κ	M1/70	eBioscience	eFluor450
CD11c	Ham Arm IgG1, λ2	HL3	BD PharMingen	PE-Cy7
CD16/CD32	Rat IgG2b, κ	24G2	BD PharMingen	Purified
CD19	Rat IgG2a κ	1D3	BD PharMingen	APC
CD19	Rat IgG2a κ	1D3	BD PharMingen	APC-Cy7
CD21/CD35	Rat IgG2b, κ	7G6	BD PharMingen	FITC
CD23	Rat IgG2a, κ	B3B4	BD PharMingen	PE
CD35	Rat IgG2a, κ	8C12	BD PharMingen	Biotin
CD38	Rat IgG2a κ	90	BD PharMingen	Pacific Blue
CD45.1	Mouse IgG2a, κ	A20	BD PharMingen	FITC
CD45.2	Mouse IgG2a, κ	104	BD PharMingen	PerCP-Cy5.5
CD45.2	Mouse IgG2a, κ	104	eBioscience	FITC
CD117 (c-kit)	Rat IgG2b, κ	2B8	eBioscience	PE
CD138	Rat	281-2	BD Pharmingen	Purified
CD138	Rat IgG2a, κ	281-2	BD PharMingen	APC
CD138	Rat IgG2a, κ	281-2	Biolegend	Brilliant violet
CD138	Rat IgG2a, κ	281-2	BD PharMingen	PE
CD169	Rat	MOMA-1	AbD serotec	Purified
Cell Trace™	N/A	N/A	Molecular Probes	Violet
ChemR23	Rat IgG2b	477806	R&D Systems	Alexa488
F4/80	Rat	Cl:A3-1	AbD serotec	Purified
F4/80	Rat	BM8	eBioscience	FITC
Fas (CD95)	Hamster IgG	Jo2	BD Pharmingen	PE-Cy7

Specificity	Isotype	Clone	Source	Conjugation
FITC	Rabbit	Polyclonal	Molecular Probes	Alexa488
GL7	Rat IgG2a	MP1-22E9	BD PharMingen	FITC
Goat Ig	Rabbit	Polyclonal	Dako	Biotin
Hamster IgG	Goat	Polyclonal	Vector	Biotin
IgD	Rat	11-26c2a	BD Pharmingen	Purified
IgD	Sheep	Polyclonal	ABCAM	Purified
IgD	Rat IgG2a, κ	11-26c	eBioscience	Pacific Blue
IgD	Rat IgG2a, κ	11-26	Southern Biotech	PE
IgE	Rat IgG1, κ	23G3	Southern Biotech	Alkaline Phosphatase
IgG1	Goat	Polyclonal	Southern Biotech	Alkaline Phosphatase
IgG2a	Goat	Polyclonal	Southern Biotech	Alkaline Phosphatase
IgG2b	Goat	Polyclonal	Southern Biotech	Alkaline Phosphatase
IgG2b	Goat	Polyclonal	Southern Biotech	FITC
IgG2c	Goat	Polyclonal	Southern Biotech	Alkaline Phosphatase
IgG2c	Goat	Polyclonal	Southern Biotech	FITC
IgG3	Goat	Polyclonal	Southern Biotech	Alkaline Phosphatase
IgM	Rat IgG2a, κ	II/41	eBioscience	PE-Cy7
IgM	Goat	Polyclonal	Southern Biotech	FITC
IgMa	Mouse	DS-1	BD PharMingen	Biotin
IgMb	Mouse	AF6-78	BD PharMingen	Biotin
Ki67	Rabbit	In House		Purified
Ly6G (gr1)	Rat IgG2a, κ	RB6-8C5	eBioscience	PE
NP	Sheep	In House		Purified
NP	Rabbit	In House		Purified
NP		In House		PE
Rabbit Ig	Swine	Polyclonal	Dako	Alkaline Phosphatase
Rabbit Ig	Swine	Polyclonal	Dako	Biotin
Rabbit IgG	Donkey	Polyclonal	Jackson	Cy3

Specificity	Isotype	Clone	Source	Conjugation
Rat Ig	Sheep	Polyclonal	The Binding Site	Horseradish Peroxidase
Rat Ig	Rabbit	Polyclonal	Dako	Horseradish Peroxidase
Rat Ig	Sheep	Polyclonal	The Binding Site	Biotin
Rat Ig	Rabbit	Polyclonal	Dako	Biotin
Rat IgG	Donkey	Polyclonal	Jackson	Cy3
Rat IgG	Donkey	Polyclonal	Jackson	APC
Sheep/Goat Ig	Donkey	Polyclonal	Jackson	Biotin
Sheep/Goat Ig	Donkey	Polyclonal	Jackson	Horseradish Peroxidase
TACI (CD267)	Rat IgG2a, κ	8F10	BD PharMingen	Alexa647

Appendix C – Primer Sequences for RT-qPCR

Name	Forward Primer Sequence	Reverse Primer Sequence	Probe Sequence
β-actin	CGTGAAAAGATGACCCAGATCA	TGGTACGACCAGAGGCATACAG	TCAACACCCCAGCCATGTACGTAGCC
β2-Microglobulin	CATACGCCTGCAGAGTTAAGCA	ATCACATGTCTCGATCCCAGTAGA	CAGTATGGCCGAGCCCAAGACCG
AID	GTCCGGCTAACCAGACAACTTC	GCTTTCAAAATCCCAACATACGA	TGCATCTCGCAAGTCATCGACTTCGT
APRIL	CGAGTCTGGGACACTGGAATTT	AGATACCACCTGACCCATTGTGA	CTGCTCTATAGTCAGGTCCTGTTTCATGATGTGAC
BAFF	GAAGTGTGCCATGTGAGTTATGAGA	TCACCCAAGGCAAAAAGCA	TCCTTTGCCAACACGCACCGC
BAFFR	ACTTCAGAAGGAGTCCAGCAAGAG	CAGGTAGGAGCTGAGGCATGAG	CCCTGGAAAATGTCTTTGTACCCTCCTCA
Bcl6	CAGACGCACAGTGACAAACCA	ACTGCGCTCCACAAATGTTACA	CAGCCACAAGACTGTCCACACGGGT
BCMA	TCCAACCCTCCTGCAACCT	CGTGTACGTCCCTTTCACTGAA	TCAGCCTTACTGTGATCCAAGCGTGACC
Blimp-1	CAAGAATGCCAACAGGAAGTATTTT	CCATCAATGAAGTGGTGGAACTC	TCTCTGGAATAGATCCGCCA-MGB
CCRL2	GTCCGGTGAGCAAGGACAG	CCCACTGTTGTCCAGGTAGTC	TCCGATGGATAACTACACAGTGGCC
IRF4	GGAGGACGCTGCCCTCTT	TCTGGCTTGTCGATCCCTTCT	AGGCTTGGGCATTGTTTAAAGGCAAGTTC
TACI	CATTCTGCCCCAAAGATCAGTAC	TGCTCTTTTCGGCAATTGATG	CAGCCAGAGGAGCCAGCGCAC

References

ACHTMAN, A. H., HOPKEN, U. E., BERNERT, C. & LIPP, M. 2009. CCR7-deficient mice develop atypically persistent germinal centers in response to thymus-independent type 2 antigens. *J Leukoc Biol,* 85**,** 409-17.

AICHELE, P., ZINKE, J., GRODE, L., SCHWENDENER, R. A., KAUFMANN, S. H. & SEILER, P. 2003. Macrophages of the splenic marginal zone are essential for trapping of blood-borne particulate antigen but dispensable for induction of specific T cell responses. *J Immunol,* 171**,** 1148-55.

ALLEN, C. D., ANSEL, K. M., LOW, C., LESLEY, R., TAMAMURA, H., FUJII, N. & CYSTER, J. G. 2004. Germinal center dark and light zone organization is mediated by CXCR4 and CXCR5. *Nat Immunol,* 5**,** 943-52.

ALLEN, C. D., OKADA, T. & CYSTER, J. G. 2007. Germinal-center organization and cellular dynamics. *Immunity,* 27**,** 190-202.

ALTSCHUL, S. F., GISH, W., MILLER, W., MYERS, E. W. & LIPMAN, D. J. 1990. Basic local alignment search tool. *J Mol Biol,* 215**,** 403-10.

ALUGUPALLI, K. R., LEONG, J. M., WOODLAND, R. T., MURAMATSU, M., HONJO, T. & GERSTEIN, R. M. 2004. B1b lymphocytes confer T cell-independent long-lasting immunity. *Immunity,* 21**,** 379-90.

BACHELERIE, F., BEN-BARUCH, A., BURKHARDT, A. M., COMBADIERE, C., FARBER, J. M., GRAHAM, G. J., HORUK, R., SPARRE-ULRICH, A. H., LOCATI, M., LUSTER, A. D., MANTOVANI, A., MATSUSHIMA, K., MURPHY, P. M., NIBBS, R., NOMIYAMA, H., POWER, C. A., PROUDFOOT, A. E., ROSENKILDE, M. M., ROT, A., SOZZANI, S., THELEN, M., YOSHIE, O. & ZLOTNIK, A. 2014. International Union of Basic and Clinical Pharmacology. [corrected]. LXXXIX. Update on the extended family of chemokine receptors and introducing a new nomenclature for atypical chemokine receptors. *Pharmacol Rev,* 66**,** 1-79.

BAGGIOLINI, M., DEWALD, B. & MOSER, B. 1997. Human chemokines: an update. *Annu Rev Immunol,* 15**,** 675-705.

BALAZS, M., MARTIN, F., ZHOU, T. & KEARNEY, J. 2002. Blood dendritic cells interact with splenic marginal zone B cells to initiate T-independent immune responses. *Immunity,* 17**,** 341-52.

BANNARD, O., HORTON, R. M., ALLEN, C. D., AN, J., NAGASAWA, T. & CYSTER, J. G. 2013. Germinal center centroblasts transition to a centrocyte phenotype according to a timed program and depend on the dark zone for effective selection. *Immunity,* 39**,** 912-24.

BARNEA, G., STRAPPS, W., HERRADA, G., BERMAN, Y., ONG, J., KLOSS, B., AXEL, R. & LEE, K. J. 2008. The genetic design of signaling cascades to record receptor activation. *Proc Natl Acad Sci U S A,* 105**,** 64-9.

BASSO, K., SAITO, M., SUMAZIN, P., MARGOLIN, A. A., WANG, K., LIM, W. K., KITAGAWA, Y., SCHNEIDER, C., ALVAREZ, M. J., CALIFANO, A. & DALLA-FAVERA, R. 2010. Integrated biochemical and computational approach identifies BCL6 direct target genes controlling multiple pathways in normal germinal center B cells. *Blood,* 115**,** 975-84.

BASSO, K., SCHNEIDER, C., SHEN, Q., HOLMES, A. B., SETTY, M., LESLIE, C. & DALLA-FAVERA, R. 2012. BCL6 positively regulates AID and germinal center gene expression via repression of miR-155. *J Exp Med,* 209**,** 2455-65.

BAUMGARTH, N., HERMAN, O. C., JAGER, G. C., BROWN, L., HERZENBERG, L. A. & HERZENBERG, L. A. 1999. Innate and acquired humoral immunities to influenza virus are mediated by distinct arms of the immune system. *Proc Natl Acad Sci U S A,* 96**,** 2250-5.

BELNOUE, E., PIHLGREN, M., MCGAHA, T. L., TOUGNE, C., ROCHAT, A. F., BOSSEN, C., SCHNEIDER, P., HUARD, B., LAMBERT, P. H. & SIEGRIST, C. A. 2008. APRIL is critical for plasmablast survival in the bone marrow and poorly expressed by early-life bone marrow stromal cells. *Blood,* 111**,** 2755-64.

BEREK, C., BERGER, A. & APEL, M. 1991. Maturation of the immune response in germinal centers. *Cell,* 67**,** 1121-9.

BERLAND, R. & WORTIS, H. H. 2002. Origins and functions of B-1 cells with notes on the role of CD5. *Annu Rev Immunol,* 20**,** 253-300.

BIBER, K., ZUURMAN, M. W., HOMAN, H. & BODDEKE, H. W. 2003. Expression of L-CCR in HEK 293 cells reveals functional responses to CCL2, CCL5, CCL7, and CCL8. *J Leukoc Biol,* 74**,** 243-51.

BOBAT, S. 2011. Characterising the immune response to Salmonella and Salmonella surface antigens during a systemic infection. *Thesis, School of Immunity and Infection, The University of Birmingham*.

BORTNICK, A., CHERNOVA, I., QUINN, W. J., 3RD, MUGNIER, M., CANCRO, M. P. & ALLMAN, D. 2012. Long-lived bone marrow plasma cells are induced early in response to T cell-independent or T cell-dependent antigens. *J Immunol,* 188**,** 5389-96.

BOSSEN, C. & SCHNEIDER, P. 2006. BAFF, APRIL and their receptors: structure, function and signaling. *Semin Immunol,* 18**,** 263-75.

BOTHWELL, A. L., PASKIND, M., RETH, M., IMANISHI-KARI, T., RAJEWSKY, K. & BALTIMORE, D. 1981. Heavy chain variable region contribution to the NPb family of antibodies: somatic mutation evident in a gamma 2a variable region. *Cell,* 24**,** 625-37.

BOULIANNE, B., ROJAS, O. L., HADDAD, D., ZAHEEN, A., KAPELNIKOV, A., NGUYEN, T., LI, C., HAKEM, R., GOMMERMAN, J. L. & MARTIN, A. 2013. AID and caspase 8 shape the germinal center response through apoptosis. *J Immunol,* 191**,** 5840-7.

BROUWER, N., ZUURMAN, M. W., WEI, T., RANSOHOFF, R. M., BODDEKE, H. W. & BIBER, K. 2004. Induction of glial L-CCR mRNA expression in spinal cord and brain in experimental autoimmune encephalomyelitis. *Glia,* 46**,** 84-94.

CANCRO, M. P. 2004. Tipping the scales of selection with BAFF. *Immunity,* 20**,** 655-6.

CASCALHO, M., MA, A., LEE, S., MASAT, L. & WABL, M. 1996. A quasi-monoclonal mouse. *Science,* 272**,** 1649-52.

CASH, J. L., CHRISTIAN, A. R. & GREAVES, D. R. 2010. Chemerin peptides promote phagocytosis in a ChemR23- and Syk-dependent manner. *J Immunol,* 184**,** 5315-24.

CASTIGLI, E., WILSON, S. A., ELKHAL, A., OZCAN, E., GARIBYAN, L. & GEHA, R. S. 2007. Transmembrane activator and calcium modulator and cyclophilin ligand interactor

enhances CD40-driven plasma cell differentiation. *J Allergy Clin Immunol,* 120**,** 885-91.

CATUSSE, J., LEICK, M., GROCH, M., CLARK, D. J., BUCHNER, M. V., ZIRLIK, K. & BURGER, M. 2010. Role of the atypical chemoattractant receptor CRAM in regulating CCL19 induced CCR7 responses in B-cell chronic lymphocytic leukemia. *Mol Cancer,* 9**,** 297.

CESTA, M. F. 2006. Normal structure, function, and histology of the spleen. *Toxicol Pathol,* 34**,** 455-65.

CHOI, Y. S., YANG, J. A. & CROTTY, S. 2013. Dynamic regulation of Bcl6 in follicular helper CD4 T (Tfh) cells. *Curr Opin Immunol,* 25**,** 366-72.

CHU, V. T., BELLER, A., RAUSCH, S., STRANDMARK, J., ZANKER, M., ARBACH, O., KRUGLOV, A. & BEREK, C. 2014. Eosinophils promote generation and maintenance of immunoglobulin-A-expressing plasma cells and contribute to gut immune homeostasis. *Immunity,* 40**,** 582-93.

CHU, V. T., FROHLICH, A., STEINHAUSER, G., SCHEEL, T., ROCH, T., FILLATREAU, S., LEE, J. J., LOHNING, M. & BEREK, C. 2011. Eosinophils are required for the maintenance of plasma cells in the bone marrow. *Nat Immunol,* 12**,** 151-9.

CHUSED, T. M., KASSAN, S. S. & MOSIER, D. E. 1976. Macrophage requirement for the in vitro response to TNP Ficoll: a thymic independent antigen. *J Immunol,* 116**,** 1579-81.

CINAMON, G., MATLOUBIAN, M., LESNESKI, M. J., XU, Y., LOW, C., LU, T., PROIA, R. L. & CYSTER, J. G. 2004. Sphingosine 1-phosphate receptor 1 promotes B cell localization in the splenic marginal zone. *Nat Immunol,* 5**,** 713-20.

CINAMON, G., ZACHARIAH, M. A., LAM, O. M., FOSS, F. W., JR. & CYSTER, J. G. 2008. Follicular shuttling of marginal zone B cells facilitates antigen transport. *Nat Immunol,* 9**,** 54-62.

COMERFORD, I., MILASTA, S., MORROW, V., MILLIGAN, G. & NIBBS, R. 2006. The chemokine receptor CCX-CKR mediates effective scavenging of CCL19 in vitro. *Eur J Immunol,* 36**,** 1904-16.

COMERFORD, I., NIBBS, R. J., LITCHFIELD, W., BUNTING, M., HARATA-LEE, Y., HAYLOCK-JACOBS, S., FORROW, S., KORNER, H. & MCCOLL, S. R. 2010. The atypical chemokine receptor CCX-CKR scavenges homeostatic chemokines in circulation and tissues and suppresses Th17 responses. *Blood,* 116**,** 4130-40.

COOK, S. 2011. The role of CCRL2 in the Regulation of Germinal Centre B-Cell Migration. *Thesis, School of Immunity and Infection, The University of Birmingham*.

CUNNINGHAM, A. F., GASPAL, F., SERRE, K., MOHR, E., HENDERSON, I. R., SCOTT-TUCKER, A., KENNY, S. M., KHAN, M., TOELLNER, K. M., LANE, P. J. & MACLENNAN, I. C. 2007. Salmonella induces a switched antibody response without germinal centers that impedes the extracellular spread of infection. *J Immunol,* 178**,** 6200-7.

DE VINUESA, C. G., COOK, M. C., BALL, J., DREW, M., SUNNERS, Y., CASCALHO, M., WABL, M., KLAUS, G. G. & MACLENNAN, I. C. 2000. Germinal centers without T cells. *J Exp Med,* 191**,** 485-94.

DEL PRETE, A., BONECCHI, R., VECCHI, A., MANTOVANI, A. & SOZZANI, S. 2013. CCRL2, a fringe member of the atypical chemoattractant receptor family. *Eur J Immunol,* 43**,** 1418-22.

DICKINSON, G. S., SUN, G., BRAM, R. J. & ALUGUPALLI, K. R. 2014. Efficient B cell responses to Borrelia hermsii infection depend on BAFF and BAFFR but not TACI. *Infect Immun,* 82**,** 453-9.

DONA, E., BARRY, J. D., VALENTIN, G., QUIRIN, C., KHMELINSKII, A., KUNZE, A., DURDU, S., NEWTON, L. R., FERNANDEZ-MINAN, A., HUBER, W., KNOP, M. & GILMOUR, D. 2013. Directional tissue migration through a self-generated chemokine gradient. *Nature,* 503**,** 285-9.

DOUGLAS, R. M., CHEN, A. H., INIGUEZ, A., WANG, J., FU, Z., POWELL, F. L., JR., HADDAD, G. G. & YAO, H. 2013. Chemokine receptor-like 2 is involved in ischemic brain injury. *J Exp Stroke Transl Med,* 6**,** 1-6.

ELLYARD, J. I., AVERY, D. T., MACKAY, C. R. & TANGYE, S. G. 2005. Contribution of stromal cells to the migration, function and retention of plasma cells in human spleen: potential roles of CXCL12, IL-6 and CD54. *Eur J Immunol,* 35**,** 699-708.

FAN, P., KYAW, H., SU, K., ZENG, Z., AUGUSTUS, M., CARTER, K. C. & LI, Y. 1998. Cloning and characterization of a novel human chemokine receptor. *Biochem Biophys Res Commun,* 243**,** 264-8.

FORSTER, R., SCHUBEL, A., BREITFELD, D., KREMMER, E., RENNER-MULLER, I., WOLF, E. & LIPP, M. 1999. CCR7 coordinates the primary immune response by establishing functional microenvironments in secondary lymphoid organs. *Cell,* 99**,** 23-33.

FREDRIKSSON, R., LAGERSTROM, M. C., LUNDIN, L. G. & SCHIOTH, H. B. 2003. The G-protein-coupled receptors in the human genome form five main families. Phylogenetic analysis, paralogon groups, and fingerprints. *Mol Pharmacol,* 63**,** 1256-72.

GALLIGAN, C. L., MATSUYAMA, W., MATSUKAWA, A., MIZUTA, H., HODGE, D. R., HOWARD, O. M. & YOSHIMURA, T. 2004. Up-regulated expression and activation of the orphan chemokine receptor, CCRL2, in rheumatoid arthritis. *Arthritis Rheum,* 50**,** 1806-14.

GARCIA DE VINUESA, C., GULBRANSON-JUDGE, A., KHAN, M., O'LEARY, P., CASCALHO, M., WABL, M., KLAUS, G. G., OWEN, M. J. & MACLENNAN, I. C. 1999a. Dendritic cells associated with plasmablast survival. *Eur J Immunol,* 29**,** 3712-21.

GARCIA DE VINUESA, C., O'LEARY, P., SZE, D. M., TOELLNER, K. M. & MACLENNAN, I. C. 1999b. T-independent type 2 antigens induce B cell proliferation in multiple splenic sites, but exponential growth is confined to extrafollicular foci. *Eur J Immunol,* 29**,** 1314-23.

GATTO, D., PAUS, D., BASTEN, A., MACKAY, C. R. & BRINK, R. 2009. Guidance of B cells by the orphan G protein-coupled receptor EBI2 shapes humoral immune responses. *Immunity,* 31**,** 259-69.

GHOSN, E. E., CASSADO, A. A., GOVONI, G. R., FUKUHARA, T., YANG, Y., MONACK, D. M., BORTOLUCI, K. R., ALMEIDA, S. R., HERZENBERG, L. A. & HERZENBERG, L. A. 2010. Two physically, functionally, and developmentally distinct peritoneal macrophage subsets. *Proc Natl Acad Sci U S A,* 107**,** 2568-73.

GHOSN, E. E., YANG, Y., TUNG, J., HERZENBERG, L. A. & HERZENBERG, L. A. 2008. CD11b expression distinguishes sequential stages of peritoneal B-1 development. *Proc Natl Acad Sci U S A,* 105**,** 5195-200.

GIL-CRUZ, C., BOBAT, S., MARSHALL, J. L., KINGSLEY, R. A., ROSS, E. A., HENDERSON, I. R., LEYTON, D. L., COUGHLAN, R. E., KHAN, M., JENSEN, K. T., BUCKLEY, C. D., DOUGAN, G., MACLENNAN, I. C., LOPEZ-MACIAS, C. & CUNNINGHAM, A. F. 2009. The porin OmpD from nontyphoidal Salmonella is a key target for a protective B1b cell antibody response. *Proc Natl Acad Sci U S A,* 106**,** 9803-8.

GITLIN, A. D., SHULMAN, Z. & NUSSENZWEIG, M. C. 2014. Clonal selection in the germinal centre by regulated proliferation and hypermutation. *Nature,* 509**,** 637-40.

GLYNNE, R., GHANDOUR, G., RAYNER, J., MACK, D. H. & GOODNOW, C. C. 2000. B-lymphocyte quiescence, tolerance and activation as viewed by global gene expression profiling on microarrays. *Immunol Rev,* 176**,** 216-46.

GOENKA, R., MATTHEWS, A. H., ZHANG, B., O'NEILL, P. J., SCHOLZ, J. L., MIGONE, T. S., LEONARD, W. J., STOHL, W., HERSHBERG, U. & CANCRO, M. P. 2014. Local BLyS production by T follicular cells mediates retention of high affinity B cells during affinity maturation. *J Exp Med,* 211**,** 45-56.

GONZALVO-FEO, S., DEL PRETE, A., PRUENSTER, M., SALVI, V., WANG, L., SIRONI, M., BIERSCHENK, S., SPERANDIO, M., VECCHI, A. & SOZZANI, S. 2014. Endothelial cell-derived chemerin promotes dendritic cell transmigration. *J Immunol,* 192**,** 2366-73.

GRAHAM, G. J., LOCATI, M., MANTOVANI, A., ROT, A. & THELEN, M. 2012. The biochemistry and biology of the atypical chemokine receptors. *Immunol Lett,* 145**,** 30-8.

GRAS, M. P., LAABI, Y., LINARES-CRUZ, G., BLONDEL, M. O., RIGAUT, J. P., BROUET, J. C., LECA, G., HAGUENAUER-TSAPIS, R. & TSAPIS, A. 1995. BCMAp: an integral membrane protein in the Golgi apparatus of human mature B lymphocytes. *Int Immunol,* 7**,** 1093-106.

GREEN, J. A. & CYSTER, J. G. 2012. S1PR2 links germinal center confinement and growth regulation. *Immunol Rev,* 247**,** 36-51.

GREEN, J. A., SUZUKI, K., CHO, B., WILLISON, L. D., PALMER, D., ALLEN, C. D., SCHMIDT, T. H., XU, Y., PROIA, R. L., COUGHLIN, S. R. & CYSTER, J. G. 2011. The sphingosine 1-phosphate receptor S1P(2) maintains the homeostasis of germinal center B cells and promotes niche confinement. *Nat Immunol,* 12**,** 672-80.

GUNN, M. D., KYUWA, S., TAM, C., KAKIUCHI, T., MATSUZAWA, A., WILLIAMS, L. T. & NAKANO, H. 1999. Mice lacking expression of secondary lymphoid organ chemokine have defects in lymphocyte homing and dendritic cell localization. *J Exp Med,* 189**,** 451-60.

HAMBY, M. E., COPPOLA, G., AO, Y., GESCHWIND, D. H., KHAKH, B. S. & SOFRONIEW, M. V. 2012. Inflammatory mediators alter the astrocyte transcriptome and calcium signaling elicited by multiple G-protein-coupled receptors. *J Neurosci,* 32**,** 14489-510.

HANSELL, C. A., SCHIERING, C., KINSTRIE, R., FORD, L., BORDON, Y., MCINNES, I. B., GOODYEAR, C. S. & NIBBS, R. J. 2011. Universal expression and dual function of the atypical chemokine receptor D6 on innate-like B cells in mice. *Blood,* 117**,** 5413-24.

HARDENBERG, G., VAN BOSTELEN, L., HAHNE, M. & MEDEMA, J. P. 2008. Thymus-independent class switch recombination is affected by APRIL. *Immunol Cell Biol,* 86**,** 530-4.

HARDTKE, S., OHL, L. & FORSTER, R. 2005. Balanced expression of CXCR5 and CCR7 on follicular T helper cells determines their transient positioning to lymph node follicles and is essential for efficient B-cell help. *Blood,* 106**,** 1924-31.

HARTMANN, T. N., LEICK, M., EWERS, S., DIEFENBACHER, A., SCHRAUFSTATTER, I., HONCZARENKO, M. & BURGER, M. 2008. Human B cells express the orphan chemokine receptor CRAM-A/B in a maturation-stage-dependent and CCL5-modulated manner. *Immunology,* 125**,** 252-62.

HAUSER, A. E., DEBES, G. F., ARCE, S., CASSESE, G., HAMANN, A., RADBRUCH, A. & MANZ, R. A. 2002. Chemotactic responsiveness toward ligands for CXCR3 and CXCR4 is regulated on plasma blasts during the time course of a memory immune response. *J Immunol,* 169**,** 1277-82.

HAYAKAWA, K., HARDY, R. R., HERZENBERG, L. A. & HERZENBERG, L. A. 1985. Progenitors for Ly-1 B cells are distinct from progenitors for other B cells. *J Exp Med,* 161**,** 1554-68.

HESS, J., LADEL, C., MIKO, D. & KAUFMANN, S. H. 1996. Salmonella typhimurium aroA-infection in gene-targeted immunodeficient mice: major role of CD4+ TCR-alpha beta cells and IFN-gamma in bacterial clearance independent of intracellular location. *J Immunol,* 156**,** 3321-6.

HOISETH, S. K. & STOCKER, B. A. 1981. Aromatic-dependent Salmonella typhimurium are non-virulent and effective as live vaccines. *Nature,* 291**,** 238-9.

HSU, M. C., TOELLNER, K. M., VINUESA, C. G. & MACLENNAN, I. C. 2006. B cell clones that sustain long-term plasmablast growth in T-independent extrafollicular antibody responses. *Proc Natl Acad Sci U S A,* 103**,** 5905-10.

HUMPHREY, J. L. 1979. Marginal zone and marginal sinus macrophages in the mouse are distinct populations. *Adv Exp Med Biol,* 114**,** 381-8.

IMANISHI, T. & MAKELA, O. 1974. Inheritance of antibody specificity. I. Anti-(4-hydroxy-3-nitrophenyl)acetyl of the mouse primary response. *J Exp Med,* 140**,** 1498-510.

INABA, K., METLAY, J. P., CROWLEY, M. T. & STEINMAN, R. M. 1990. Dendritic cells pulsed with protein antigens in vitro can prime antigen-specific, MHC-restricted T cells in situ. *J Exp Med,* 172**,** 631-40.

JACK, R. S., IMANISHI-KARI, T. & RAJEWSKY, K. 1977. Idiotypic analysis of the response of C57BL/6 mice to the (4-hydroxy-3-nitrophenyl)acetyl group. *Eur J Immunol,* 7**,** 559-65.

JACKSON, A., NANTON, M. R., O'DONNELL, H., AKUE, A. D. & MCSORLEY, S. J. 2010. Innate immune activation during Salmonella infection initiates extramedullary erythropoiesis and splenomegaly. *J Immunol,* 185**,** 6198-204.

KANSWAL, S., KATSENELSON, N., SELVAPANDIYAN, A., BRAM, R. J. & AKKOYUNLU, M. 2008. Deficient TACI expression on B lymphocytes of newborn mice leads to defective Ig secretion in response to BAFF or APRIL. *J Immunol,* 181**,** 976-90.

KLEIN, U., CASOLA, S., CATTORETTI, G., SHEN, Q., LIA, M., MO, T., LUDWIG, T., RAJEWSKY, K. & DALLA-FAVERA, R. 2006. Transcription factor IRF4 controls plasma cell differentiation and class-switch recombination. *Nat Immunol,* 7**,** 773-82.

KRAAL, G., SCHORNAGEL, K., STREETER, P. R., HOLZMANN, B. & BUTCHER, E. C. 1995. Expression of the mucosal vascular addressin, MAdCAM-1, on sinus-lining cells in the spleen. *Am J Pathol,* 147**,** 763-71.

KUMARARATNE, D. S. & MACLENNAN, I. C. 1981. Cells of the marginal zone of the spleen are lymphocytes derived from recirculating precursors. *Eur J Immunol,* 11**,** 865-9.

KUO, T. C. & CALAME, K. L. 2004. B lymphocyte-induced maturation protein (Blimp)-1, IFN regulatory factor (IRF)-1, and IRF-2 can bind to the same regulatory sites. *J Immunol,* 173**,** 5556-63.

LAM, K. P. & RAJEWSKY, K. 1999. B cell antigen receptor specificity and surface density together determine B-1 versus B-2 cell development. *J Exp Med,* 190**,** 471-7.

LANE, P. J., GRAY, D., OLDFIELD, S. & MACLENNAN, I. C. 1986. Differences in the recruitment of virgin B cells into antibody responses to thymus-dependent and thymus-independent type-2 antigens. *Eur J Immunol,* 16**,** 1569-75.

LAUFFENBURGER, D. A. & HORWITZ, A. F. 1996. Cell migration: a physically integrated molecular process. *Cell,* 84**,** 359-69.

LEICK, M., CATUSSE, J., FOLLO, M., NIBBS, R. J., HARTMANN, T. N., VEELKEN, H. & BURGER, M. 2010. CCL19 is a specific ligand of the constitutively recycling atypical human chemokine receptor CRAM-B. *Immunology,* 129**,** 536-46.

LI, L., MA, P., HUANG, C., LIU, Y., ZHANG, Y., GAO, C., XIAO, T., REN, P. G., ZABEL, B. A. & ZHANG, J. V. 2014. Expression of chemerin and its receptors in rat testes and its action on testosterone secretion. *J Endocrinol,* 220**,** 155-63.

LIN, Y., WONG, K. & CALAME, K. 1997. Repression of c-myc transcription by Blimp-1, an inducer of terminal B cell differentiation. *Science,* 276**,** 596-9.

LIU, Y. J., ZHANG, J., LANE, P. J., CHAN, E. Y. & MACLENNAN, I. C. 1991. Sites of specific B cell activation in primary and secondary responses to T cell-dependent and T cell-independent antigens. *Eur J Immunol,* 21**,** 2951-62.

LOPES-CARVALHO, T. & KEARNEY, J. F. 2004. Development and selection of marginal zone B cells. *Immunol Rev,* 197**,** 192-205.

MACLENNAN, I. C. 1994. Germinal centers. *Annu Rev Immunol,* 12**,** 117-39.

MANTCHEV, G. T., CORTESAO, C. S., REBROVICH, M., CASCALHO, M. & BRAM, R. J. 2007. TACI is required for efficient plasma cell differentiation in response to T-independent type 2 antigens. *J Immunol,* 179**,** 2282-8.

MARINESCU, V. D., KOHANE, I. S. & RIVA, A. 2005. The MAPPER database: a multi-genome catalog of putative transcription factor binding sites. *Nucleic Acids Res,* 33**,** D91-7.

MARSHALL, J. 2009. Early divergent B cell differentiation during antibody responses. *Thesis, School of Immunity and Infection, The University of Birmingham*.

MARSHALL, J. L., FLORES-LANGARICA, A., KINGSLEY, R. A., HITCHCOCK, J. R., ROSS, E. A., LOPEZ-MACIAS, C., LAKEY, J., MARTIN, L. B., TOELLNER, K. M., MACLENNAN, C. A., MACLENNAN, I. C., HENDERSON, I. R., DOUGAN, G. & CUNNINGHAM, A. F. 2012. The capsular polysaccharide Vi from Salmonella typhi is a B1b antigen. *J Immunol,* 189**,** 5527-32.

MARSHALL, J. L., ZHANG, Y., PALLAN, L., HSU, M. C., KHAN, M., CUNNINGHAM, A. F., MACLENNAN, I. C. & TOELLNER, K. M. 2011. Early B blasts acquire a capacity for Ig

class switch recombination that is lost as they become plasmablasts. *Eur J Immunol,* 41**,** 3506-12.

MARTIN, F., OLIVER, A. M. & KEARNEY, J. F. 2001. Marginal zone and B1 B cells unite in the early response against T-independent blood-borne particulate antigens. *Immunity,* 14**,** 617-29.

MATSUYAMA, T., GROSSMAN, A., MITTRUCKER, H. W., SIDEROVSKI, D. P., KIEFER, F., KAWAKAMI, T., RICHARDSON, C. D., TANIGUCHI, T., YOSHINAGA, S. K. & MAK, T. W. 1995. Molecular cloning of LSIRF, a lymphoid-specific member of the interferon regulatory factor family that binds the interferon-stimulated response element (ISRE). *Nucleic Acids Res,* 23**,** 2127-36.

MCSORLEY, S. J. & JENKINS, M. K. 2000. Antibody is required for protection against virulent but not attenuated Salmonella enterica serovar typhimurium. *Infect Immun,* 68**,** 3344-8.

MEBIUS, R. E. & KRAAL, G. 2005. Structure and function of the spleen. *Nat Rev Immunol,* 5**,** 606-16.

MEDER, W., WENDLAND, M., BUSMANN, A., KUTZLEB, C., SPODSBERG, N., JOHN, H., RICHTER, R., SCHLEUDER, D., MEYER, M. & FORSSMANN, W. G. 2003. Characterization of human circulating TIG2 as a ligand for the orphan receptor ChemR23. *FEBS Lett,* 555**,** 495-9.

MIGEOTTE, I., FRANSSEN, J. D., GORIELY, S., WILLEMS, F. & PARMENTIER, M. 2002. Distribution and regulation of expression of the putative human chemokine receptor HCR in leukocyte populations. *Eur J Immunol,* 32**,** 494-501.

MINGUET, S., DOPFER, E. P., POLLMER, C., FREUDENBERG, M. A., GALANOS, C., RETH, M., HUBER, M. & SCHAMEL, W. W. 2008. Enhanced B-cell activation mediated by TLR4 and BCR crosstalk. *Eur J Immunol,* 38**,** 2475-87.

MOHR, E., SERRE, K., MANZ, R. A., CUNNINGHAM, A. F., KHAN, M., HARDIE, D. L., BIRD, R. & MACLENNAN, I. C. 2009. Dendritic cells and monocyte/macrophages that create the IL-6/APRIL-rich lymph node microenvironments where plasmablasts mature. *J Immunol,* 182**,** 2113-23.

MOMBAERTS, P., IACOMINI, J., JOHNSON, R. S., HERRUP, K., TONEGAWA, S. & PAPAIOANNOU, V. E. 1992. RAG-1-deficient mice have no mature B and T lymphocytes. *Cell,* 68**,** 869-77.

MOND, J. J., LEES, A. & SNAPPER, C. M. 1995. T cell-independent antigens type 2. *Annu Rev Immunol,* 13**,** 655-92.

MONNIER, J., LEWEN, S., O'HARA, E., HUANG, K., TU, H., BUTCHER, E. C. & ZABEL, B. A. 2012. Expression, regulation, and function of atypical chemerin receptor CCRL2 on endothelial cells. *J Immunol,* 189**,** 956-67.

MORIYAMA, S., TAKAHASHI, N., GREEN, J. A., HORI, S., KUBO, M., CYSTER, J. G. & OKADA, T. 2014. Sphingosine-1-phosphate receptor 2 is critical for follicular helper T cell retention in germinal centers. *J Exp Med,* 211**,** 1297-305.

MOSIER, D. E., MOND, J. J. & GOLDINGS, E. A. 1977. The ontogeny of thymic independent antibody responses in vitro in normal mice and mice with an X-linked B cell defect. *J Immunol,* 119**,** 1874-8.

MOSIER, D. E., SCHER, I. & PAUL, W. E. 1976. In vitro responses of CBA/N mice: spleen cells of mice with an X-linked defect that precludes immune responses to several

thymus-independent antigens can respond to TNP-lipopolysaccharide. *J Immunol,* 117**,** 1363-9.

MUPPIDI, J. R., ARNON, T. I., BRONEVETSKY, Y., VEERAPEN, N., TANAKA, M., BESRA, G. S. & CYSTER, J. G. 2011. Cannabinoid receptor 2 positions and retains marginal zone B cells within the splenic marginal zone. *J Exp Med,* 208**,** 1941-8.

MURRAY, C. J. & LOPEZ, A. D. 1997. Alternative projections of mortality and disability by cause 1990-2020: Global Burden of Disease Study. *Lancet,* 349**,** 1498-504.

NERA, K. P., KOHONEN, P., NARVI, E., PEIPPO, A., MUSTONEN, L., TERHO, P., KOSKELA, K., BUERSTEDDE, J. M. & LASSILA, O. 2006. Loss of Pax5 promotes plasma cell differentiation. *Immunity,* 24**,** 283-93.

NIBBS, R. J. & GRAHAM, G. J. 2013. Immune regulation by atypical chemokine receptors. *Nat Rev Immunol,* 13**,** 815-29.

NIETO, M., FRADE, J. M., SANCHO, D., MELLADO, M., MARTINEZ, A. C. & SANCHEZ-MADRID, F. 1997. Polarization of chemokine receptors to the leading edge during lymphocyte chemotaxis. *J Exp Med,* 186**,** 153-8.

NIEUWENHUIS, P. & FORD, W. L. 1976. Comparative migration of B- and T-Lymphocytes in the rat spleen and lymph nodes. *Cell Immunol,* 23**,** 254-67.

OBUKHANYCH, T. V. & NUSSENZWEIG, M. C. 2006. T-independent type II immune responses generate memory B cells. *J Exp Med,* 203**,** 305-10.

OCHIAI, K., MAIENSCHEIN-CLINE, M., SIMONETTI, G., CHEN, J., ROSENTHAL, R., BRINK, R., CHONG, A. S., KLEIN, U., DINNER, A. R., SINGH, H. & SCIAMMAS, R. 2013. Transcriptional regulation of germinal center B and plasma cell fates by dynamical control of IRF4. *Immunity,* 38**,** 918-29.

OKADA, T., MILLER, M. J., PARKER, I., KRUMMEL, M. F., NEIGHBORS, M., HARTLEY, S. B., O'GARRA, A., CAHALAN, M. D. & CYSTER, J. G. 2005. Antigen-engaged B cells undergo chemotaxis toward the T zone and form motile conjugates with helper T cells. *PLoS Biol,* 3**,** e150.

OLIVER, A. M., MARTIN, F. & KEARNEY, J. F. 1997. Mouse CD38 is down-regulated on germinal center B cells and mature plasma cells. *J Immunol,* 158**,** 1108-15.

OOSTENDORP, J., HYLKEMA, M. N., LUINGE, M., GEERLINGS, M., MEURS, H., TIMENS, W., ZAAGSMA, J., POSTMA, D. S., BODDEKE, H. W. & BIBER, K. 2004. Localization and enhanced mRNA expression of the orphan chemokine receptor L-CCR in the lung in a murine model of ovalbumin-induced airway inflammation. *J Histochem Cytochem,* 52**,** 401-10.

OTERO, K., VECCHI, A., HIRSCH, E., KEARLEY, J., VERMI, W., DEL PRETE, A., GONZALVO-FEO, S., GARLANDA, C., AZZOLINO, O., SALOGNI, L., LLOYD, C. M., FACCHETTI, F., MANTOVANI, A. & SOZZANI, S. 2010. Nonredundant role of CCRL2 in lung dendritic cell trafficking. *Blood,* 116**,** 2942-9.

OU, X., XU, S. & LAM, K. P. 2012. Deficiency in TNFRSF13B (TACI) expands T-follicular helper and germinal center B cells via increased ICOS-ligand expression but impairs plasma cell survival. *Proc Natl Acad Sci U S A,* 109**,** 15401-6.

OZCAN, E., GARIBYAN, L., LEE, J. J., BRAM, R. J., LAM, K. P. & GEHA, R. S. 2009. Transmembrane activator, calcium modulator, and cyclophilin ligand interactor drives plasma cell differentiation in LPS-activated B cells. *J Allergy Clin Immunol,* 123**,** 1277-86 e5.

PASQUALUCCI, L., MIGLIAZZA, A., BASSO, K., HOULDSWORTH, J., CHAGANTI, R. S. & DALLA-FAVERA, R. 2003. Mutations of the BCL6 proto-oncogene disrupt its negative autoregulation in diffuse large B-cell lymphoma. *Blood,* 101**,** 2914-23.

PELED, J. U., KUANG, F. L., IGLESIAS-USSEL, M. D., ROA, S., KALIS, S. L., GOODMAN, M. F. & SCHARFF, M. D. 2008. The biochemistry of somatic hypermutation. *Annu Rev Immunol,* 26**,** 481-511.

PEREIRA, J. P., KELLY, L. M., XU, Y. & CYSTER, J. G. 2009. EBI2 mediates B cell segregation between the outer and centre follicle. *Nature,* 460**,** 1122-6.

PERLMUTTER, R. M., HANSBURG, D., BRILES, D. E., NICOLOTTI, R. A. & DAVIE, J. M. 1978. Subclass restriction of murine anti-carbohydrate antibodies. *J Immunol,* 121**,** 566-72.

PIE, S., TRUFFA-BACHI, P., PLA, M. & NAUCIEL, C. 1997. Th1 response in Salmonella typhimurium-infected mice with a high or low rate of bacterial clearance. *Infect Immun,* 65**,** 4509-14.

PONE, E. J., ZHANG, J., MAI, T., WHITE, C. A., LI, G., SAKAKURA, J. K., PATEL, P. J., AL-QAHTANI, A., ZAN, H., XU, Z. & CASALI, P. 2012. BCR-signalling synergizes with TLR-signalling for induction of AID and immunoglobulin class-switching through the non-canonical NF-kappaB pathway. *Nat Commun,* 3**,** 767.

PRUENSTER, M., MUDDE, L., BOMBOSI, P., DIMITROVA, S., ZSAK, M., MIDDLETON, J., RICHMOND, A., GRAHAM, G. J., SEGERER, S., NIBBS, R. J. & ROT, A. 2009. The Duffy antigen receptor for chemokines transports chemokines and supports their promigratory activity. *Nat Immunol,* 10**,** 101-8.

RAHMAN, Z. S., RAO, S. P., KALLED, S. L. & MANSER, T. 2003. Normal induction but attenuated progression of germinal center responses in BAFF and BAFF-R signaling-deficient mice. *J Exp Med,* 198**,** 1157-69.

RASHEED, M. A., LATNER, D. R., AUBERT, R. D., GOURLEY, T., SPOLSKI, R., DAVIS, C. W., LANGLEY, W. A., HA, S. J., YE, L., SARKAR, S., KALIA, V., KONIECZNY, B. T., LEONARD, W. J. & AHMED, R. 2013. Interleukin-21 is a critical cytokine for the generation of virus-specific long-lived plasma cells. *J Virol,* 87**,** 7737-46.

REIF, K., EKLAND, E. H., OHL, L., NAKANO, H., LIPP, M., FORSTER, R. & CYSTER, J. G. 2002. Balanced responsiveness to chemoattractants from adjacent zones determines B-cell position. *Nature,* 416**,** 94-9.

REVY, P., MUTO, T., LEVY, Y., GEISSMANN, F., PLEBANI, A., SANAL, O., CATALAN, N., FORVEILLE, M., DUFOURCQ-LABELOUSE, R., GENNERY, A., TEZCAN, I., ERSOY, F., KAYSERILI, H., UGAZIO, A. G., BROUSSE, N., MURAMATSU, M., NOTARANGELO, L. D., KINOSHITA, K., HONJO, T., FISCHER, A. & DURANDY, A. 2000. Activation-induced cytidine deaminase (AID) deficiency causes the autosomal recessive form of the Hyper-IgM syndrome (HIGM2). *Cell,* 102**,** 565-75.

ROSADO, M. M., ARANBURU, A., CAPOLUNGHI, F., GIORDA, E., CASCIOLI, S., CENCI, F., PETRINI, S., MILLER, E., LEANDERSON, T., BOTTAZZO, G. F., NATALI, P. G. & CARSETTI, R. 2009. From the fetal liver to spleen and gut: the highway to natural antibody. *Mucosal Immunol,* 2**,** 351-61.

ROSAS, L. E., BARBI, J., LU, B., FUJIWARA, Y., GERARD, C., SANDERS, V. M. & SATOSKAR, A. R. 2005. CXCR3-/- mice mount an efficient Th1 response but fail to control Leishmania major infection. *Eur J Immunol,* 35**,** 515-23.

ROT, A. & VON ANDRIAN, U. H. 2004. Chemokines in innate and adaptive host defense: basic chemokinese grammar for immune cells. *Annu Rev Immunol,* 22**,** 891-928.

SCHOLZEN, T. & GERDES, J. 2000. The Ki-67 protein: from the known and the unknown. *J Cell Physiol,* 182**,** 311-22.

SCIAMMAS, R., SHAFFER, A. L., SCHATZ, J. H., ZHAO, H., STAUDT, L. M. & SINGH, H. 2006. Graded expression of interferon regulatory factor-4 coordinates isotype switching with plasma cell differentiation. *Immunity,* 25**,** 225-36.

SEO, B. S., LEE, S. H., LEE, J. E., YOO, Y. C., LEE, J. & PARK, S. R. 2013. Dectin-1 Stimulation Selectively Reinforces LPS-driven IgG1 Production by Mouse B Cells. *Immune Netw,* 13**,** 205-12.

SERRE, K., CUNNINGHAM, A. F., COUGHLAN, R. E., LINO, A. C., ROT, A., HUB, E., MOSER, K., MANZ, R., FERRARO, A., BIRD, R., TOELLNER, K. M., DEMENGEOT, J., MACLENNAN, I. C. & MOHR, E. 2012. CD8 T cells induce T-bet-dependent migration toward CXCR3 ligands by differentiated B cells produced during responses to alum-protein vaccines. *Blood,* 120**,** 4552-9.

SESHASAYEE, D., VALDEZ, P., YAN, M., DIXIT, V. M., TUMAS, D. & GREWAL, I. S. 2003. Loss of TACI causes fatal lymphoproliferation and autoimmunity, establishing TACI as an inhibitory BLyS receptor. *Immunity,* 18**,** 279-88.

SHAFFER, A. L., LIN, K. I., KUO, T. C., YU, X., HURT, E. M., ROSENWALD, A., GILTNANE, J. M., YANG, L., ZHAO, H., CALAME, K. & STAUDT, L. M. 2002. Blimp-1 orchestrates plasma cell differentiation by extinguishing the mature B cell gene expression program. *Immunity,* 17**,** 51-62.

SHAFFER, A. L., SHAPIRO-SHELEF, M., IWAKOSHI, N. N., LEE, A. H., QIAN, S. B., ZHAO, H., YU, X., YANG, L., TAN, B. K., ROSENWALD, A., HURT, E. M., PETROULAKIS, E., SONENBERG, N., YEWDELL, J. W., CALAME, K., GLIMCHER, L. H. & STAUDT, L. M. 2004. XBP1, downstream of Blimp-1, expands the secretory apparatus and other organelles, and increases protein synthesis in plasma cell differentiation. *Immunity,* 21**,** 81-93.

SHAFFER, A. L., YU, X., HE, Y., BOLDRICK, J., CHAN, E. P. & STAUDT, L. M. 2000. BCL-6 represses genes that function in lymphocyte differentiation, inflammation, and cell cycle control. *Immunity,* 13**,** 199-212.

SHAPIRO-SHELEF, M., LIN, K. I., MCHEYZER-WILLIAMS, L. J., LIAO, J., MCHEYZER-WILLIAMS, M. G. & CALAME, K. 2003. Blimp-1 is required for the formation of immunoglobulin secreting plasma cells and pre-plasma memory B cells. *Immunity,* 19**,** 607-20.

SHI, G. X., HARRISON, K., WILSON, G. L., MORATZ, C. & KEHRL, J. H. 2002. RGS13 regulates germinal center B lymphocytes responsiveness to CXC chemokine ligand (CXCL)12 and CXCL13. *J Immunol,* 169**,** 2507-15.

SHIH, T. A., MEFFRE, E., ROEDERER, M. & NUSSENZWEIG, M. C. 2002. Role of BCR affinity in T cell dependent antibody responses in vivo. *Nat Immunol,* 3**,** 570-5.

SHIMADA, T., MATSUMOTO, M., TATSUMI, Y., KANAMARU, A. & AKIRA, S. 1998. A novel lipopolysaccharide inducible C-C chemokine receptor related gene in murine macrophages. *FEBS Lett,* 425**,** 490-4.

SHOKAT, K. M. & GOODNOW, C. C. 1995. Antigen-induced B-cell death and elimination during germinal-centre immune responses. *Nature,* 375**,** 334-8.

SMITH, F. I., CUMANO, A., LICHT, A., PECHT, I. & RAJEWSKY, K. 1985. Low affinity of kappa chain bearing (4-hydroxy-3-nitrophenyl)acetyl (NP)-specific antibodies in the primary antibody repertoire of C57BL/6 mice may explain lambda chain dominance in primary anti-NP responses. *Mol Immunol,* 22**,** 1209-16.

SMITH, J. P., BURTON, G. F., TEW, J. G. & SZAKAL, A. K. 1998. Tingible body macrophages in regulation of germinal center reactions. *Dev Immunol,* 6**,** 285-94.

SONG, H. & CERNY, J. 2003. Functional heterogeneity of marginal zone B cells revealed by their ability to generate both early antibody-forming cells and germinal centers with hypermutation and memory in response to a T-dependent antigen. *J Exp Med,* 198**,** 1923-35.

SORO, P. G., MORALES, A. P., MARTINEZ, M. J., MORALES, A. S., COPIN, S. G., MARCOS, M. A. & GASPAR, M. L. 1999. Differential involvement of the transcription factor Blimp-1 in T cell-independent and -dependent B cell differentiation to plasma cells. *J Immunol,* 163**,** 611-7.

STAVNEZER, J., GUIKEMA, J. E. & SCHRADER, C. E. 2008. Mechanism and regulation of class switch recombination. *Annu Rev Immunol,* 26**,** 261-92.

STOLL, S., DELON, J., BROTZ, T. M. & GERMAIN, R. N. 2002. Dynamic imaging of T cell-dendritic cell interactions in lymph nodes. *Science,* 296**,** 1873-6.

STREETER, P. R., BERG, E. L., ROUSE, B. T., BARGATZE, R. F. & BUTCHER, E. C. 1988. A tissue-specific endothelial cell molecule involved in lymphocyte homing. *Nature,* 331**,** 41-6.

SUN, Y., MCGARRIGLE, D. & HUANG, X. Y. 2007. When a G protein-coupled receptor does not couple to a G protein. *Mol Biosyst,* 3**,** 849-54.

SUZUKI, K., GRIGOROVA, I., PHAN, T. G., KELLY, L. M. & CYSTER, J. G. 2009. Visualizing B cell capture of cognate antigen from follicular dendritic cells. *J Exp Med,* 206**,** 1485-93.

SZE, D. M., TOELLNER, K. M., GARCIA DE VINUESA, C., TAYLOR, D. R. & MACLENNAN, I. C. 2000. Intrinsic constraint on plasmablast growth and extrinsic limits of plasma cell survival. *J Exp Med,* 192**,** 813-21.

TAILLARDET, M., HAFFAR, G., MONDIERE, P., ASENSIO, M. J., GHEIT, H., BURDIN, N., DEFRANCE, T. & GENESTIER, L. 2009. The thymus-independent immunity conferred by a pneumococcal polysaccharide is mediated by long-lived plasma cells. *Blood,* 114**,** 4432-40.

TAKAHASHI, M., OKIMURA, Y., IGUCHI, G., NISHIZAWA, H., YAMAMOTO, M., SUDA, K., KITAZAWA, R., FUJIMOTO, W., TAKAHASHI, K., ZOLOTARYOV, F. N., HONG, K. S., KIYONARI, H., ABE, T., KAJI, H., KITAZAWA, S., KASUGA, M., CHIHARA, K. & TAKAHASHI, Y. 2011. Chemerin regulates beta-cell function in mice. *Sci Rep,* 1**,** 123.

TARTE, K., ZHAN, F., DE VOS, J., KLEIN, B. & SHAUGHNESSY, J., JR. 2003. Gene expression profiling of plasma cells and plasmablasts: toward a better understanding of the late stages of B-cell differentiation. *Blood,* 102**,** 592-600.

TAYLOR, P. R., PICKERING, M. C., KOSCO-VILBOIS, M. H., WALPORT, M. J., BOTTO, M., GORDON, S. & MARTINEZ-POMARES, L. 2002. The follicular dendritic cell restricted epitope, FDC-M2, is complement C4; localization of immune complexes in mouse tissues. *Eur J Immunol,* 32**,** 1888-96.

TEW, J. G., WU, J., QIN, D., HELM, S., BURTON, G. F. & SZAKAL, A. K. 1997. Follicular dendritic cells and presentation of antigen and costimulatory signals to B cells. *Immunol Rev,* 156**,** 39-52.

TOELLNER, K. M., LUTHER, S. A., SZE, D. M., CHOY, R. K., TAYLOR, D. R., MACLENNAN, I. C. & ACHA-ORBEA, H. 1998. T helper 1 (Th1) and Th2 characteristics start to develop during T cell priming and are associated with an immediate ability to induce immunoglobulin class switching. *J Exp Med,* 187**,** 1193-204.

TSUJI, S., CORTESAO, C., BRAM, R. J., PLATT, J. L. & CASCALHO, M. 2011. TACI deficiency impairs sustained Blimp-1 expression in B cells decreasing long-lived plasma cells in the bone marrow. *Blood,* 118**,** 5832-9.

TUNYAPLIN, C., SHAFFER, A. L., ANGELIN-DUCLOS, C. D., YU, X., STAUDT, L. M. & CALAME, K. L. 2004. Direct repression of prdm1 by Bcl-6 inhibits plasmacytic differentiation. *J Immunol,* 173**,** 1158-65.

TURNER, C. A., JR., MACK, D. H. & DAVIS, M. M. 1994. Blimp-1, a novel zinc finger-containing protein that can drive the maturation of B lymphocytes into immunoglobulin-secreting cells. *Cell,* 77**,** 297-306.

ULVMAR, M. H., HUB, E. & ROT, A. 2011. Atypical chemokine receptors. *Exp Cell Res,* 317**,** 556-68.

ULVMAR, M. H., WERTH, K., BRAUN, A., KELAY, P., HUB, E., ELLER, K., CHAN, L., LUCAS, B., NOVITZKY-BASSO, I., NAKAMURA, K., RULICKE, T., NIBBS, R. J., WORBS, T., FORSTER, R. & ROT, A. 2014. The atypical chemokine receptor CCRL1 shapes functional CCL21 gradients in lymph nodes. *Nat Immunol,* 15**,** 623-30.

VENKITESWARAN, G., LEWELLIS, S. W., WANG, J., REYNOLDS, E., NICHOLSON, C. & KNAUT, H. 2013. Generation and dynamics of an endogenous, self-generated signaling gradient across a migrating tissue. *Cell,* 155**,** 674-87.

VINUESA, C. G. 2000. Exploring the limits of thymus independence. *Thesis, School of Immunity and Infection, The University of Birmingham*.

VINUESA, C. G. & CHANG, P. P. 2013. Innate B cell helpers reveal novel types of antibody responses. *Nat Immunol,* 14**,** 119-26.

VINUESA, C. G., SUNNERS, Y., PONGRACZ, J., BALL, J., TOELLNER, K. M., TAYLOR, D., MACLENNAN, I. C. & COOK, M. C. 2001. Tracking the response of Xid B cells in vivo: TI-2 antigen induces migration and proliferation but Btk is essential for terminal differentiation. *Eur J Immunol,* 31**,** 1340-50.

WANG, H., BEATY, N., CHEN, S., QI, C. F., MASIUK, M., SHIN, D. M. & MORSE, H. C., 3RD 2012. The CXCR7 chemokine receptor promotes B-cell retention in the splenic marginal zone and serves as a sink for CXCL12. *Blood,* 119**,** 465-8.

WEIBEL, E. R. 1963. Principles and methods for the morphometric study of the lung and other organs. *Lab Invest,* 12**,** 131-55.

WINKELMANN, R., SANDROCK, L., PORSTNER, M., ROTH, E., MATHEWS, M., HOBEIKA, E., RETH, M., KAHN, M. L., SCHUH, W. & JACK, H. M. 2011. B cell homeostasis and plasma cell homing controlled by Kruppel-like factor 2. *Proc Natl Acad Sci U S A,* 108**,** 710-5.

WITTAMER, V., FRANSSEN, J. D., VULCANO, M., MIRJOLET, J. F., LE POUL, E., MIGEOTTE, I., BREZILLON, S., TYLDESLEY, R., BLANPAIN, C., DETHEUX, M., MANTOVANI, A., SOZZANI, S., VASSART, G., PARMENTIER, M. & COMMUNI, D. 2003. Specific

recruitment of antigen-presenting cells by chemerin, a novel processed ligand from human inflammatory fluids. *J Exp Med,* 198**,** 977-85.

XU, Z., ZAN, H., PONE, E. J., MAI, T. & CASALI, P. 2012. Immunoglobulin class-switch DNA recombination: induction, targeting and beyond. *Nat Rev Immunol,* 12**,** 517-31.

YANG, H., LI, F., KONG, X., YUAN, X., WANG, W., HUANG, R., LI, T., GENG, M., WU, G. & YIN, Y. 2012. Chemerin regulates proliferation and differentiation of myoblast cells via ERK1/2 and mTOR signaling pathways. *Cytokine,* 60**,** 646-52.

YIN, F., XU, Z., WANG, Z., YAO, H., SHEN, Z., YU, F., TANG, Y., FU, D., LIN, S., LU, G., KUNG, H. F., POON, W. S., HUANG, Y. & LIN, M. C. 2012. Elevated chemokine CC-motif receptor-like 2 (CCRL2) promotes cell migration and invasion in glioblastoma. *Biochem Biophys Res Commun,* 429**,** 168-72.

ZABEL, B. A., NAKAE, S., ZUNIGA, L., KIM, J. Y., OHYAMA, T., ALT, C., PAN, J., SUTO, H., SOLER, D., ALLEN, S. J., HANDEL, T. M., SONG, C. H., GALLI, S. J. & BUTCHER, E. C. 2008. Mast cell-expressed orphan receptor CCRL2 binds chemerin and is required for optimal induction of IgE-mediated passive cutaneous anaphylaxis. *J Exp Med,* 205**,** 2207-20.

ZHANG, Y. 2010. Signals for B cell activation in antibody response. *Thesis, School of Immunity and Infection, The University of Birmingham*.

ZHANG, Y., MEYER-HERMANN, M., GEORGE, L. A., FIGGE, M. T., KHAN, M., GOODALL, M., YOUNG, S. P., REYNOLDS, A., FALCIANI, F., WAISMAN, A., NOTLEY, C. A., EHRENSTEIN, M. R., KOSCO-VILBOIS, M. & TOELLNER, K. M. 2013. Germinal center B cells govern their own fate via antibody feedback. *J Exp Med,* 210**,** 457-64.

ZHAO, P., YANG, Y., FENG, H., ZHAO, L., QIN, J., ZHANG, T., WANG, H., YANG, S. & XIA, X. 2013. Global gene expression changes in BV2 microglial cell line during rabies virus infection. *Infect Genet Evol,* 20**,** 257-69.

ZUBLER, R. H. 2001. Naive and memory B cells in T-cell-dependent and T-independent responses. *Springer Semin Immunopathol,* 23**,** 405-19.

ZUURMAN, M. W., HEEROMA, J., BROUWER, N., BODDEKE, H. W. & BIBER, K. 2003. LPS-induced expression of a novel chemokine receptor (L-CCR) in mouse glial cells in vitro and in vivo. *Glia,* 41**,** 327-36.